MEMOIR OF THE
GEOLOGICAL SURVEY OF NAMIBIA

GEOLOGICAL PROCESSES AND STRATIGRAPHY OF THE DIAMOND PLACERS OF THE NORTHERN SPERRGEBIET

Edited by Martin Pickford

MINISTRY OF MINES AND ENERGY

MEMOIR 22
2016

GEOLOGICAL SURVEY OF NAMIBIA

MINISTRY OF MINES AND ENERGY

Acting Director: G. Simubali

MEMOIR 22

GEOLOGICAL PROCESSES AND STRATIGRAPHY OF THE DIAMOND PLACERS OF THE NORTHERN SPERRGEBIET

Editor: M. Pickford

Manuscripts reviewed by: M. Pickford, U. Schreiber

Obtainable from the Geological Survey of Namibia,
Private Bag 13297, Windhoek, Namibia

ISSN: 2026-8262 (Online)
ISSN: 2026-8270 (CD-ROM)

ISBN: 978-99945-0-093-2 (Online)

MEMOIR OF THE GEOLOGICAL SURVEY OF NAMIBIA

MEMOIR 22
2016

CONTENTS

PAPERS

Cover Image : The 120 metre high Buntfeldschuh Escarpment and Kakaoberg viewed from the North. The low-lying ground comprises altered Precambrian schist and dolomite (Bo Alterite) overlain successively by Eocene Buntfeldschuh Formation (deltaic-marine sediments), Oligocene Terrestre Sandstone (aeolianite which was densely ferruginised on Kakaoberg during the Oligo-Miocene), Middle Miocene Namib 1 Calc-crust, and finally loose sand and regolith. The dark knolls in the foreground are densely ferruginised palaeoregolith overlying Bo Alterite but of the same age as the ferricrete forming Kakaoberg.

PREFACE

Memoir 22 of the Geological Survey of Namibia

Geological Processes and Stratigraphy of the Diamond Placers of the Northern Sperrgebiet

The discovery of alluvial diamonds in Namibia in 1908 not only sparked off over a century of exploitation of the richest and most areally extensive diamond placers ever recognised, but it also set in motion the inquisitive minds of scientists who have laboured to understand the processes that led to the formation of the placers. Within a year of the initial discovery, geologists such as Merensky (1909) and Krause (1910) had proposed a source (or sources) for the diamonds, had suggested transport pathways from source to sink, and had investigated concentration mechanisms as well as estimated the timing of some of the geological events in the region. A few of the early ideas, such as the supposed presence of Cretaceous rocks in the region, were poorly supported by evidence, in this case being based on mis-identified marine molluscs (Merensky, 1909) of Late Eocene age.

In 1910, the region was declared the Sperrgebiet (Forbidden Territory) by the German Government, and for the next century, in the interests of diamond security, there has been strict control on movements within the region.

The sector of the Northern Sperrgebiet from Buntfeldshuch to Grillental was mapped in detail by Kaiser & Beetz (1926). The six geological maps and the two-volume monograph (Kaiser, 1926) that resulted from this immense task have formed the basis for all subsequent interpretations of the succession of events, the timing of events and of the geological processes that led to the formation of the diamond placers. But as was realised by Kaiser & Beetz (1926) themselves, the last word had not been written about the genesis of the diamond deposits, the geomorphology of the Trough Namib, where the bulk of the diamonds occurred, and the Plain Namib in the interior. These authors in particular stressed the importance of fossils for providing chronological anchors upon which the timing of events and the rates of geological processes could be estimated. For example, the legends in the geological maps mention the presence of fossiliferous Miocene marine deposits in the Granitberg-Bogenfels sector, but by the time that the monograph had been written, the fossils had been restudied (Böhm, 1926) and dated to the Eocene, which more than doubled the time span over which geological processes were thought to have been active. These authors did not recognise any undoubted Cretaceous rocks in the region (that was to come later with the announcement of the discoverty of Cretaceous ammonites at Wanderfeld IV by Haughton (1930a, 1930b)) and they were perspicacious enough to correlate the post-Basement strata of the region to the Prämitteleocän. The only unit that they thought might have resulted from geological processes active during the Cretaceous were the deep weathering of the Basement and the formation of ferruginous surface crusts at the base of what they called the Pomona Schichten.

There was thus a serious difference of opinion between Kaiser & Beetz (1926) on the one hand, and Merensky (1909) on the other, concerning the ages of the oldest post-basement strata in the Sperrgebiet, which impacted on aspects of the geomorphology of the region (the timing of the formation of endorheic basins, for instance) and the develoment of the placers themselves.

Major difficulties encountered while studying Sperrgebiet Geology were recognised by Kaiser & Beetz (1926). Among these were :-

1) the scattered and discontinuous nature of the post-basement deposits, which sometimes rendered the determination of the succession of geological events difficult,

2) the fact that the region of interest was close to the interface between continent and ocean and had thereby been affected by processes related to both,

3) the dominant role played by the wind in deflating sediments and facetting the basement relief,

4) the role of infrequent rainfall in the desert, resulting in ephemeral flow in the local hydrographic networks which comprised many endorheic basins as well as valleys debouching into the Atlantic,

5) the role of fog in shaping the landscape via the formation of calc-crusts and the

promotion of growth of desert-adapted vegetation,

6) the deposition of salt in the so-called Salt Namib, important because it promotes breakdown of sediment cohesion via salt-weathering processes (Corbett, 1989),

7) the role played by the Benguela Current in transporting sediments northwards along the Atlantic coast,

8) bioturbation, which disturbs the desert floor, thereby enhancing the deflation action of the wind,

9) eustatic changes in sea-level,

10) vertical land movements,

11) volcanic activity, notably in the Klinghardt Phonolite Cluster in the Plain Namib,

12) climatic change,

13) the scarcity of chronological anchors (fossils in particular) for the post-Proterozoic strata,

14) the presence of intense but variable weathering of the basement rocks,

15) the presence of superficial 'karst' features (called dolines by Kaiser & Beetz, 1926).

Closure of the Sperrgebiet effectively rendered impossible the solution or elucidation of most of these difficulties. In effect, declaration of the Sperrgebiet adversely affected scientific endeavour, because it prevented unhindered access to outcrops and thereby stifled debate about them. Geologists who were anxious to see the evidence for themselves in a free and open way were generally unable to do so.

The Consolidated Diamond Mines (Pty) Ltd, and subsequently Namdeb, employed in-house geologists to continue geological investigations in the region, especially in the inland sectors, but the results of these surveys were in the form of unpublished internal reports to the company with restricted circulation. From time to time consultants were invited to investigate selected target areas or sections, but few if any of these people were able to wander freely through the area to study other outcrops.

The outcome was that, instead of letting the geology of the region to speak for itself, there was often an imposition of « foreign » or "external" ideas and concepts on interpretations of Sperrgebiet geology. Over the years, the variety of such impositions has become quite bewildering, ranging from the correlation of strata and erosion surfaces to the Gondwana Surface or the African Surface of King (1949) on the scantiest of evidence (Hallam, 1964) (most of the Sperrgebiet strata previously correlated to the Mid- or Late Cretaceous « African Surface » are Lutetian to Bartonian in age as shown by their fossil content (Pickford *et al.* 2008)), to interpreting low altitude raised beaches (less than 20 masl) and shallow-water sub-marine beaches in terms of Quaternary Glacial-Interglacial cycles, correlating high raised beaches (between 30 and 160 masl) and deep-water sub-marine beaches to eustatic sea-level curves, including sea-level changes due to Polar Ice-cap growth in the Antarctic (Eo-Oligocene) and Arctic (Late Miocene to Present-day), not omitting the correlation of deposits and geological events to palaeo-climatic curves.

The ferruginous crust that Beetz (1926) called the « Verwitterungskruste einer alten Landoberfläche » was correlated by him to the « Wahrscheinlich Kreide » (probably Cretaceous) because his mapping showed that it comprised the base of the Prämitteleocän Pomona Schichten. However, remapping by the Namibia Palaeontology Expedition has revealed that all studied occurrences of this Verwitterungskruste, including those in the type area near Pomona, represent ferricrete deposited during the Oligo-Miocene. The ferricrete often occurs topographically beneath outcrops of Pomona Schichten, but stratigraphically it is considerably younger, being banked up against pre-existing relief eroded well after the silicification of the Kätchen Plateau Formation (which was originally included in the Pomona Schichten). From an economic point of view, the Cretaceous date that got attached to these and other deposits suggested that the presence of ferricrete (often called ferrugination) in an area or a section indicated that the footwall of the diamond placers had been detected. However, this is erroneous, the genesis of the ferricrete long post-dated the first arrival of diamonds in the region.

The Namib Calc-crusts were named « Oberflächenkalkdecke » by Beetz (1926) because they differed from classic calcretes, but the distinction got lost in translation when the word (and concept underlying it) was rendered in English as Calcrete or Pedogenic Hard Pan (Corbett, 1989). In general, these calc-crusts which crop out widely in the Plain

Namib, were thought to be relatively young (Pliocene in Beetz, 1926) which is not a bad assessment their age. However, the same deposits occur in the Trough Namib, and in most places they were included in the Pomona Schichten, either as Mid- to Late Cretaceous « calcretes », precursors of the « silcretes associated with the African Surface » (Liddle, 1971) or as Prämitteleocän Pomonakalk (Beetz, 1926). The Namib 1 Calc-crust is of Middle Miocene age, the Namib 2 Calc-crust is Plio-Pleistocene, as shown by the fossils that occur in it (including in the type section of the supposedly Middle Eocene Pomonakalk at Marienberg near Pomona).

General acceptance of the stratigraphic miscorrelation of the Sperrgebiet ferricrete and the Pomonakalk represented huge obstacles to the proper interpretation of the sequence of geological events in the region. But frequent repetition gave them a veneer of veracity which obscured the reality, thereby biasing almost all correlations of strata in the Sperrgebiet. Chronological offsets range from 20 to 40 m.y. too old. Papers published as recently as 2015 are affected by these offsets.

The Geological Time Scale has evolved over the past Century, as explained by Pickford (2015). Thus the fossiliferous marine *Turritella* Beds at Wanderfeld IV, near Bogenffels, were correlated to the Middle Eocene by Böhm (1926) a conclusion accepted by Beetz (1926) but would in today's version of the time scale be termed Priabonian (i.e. Latest Eocene). Reading of the unpublished reports on Sperrgebiet geology indicates that all authors accepted a Mid- to Late Cretaceous age for the strata formerly included in the Pomona Schichten (and the supposed erosion surfaces associated with them) and that many of them accepted Beetz's correlations to the Geological Time Scale without realising that there was an offset introduced by the evolution of the terms in it.

The present Memoir comprises three papers that deal with some of the aspects of Sperrgebiet geology evoked above. Corbett's (2016) contribution is an in-depth analysis of the Namib Aeolian Erosion Basin, or broadly speaking, the Flächen-Namib (Trough Namib) of Kaiser (1926). It examines aeolian processes at various scales, especially those related to deflation of sand and lighter clasts from the sediment load in the region, and it evokes fluvial reworking in endorheic basins as a background to explaining how immense concentrations of diamonds could be formed. It examines the role of the longshore currents which transport clasts northwards along the Atlantic coast from the mouth of the Orange River, and how the geomorphology of the coastline played a role in the formation of diamondiferous sediments (pocket beaches for example) at various altitudes depending on transgressions and regressions of the sea, which resulted in the genesis of onshore and offshore placers. The role of bioturbation is evoked briefly, in that animals walking on the surface of stone pavements and sediments scuff up the surface, thereby promoting aeolian deflation of previously inaccessible fines.

The paper by Pickford (2016) comprises a detailed examination of ferricrete outcrops of the Northern Sperrgebiet. The presence of ferruginised deposits (the « Brauneisenquartzit der Pomonaschichten » of Kaiser & Beetz, 1926) has long been taken to represent the earliest deposit overlying the deep weathering profile developed on the Basement rocks of the Sperrgebiet (i.e. the Bo Alterite of Pickford, 2015). It was considered by Beetz (1926) to be the horizon (of probable Cretaceous age) upon which the rest of the Pomona Schichten were deposited. On this basis, it has been widely accepted that the presence of ferruginised levels in a section or area denote the presence of the footwall of the diamond placers, in the belief that ferruginisation predated the first input of diamonds to the region. However, this is now known to be false, the initial diamond input dating from the Eocene (if not earlier) and the ferricrete formation dating from the Oligo-Miocene.

The paper by Pickford & Senut (2016) records the discovery of marine fossils at Hexen Kessel, in the heart of the Trough Namib, not far from the locality that yielded the richest concentration of alluvial diamonds ever found (Corbett, 2016). These deposits lie at an altitude of ca 30 masl, but correlative sands occur in the same area up to ca 50 masl. These sediments probably correlate to the 50-metre marine package of Pether (1986), defined in Namaqualand, South Africa, where it has been estimated to be of Pliocene age. The Hexen Kessel fossils thus indicate that part of the Trough Namib was inundated by the sea during the Pliocene, which implies that there was probably an influx of diamonds at this time, along with the sand and fossils. This

influx would have added to previous ore reserves that were brought in during the Eocene, and possibly the Early Miocene, but of which there remains no tangible evidence in terms of sediments, so complete has been aeolian winnowing and allied erosional processes that have been active since the period of deposition. The immense diamond placers of the Trough Namib in the vicinity of Pomona are thus concluded to have resulted from several pulses of diamond input related to marine transgressions between 50 masl and 160 masl.

In the past, the role of bioturbation in a wind-dominated environment such as the Sperrgebiet has usually been underestimated. It is now known to have contributed significantly to the remodelling of the landscape. Animals not only scuff the surface of stone pavements as they pass by, as describeed by Corbett (1989, 2016) but also a miriad of insects, scorpions and spiders burrow beneath stones and bring to the surface fine sand and silt from underlying marls and alterite, which, once exposed at the surface are rapidly blown away by the boisterous winds of the Sperrgebiet. Rodents burrow extensively in the loose surface deposits of the Innen-Namib (Plain Namib) with the same result - fines brought to the surface are blown away, leading to a gradual but inevitable coarsening of the residual deposits, best seen as poorly sorted grits and gravels exposed widely in the region. The downwasting that can be brought about by biotubation is impressive, and can cause problems of interpretation. Silicified tree trunks in the vicinity of Blaubok Beacon, near Bogenfels, were for many years thought to have been fossilised in the Blaubok Conglomerate, but it is now known that they were initially preserved in marl underlying the conglomerate, and that their present-day occurrence side-by-side with Blaubok clasts is due to downwasting of the cobbles of this unit to the same levels as the tree trunks. Indeed, the Blaubok Conglomerate, as currently defined, comprises many reworked fractions lying in varied stratigraphic contexts (Oligocene, Miocene, Pliocene, Pleistocene and Recent) so, as currenly mapped, it is in effect a composite unit with an exceptionally complex history.

Finally, even though this Memoir adds significantly to our understanding of the succession and timing of geological events in the Sperrgebiet, as well as to the various processess which shaped the landscape (geomorphological processes such as erosion, deposition, tectonics, volcanic activity, the formation of desert encrustations and eustatic changes in sea-level, among others), and which transport sediments into and out of the region, there remains a great deal to be done to obtain a reliable view of what actually happened in the region since the weathering phase that resulted in the Bo Alterite. It also contributes to the understanding of the timing of events in Sperrgebiet geology.

In the future, advances in understanding of the geology of the Sperrgebiet will only be possible if the region is made more accessible to researchers motivated by testing oft-repeated supposedly « established » interpretations, rather than by those interested in imposing ideas on the region and in practicing « conclusion driven » science.

References

Böhm, J., 1926. Über Tertiäre Versteinerungen von den Bogenfelser Diamantefeldern. *In*: E. Kaiser (Ed.) *Die Diamantenwüste SüdwestAfrikas*, **2**, 55-87, D. Reimer, Berlin.

Corbett, I.B., 1989. *The Sedimentology of the Diamond Deflation Deposits within the Sperrgebiet, Namibia*. PhD Thesis, University of Cape Town, 430 pp.

Corbett, IB., 2016. Sediment Dynamics of the Namib Aeolian Erosion Basin and the Sedimentology of the Diamond Placers of the Northern Sperrgebiet, Namibia. *Memoir of the Geological Survey of Namibia,* **22**, 6-171.

Hallam, C.D., 1964. The Geology of the coastal diamond deposits of southern Africa. *In*: S.H. Haughton (Ed.) The Geology of Some Ore Deposits of Southern Africa. *Geological Society of South Africa*, **2**, 671-728.

Haughton, S.H., 1930a. Note on the occurrence of Upper Cretaceous marine beds in South West Africa. *Transactions of the Geological Society of South Africa*, **33**, 61-63.

Haughton, S.H., 1930b. On the occurrence of Upper Cretaceous marine fossils near Bogenfels, S.W. Africa. *Transactions of the Royal Society of South Africa*, **18**, 361-365.

Kaiser, E., 1926. *Die Diamantenwüste SüdwestAfrikas*. D. Reimer, Berlin, Vol. 2, 535 pp.

Kaiser, E., & Beetz, W. 1926. Geological Maps *In*: E. Kaiser (Ed.) *Die Diamantenwüste SüdwestAfrikas.* Reimer, Berlin, **2**, p. 158.

King, L.C., 1949. On the ages of African land surfaces. *Quarterly Journal of the Geological Society of London*, **104**, 438-459.

Krause, G., 1910. Notes on the German South-West African Diamonds. *Transactions of the Geological Society of South Africa*, **13**, 61-64.

Liddle, R.S., 1971. The Cretaceous deposits of the North West Sperrgebiet. Sperrgebiet Geological Investigation, *Unpublished Report, Consolidated Diamond Mines of South West Africa (Pty) Ltd*, (Namdeb archives ref. 78127). 22 pp + 2 annexes of 10 pp.

Merensky, H., 1909. The Diamond deposits of Lüderitzland, German South-West Africa. *Transactions of the Geological Society of South Africa*, **12**, 13-23.

Pether, J., 1986. Late Tertiary and Early Quaternary marine deposits of the Namaqualand coast, Cape Province: New perspectives. *South African Journal of Science*, **82**, 464-470.

Pickford, M., 2015. Cenozoic Geology of the Northern Sperrgebiet, Namibia, accenting the Palaeogene. *Communications of the Geological Survey of Namibia*, **16**, 10-104.

Pickford, M. 2016. Ferricrete in the Sperrgebiet, Namibia: age, palaeoclimate and economic implications. *Memoir of the Geological Survey of Namibia*, **22**, 172-198.

Pickford, M., & Senut, B., 2016. The fossiliferous sands of Hexen Kessel, Sperrgebiet, Namibia. *Memoir of the Geological Survey of Namibia*, **22**, 199-208.

Pickford, M., Senut, B., Morales, J., & Sanchez, I., 2008. Fossiliferous Cainozoic Carbonates of the Northern Sperrgebiet. *Communications of the Geological Survey of Namibia*, **20**, 25-42.

Martin Pickford

Sediment Dynamics of the Namib Aeolian Erosion Basin and the Arid Zone Diamond Placers of the Northern Sperrgebiet, Namibia

Ian B. Corbett

8, Well Way, Hout Bay, Cape Town, 7806, South Africa
e-mail: <ian.corbett@knoco.co.za>

Abstract: The Namib Aeolian Erosion Basin to the south of the Namib Sand Sea presents a unique opportunity to use knowledge of diamond placer distribution to develop an understanding of arid zone sediment dynamics in one of the windiest places on Earth. This paper integrates knowledge of the sedimentary systems that characterise the Namib with a new structural dataset. Recent research has proven beyond doubt that this supposedly "passive" continental margin is subjected to periodic tectonic reactivation of old structures. The implications of this are examined in detail to provide a more comprehensive perspective of a system that has been influenced by structural movement on a local scale, as opposed to the entrenched view of epeirogenic uplift. As a result subtle interaction between tectonism and sediment transport pathways can be deduced.

The erosional architecture within the Namib Aeolian Erosion Basin provides some of the most dramatic examples of aeolian erosional landforms known on the planet that are sculpted in a variety of crystalline rock types. Many of the diamond placers occur within closed, endorheic basins distributed along the Atlantic coast of Namibia. Topographic inversion has created sub-basins in response to weathering and aeolian erosion. The sub-basins are as much as 120 m deep, and the floor of the Idatal basin is 2 mbsl. The geological structure has strongly influenced their development and they are coincidentally aligned parallel with the unimodal southerly windflow, which governs high-energy aeolian processes in the 20 km wide coastal tract.

Sand primarily enters the Namib aeolian system through the deflation of fine-grained sandy beaches in log-spiral bays which provide widely dispersed coastal point-sources. Deflated sand is transported through the erosional basin within wind-aligned, 1 to 2 km wide linear zones called aeolian transport corridors delineated by barchan dune trains. Southerly wind velocities frequently average 50 to 60 km/hr between October and March, and gust at 80 to 90 km/hr. At these velocities, saltating quartz grains exceeding -1.5 phi (2.5 mm) in diameter propagate reptation and creep transport of particles on impact with the bed. Experiments show that garnet (and hence diamond) between 0 and -2 phi (1 to 4 mm) in diameter are rapidly transported and sorted by aeolian processes according to size, density and shape. Heavy minerals transported with coarse-grained aeolian bedload are incorporated into a variety of aeolian bedforms of different scales.

These observations show that size-density-shape sorting of particles incorporated in migrating aeolian bedforms lead to the concentration of heavy minerals – possibly related to particle residence time at specific locations within the bedform. Aeolian transport of diamonds explains the northward-fining diamond dispersal pattern evident in endorheic sub-basins from the original prospecting data. Remarkable concentrations of diamonds were located within the aeolian erosion basin during exploration and mining operations. These can be explained by the presence of east-west oriented obstacles to aeolian bedload transport at a variety of scales oriented transverse to the dominant northbound bedload migration direction. The progressive segregation of diamonds resulting in placer formation at these sites can be accounted for by kinematic wave theory.

Although rainfall seldom exceeds 50 mm/year in the southern Namib deflation basin, ephemeral fluvial systems are instrumental in forming the diamond placers. Dendritic tributary networks at the northern end of endorheic basins feed trunk streams which flow south into ponded water bodies situated at base-level. Coarse-grained aeolian bedload, including diamonds, flooring endorheic basins which has been transported north by aeolian processes, is eroded by ephemeral streams and transported back to the south. "Aeolian" diamonds returned to the base-level of individual endorheic basins are reworked by aeolian processes, resulting in the concentration of the larger diamonds at the southern end of the endorheic basins.

Previous explanations of the formation of the diamond placers within endorheic basins invoked progressive deflation and surface-lowering of a pre-existing diamondiferous sediment pile. The integrated understanding that has developed subsequently, incorporates knowledge of the fluvial and marine (beach, nearshore and deep-water shelf) placers that earlier workers knew nothing of. The placers within the endorheic basins are now seen to be the result of aeolian bedload transport and dynamic interaction between the aeolian and ephemeral stream systems. Deflation has been responsible for the removal of fine-grained sediment produced by a variety of forms of weathering.

The extreme bimodality of the diamond population provides clear evidence that the destruction of raised palaeoshorelines (as well as those now submerged on the continental shelf) containing rich beach diamond placers introduced diamonds to both the aeolian and ephemeral stream systems. A new structural dataset is used to develop an alternative hypothesis to explain the presence of an onshore extension of the Orange Basin within the Namib Aeolian Erosion Basin.

Changes in coastal morphology resulting from sea level movement alter the frequency and spacing of beaches suitable for aeolian deflation. Consequently, the location of active aeolian transport corridors changes through time. Aeolian processes eroded diamonds from marine beaches influenced by arid zone weathering processes and progressively transported them northwards. On entry to endorheic basins within the main deflation basin, the diamonds are size-sorted. Diamonds of approximately 0.2 cts or less, being more frequently entrained and transported by aeolian bedload transport processes, migrate northwards into successive endorheic basins producing a series of progressively northward-fining diamond placers. The plinth at the south-western end of the Namib Sand Sea effectively acts as a barrier to the transport of coarse heavy minerals by aeolian creep and reptation. This resulted in the concentration of diamonds along the active plinth margin.

Mapping the location of inactive palaeo-yardangs together with the regional pattern of diamond dispersal throughout the aeolian erosion basin proves that the location of aeolian transport corridors has varied through time. Consequently the boundary conditions that determine the architecture of the Namib Sand Sea are shown to have varied. In particular, changes in the spatial location of the tract influenced by high-energy wind has varied in response to sea-level change together with the nature of sand sources and the volume of sediment available for deflation by the aeolian system. It is predicted that this would result in changes in the location of the active plinth of the sand sea. The active Elisabeth Bay – Kolmanskop-Charlottental placer domain may be an example of aeolian system response to transgression. It is suggested that features mapped at the southern end of the Namib Depositional Basin may provide evidence of aeolian system response to changing boundary conditions resulting from modification of the coastal morphology due to transgression.

The integration of a structural framework with data on the aeolian and alluvial sedimentary systems within the Sperrgebiet indicates that both systems have probably been influenced by reactivation tectonics. Regional mapping of aeolian transport pathways supplying sand to the Namib Depositional Basin provide evidence for subtle offsets in direction as well as variation in deposition across faults. There is also an indication that the gross morphology of the Namib Depositional Basin may also be influenced by reactivation tectonics. In particular the location of the present-day plinth directly above a major structural boundary suggests that the location of

deposition for the main Namib Sand Sea might have been controlled by the provision of accommodation space by movement along the fault. A number of spurs along the south-eastern margin of the present-day sand sea are also directly above, and aligned with, major faults mapped from a high-resolution aeromagnetic dataset. These faults are shown to have controlled the development of fault scarps from which major alluvial fan systems were generated – presumably also in response to reactivation tectonics.

Key Words: Namib Aeolian Erosion Basin, Sperrgebiet, Aeolian Bedload Dynamics, Diamond Placer, Sedimentology

To cite this paper: Corbett, I.B., 2016. Sediment Dynamics of the Namib Aeolian Erosion Basin and the Sedimentology of the Diamond Placers of the Northern Sperrgebiet, Namibia. *Memoir of the Geological Survey of Namibia,* **22**, 6-171.

Submitted August, 2016

Introduction

Diamond Placer Discovery

Diamonds were first discovered on the west coast of southern Africa at Graskop, inland of Lüderitz (Fig. 1) by a railway labourer named Zacharias Lewala during 1908. Lewala handed the stone to August Stauch, a bahnmeister responsible for ensuring that the railway line from the port of Lüderitz to the interior was kept clear of sand dunes.

When Professor Scheibe at Rhodes University confirmed that the stone was a diamond, the two men proceeded south through the inhospitable Namib Aeolian Erosion Basin (NAEB) pegging claims on behalf of the German Government. They reached the valley which Stauch later named Idatal, after his wife, in the dark. However, the concentration of diamonds on the stony desert floor was so great that they are reputed to have continued prospecting into the night, aided only by the light of the moon. The two men had not only located some of the richest gem diamond placers that are ever likely to be found, but had also initiated a search which would lead to the discovery of the world's greatest gem diamond placer system incorporating high-energy fluvial, marine and aeolian sub-systems. Mining operations subsequently endured for more than a century, with onshore production progressively being replaced by expansion of the deep-water offshore mining operation.

As geologists flocked to the region to verify the claims of vast diamond deposits it became clear that the hostile southerly wind system which sweeps through this narrow coastal region had strongly influenced the formation of the diamond deposits (Lotz, 1909; Merensky 1909; Krause 1910; Wagner 1910, 1914).

The observations of numerous researchers were published collectively during 1926 in an outstanding treatise entitled "Die Diamantenwüste SüdwestAfrikas" which was edited by Erich Kaiser. Many of the processes governing the concentration of diamonds within the Namib Aeolian Erosion Basin were described by Kaiser, Beetz and other contributors to this work. Although the significance of the interaction between aeolian and ephemeral stream processes was identified, the dynamic nature of the pavements covered by small pebble gravels that contain the placers was not fully appreciated at the time. The progressive removal of smaller particles by wind action (classically termed aeolian deflation) was therefore identified as the major process concentrating diamonds within the region. Whilst the deflation process has undoubtedly contributed to increasing the diamond content of the residual sediment, sustained diamond transport through the region is required to explain the:-

- Spatial geometry of the diamond placers;
- Extraordinarily high diamond concentrations which made the region famous;
- Remarkably well-sorted nature of the diamond deposits.

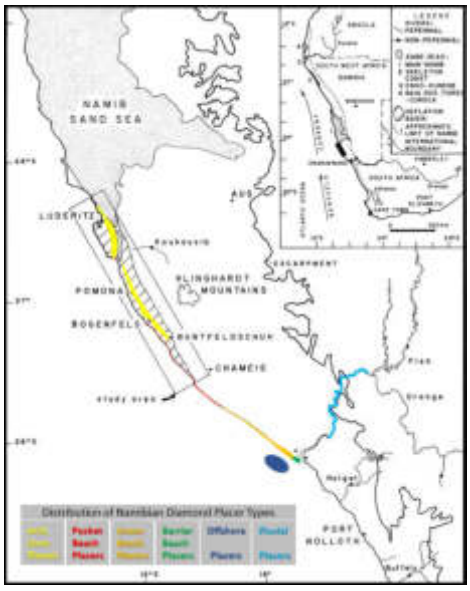

Figure 1. Map showing the spatial distribution of placer types in southern Namibia comprising the Diamond Placer System. A number of theses and dissertations were written by geologists working for CDM (Pty) Ltd / Namdeb (Pty) Ltd on different aspects of the placer system. The sedimentology of the fluvial placers was researched by Fowler (1976; 1982) and Jacob (2005), the sedimentology of the barrier beach placers was studied by Spaggiari (2011), the wave platforms of the linear beaches were studied by Jacob (2001), the pocket beach at Chameis was researched by Apollus (1995), shallow marine offshore diamond placers were studied by Oelofsen (2008) and the sedimentology of the arid zone placers was studied by Corbett (1989). A number of papers arising from this, and other research have been published. Ian McMillan has published extensively on the micropalaeontology of shelf sequences and Martin Pickford and Brigitte Senut and their co-workers on vertebrate palaeontology. John Ward and Brian Bluck authored numerous papers with various co-workers on different sedimentological aspects of the placer system.

Background to this Paper

The observations included in this paper formed the basis of a PhD thesis by the author that was completed in 1989.

The research has been significantly updated and the original material has been reviewed extensively in the context of the numerous unpublished theses and publications that have emerged through studies supported by Namdeb Pty Ltd and De Beers. New literature on aeolian transport and sedimentological research in other desert regions has also been sourced.

The original mapping relied on aerial photography. I am indebted to Dr Jürgen Jacob at Namdeb (Pty) Ltd for generously allowing access to a remarkable high-resolution proprietary Airborne Laser Scanner (ALS) dataset that covers virtually the entire NAEB, as well as high resolution aeromagnetic data and diamond prospecting data.

Against the ALS backdrop it has been possible for the first time to build a GIS-dataset to integrate many different sources of published data and information as well as unpublished reports.

Together with developments in many aspects of geological thinking this presents a fundamentally different perspective with which not only to examine the development and dynamics of the Namib aeolian system, but also to critically reappraise apparent contradictions highlighted by previous research.

In particular, since the late 1980s the region discussed in this paper has yielded significant quantities of unusually detailed biostratigraphic information – primarily through the research of Ian McMillan and John Pether in the offshore and Martin Pickford and Brigitte Senut together with their co-workers of the Namibia Palaeontology Expedition.

These studies not only shed new light on faunas and palaeoenvironments, but they also provide important new insights into the post-rift tectonic stability of this margin. This new knowledge raises the possibility that an improved level of understanding of how the onshore-offshore sedimentary systems have interacted. This requires a more holistic approach that not only takes cognisance of sediment supply, climate change and eustatic sea-level movement, but also of tectonic activity.

Consequently, a new perspective on the geomorphic evolution and erosional architecture of the region is presented based on evidence that post-break-up tectonics and volcanic activity have played (and in the case of tectonics continue to play) an important role in determining both the development and preservation of sedimentary sequences in the NAEB.

At a more detailed scale, the ALS data coverage enables a new understanding of the spatial distribution of bedforms produced by aeolian bedload transport within the NAEB to be developed. These observations further refine our knowledge of the pattern of aeolian transport through the NAEB, and in particular the nature of coarse-grained aeolian bedload transport and deposition associated with Aeolian Transport Corridors (ATC). These observations are used to examine the role that aeolian bedload transport played in the development of extremely high-grade diamond placers in this hyper-arid zone.

The Namib Aeolian Erosion Basin

The Namib Aeolian Erosion Basin (NAEB) forms a 150 km long coastal belt ranging from 0 to 15 km wide between 26°'30'S and 27°40'S on the Atlantic coast of Namibia (Figs 1 and 4). It is located in the hyper-arid core between 18°S to 29°S (Meigs, 1966) of a coastal desert that extends from the Olifants River in South Africa to the Carunjamba River in the Moçamedes District of Angola.

The NAEB lies within a winter rainfall region and the annual rainfall is less than 10 mm for 50 percent of the available records between 15°S and 33°S (van Zinderen

Bakker, 1975). Rainfall, when it occurs, is ephemeral and short-lived. The advective Benguela Fog has been shown to be a more reliable moisture source (Pietruszka & Seely 1985) that plays an important role geologically (e.g. Eckardt *et al.* 2001; Goudie *et al.* 2002) and for sustaining the fauna and flora that exist there.

The NAEB extends from the first log-spiral bay at Chameis Bay situated approximately 100 km north of the Orange River. It then broadens downwind to form a wedge-shaped tract about 20 km in width with the western margin provided by the high-energy Atlantic coastline.

The region has enjoyed notoriety for its spectacular aeolian erosion features which bear testimony to the extreme energy of the aeolian system which has led to the formation of some of the best examples of hard-rock yardangs known on Earth (Corbett, 1989; Goudie, 2007) and possibly for the antiquity of the aeolian system.

The Wind Regime

The surface wind regime of the Namib Desert is distinctly zonal (Lancaster, 1985). The highest-energy winds occur within a narrow coastal tract approximately 20 km in width in which the NAEB is wholly located. This coastal tract is dominated by unimodal high-energy south-south-westerly to south-south-easterly surface winds (Corbett 1989; Corbett, 1993), and it has been described as one of the windiest places on Earth (Rogers *et al*. 1990). This strongly influences the aeolian landscape.

The annual peak in the unimodal southerly wind regime (Fig. 2), which is the primary driver of the aeolian system within the NAEB, occurs seasonally between October and March. Winds during this time are strongly diurnal and gusts of 80 km/hr to 100 km/hr commonly occur on a daily basis between 13h00 to 16h00.

Periodically, between April and August, rapid high-energy northerly wind reversals occur.

The inland wind regime increases in variability towards the east, becoming bimodal and then trimodal as the influence of the South Atlantic anticyclone diminishes.

The wind regime thus shows a broad similarity with that described for the Namib Depositional Basin to the north (Fryberger & Dean, 1979; Ward, 1984)

The topics of aeolian dust in relation to aeolian erosion and abrasion and aerosols in relation to the development of duricrusts have received much attention since the original research was completed.

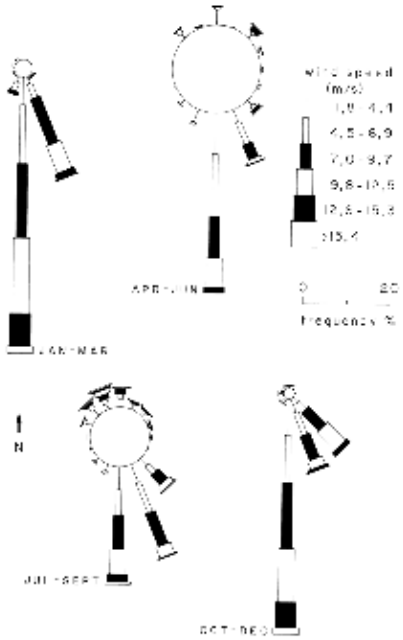

Figure 2. Wind roses summarising the seasonal variation in surface wind direction at Bogenfels during 1987.

A number of hot, dry east winds were experienced during the years when the author lived at Bogenfels and Pomona. In some instances these winds were observed to introduce very fine red sand and dust onto the NAEB but these winds are usually of short duration (1 to 2 days). On one occasion an east wind was seen to come in towards the coast before veering upwards along an almost vertical boundary some thousands of metres before streaming over the NAEB to form elongate plumes of red fine-grained sand and dust extending out to sea that are visible from space (Eckardt *et al*. 2001). In the Central Namib dust plume events such as these have been observed to occur when hydrogen sulphide has been erupting through the nearshore water column (Scott & Schmaltz, 2010).

The Pattern of Sandflow and the Definition of Aeolian Transport Corridors

The NAEB is bordered by the high-energy Atlantic coastline which is characterised by widely-spaced, steep beaches interspersed along a largely rocky shoreline.

The steep, coarse-grained beaches are composed predominantly of granules and small pebbles. Sandy beaches, which act as point sources for sand supply to the Namib Aeolian System (Fig. 4) principally occur as log-spiral embayments or south-facing re-entrant bays (Corbett, 1993).

Figure 3. Oblique aerial view to the south-south east showing dome dunes, proto-barchans and barchans immediately downwind of the sand point-source within the Baker's Bay log-spiral embayment.

Sandflow in the form of aeolian saltation plays a crucial role in both aeolian erosion and the transport of coarser bedload particles through aeolian reptation and creep transport processes. Sand traps were deployed at Bogenfels to investigate the pattern of sandflow through the area to aid understanding of the regional pattern throughout the NAEB.

Trains of large barchan dunes that are up to 30 m high migrate through the NAEB at rates of 30 m to 50 m/year (Kaiser, 1926a; Corbett, 1989, 1993). They have recently been studied in some detail and have been compared to those identified on Mars by Bourke & Goudie (2009) whose classification system was used to map the trains covered by ALS data for this study. The barchan dune trains form downwind of the point sand sources along the coast. Because initial results from the first sand trap deployed to the south of Bogenfels were disappointing, additional traps were deployed to the east closer to the barchan dune train that is maintained by beach deflation within the log-spiral embayment at Baker's Bay (Fig. 4). The sand traps were designed to measure the variation in the sandflow rate within the main saltation layer as well as the vertical variation in sandflow over a height of 1.83 m (Fig. 5). The most complete data set was collected during 1987. A major sand storm occurred on 10 February in that year. Sandflow was found to be orders of magnitude greater within 0.5 km of the barchan dune train. The analysis of the trapped sediment also provided further evidence that sand transport within a narrow zone on either side of barchan dune trains creates optimal conditions for coarse bedload transport by aeolian processes. This conclusion was reached because not only was the sediment flux greatest at site C but also the grain size of the sandflow was consistently coarser than at either site B or A (Fig. 6).

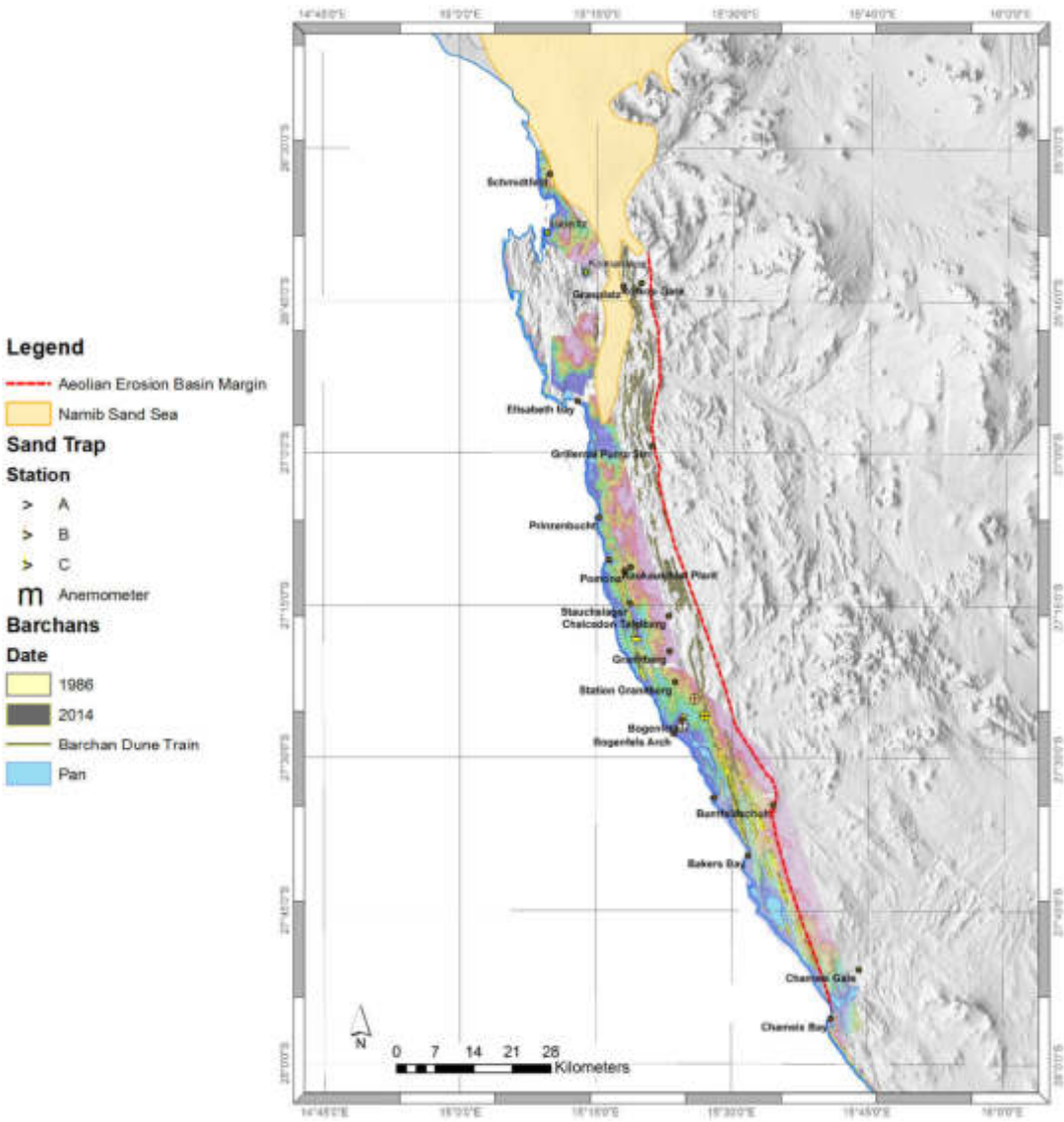

Figure 4. Map summarising the present-day pattern of sandflow through the Namib Aeolian Erosion Basin and the southern part of the Namib Depositional Basin. The coloured DEM background within the NAEB shows the distribution of high-resolution Airborne Laser Scanner (ALS) and photographic coverage used for this study. Two anemometer stations were used during the original study. The anemometer at Bogenfels provided higher resolution data whilst the anemometer at Idatal provided averaging data only. The location of the sand trap stations at Bogenfels that were used to measure sandflow are also shown.

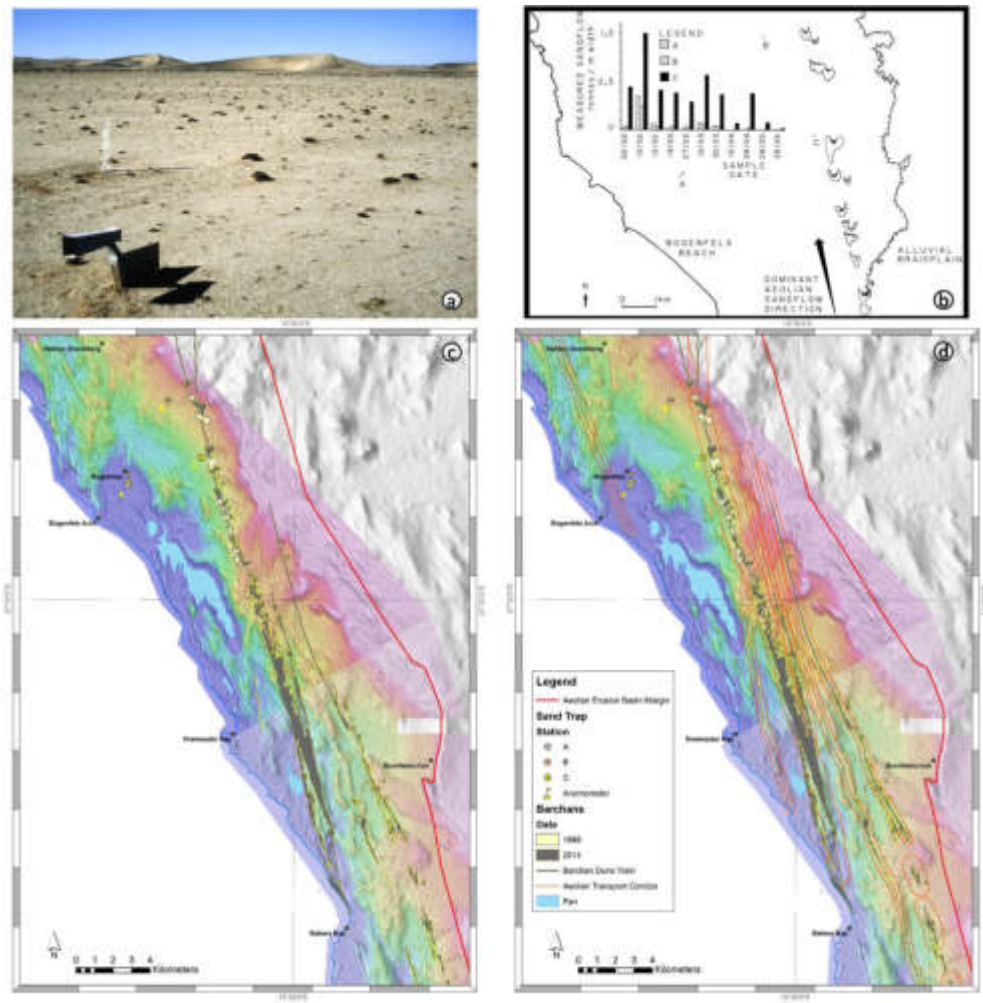

Figure 5. a) Sand trap site C showing two of the different sand traps used to monitor sandflow and the vertical distribution of saltation load driven by southerly winds. b) Variation in sandflow across the area monitored show significantly higher sandflow in close proximity to the Baker's Bay dune train. c) Map showing the monitoring sites in relation to the Baker's Bay barchan dune train. Sand trap site C is about 26 km downwind of the sand source at Baker's Bay. d) Interpreted sandflow pattern based on the sand trap results showing the detailed distribution of Aeolian Transport Corridors within the part of the Namib Aeolian Erosion Basin produced by detailed mapping of the ALS data which provides the backdrop to maps c and d.

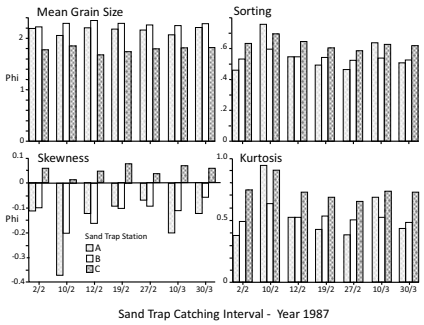

Figure 6. Characteristics of some of the saltation load trapped at sites A, B and C between early February and the end of March 1987.

Sand from site C was also less sorted and it was the only site that showed positive skewness.

These observations led to the definition of Aeolian Transport Corridors (ATC) along which aeolian bedload transport should be especially effective on the basis that high saltation loads of coarse sand should provide optimal conditions to drive aeolian bedload transport processes.

The sand trap records showed that in a sand-starved, strongly unimodal aeolian regime such as exists in the NAEB, sandflow tends to be regulated by the progressive storage of sand at stable sites of deposition, such as aeolian current shadows from micro- to macro-scales within the system. Sand from these storage sites is rapidly entrained during northerly wind reversals, which deposit the sand in unstable sites with respect to the southerly wind regime. The importance of sand storage in stone pavements has recently been confirmed through innovative field-based wind tunnel experiments by D. Zhang *et al*. (2014). Rapid switching in aeolian transport direction destabilises the sandflow system and releases large quantities of sand from southerly wind storage sites. When southerly winds resume it thus results in the rapid entrainment of unusually large volumes of sand into saltation. These peaks in sandflow cannot be achieved through the deflation of isolated point-sources provided by beaches. One such event occurred on 10 February 1987, which accounted for the sudden change in the availability of sand for transport – it was dramatic to witness.

Aeolian Transport Corridors as Pathways for Accelerated Aeolian Bedload Transport

Two aeolian bedload transport processes have been identified:

- Reptation : which produces a low hopping motion of grains over short distances on the impact of a saltating particle with a loose bed (Anderson & Haff, 1988) and
- Creep : which results in coarse particles rolling on the loose bed following the impact of a saltating grain.

Observation of grains trapped in cracks in wooden telegraph poles showed that coarse grains (3 to 5 mm diameter) were trapped at heights between 3 m to 4 m above the ground surface. Based on simple experiments holding plastic bags at head height during sand storms it became clear that the sand trap catching the saltation load to a height of 47 cm above the bed at site C did not properly reflect the size frequency distribution of the saltation load migrating across the stone pavement at this locality.

A compartmentalised sand trap was then built to trap saltating grains between 0 to 16 cm, 16 to 50 cm, 50 to 100 cm, 100 to 140 cm and 140 to 183 cm above the bed.

Some interesting results were produced despite the limited time that the trap was deployed for (Fig. 7). It was found that 40% to 50% of the saltation load travelled in the lowest 16 cm above the stone pavement surface. A further 30% of the sandflow was trapped between 16 to 50 cm above the bed and 20% was trapped 50 to 100 cm above the bed.

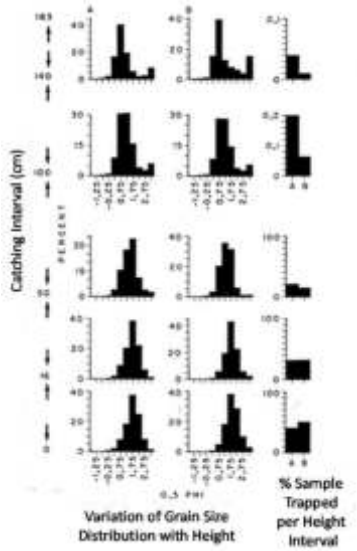

Figure 7. Graphs illustrating the variation in the quantity and grain size of saltation load being transported over the stone pavement at sand trap site C. Dataset "A" is for a major wind reversal on 18 July, 1987. Dataset "B" shows the sandflow transported by southerly winds between 20 July and 22 September 1987.

Above this height the quantity of sediment trapped declined rapidly. The coarsest saltation load was trapped between 140 cm to 183 cm above the stone pavement – the largest single grain was almost 2.8 mm in diameter and weighed 0.042 gm. Larger grains might have been recorded had this trap been used over a longer period – as grains of 5 mm diameter were caught in plastic bags held between 2.5 and 3 m above the stone pavement.

Interestingly, results showed that the percentage of particles finer than 3 phi also increased in the highest compartment, indicating that the suspended load probably also travels above the main saltation layer within the first metre above the bed.

It has been shown that saltating grains typically attain 50% to 70% of the free stream wind velocity (Greeley *et al.* 1983). Within the NAEB free stream wind velocities of 60 to 90 km/hr commonly occur. As a result saltating grains strike the bed with considerable force. Even though there may be comparatively few such grains at any one time, they exert an important influence on the modification of the particle configuration on the bed where they impact. It seems reasonable to predict that the frequency of what are effectively ballistic impacts should be greatest on the sediment surface beneath Aeolian Transport Corridors. As a stochastic process, the probability of bedload entrainment along these relatively narrow pathways should therefore be greater than it is in the areas between them, resulting in accelerated transport with respect to areas outside these pathways. When Aeolian Transport Corridors traverse stone pavement surfaces, saltating grains impacting larger clasts (immobile roughness elements) should follow higher particle trajectories into the windstream creating optimal conditions for the transport of coarse bedload, including diamonds. In the NAEB, based on field observations, coarse bedload includes quartz particles of at least 12 mm diameter. Figure 8 presents a detailed overview of the spatial distribution of the currently active Aeolian Transport Corridors through the NAEB.

Before describing the transport of coarse bedload by aeolian processes and discussing arid zone process interaction in relation to diamond placer formation it is important to understand the erosional architecture of the NAEB. This requires an appreciation of the structural context in which the NAEB occurs.

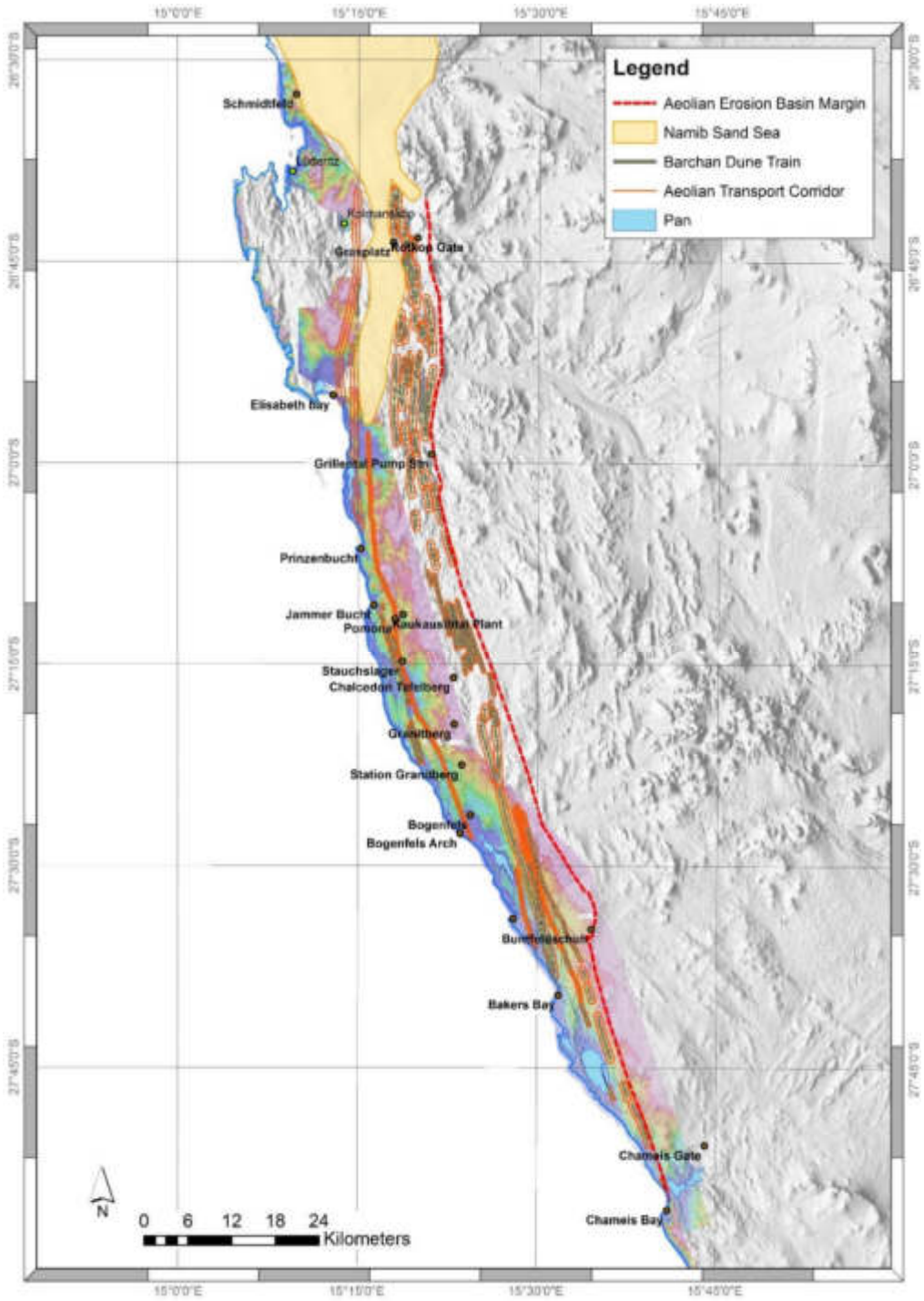

Figure 8. Map showing the distribution of Aeolian Transport Corridors through the Namib Aeolian Erosion Basin which currently maintain the Namib Sand Sea. Note that the majority of the currently active ATCs are located to the east of the area covered by ALS data in which the arid zone diamond placer deposits were located.

The Structural Setting of the Namib Aeolian Erosion Basin

A summary of the main structures within the region is shown in Fig. 9.

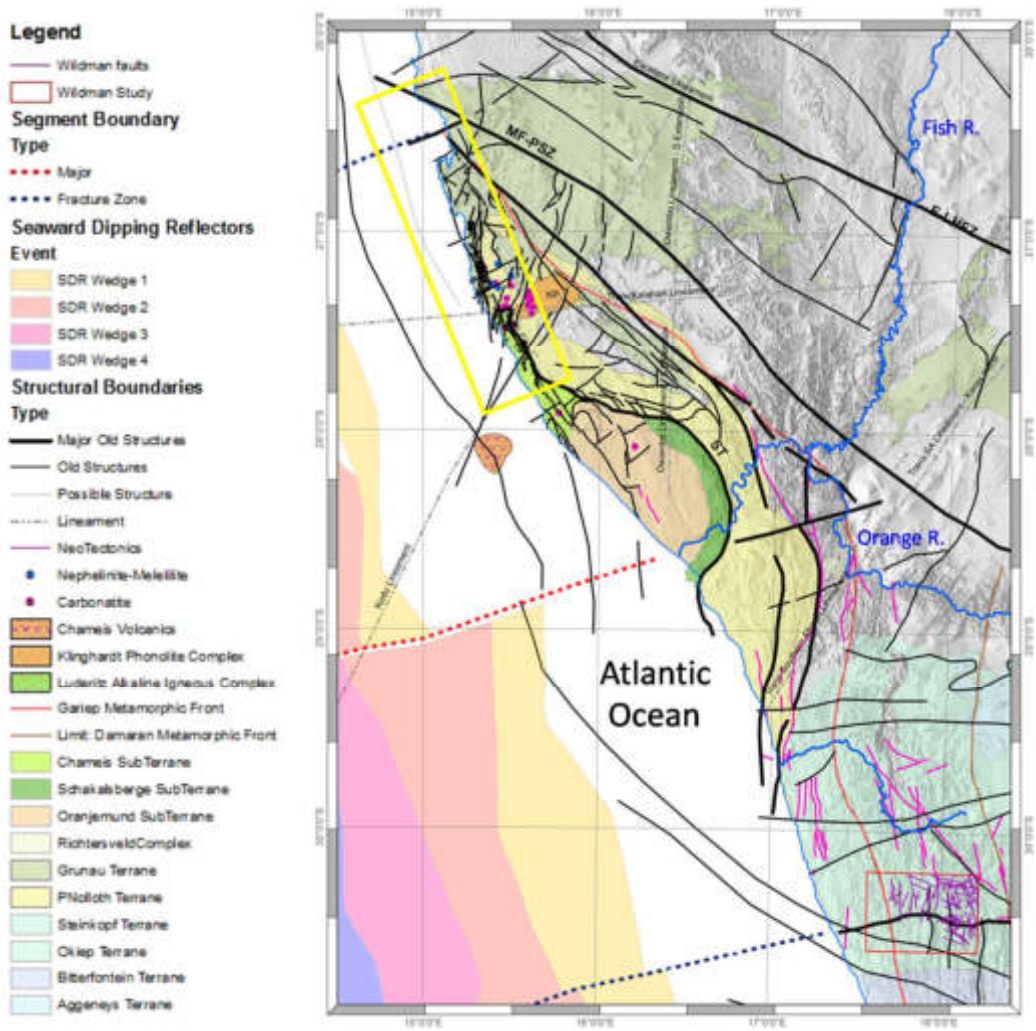

Figure 9. The structural setting of the Namib Aeolian Deflation Basin (study area shown by yellow rectangle). The major structural features and Namaqua Metamorphic terranes were compiled from Frimmel (2000a, 2000b), Corner (2008) and (Colliston *et al*. 2012). ST= Schakalsberg Thrust, MF-PSZ Marshall Fork – Pofadder Shear Zone, E-LHEZ = Excelsior-H Lineament. Additional structural detail has been added through mapping of regional gravity and magnetic data and a more detailed TMI image for southern Namibia (provided by Namdeb Pty Ltd) for this study as well as from Wildman (2015) and (Wildman *et al*. 2015). The offshore segment boundaries and seaward dipping reflectors are from Koopmann *et al.* (2014). Volcanics offshore Chameis were mapped by Mike Shaw (pers. comm. 2006). Evidence of neotectonic activity has been compiled from numerous sources including Borg (2003) Brandt *et al*. (2005) and Viola *et al*. (2005, 2012) and through involvement in numerous exploration programmes for De Beers.

The major structures define a number of tectonic domains at a sub-regional scale and a number of prominent structural trends can be identified.

When the original research was undertaken the possibility that local tectonics could be influencing the sedimentary system responsible for the development of the diamond placers was largely excluded from the geological model. Climate change was seen to be the primary driver e.g. Ward & Corbett (1990) operating on the margin. Any thinking on the possibility of a tectonic influence was dominated by proponents of regional scale events linked to epeirogenic events (e.g. Partridge & Maud, 1987; Burke & Gunnell, 2008) which built on the earlier concept of the African Surface proposed by King (1951). Post-rifting, the margin was

therefore deemed to be passively quiescent. This concept is progressively being challenged.

One of the more interesting developments in structural geology has been the recognition in oil and gas exploration that structural segmentation of margins related to rift development plays an important role in controlling the distribution of economic oil and gas reservoirs. The conjugate Atlantic margin of Brazil is one of the areas in which this thinking has evolved (Cobbold *et al*. 2001; Cogné *et al*. 2011; Meisling *et al*. 2001).

It is intriguing to speculate on whether similar concepts might be applied to the diamond placer mineral system on the southwestern margin of Africa. Investigation of this required the compilation of a large structural GIS dataset which has involved the integration of information from many disparate sources. A regional map by Corner (2008) has been invaluable. It has been supplemented by the interpretation of regional gravity and magnetic datasets and local-scale proprietary data and information.

Offsets in the seaward dipping reflectors together with the distribution of volcanic activity along the South African and Namibian margins (Koopmann *et al*. 2014) confirm the presence of prominent segment boundaries, some of which were previously interpreted to be transfer zones along the Namibian margin (Clemson *et al*. 1997). Two of the major boundaries identified bound the region in southern Namibia in which the diamond placers are located.

Faults affected by neotectonic activity demarcate areas in which evidence for the reactivation of old structures has been recognised. In southern Namibia evidence of neotectonic activity was recorded in the walls of the open pit at the Skorpion Mine near Rosh Pinah (Borg *et al*. 2003). These observations confirm the likelihood that reactivation of Gariep structures extends across the Orange River at several points along its course. It is probable that the reactivation of old structures influenced the course of the Orange River and consequently, the development of the diamond placers in the lower Orange Valley. Based on the conclusion of Mvondo *et al*. (2011) in terms of the development of the Fish River graben system, the faults trending SSW-NNE were probably active in the Late Palaeocene – Early Eocene.

Based on this study, a linear feature to the north of Oranjemund at about 90 masl may provide further evidence of neotectonic movement.

Reviewing the history of exploration projects along the west coast within the context of a margin that has remained tectonically active since continental break-up has enabled new insights to evolve leading to the realisation that striking similarities exist between the south-eastern Brazilian margin and the Namaqua-Namibian margin in terms of the reactivation of old structures (especially those related to the Gariep orogeny) and the effects these have had on sediment transport and deposition in southern Namibia.

The Erosional Architecture of the Namib Aeolian Erosion Basin

Kaiser (1926a) recognised two principal geomorphic domains within the "Sperrgebiet". Aided by the structural dataset presented here and a regional bedrock dataset (Fig. 10a) that was kindly provided by Hartwig Frimmel the region has been subdivided into a number of different geomorphic domains (Fig. 9).

Kaiser (1926a) identified two geo-morphologic domains:-

- The Plain Namib – the region east of the NAEB characterised by extensive sandy plains and isolated mountainous areas;
- The Trough Namib – The main region of the NAEB containing diamond placer deposits characterised by elongate, narrow primarily endorheic valley systems oriented broadly SSE to NNW.

The Plain Namib lies beyond the eastern boundary of the NAEB, and is not included in the scope of this paper.

Kaiser's (1926a) Trough Namib represents an important domain – both in terms of understanding the erosional architecture of the NAEB and the development of the diamond placer deposits that it contains.

Additional domains have been identified through this study (Fig. 10b). Their distribution is primarily controlled by a combination of geological structure and bedrock lithology. The primary process is provided by the pattern of sandflow through the NAEB which controls the pathways along which aeolian erosion due to abrasion by saltating particles is most effective. The other process that strongly influences the macro-scale erosional architecture is provided by ephemeral streams and pans, many of which become saline. Surface water run-off after rare rain events together with precipitation from the Benguela Fog promotes salt weathering, which renders surficial material loosened by salt crusts susceptible to aeolian abrasion and deflation.

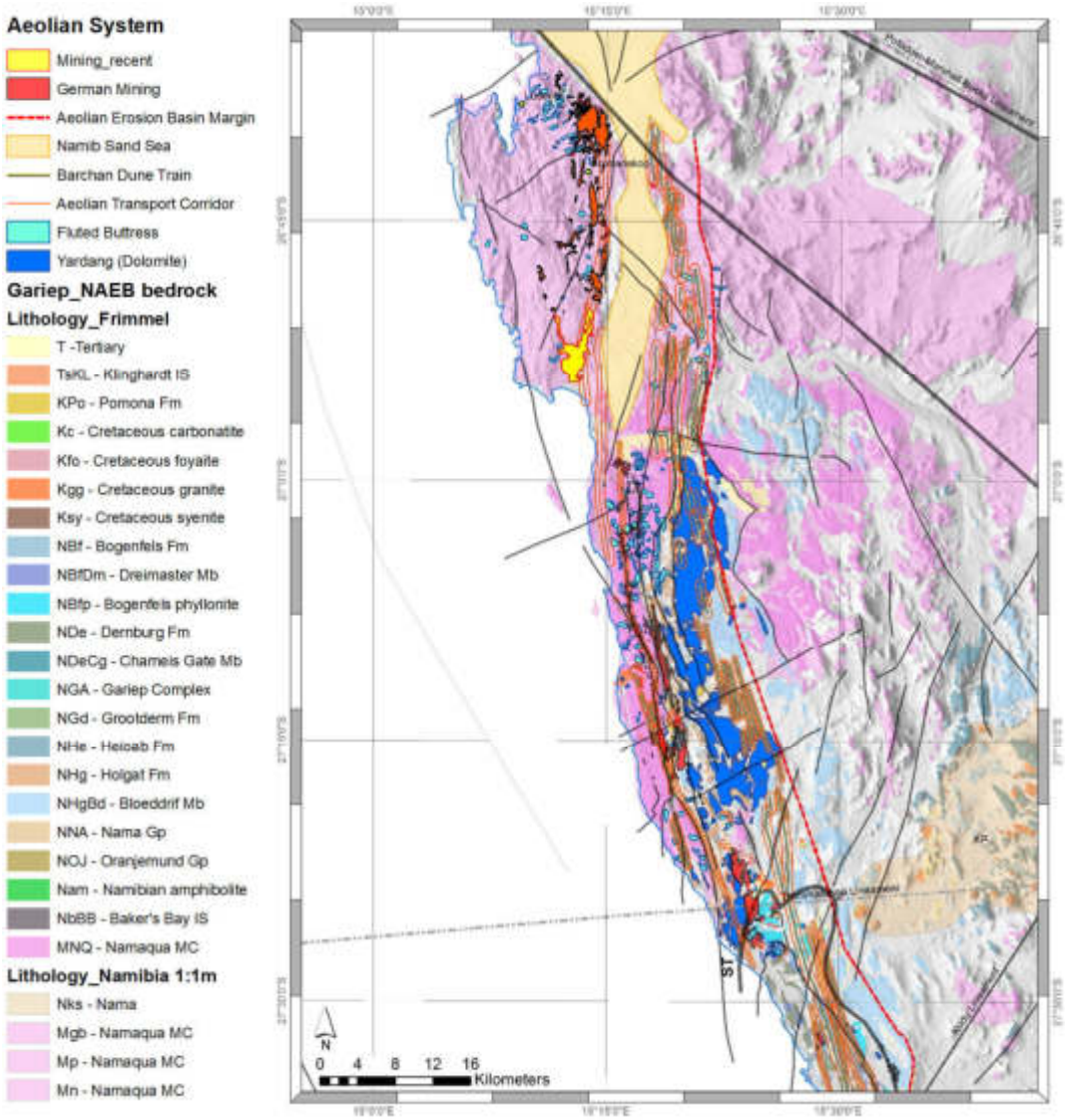

Figure 10a. Map showing the structure and bedrock geology between Dreimaster Bay and Marshall Rocks north of Lüderitz with the present-day sandflow along Aeolian Transport Corridors shown together with areas in which mining has taken place.

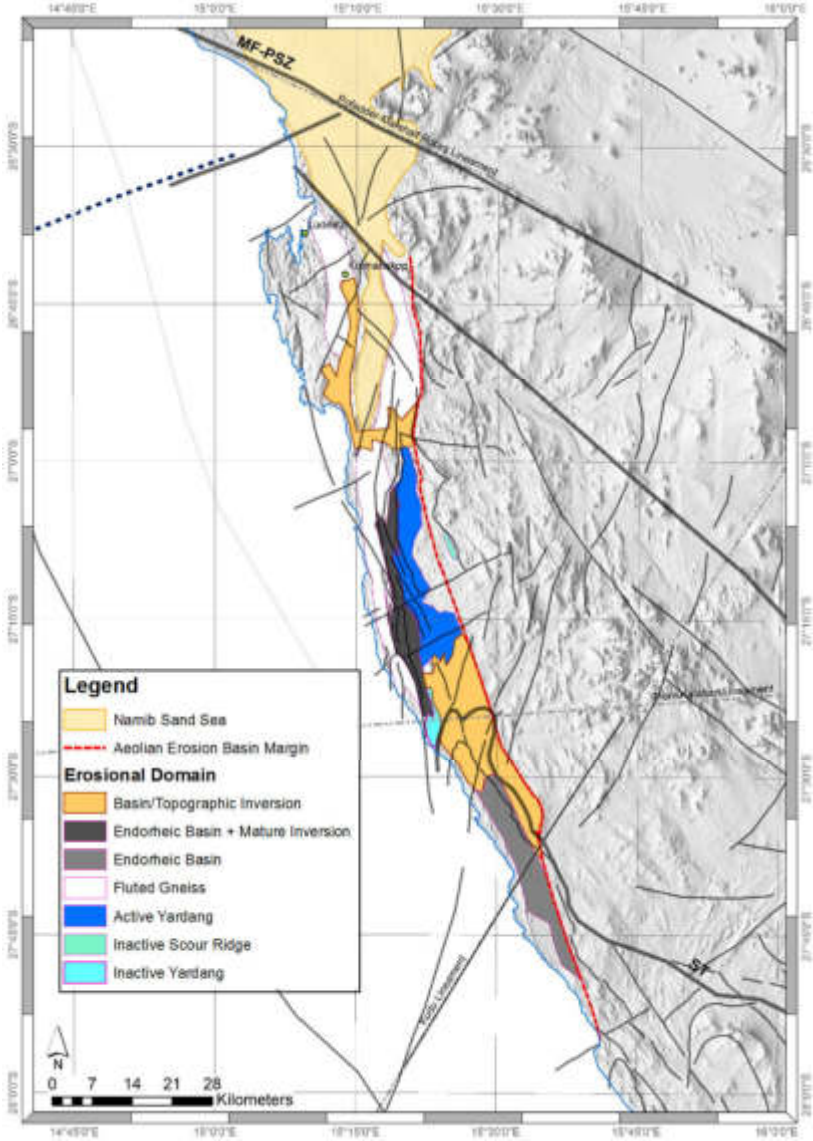

Figure 10b. Distribution of the macro-erosional domains of the Namib Aeolian Erosion Basin bordered to the east by Kaiser's (1926a) "Plain Namib". Kaiser's (1926a) Trough Namib has been subdivided to reflect the spatial distribution of key features of the aeolian landscape based on current knowledge. Between Buntfeldschuh and Bogenfels-Granitberg active Basin / Topographic Inversion is currently taking place. The main Trough Namib located between Granitberg and Grillental also represents a mature domain of Basin / Topographic Inversion. Two domains characterised by dolomite yardangs were identified by Corbett (1989). The Active Yardang Domain in the east lies within the path of currently active Aeolian Transport Corridors. The southwestern Inactive Yardang Domain lies outside the present-day distribution of Aeolian Transport Corridors. Analysis of a high resolution DEM created from the ALS dataset led to definition of another domain termed "Fluted Gneiss". This domain shows widespread evidence of aeolian erosion that has created large-scale fluting – especially along the south-facing slopes/buttresses of gneissic hills that show aeolian modification and streamlining without attaining the classic yardang form. A northern domain characterised by Basin/Topographic inversion is recognised based on the exhumation of Lower Miocene alluvial sequences infilling depressions in the gneiss landscape.

Kaiser (1926a) chose the term "Trough Namib" to refer to the coastal tract characterised by elongate, sub-parallel, narrow valleys which are oriented almost parallel to the prevailing unimodal southerly wind regime.

The structural trends mapped from the ALS and geophysical data confirm that the orientation of these features is controlled by a combination of structure and variation in bedrock lithology. In many instances the valleys have no exit to the coast, so they form classic endorheic basins (Fig. 11) in which alluvial systems form ponded water-bodies at their base-level after rain. These basins played a critical role in the development of some of the main diamond placers within the NAEB.

Two main areas of the Endorheic Basin Domain are present to the south and north of Bogenfels:

- Chameis - Fröhe Hoffnüng,
- Daheimtal - Pomona-Grillental.

In the south, the Chameis-Fröhe Hoffnüng Endorheic Basin Domain is situated within the area bounded by the toe of the Schakalsberge Thrust, whilst the bedrock lithologies form part of the Chameis Sub-Terrane of the Gariep Metamorphic Complex. The basins within this area are smaller than those in the Daheimtal-Pomona-Grillental area – possibly because the volcano-clastic metasediments in which they are eroded are prone to salt weathering.

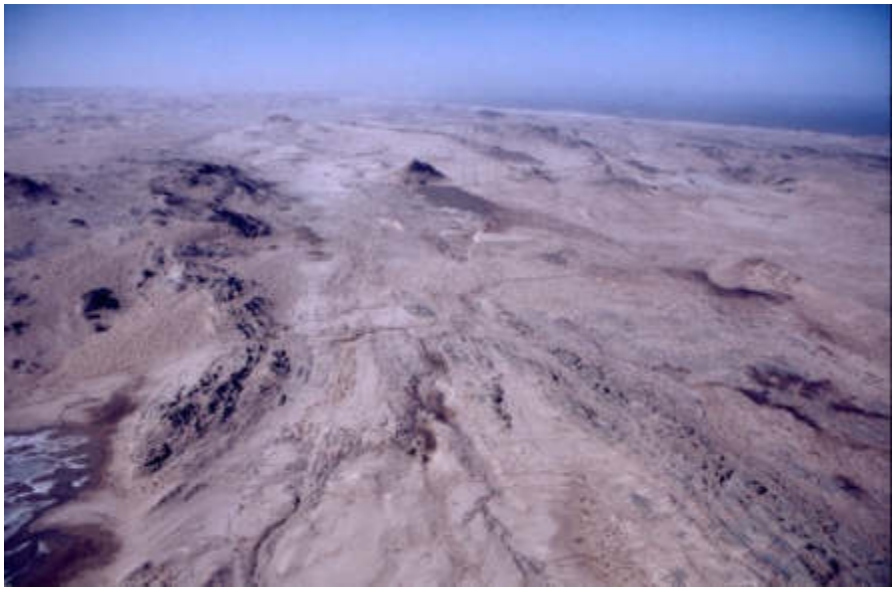

Figure 11. Aerial view south down the Fröhe Hoffnüng endorheic basin in which some of the southernmost diamond placer mining took place. A ponded water body in front of the dark hill in the middle distance marks the base-level after a rainstorm.

Lithologies within the northern domain are not as affected by salt weathering and perhaps due to uplift related to carbonatite volcanism (Pickford, 2015) the basins are far larger reaching depths of 120 m in the case of the Idatal, which is the only endorheic basin within the NAEB with a base-level below sea-level. Based on the scale of the basins together with the nature of the diamond placers that the Idatal and its associated valley systems contained (see later sections), it is implied that this area of the NAEB has been subjected to the most intense topographic inversion resulting in a mature aeolian erosion landscape through

the combined effects of aeolian abrasion and deflation coupled with salt weathering.

The northern Endorheic Basin Domain contains a number of important duricrust localities which form “tafelberg” (Fig. 12).

Figure 12. Oblique aerial view to the SSE across the eastern edge of the northern Endorheic Basin Domain – a number of smaller tafelberge provide evidence of advanced topographic inversion. One of the main Active Yardang fields can be seen in the left middle distance.

Detailed study by the Namibia Palaeontology Expedition has resulted in revision of the stratigraphic relationships of the different duricrusts and their differentiation from sediments produced by a silicification event (Sperrgebiet Siliceous Suite) linked to widespread carbonatite / phonolite volcanism (Pickford, 2015). Onshore and offshore biostratigraphic ages for this event consistently place it in the mid-Lutetian-Bartonian stage of the Eocene. These new insights into the correct stratigraphic relationships between the so-called ‘silcretes’ and the later calcretes (calc-crusts) have implications for interpreting the erosional history. The silcretes, which occur well below the escarpment within the NAEB were previously considered to indicate the presence of the African Surface of King by Partridge & Maud (1987). However, this concept was challenged by Corbett (1989) who interpreted them as valley remnants left high above the surrounding depressions due to topographic inversion. Interestingly a number of the tafelberge remnants capped by what Miller (2008) called the Kätchen Plateau Formation appear to be associated with faults mapped during this study. In Namaqualand a similar relationship has emerged from detailed mapping of the Vaalputs area (Brandt *et al*. 2003, 2005). It is thus probable that the silcretes in the NAEB do not represent the end-Cretaceous land surface but owe their origin to groundwater movement along faults which, in the case of the NAEB, may well have acted as conduits for migrating hydrothermal fluids during phases of volcanic activity which is now known to have widely influenced the NAEB (Pickford, 2015).

The endorheic basins are well-developed in the southern part of this domain in which relief is more subdued in its northern parts Several valley features have been mapped in the area which are discussed in more detail in the section that reviews the influence of structure on the development of alluvial systems within the Sperrgebiet. The marine sequences preserved within the region are also discussed in a later section on the structural influence of onshore extensions to marine basins.

In terms of the aeolian erosional architecture of the NAEB, this domain is actively undergoing extensive basin and topographic inversion which is a classic characteristic of areas subject to high levels of aeolian abrasion and deflation. The topographic inversion is most readily identified in those areas in which the Gemsboktal Conglomerates provide extensive stone pavement surfaces (Fig. 13) due to the development of the Namib I Calc-crust, sensu Pickford (2015). The pattern of topographic inversion displayed tells a story, revealing that inversion has advanced further in the west than it has in the east along the boundary with the Plain Namib.

Figure 13. Oblique aerial **v**iew towards the north east across the Bogenfels Pan backed by the Gemsboktal Conglomerates which provide evidence of topographic inversion. On the horizon the subdued topography of Kaiser's (1926a) "Plain Namib" stretches into the distance.

Although inversion is less advanced in the east, ALS data shows that surfaces are progressively being actively lowered through aeolian erosion and arid zone weathering processes. This is not surprising as they lie beneath a concentration of the most active Aeolian Transport Corridors which currently operate within the NAEB.

Grillental-Kolmanskop Basin / Topographic Inversion Domain

A second Basin /Topographic Inversion domain begins in the Grillental (Fig. 14) immediately east of Elisabeth Bay and extends northwards into the Kolmanskop area.

Figure 14. Oblique aerial view due west down the Grillental showing active topographic inversion. Barchan dune trains mark the path of three parallel Aeolian Transport Corridors. The two bright white areas in the foreground and middle distance consist of a fluvial bar facies within the Burdigalian sequence. The tongue of dark coloured sediment extending diagonally from the bottom right corner towards the top left of the picture is the Tortonian Gemsboktal Conglomerate. The bright area in the top left is Wüstenkönig – a Pleistocene sequence of interbedded aeolian dune and coastal pan sediments.

Within this domain, depressions infilled by fine-grained green clays of the Elisabeth Bay Formation have produced an astonishing array of palaeontological discoveries – first in the 1900s which were recorded in Kaiser (1926a), and subsequently by the Namibia Palaeontology Expedition which has worked extensively on them (Pickford 2000; Pickford *et al*. 2008, 2013) and which has correlated them to the Burdigalian.

In the vicinity of Fiskus Pan, a Pliocene precursor to the present-day Namib Sand Sea is also being eroded as part of the exhumation and inversion process.

Active / Inactive Yardang Domains

Corbett (1989) showed that the location of the Aeolian Transport Corridors, along which saltation flux is at its highest levels, change through time. These changes are identifiable on the basis of yardang distribution in particular.

The main yardang fields containing classic inverted boat-hull-shaped features occur where the NAEB is floored by dolomite, as shown in Figure 10b. Where they are subjected to active sandflow resulting in ongoing abrasion, the surfaces the yardangs are polished smooth, and they often exhibit streamlines marked by beautifully elongate flutes and grooves (Fig. 15). However, if sandflow declines due to the spatial reorganisation of coastal point sources to Aeolian Transport

Corridors in response to changes in shoreline configuration due to regression and/or transgression, their surfaces are etched by dissolution features – especially if they are in the area influenced by the Benguela Fog. One such area is located immediately west of the town of Bogenfels, where yardangs today occur within a densely vegetated sand sheet. The surfaces of the yardangs are lichen-covered, in contract to those that occur in areas of active sandflow.

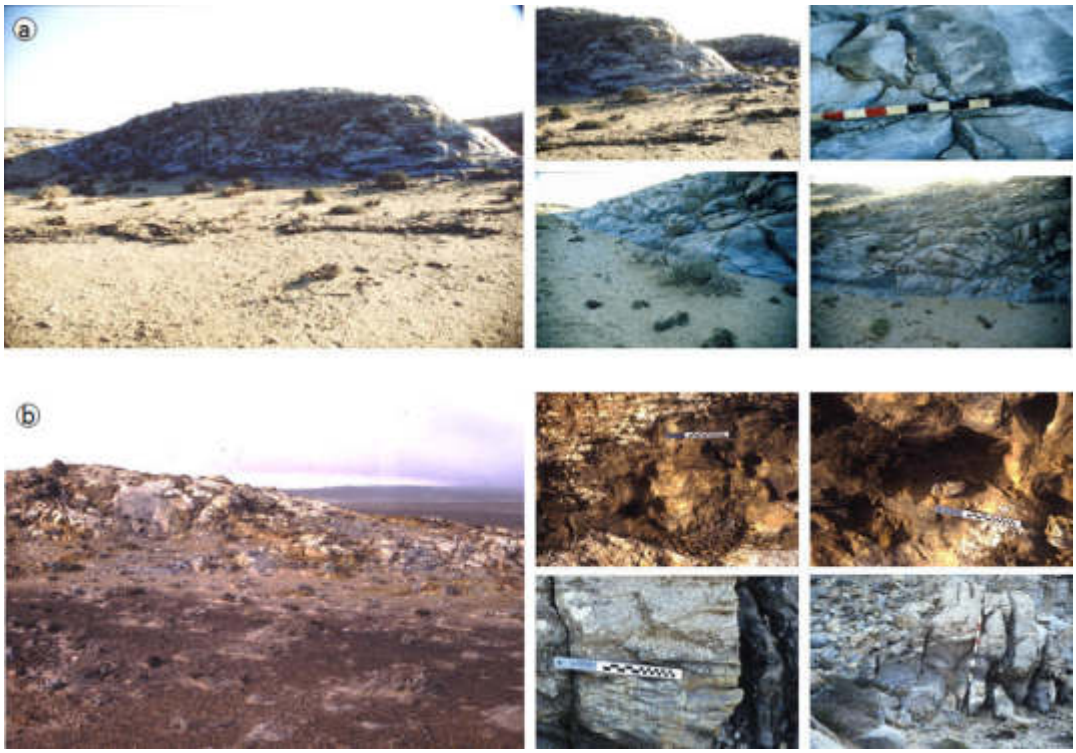

Figure 15. Two quite different examples of yardangs in Precambrian dolomite to demonstrate the Active vs Inactive form. a) Yardang located in high sandflow within an active Aeolian Transport Corridor showing polished, fluted surfaces. b) Yardang showing widespread surface modification due to dissolution by surface water (rain/fog condensation) and extensive growth of lichens and succulent flora. Note also that difference in the area immediately in front of the yardangs – in the active system vegetation cover is minimal.

As will be shown in a later section, further evidence that the path of Aeolian Transport Corridors through the NAEB has changed through time is provided by the geometry, sedimentological characteristics and size distribution of the diamond placers that occur within the NAEB.

Fluted Gneiss Domain

This domain was not recognised during the initial period of research. It has come to light through a review of the ALS data, which provides a detailed model of the relief. The macro-fluting of the exposed gneiss is particularly well-developed between Pomona and Grillental immediately downwind (i.e. north) of the famous Idatal-Hexenkessel-Kaukausibtal endorheic basins. The fluting is visible on the south-facing slopes of the gneissic hills (Fig. 16). In a number of places the fluting almost develops into classical yardang forms visible in the high-resolution ALS DEM (Fig. 17). Presumably this shape is more difficult to erode due to the fabric of the gneiss than it is in the bedded dolomite.

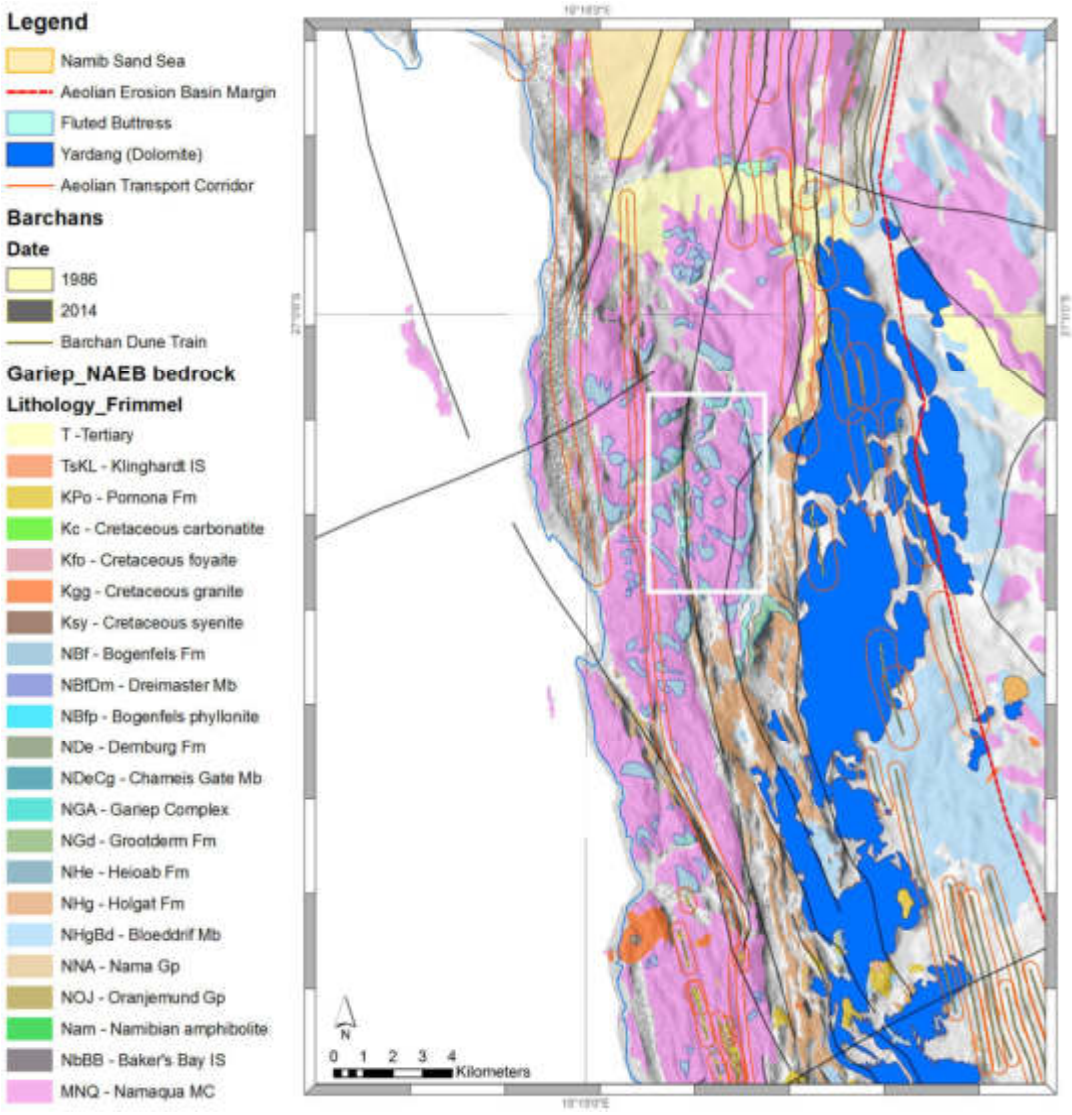

Figure 16. The best-developed area of Fluted Gneiss Domain occurs between Pomona and Grillental. Note that the area in which the domain is most maturely developed lies between Aeolian Transport Corridors. Effectively this region is currently by-passed by high sandflow pathways suggesting that this is a relic of a previous sandflow pattern that no longer exists. The white rectangle shows the position of the map in the next figure.

It is possible that the maturity of this domain at this locality is further evidence of the extent to which topographic inversion has progressed, creating large gneiss hills with south-facing ramps / buttresses for the erosional regime to sculpt in time.

Figure 17 shows a closer view of the relief shown by the ALS DEM. The larger gneiss feature consists of a number of smaller hills which appear to have been formed by aeolian erosion. The streamlined form resembles that of yardangs, but they are much larger – some are more than 2 km in length and 0.7 km wide. The surfaces are covered by patterns formed by smaller-scale fluting.

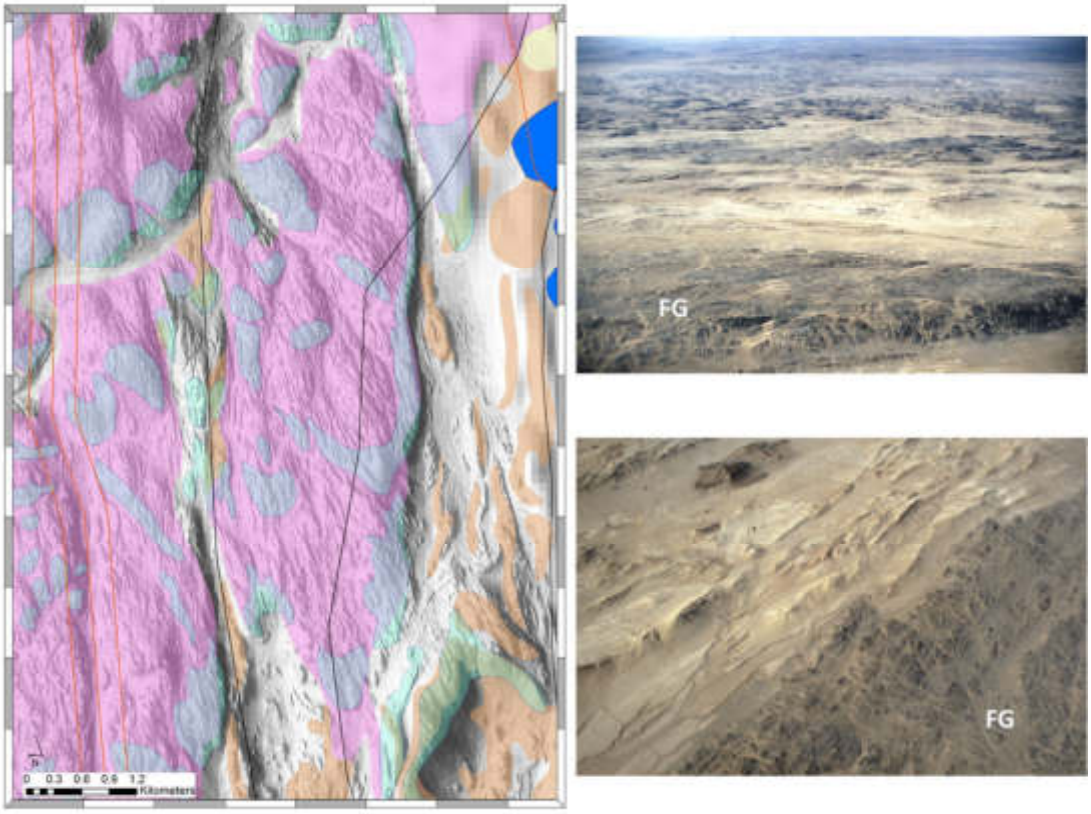

Figure 17. Closer view of the ALS DEM showing large streamlined features in gneiss – the legend for the previous figure applies to the map. The central feature consists of a series of streamlined hills. The centre-left hill that closely resembles a yardang is 2.3 km long and 0.7 km wide and has smaller fluted relief on its surface, making these streamlined hills considerably larger than the dolomite yardangs. The top photograph shows an oblique aerial view to the east across the Fluted Gneiss Domain towards the Active Yardang Domain. The lower photograph is an aerial view showing some of the smaller scale fluting that is superimposed on the larger features. The Endorheic Basin Domain is adjacent to the Fluted Gneiss.

Gneiss surfaces in the vicinity of the features are highly fluted at a smaller scale as well, bearing testimony to the erosional power of the system that sculpted them (Fig. 18).

Abrasion vs Dust as an Agent of Erosion

An extensive literature exists on whether aeolian erosion is effected by dust or the sandflow in saltation. This aspect was not studied in detail during the initial research period. However, based on observations during 3 years of living and working within the NAEB there is little doubt that abrasion by the saltation load must play a key role. My reason for stating this is that watching sandflow around dolomite yardangs it would seem to be the most logical explanation for the surface bevel cut around the skirt of the yardangs given the sand trap results on the vertical distribution of the saltation load. The form of the smaller-scale erosion features such as knobs and bosses on surfaces exposed to the southerly wind regime (Fig. 18) also suggest that abrasion by the impacting saltation load must play a major role – you can even hear it chiming on the quartz veins standing proud of fluted dolomite surfaces if you stand in Aeolian Transport Corridors during sandstorms!

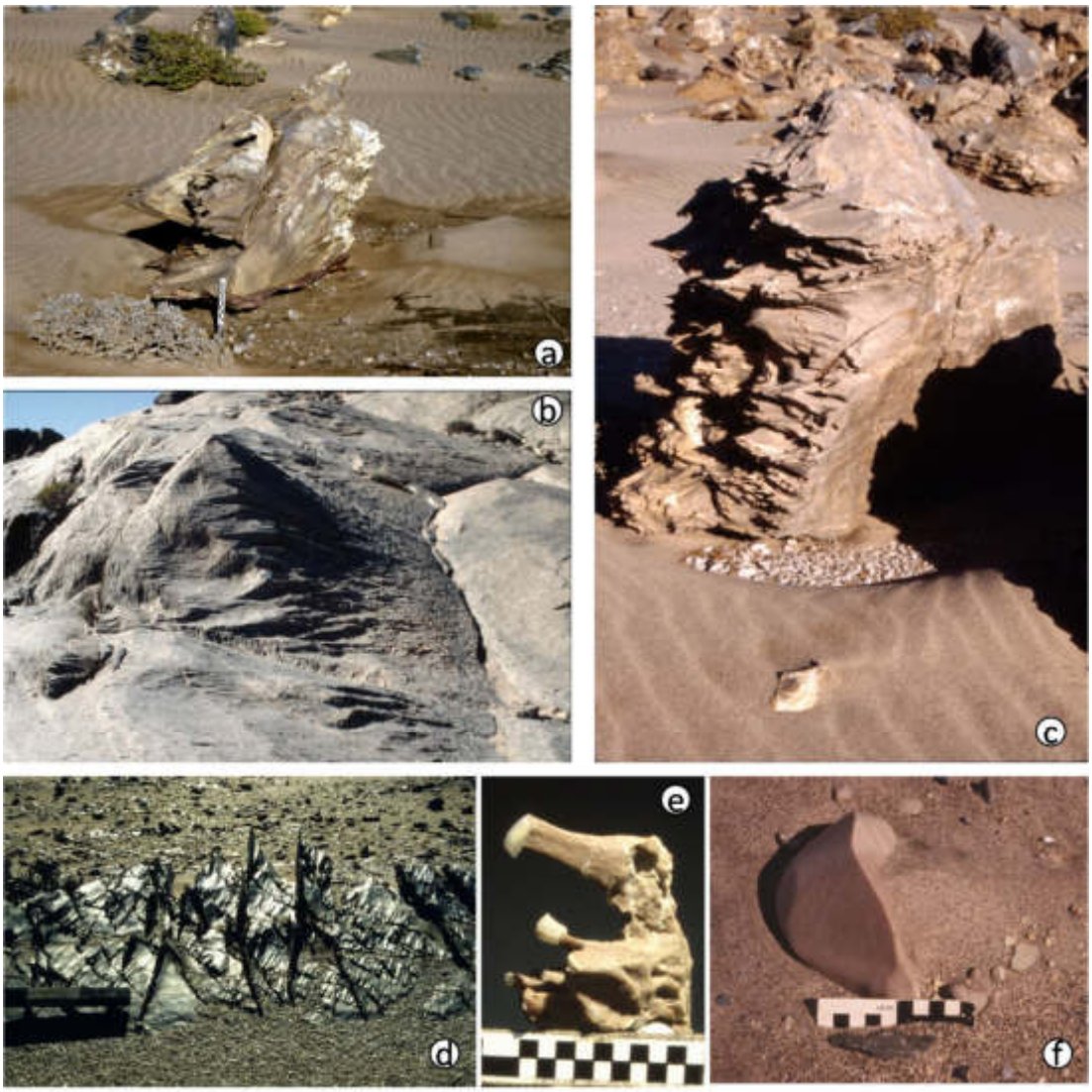

Figure 18. Examples of aeolian abrasion from different localities within the NAEB. a) and c) show the difference in abrasion on south-facing dolomite surfaces and the northern surface. The scale in (a) is 10 cm long and the form suggests that intense abrasion has cut the face back in the first 20 cm above the bed – this is the zone in which sand traps caught 50% of the saltation load. In (c) the overall height is 75 cm and there is evidence of fluting and abrasion to a height of 50 to 60 cm above the bed, in which 80% of the saltation load travels according to this study. b) shows fluting of the gneiss surface on the western valley wall of northern Windhuktal. d) shows fluting on the surface of dolomite with quartz veins standing proud of the surface providing evidence of differential erosion rates. e) is a sample of Namib 1 Calc-crust (terminology of Pickford, 2015) from the Terrassen Felder claim area east of Bogenfels where Aeolian Transport Corridors cross the Gemsboktal Conglomerates. Quartz clasts have protected the calcrete behind them from abrasion by the saltation load from the south. Note that the northern surface is relatively unaffected. f) Quartzite ventifact developing on the surface of the Gemsboktal Conglomerates – southerly wind from left to right.

Goudie (2007) stated that *"there is very little evidence as to the age and rate of formation of mega-yardangs developed in hard rocks.....Mega-Yardangs may be old and persistent features that have been shaped over millions of years, not least by high-velocity glacial age trade winds* (Rea, 1994)*"*.

The in-depth review of the Palaeogene deposits within the Sperrgebiet by Pickford (2015) suggests that this extreme example of an erosional aeolian landscape may be younger than previously thought.

Corbett (1989) suggested that some of the aeolian landscape, such as the extensive fields of dolomite yardangs might be a karst topography that was later modified by aeolian abrasion. This may still be true given the presence of thick saprolite sequences (Alterites in the terminology of Pickford, 2015).

The prominent geomorphological features termed "tafelberge", which are commonly capped by flat or gently undulating silicified sediments (termed the Kätchen Plateau Formation by Miller, 2008) have been extensively reviewed by the Namibia Palaeontology Expedition. According to Pickford (2015) "*Erosion has left the tafelberge as positive relief features isolated from each other, comprising classic examples of inverted relief – what were shallow (pre-Eocene?) depressions infilled with rubble and sand are today tall ridges and mesas standing high above the neighbouring low ground*". Corbett (1989) interpreted these sediments to mark topographically-inverted valley floor deposits. Based on the structural mapping for this study, many of the tafelberge either lie on, or are adjacent to faults, which supports the notion that the saprolites were the result of groundwater movement and that silicification might have taken place at or close to the water-table.

Importantly, Pickford (2015) concludes that undulating topography with well-defined valleys was present in the vicinity of the Kätchen Plateau – Elfert's Tafelberg area within the Pomona Claim, concluding that the Idatal and Hexenkessel valleys "*existed much in their present form before the Middle Miocene, probably down cut during the Oligocene low sea-stand*".

This observation potentially has a bearing on the subsequent development of the famous diamond placers that existed within the Pomona Claim.

It is also testimony to the extremely harsh erosional conditions that prevailed after aridification within the Namib region intensified from the mid-Miocene onwards. Based upon Pickford's (2015) revision of the stratigraphy and the biostratigraphic ages of the units studied by the Namibia Palaeontology Expedition, the aeolian erosion landscape within the NAEB has probably taken at least 14 m.y. to develop. It is virtually impossible to say whether any of the erosional features were inherited from earlier periods of aeolian activity, but there is evidence that such systems existed on rifting and later in the late Eocene based on the Buntfeldschuh aeolianites, depending upon how these are interpreted to have developed.

An evidence base is emerging in support of significantly greater wind energy during the Last Glacial Maximum. Lancaster (1985) first raised this possibility for the Namib. More recently Rohrmann *et al*. (2013) used cosmogenic dating to quantitatively determine wind erosion rates the Qaidam Basin, China. Based on biostratigraphic data for sequences in the NAEB, accelerated aeolian erosion might have taken place here during the Last Glacial Maximum. Whether this would have extended far enough to the west to affect the area of the present-day NAEB from the regressive coastline out on the exposed shelf at that time is unknown.

The Influence of Structure on the Namib Depositional Basin

The Namib Aeolian Depositional Basin is located immediately downwind (i.e. to the north) of the NAEB (Fig. 19). NNE-SSW structures intersecting the coastline exert a strong influence on the location of log-spiral bays which determine where entry points for sand supply to the NAEB occur.

Observations during diamond exploration on the coastal plain of Namaqualand showed that aeolian systems are extremely sensitive indicators of change in surface morphology due to fault reactivation and/or neotectonic fault movements.

In southern Namibia an interesting pattern is observed between the major SE-NW trending lineaments and the location and geometry of the Namib Sand Sea within the depositional basin of the system. East of Lüderitz it is possible that the southernmost of the major SE-NW trending faults shown in Figure 19 has controlled the location of the leading edge of the depression in which the depositional basin starts. There is also a striking similarity in the orientation of this structural feature and the currently active plinth of the Namib Sand Sea.

Moving north, successive SE-NW trending lineaments as well as similarly oriented smaller structures appear to exert a strong influence on the geometry of the eastern sand sea margin. It is suggested that reactivation and/or neotectonic movement is controlling the position of these offsets. Deposition along the features has produce a "stepped" geometry mimicking the distribution of the faulting which may indicate that fault movement is creating accommodation space - especially in the areas of larger sand accumulation, e.g. north of Aus. Alternatively, fault movement could be subtly modifying surface relief and thereby influencing windflow patterns which might be further enhanced by the localisation of erosion along faults which could further modify surface windflow patterns.

Recognition of a possible relationship between the geometry of the sand sea margin and fault reactivation / neotectonics may be important in explaining why earlier aeolian depocentres such as Rooilepel, to the north of the Orange River, came into existence and why the sequences they contain (which are about 100 m thick) have subsequently been preserved. These aeolianite sequences, which today form isolated remnants, were potentially part of a far more extensive Namib Erg when the aeolian systems responsible for their deposition were active.

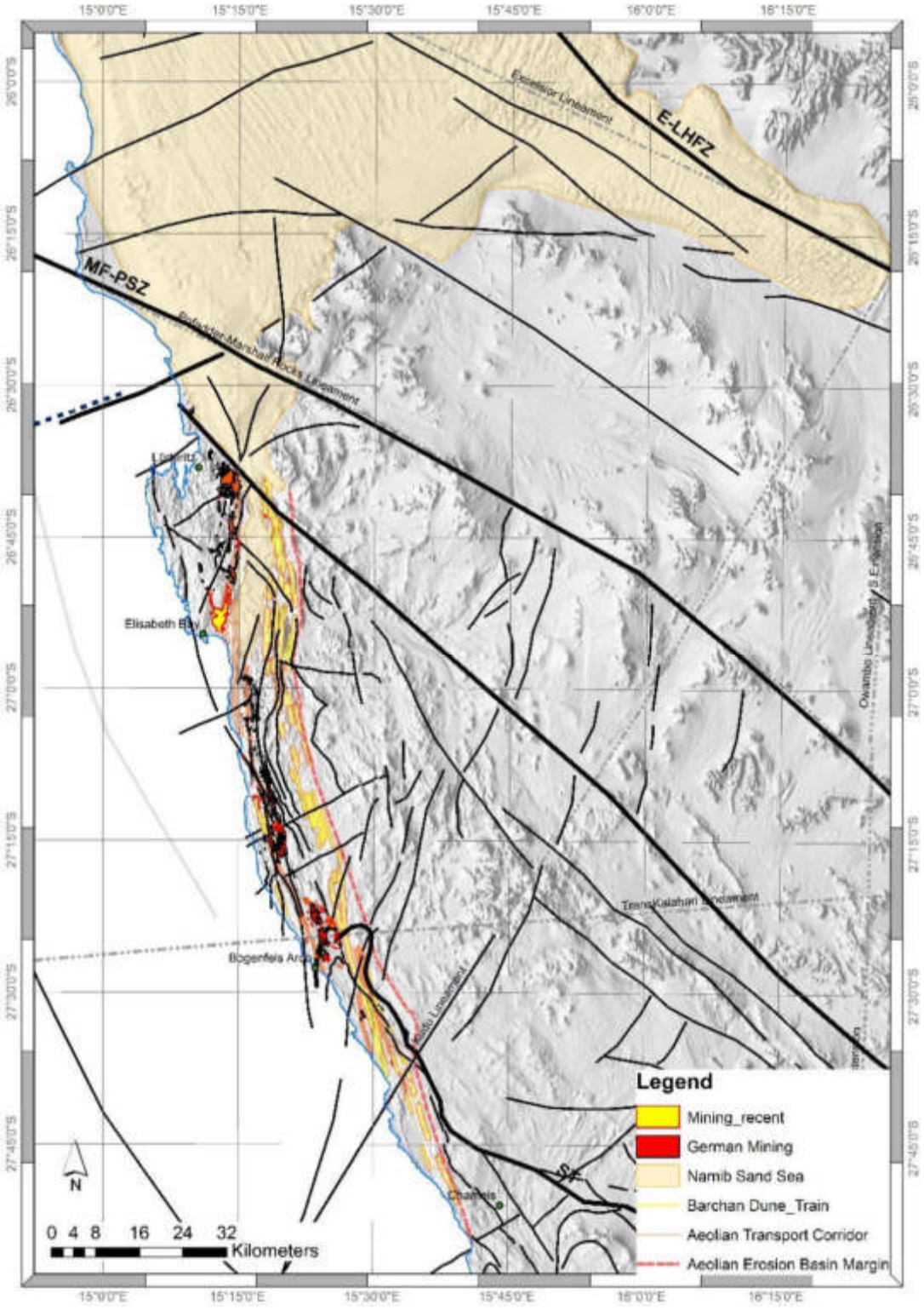

Figure 19. Structural setting of the southern end of the Namib Aeolian System. The wedge-shaped Namib Aeolian Erosion Basin is located to the south of the Namib Depositional Basin. Note the apparent relationship between the start of the main Namib Sand Sea east of Lüderitz and the form of the eastern boundary in relation to the major SE-NW trending structures. The toe of the Schakalsberge Thrust (ST) forms a major structural boundary that is intersected by a series of NNE-SSW trending faults at Bogenfels that have a similar orientation to the Kudu Lineament identified by Corner (2008).

Aeolian Bedload Transport in the NAEB

Introduction to Study Area

Later sections will show that mining has taken place extensively throughout the length of the NAEB. Fortunately the initial research on which this paper is based recorded observations on aeolian bedload dynamics in areas which were unaffected by mining at the time. In many instances these have subsequently been sampled and/or mined.

The area east of Bogenfels, extending south towards Buntfeldschuh and Baker's Bay provides an excellent area for research into the dynamic nature of the NAEB aeolian transport system. Many of the features observed within this part of the system probably existed throughout the region in which placer diamond mining occurred (see Fig. 5).

ALS data and the associated photographic coverage over the NAEB were used to map the active Aeolian Transport Corridors in detail. This dataset has also made it possible to map bedforms related to aeolian bedload transport throughout virtually the entire NAEB between Chameis and Grillental. Patterns formed by large-scale sheet-like bedforms which are not easily discerned using aerial photographic coverage can readily be recognised using the ALS DEM. The scale and distribution of these bedforms provide new insights into the pattern of aeolian bedload transport and deposition through the NAEB and allow our understanding of diamond placer formation to be refined (see later section).

Aeolian Bedload Transport Processes

In the introduction to the NAEB it was shown that sandflow rates within ATCs are significantly greater than they are within the intervening low sandflow zones that separate them. The sand is transported principally by aeolian saltation, which results in particles saltating (bouncing) across the deflation basin floor which generally consists either of Precambrian bedrock or of loose surficial gravel forming a stone pavement capping a vesicular soil horizon.

The saltating grains travel along a characteristic trajectory, for which the horizontal path length is equal to about eight times the vertical height attained by the particle (Bagnold, 1941; Chepil, 1945a). As particles in saltation commonly travel at 50% to 70% of the free stream wind velocity (Greeley *et al*. 1983), sandflow particles in the Southern Namib regularly collide with the bed at velocities of between 60 and 90 km/hr whereupon the saltating grains lose about 40% of their velocity on rebound after impact with the bed (Willetts & Rice 1989). Quartz grains almost 2.8 mm in diameter have been caught in sediment traps at heights of between 1.4 and 1.83 m above the stone pavement flooring the Baker's Bay ATC a few kilometres to the east of Bogenfels, and grains of almost 5 mm diameter have been caught in bags held at head height during major sand storm events (Corbett, 1989). Under these high-energy conditions saltating particles act as small ballistic missiles when they collide with the bed making stone pavements dynamic surfaces for aeolian transport, especially when they lie beneath ATCs.

Comparatively few studies of aeolian bedload transport process have been made. The basic concept that saltation impact propels larger grains over the bed is well established (Bagnold, 1941).

Willetts & Rice (1986) experimentally examined the mechanics of the collision process. According to Anderson & Haff (1988) on collision with the bed a saltating particle can eject larger particles through the process of reptation. As a result several large particles might move a variable, but short distance with a low, hopping

movement driven by the impact. Alternatively, particles can creep with a rolling action as a result of the combined effect of wind drag on particles as well as the transfer of energy on impact of high-velocity grains in saltation (Fig. 20).

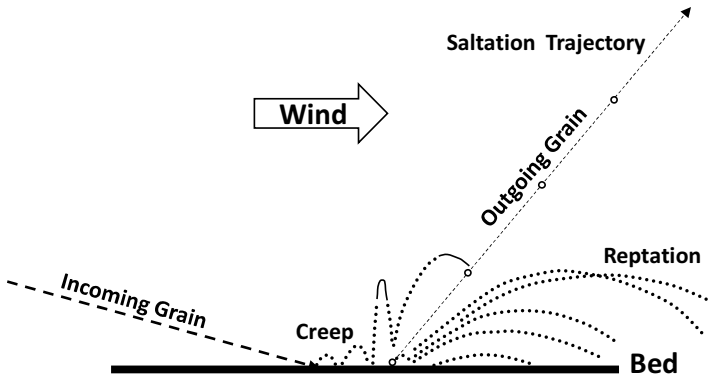

Figure 20. Illustration of the key transport processes – reptation by high-velocity grain collisions with the bed eject grains into the airflow. This either results in saltation of the particle or movement along a much shorter trajectory, whilst creep results in very localised movement by rolling. Reptation and creep play an important role in enabling organisation of bedload particles on the bed.

In the NAEB the coarsest aeolian ripples observed consisted of particles of 10 to 12 mm diameter (pers. comm. John Ward), which proves that this aeolian system is capable of transporting medium-pebble sized clasts by reptation and bedload creep.

It was impossible to study the processes or reptation and creep in detail under controlled conditions during the original study, and field observations cannot reliably be made when it is barely possible to see the ground surface, let alone to attempt time lapsed photography. As a result the main aim was to confirm whether reptation and/or creep occurs or not and record the bed configurations and bedforms that develop as a result, with the ultimate goal of relating these to the process of sediment dispersal and diamond placer formation within the NAEB.

Due to the spatial variation in sandflow outlined previously, optimal conditions for reptation and creep occur on the desert floor immediately beneath ATCs. As a consequence ATCs act as high-energy pathways along which ideal conditions for aeolian bedload transport occur. As will become evident, the pattern that develops is also strongly influenced by the topography created by the erosional architecture.

Sediment Dispersal by Reptation and Creep

Proving Reptation and Creep using Garnet Tracers

Between 27/07/87 to 05/01/88 a 26 m high barchan, comprised mainly of medium- to coarse-grained quartz sand, migrated 13.2 m to the north within the Baker's Bay aeolian transport corridor.

Over the same time period, bedload creep tracers of very coarse sand- to granule-sized garnet grains released about 200 m west of the measured dune, migrated approximately 1.5 m (Fig. 21). By the time the bed was sampled again on 23/11/88, the main concentration of garnet grains had moved 2 m to 3 m north of the starting position. This implies that a garnet creep bedload population advances about 8 or 9 times more slowly than a barchan at this point within the aeolian transport corridor. Geologically speaking, this is surprisingly fast.

Figure 21. Dispersal of the garnet bedload creep tracers by aeolian processes. By 05/01/88 the initial line of garnet grains had been transported about 1 to 1.5 m to the north across the stone pavement. The original starting point is marked by a pile of stones near the scale. Southerly wind flow from bottom to top, scale 1 m

Initially, the entire 1 m long line of garnet grains laid perpendicular to the southerly surface-wind flow moved forward en masse (Fig. 21, Fig. 22).

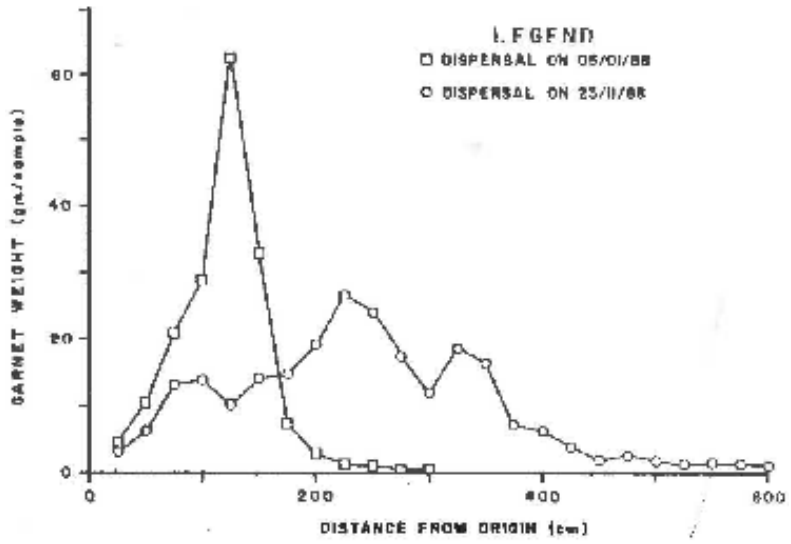

Figure 22. Graph showing the amount of creep transport undergone by garnet bedload creep tracers between 27/07/87 and 23/11/88.

As the experiment proceeded, some of the garnet grains continued to migrate to the north, whilst others remained behind. The stone pavement surface over which the garnet grains were being transported was first sampled on 05/01/88, and subsequently

on 23/11/88. The garnet bedload tracers were recovered from surficial stone pavement samples of 0 to 2 cm depth, taken in a line parallel to the southerly wind regime. Grain size distributions for the garnet creep tracers illustrate the progressive decrease in mean particle size to the north of the starting point (Fig. 22). The smallest garnet grains evidently advanced a greater distance - this is evidence of aeolian size-sorting by the combined effect of reptation and creep.

If a quarter phi sieve size class contained less than 10% of a sample's total garnet population, it was assumed to represent the migration limit of that grain size. The rate of advance for that grain size relative to the barchan dune was then calculated. An abrupt decrease in the rate is observed. Given the stochastic nature of the transport process, this is interpreted as evidence of a marked change in the probability of entrainment of the garnet grains with size. Grains smaller than -0.75 phi (1.68 mm) are more susceptible to transport by both saltation bedload reptation and creep.

Table 1. Variation in the rate of creep transport for different size fractions of garnet relative to the rate of a barchan dune between 15/10/87 to 5/01/88. Measurements were taken within the Baker's Bay aeolian transport corridor to the east of Bogenfels.

Grain Size (Phi)	Advance (m)	Rate Slower than Dune
-1.5 to -1.0	0.75	17.3
-1.0 to -.75	1.50	8.6
-.75 to -.50	7.50	1.7
-.50 to -.25	9.00	1.4

A cut-off of 3 m from the origin was employed to limit those samples used for defining the statistical parameters of the garnet grain size distribution (Fig. 23). Beyond this distance, the sample size as at 05/01/88 was found to be too small to define adequately the distribution.

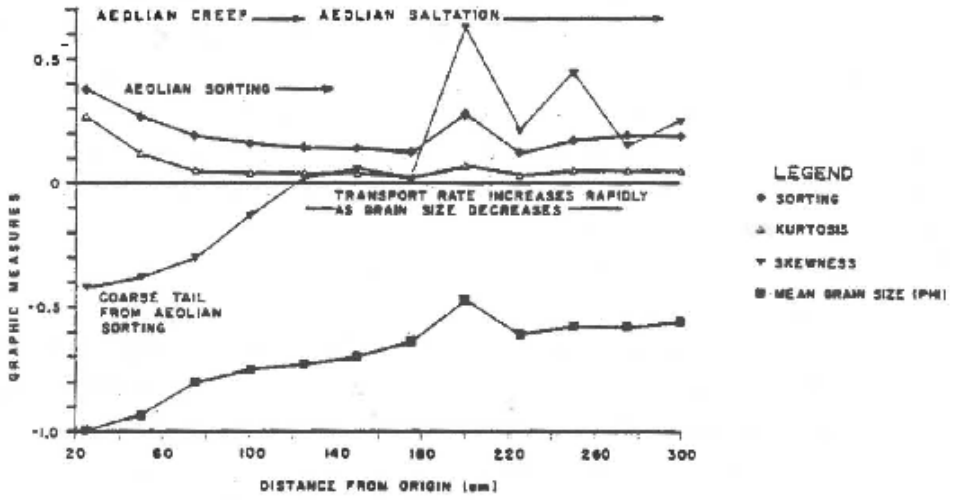

Figure 23. Graphs showing the variation of garnet grain size over the first 3 m of the stone pavement surface to the north of the release line on 05/01/87. The size of the garnet tracers decreases progressively to the north of the starting line, providing evidence for aeolian size-sorting.

Small sample size possibly explains the sharp reduction of the mean grain size and other parameters at 200 cm from the origin. The sorting of the garnet grains comprising the samples also increased to the north, confirming the subtle influence of aeolian size-sorting. The values of skewness for the distributions also systematically changes to the north. Near the origin, the samples were strongly coarsely skewed, with the change to finely skewed distributions occurring about 120 cm to the north.

The coarse tails of the initial samples are interpreted as the result of the progressive sorting of the original material. The coarser, slower moving garnet grains were left behind by the smaller faster moving ones. This probably accounts for the segregation of the garnet grains into three distinct peaks when the surface was re-sampled on 23/11/88. The change from negative to positively skewed distributions, for samples taken on 05/01/88 approximately corresponds to the point at which the rate of garnet movement slower than a barchan dune decreased abruptly. The mean grain size of the garnet at this point was -0.75 phi.

This supports the idea that the entrainment probability of garnet grains less than or equal to this grain size is much higher than it is for larger grains. This probably reflects the likelihood that the transport of smaller garnet grains is maintained during comparatively low sandflow conditions, when the force of saltation collisions should be relatively small. As the garnet grain size increases, so too does the dependence upon the collision of large saltating grains to entrain the grains into reptation, creep or proper saltation. A small percentage of the saltation population is comprised of quartz grains coarser than -1.0 phi, and observations indicate that this material is mainly active during infrequent high sandflow events. The probability of garnet grains coarser than -0.75 phi being entrained into transport is therefore reduced because these grains, which are denser than quartz grains, are probably transported primarily by creep and rare reptation ejections driven by relatively rare, large, high-velocity particles in saltation.

Bedload Streaming Within Aeolian Transport Corridors

A distinctive series of bed configurations and bedforms characterise areas of active, high-energy / frequent bedload transport. This section starts with a review of bedload features occurring in direct association with barchan dune trains that define the zones of highest sandflow within ATCs. These observations are then used to consider the regional pattern of aeolian bedload transport in the context of the spatial distribution of sandflow through the NAEB as it is today.

In order to characterise the bedload that is actively being transported within the Baker's Bay ATC surficial samples were collected from the windward slope of a 28 m high barchan dune and the surrounding stone pavement (Fig. 24) to the east of Bogenfels.

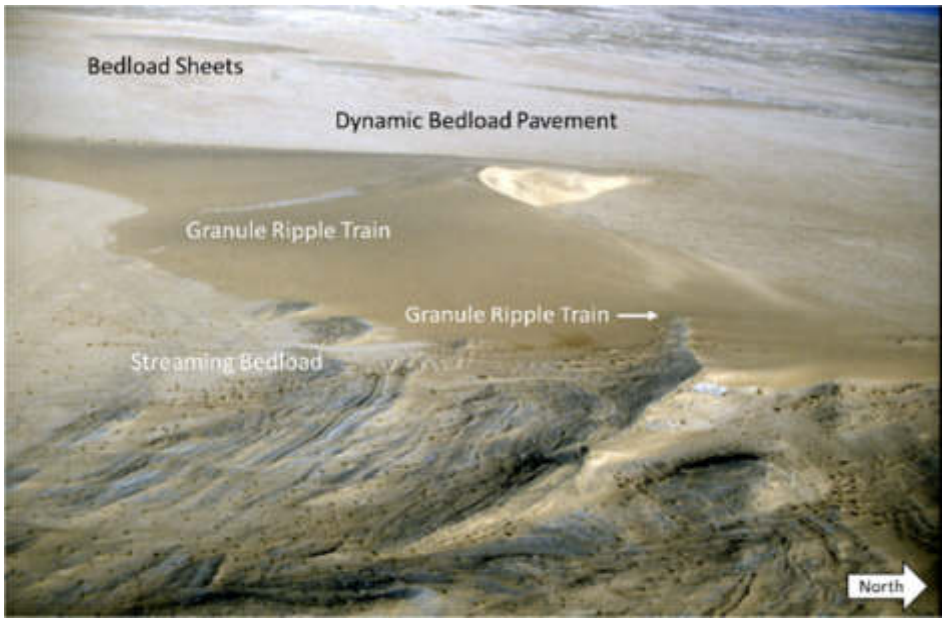

Figure 24. Oblique aerial view west, across the 28 m high barchan dune and the stone pavement which were sampled. Note the white granule ripple train on the dune's stoss slope and the large ripples on the eastern flank of the dune. Granule ripples and bedload encroachment create a white area along the skirt of the dune. White quartz granule streaks in the lee of a flow transverse, downwind-facing bedrock step provide evidence for streaming bedload transported by reptation and creep to the north.

The sand to small pebble fraction of each sample was sieved to examine whether the variable transport rates of the aeolian saltation and creep loads modify the grain size of the material composing the bed.

The grain size distributions of a selection of the samples collected are shown in Fig. 25.

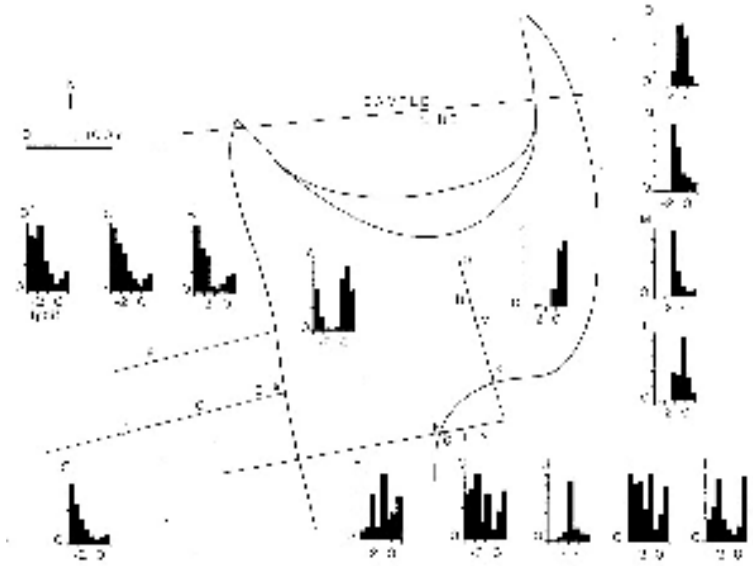

Figure 25. Grain size distributions of samples from a 28 m high barchan dune and adjacent stone pavement within the Baker's Bay Aeolian Transport Corridor near sand trap site C. The vertical axes of all graphs are in units of 10 percent.

A very coarse-grained lag deposit was present at the base of the barchan's stoss slope (sample K) (Fig. 26). This lag was separated from the underlying stone pavement by cross-stratified toesets of aeolian dune sand, marking the former dune position. Grain size analysis of this material revealed a weakly bi-modal distribution, with a minor population of quartz granules and small pebbles, but the majority of the material is very coarse quartz sand (1 to -0.5 phi).

Figure 26. Skirt of barchan stoss slope (sample K), showing very coarse-grained lag deposit overlying toesets that develop as the dune migrates to the north. Scale 11.5 cm long.

About 48 m up the stoss slope (sample L) granule ripples ascend in a wind-aligned train towards the slip-face (Fig. 27) but they do not reach it. Samples L to 0 demonstrate that the granule ripples in the centre of the street are coarser-grained than those above and below on the stoss slope. There is a tendency for the grain size to decrease up the stoss slope, but granules are still present near the crest at sites N to O.

Grain size distributions for newly exposed stone pavement along the windward base of the dune (samples F, G, and I) do not exhibit the same bimodal form as those from the stone pavement to the west of the barchan. Pronounced peaks in the distribution of sample F, suggest a tri-modal deposit. Very coarse sand forms the largest proportion of the sample, with smaller peaks of medium to coarse quartz sand and granules. Coarser fractions dominate sample G, where a pronounced peak in the quartz granule to small pebble range occurs. This reflects the start of granule ripple development at this point. The progressive increase in the percentage of the granule and small pebble fractions, together with the emergence of immobile clasts because of deflation are important factors in the stabilisation of the bed (Fig. 28).

Figure 27. Granule ripple train ascending the stoss slope of the 28 m high barchan (samples L to 0). Note that the ripples do not commence at the base of the slope, and that they do not reach the crest. Person and cat sitting for scale.

Figure 28. Stone pavement surface development is accomplished by the concentration of the granule and small pebble creep bedload on the surface, and the emergence of immobile roughness elements. Scale 11.5 cm.

Granule ripples at sample site H, near the dune skirt, are well-sorted, and material finer than 0 phi has largely been removed. Material of 0 to -2 phi is thus concentrated at the surface by aeolian size-sorting. The continued introduction of sediment between 0 to -2 phi by aeolian creep from the south blankets the bed, forming an encroachment deposit along the upwind margin of the dune skirt. No encroachment deposit was present at site I, which is relatively poorly sorted. Deflation of the sand which remains after the passage of the barchan had left pebbles, introduced by alluvial and weathering processes, forming roughness elements on the stone pavement where large quantities of aeolian sand is temporarily stored.

With increased duration of exposure to the influence of the southerly surface wind, grain size distributions become noticeably more bimodal. Sample J shows that as the coarse to very coarse sand fractions are removed by aeolian processes, there is a relative increase in the granule to small pebble fractions along the dune skirt. An encroachment deposit (see bedload transport section) is formed in response to the accumulation of creep bedload at the base of the barchan stoss slope (Fig. 29).

Figure 29. a) Oblique aerial view north showing stoss slope of sampled barchan with light-coloured quartz encroachment bedload deposition along the base of the dune skirt (E). b) Inset picture looking south from barchan crest down the ATC with an arcuate zone of encroachment deposition clearly visible along the dune skirt. Person for scale at base of granule ripple train (GRT).

Although the surficial concentration of the coarser-grained material on the bed progressively increases upwind of the barchan, after its passage over the surface the amount of sand fraction remains significant. The sand is either stored as:-

- Current shadows in the lee of vegetation, or large roughness elements (clasts) on the bed;
- In the interstices between the roughness elements on the pavement surface.

In contrast, samples from the stone pavement west of the dune train do not contain a significant sand fraction.

The grain size distributions of the stone pavement samples (B to E) are distinctly bimodal, and more strongly skewed towards the coarser fractions. Along the western margin of the dune skirt (sample A), the sand fraction remains significant due to very coarse to coarse sand ripples migrating across the stone pavement surface with the barchan (Fig. 30). Moving west, there is a rapid transformation, as the granule and pebble fractions become dominant, and the sand fraction becomes subordinate (samples B to E). There is a visible increase in the percentage of quartz granules on the bed, until this eventually becomes the dominant component (sample D) (Fig. 31). In other cases (samples C and B), the small to medium pebble fraction is the major component.

Upwind of the barchan skirt the newly exposed bed containing a large proportion of dune material is reworked by aeolian processes.

This grain size distribution is progressively modified by the removal of material by aeolian processes, as predicted by experiments and observations by Bagnold (1941).

Figure 30. Small, very coarse sand ripples of the barchan skirt migrating across the stone pavement surface on the western margin of the dune. Southerly wind blows from bottom to top of frame. Scale 11.5 cm.

Figure 31. Stone pavement west or the barchan dune train comprised mainly of quartz granules and small pebbles between widely scattered immobile roughness elements. Note the sand storage within aeolian current shadows in the lee of roughness elements. Southerly wind flow from bottom to top. Scale 11.5 cm.

Initially, the grain size distribution of material upwind of the advancing dune exhibits three peaks (sample F). The medium to coarse and coarse sand fractions represent the material transported both by saltation and creep, whilst the granule fraction predominantly migrates by creep. The variable rate of removal, which is dependent on grain size for a uni-density sediment, results in the pervasive alteration of the grain size distribution of material resting upon the bed. The granule and pebble fractions therefore accumulate on the bed, as the finer-grained material is selectively removed.

The barchan dune migration rate of about 30 to 50 m/year means that the bed immediately in their path is continuously in a state of flux, because it is alternately covered and exposed by the migrating dunes. As the removal of material progresses along the upwind margin of the dune skirt, well-sorted, very coarse sand and granules accumulate to form granule ripples oriented transverse to the southerly wind flow. Theoretically, this position within the aeolian transport corridor corresponds to the point at which the areal concentration of sandflow peaks. The collision bombardment of the creep grains by the saltation load should therefore be most frequent here, so that entrainment of the coarse material into creep, and possibly saltation is potentially greater.

According to Willetts & Rice (1986) the creep rate increases up an inclined plane. However, the vigour with which saltation is propagated declines because of the slope of the bed, which alters the magnitude of the vertical and horizontal components of saltation collision momentum. Thus a combination of the increased concentration of sandflow, and the changes in saltation grain momentum imposed by the stoss

slope, possibly explains why creep transports some of the granule fraction up the barchan stoss slope, but not completely to the dune crest. In order to maintain the granule ripple street, some granules at the base of the barchan are required to be advancing faster than the dune. About 48 m up the stoss slope granule ripples about 30 to 40 cm high form. The height of the bed forms increases up-slope until they are about 50 cm high. It is interesting that this pattern and the location of bedload on the stoss slope resembles the predicted pattern modelled by D. Zhang *et al*. (2014) based on the concept of particle residence time in migrating barchans.

From this point on, the grain size of the material declines progressively, until about 140 m up the stoss slope, there is a rapid reduction of granule ripple size, and the bed forms are only 5 to 10 cm high. Further up granules disappear and rippled dune sand separates them from the slip-face. The point where this occurs conceivably indicates the limit to which granules can be readily transported by creep, since they appear to be absent nearer the crest. Aeolian size sorting is therefore occurring on the stoss slope. This is possibly the result of a number of factors:-

1) Reduction in the concentration of the saltation load with increasing height up the stoss slope;

2) The increased dissipation of saltation grain kinetic energy on a sandy substrate resulting in reduced saltation trajectory height and path length;

3) A change in the incident angle of the saltation load relative to the sediment surface and alteration of the direction of the resultant impact force;

4) Alteration of the surface wind flow across the dune.

When the creep bedload encroaches onto the dune, observations indicate that the smaller grain sizes migrate up the slope at a faster rate. On the stoss slope of barchans to the north of the Grillental, ripples composed of very coarse sand also diminish as they approach the crest. On examples north of the Grillental, a small percentage of the coarse grains on the dune surface were observed advancing towards the crest. On reaching this point, they are incorporated into avalanche tongues, which cut back into the crestal area of the dune (Fig. 32). The coarse material associated with an individual barchan dune therefore appears to be recycled as the dune advances (Fig. 33). Groh *et al*. (2011) have observed that sand particles beneath the surface of migrating dunes are subject to a self-organising process that can lead to reverse grading with coarser particles migrating upwards. Their research shows that density-sorting leads to denser particles concentrating in a central core close to the top of the dune in the area predicted by D. Zhang *et al*. (2014) and it makes sense that residence time would be longer here too – this would appear to be borne out by field observations reported here as well as the observation that diamonds concentrate on barchan dunes (Kaiser, 1926a).

Figure 32. ATC crossing Grillental. Avalanche tongues cutting back into a barchan slip-face, and transporting very coarse sand grains from the top of the stoss slope onto the slip-face. Scale 1 m.4

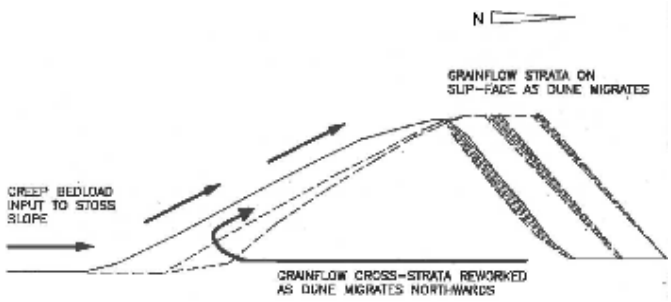

Figure 33. Sketch illustrating how aeolian bedload is incorporated into a cyclical transport process associated with barchan dunes within ATCs.

Some granules will be deposited on the bed as the dune advances. Thus to maintain the granule ripple street, some granules in the creep bedload must migrate at a similar rate to the dune, which is very fast compared to the garnet creep tracer migration rate measured about 200 m west of the sampled dune. These observations confirm that aeolian transport corridors are probably optimal sites for creep transport.

Not only do the corridors represent zones of high sandflow, they are also linear, wind-aligned zones along which the creep transport rate is very high. On the basis that the areal concentration of sandflow probably diminishes away from the dune train, it is suspected that the creep transport rate varies laterally across aeolian transport corridors (Fig. 34).

Conditions affecting the stone pavement to the west of the barchan dune train differ because the bed is not traversed by barchan dunes. It is thus a more stable environment in which aeolian processes governed by the southerly surface-wind flow operate uninterruptedly over comparatively long periods of time.

The population of garnet creep tracers released on the sampled stone pavement, near sand trap site C within the aeolian transport corridor proved that material is rapidly redistributed by creep, resulting in size-sorting of the sediment. The comparison of stone pavement samples (sites B to E), with those of granule ripples

from the barchan's stoss slope (samples L to O), and other granule ripple samples from the study area, demonstrate an interesting correlation. The peaks of the well-sorted granule ripple distributions coincide with the troughs in the bi-modal stone pavement distributions (Fig. 35). As confirmed by the garnet creep tracers, particles between -2.5 and -0.5 phi are transported northwards by creep. The absence of this range of grain size is therefore interpreted as evidence for progressive aeolian modification of the bed between immobile roughness elements. Thus from a wider starting distribution, the grain size of the sediment comprising the stone pavement surface has gradually increased through time. The continued input of creep bedload from the south over a long time period has probably further altered the grain size distribution.

This significantly influences the way in which the stone pavement environment is interpreted. Within the NAEB, and more specifically within ATCs, stone pavement surfaces are not entirely composed of immobile clasts. They in fact represent a dynamic substrate which changes continuously in response to variable sandflow conditions. As discussed in the section of dynamic bedload pavements, they are also influenced by other factors.

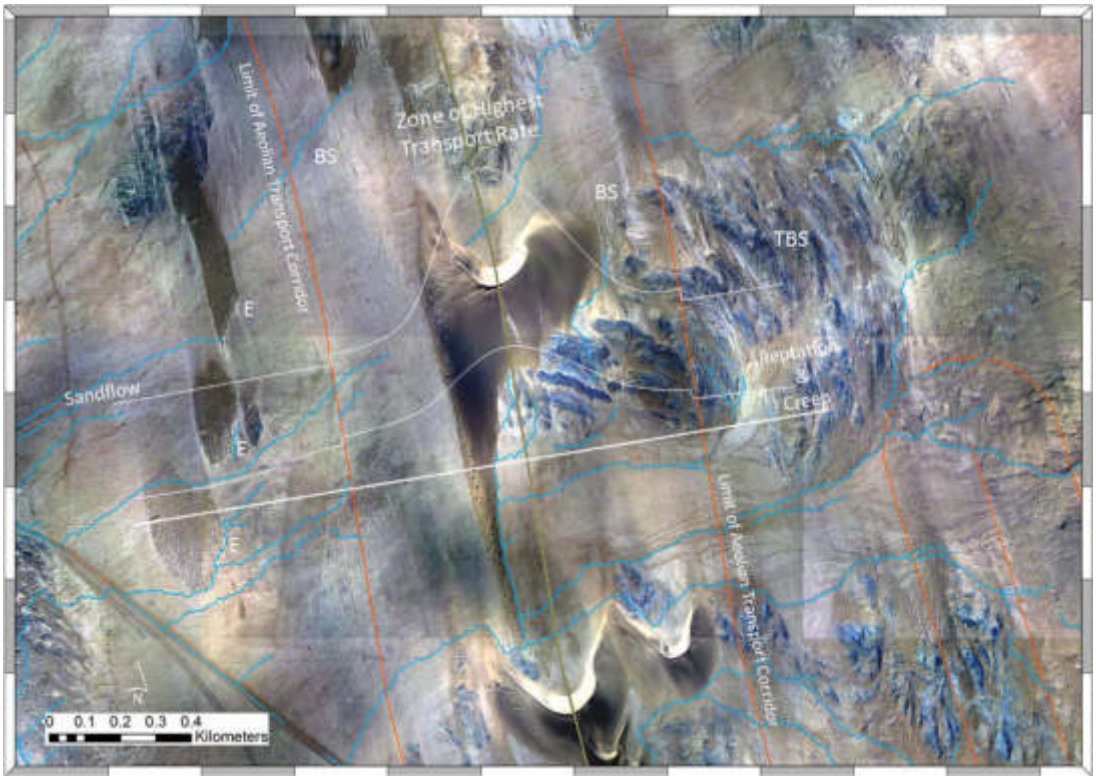

Figure 34. ALS Photomosaic of the sampled barchan showing the spectrum of bedload transport features as bright white quartz-rich deposition. The estimated limit of the Baker's Bay ATC is defined and the changes in sandflow and reptation/creep bedload transport are shown schematically on the basis of the sand trap data acquired during the original study. A subsidiary ATC is also shown. White areas annotated (BS) mark zones of bedload streaming, (TBS) highlights area in which topography controls bedload streaming direction and (E) demarcates zones in which encroachment deposition is taking place. Note the flow lines visible on the dynamic bedload pavement. The interpretation and implications of the pattern they define are discussed later in this section. The ephemeral stream network shown by blue lines was modelled using TAUDEM software. The effect of the barchans on drainage architecture is clearly seen along the trailing tail of the sampled barchan.

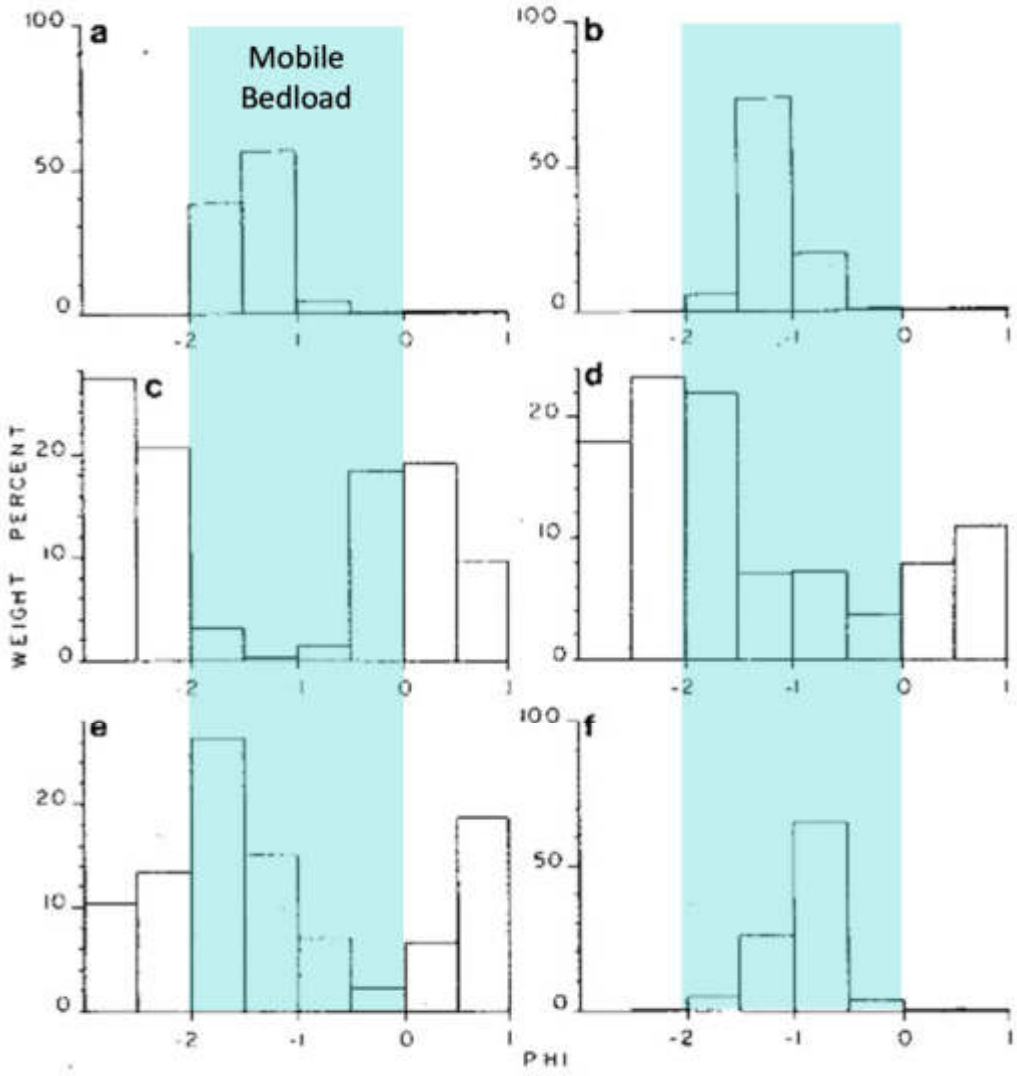

Figure 35. Comparison of stone pavement and granule ripple crest grain size distributions. Note the coincidence of the bi-modal trough with the ripple peak. (a, b, and f) granule ripples, (c, d, and e) stone pavement within the Baker's Bay aeolian transport corridor.

This understanding of bedload transport within ATCs can be applied at a larger-scale in unmined areas to look at the patterns that aeolian bedload streaming through the NAEB create (Fig. 36). As with studies seeking to understand aeolian sediment transport pathways on Mars (Bourke *et al.* 2004) the interaction of surface windflow and the associated sandflow with topography strongly influences the patterns that develop. Aeolian bedload streaming produces linear streaks elongated in the direction of the prevailing unimodal wind direction together with long trains of granule ripples.

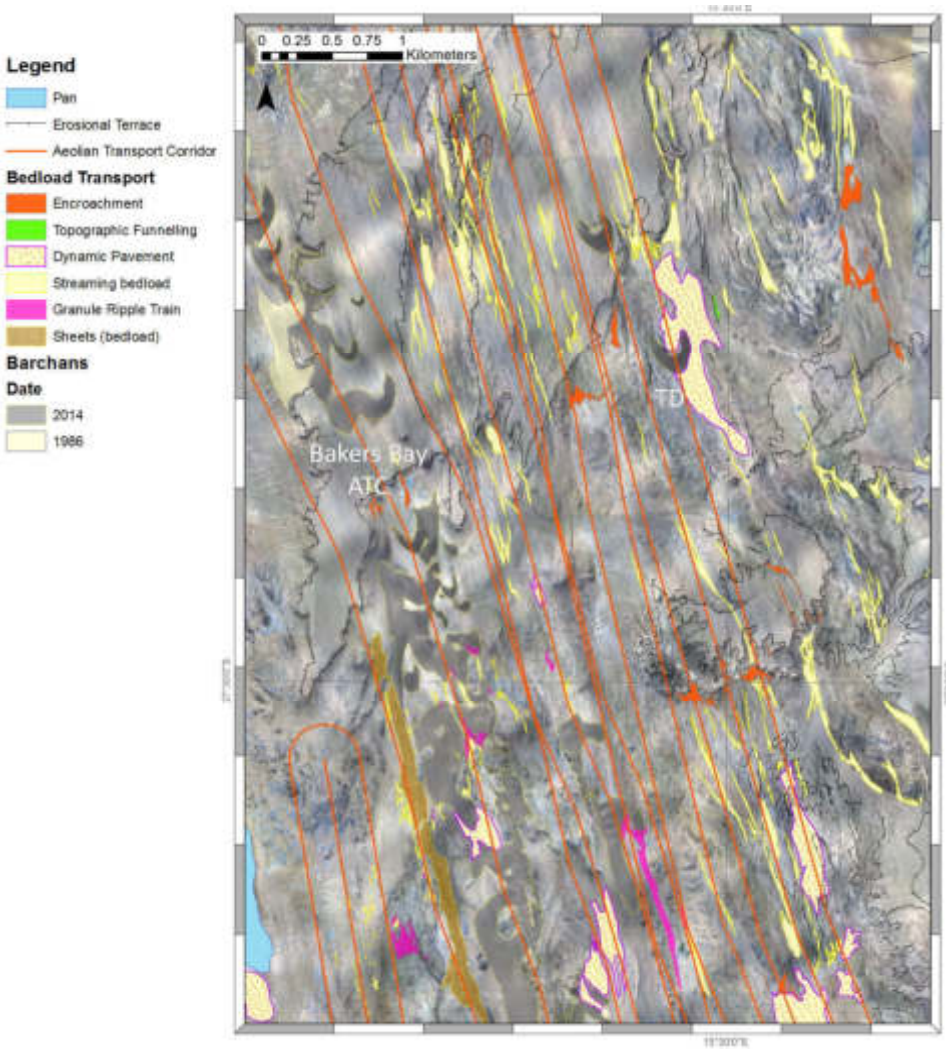

Figure 36. The convergence of Aeolian Transport Corridors within a narrow zone immediately east of Bogenfels Pan. Sandflow through the Baker's Bay ATC is sufficient to maintain a train of very large barchan dunes along its length. However the other ATCs are grossly undersaturated in respect of sandflow. In the most eastern ATC barchan dunes form as flow decelerates in a depression – the dunes then climb up the south-facing slope and dissipate as they traverse an extensive low relief stone pavement formed atop the alluvial plain of the Gemsboktal Conglomerate Formation. Bedload streaming aided by topographic funnelling has produced elongate, narrowly confined streaks of bedload migrating parallel to the prevailing southerly surface windflow. Bedload is seen to be actively migrating upslope and downslope as the ATCs traverse areas in which topographic inversion is actively occurring. Successive south-facing slopes provide temporary barriers to migration, forming sites for encroachment deposition as the bedload migration is impeded by the complex topography produced by aeolian erosion aided by other arid zone processes.

Granule Ripple Morphology and Dynamics

The granule ripples were described as "gravel waves" by earlier geologists working in the NAEB (Merensky, 1909; Krause, 1910; Wagner, 1914). These bedforms are analogous to those described by Sharp (1963) and to the pebble ridges of Bagnold (1941). Fryberger *et al.* (1992) studied granule ripples in the northern Namib where the sand availability is somewhat greater than it is within the NAEB aeolian system. These authors produced a very useful summary of the

internal stratification styles that can develop in association with these bedforms, and in particular alternation between sand ripple and granule ripple deposition. Where their study used field observations and wind tunnel experiments, the information presented below was derived in the field through direct observation of the conditions under which these bedforms migrate and the internal stratification that forms as a result of changes in surface windflow direction.

A stoss slope covered with coarse-grained material leads up to a crest that is delineated by a concentration of quartz granules and small pebbles. These form a slight step which drops abruptly down to the lee face, which is predominantly composed of medium to coarse quartz sand (Fig. 37).

In general, the stoss slope is longer than the lee face. Well-rounded granules and small pebbles consisting mainly of quartz cover the entire stoss slope surface. As noted by Kaiser (1926a) the blade-shaped particles commonly exhibit a preferred orientation, with their long axes approximately parallel to the southerly surface-wind direction. Many granules are disc-shaped. These particles frequently exhibit an imbricate shape-fabric, with the upper surfaces inclined into the southerly surface-wind (Fig. 38).

Figure 37. A large granule ripple migrating to the north with a well-defined crestal ridge and step down onto the sandy lee slope.

7

Figure 38. Densely-packed granules and small pebbles on the stoss slope of a granule ripple north of Baker's Bay. Note the close packing, imbricate shape-fabric and the alignment of particle long axes with the southerly wind flow on the stoss slope and widely scattered particles on the sandy lee slope. Scale 11.5 cm long.

During periods of reduced southerly wind-energy the lee face of granule ripples is usually composed of sand, with granules scattered across the surface. Evidence of deflation is often seen on fog-dampened lee faces (Fig. 39).

The eroded material is transported along the lee face at a slight angle to the prevailing southerly wind direction. Once the lee face dries out, small sand ripples migrate along it. The orientation of small, scour-remnant ridges (terminology of Allen, 1982), formed in the lee of granules exposed on the lee face by deflation, define the pattern of flow over the ripple crests.

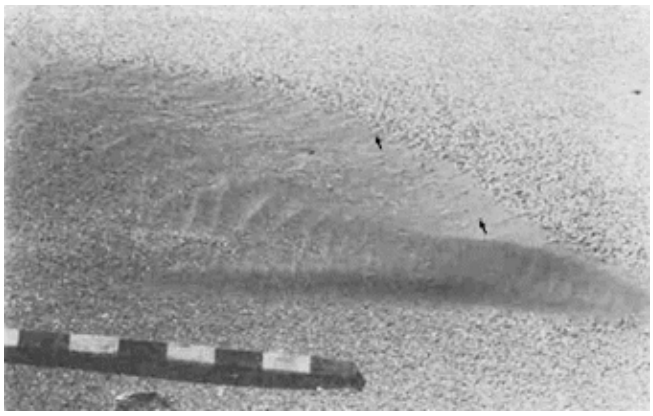

Figure 39. Scour-remnant ridges (arrowed), formed in the lee of granules exposed by deflation of the lee face of a granule ripple. The orientation of the ridges defines the pattern of surface-wind flow across the bedform. Scale 0.75 m long.

Longitudinal sections through granule ripples cut parallel to the southerly surface-wind flow, reveals that they are comprised entirely of concave, north-dipping foresets (Fig. 40). Tightly packed, wedge-shaped concentrations of quartz granules are sandwiched between the quantitatively more significant foresets of finely laminated sand which contain few granules. Sections transverse to the southerly surface-wind flow, provide oblique sections through the north-dipping foresets which are represented by laterally continuous, sharply bounded sets of low-angle strata (Fig. 41).

Figure 40. Longitudinal section through gently inclined, north-dipping foresets of a granule ripple. Note the wedges of quartz granules interspersed between sandy foresets. Scale in cm.

Figure 41. Transverse section through the granule ripple in Fig. 39. Note the low-angle stratification, and concentrations of white granules along bedding planes. Scale in cm.

Although the stoss slope is covered by tightly packed, coarse-grained material, the underlying deposit reflects the internal structure, and alternating bands of sand and granules (Fig. 42) correspond to the foresets observed in longitudinal sections.

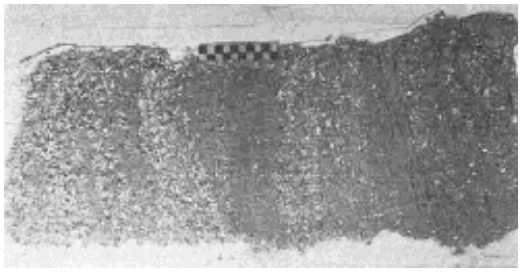

Figure 42. Cellulose acetate peel showing the stratification of the stoss slope deposits underlying the granules covering the surface. Crest of ripple is at the left end. Scale in cm.

The uniformity of foreset orientation proves that the granule ripples are migrating to the north under the influence of the southerly wind regime. The absence of steeply dipping foresets in transverse sections indicates that easterly and westerly winds have little influence on these bedforms.

The sand foresets are probably the combined result of grainfall deposition on the lee face, and translatent strata (sensu Hunter, 1977) resulting from sand ripple migration over their surface. The relative abundance of foresets composed of sand, in both longitudinal and transverse sections, strongly suggests that its deposition on the lee face contributes to the maintenance of these bedforms. During low- to moderate-energy southerly wind conditions, the deposition of fine-grained material possibly results in lee face migration. During high sandflow conditions, granules have been observed to advance up the stoss slope by creep, and to continue over the crest onto the surface of the lee face. If sufficient fine-grained sediment is added to the lee face prior to the next high sandflow event, the creep bedload crossing the former crest position, possibly tumbles onto the new sandy surface, advancing the crestal portion of the granule ripple slightly to the north.

Although the coarse component of granule ripples can probably be entrained into saltation in this high-energy aeolian environment, bedload creep appears most likely to account for their migration. Sharp (1963) interpreted the same mechanism for similar features in the Kelso Dunefield and within Coachella Valley.

The imbricate shape-fabric of granules on the stoss slope of these bed forms is probably best explained by bedload creep transport although reptation may play a role. Grain size analyses of crestal material from granule ripples in a wide variety of settings within the NAEB indicates that

particles between -2.5 to -0.75 phi are transported by bedload creep in the present-day aeolian sediment dispersal system. The possibility exists that coarser particles might have been transported during the Last Glacial Maximum when wind speeds were greater.

Early accounts by geologists visiting the mining areas record that many of the deposits were characterised by the presence of granule ripples (gravel waves). Mining may well have removed coarser-grained examples of these bedforms than those observed in this study.

A number of granule ripples were staked and measured to determine their migration rates relative to a barchan dune during the initial study. The barchan advanced 36.6 m between 15/10/86 to 5/1/88. Of four granule ripples measured over the same period, the maximum northward advance was between 0.12 to 0.17 m, with two sites showing negligible resultant movement. Despite an initial advance of 0.05 to 0.10 m winter northerly wind reversals almost returned the bed forms to their starting positions. Within the Baker's Bay ATC the northward migration rate of granule ripples is therefore potentially 200 (or more) times slower than it is for very large barchan dunes.

An examination of the rate of granule ripple advance between 15/10/86 and 12/03/87 showed that the greatest migration rates coincide with the occurrence of very high sandflow events.

Table 2. Summary of the rate of granule ripple advance in relation to the incidence of high sandflow events due to southerly windflow.

Date	Measurement Site (Advance recorded in cm)						High Sandflow Event
	1	2	3	4	5	6	
15/10/86	0.0	0.0	0.0	0.0	0.0	0.0	
01/12/86	2.8	2.0	1.0	2.0	0.6	2.4	
18/12/86	10.9	9.6	2.4	3.8	3.4	2.0	16/12/86
30/12/86	1.3	0.2	0.4		0.0	0.0	
04/02/87	2.5	1.7	0.2	-0.2	-0.2	-1.2	
12/03/87	3.5	6.5	2.5	4.0	4.7	3.0	10/02/87

The frequency of saltation collision with the bed increases during these events, and the probability of impact by large saltating grains probably also increases. This confirms that optimal conditions for creep should exist within aeolian transport corridors, where the sandflow rate is consistently higher.

In areas outside aeolian transport corridors, granule ripple advance to the south during brief high-energy wind reversals can exceed the total northward advance achieved under southerly wind conditions over a much longer time period. The rapid bedform migration rates during wind reversals is also a response to the abnormally high sandflow conditions experienced by these areas during these wind conditions. This underlines the importance of aeolian saltation in promoting the migration of these bedforms, be it by entrainment of the granule population into saltation proper or by reptation and/or creep.

Table 3. Summary of monitored granule ripple movement outside aeolian transport corridors over one year illustrating the influence of wind reversals in arresting the rate of bed form migration to the north.

Date	Measurement Site (Advance recorded in cm)					Notes
	1	2	4	5	6	
15/10/86	0.0	0.0	0.0	0.0	0.0	Observation starts
12/03/87	23.0	20.0	9.5	8.5	4.7	End of summer
05/01/88	12.0	17.0	0.0	0.0	0.0	Influence of reversals

Rain during a wind reversal on 22/9/87 allowed sections to be cut through granule ripple bedforms. Longitudinal sections were dominated by gently inclined, concave, north-dipping foresets. The lower surface of individual cross-bedded sets were formed by convex downward bounding surfaces.

Sections through the granule ripple crests demonstrated the effects of wind reversal in transforming the normally sandy lee faces during southerly wind conditions into the stoss slopes of reversed bedforms (Fig. 43, 44).

Aeolian erosion of the former, sandy lee face, results in the development of a granule lag resting upon an erosion plane. The lag is subjected to bombardment by the saltation load, and the material is transported by creep up the new stoss slope, to form a coarse-grained wedge at the crest of the bedform.

Figure 43. Longitudinal section through granule ripples to the east of Baker's Bay. Note the reversed crest, and that the former sandy lee face has been modified by the northerly wind reversal (flow from right to left) and covered by quartz granules. Cross-bedded sets are separated by convex downward erosion planes. Scale in 10 cm divisions.

If the reversal is of sufficient duration, the new crest will migrate over the former stoss slope. During the winter, frequent reversals create granule wedges in the crestal area, which are separated by fine sand and silt laminae deposited during southerly wind flow. These coarse-grained wedges become incorporated into the lee face aligned for the southerly wind, when this regime becomes dominant once more. This sensitivity to changes in the wind regime, make these bedforms useful indicators of palaeo-wind conditions in the rock record.

Figure 44. Quartz granule wedges forming a granule ripple crest as a result of a wind reversal. Note the alteration of coarse- and fine-grained material at the crest, which indicates that more than one reversal occurred. Few granules are preserved within the sand dominated sequence. Southerly wind flow from left to right, scale in 10 cm divisions.

In this example, the granule wedges formed during wind reversals were not incorporated into the sequence, which was mainly comprised of concave, sandy bottomsets. In the rock record this could perhaps be misinterpreted as the grouped bottomsets of very small aeolian dune forms, such as occur within the backshore area of log-spiral embayments which supply ATCs or in tidally flooded pan environments.

Transverse sections cut through the same bedforms exhibited low-angle stratification. Again, this is interpreted as oblique sections through the foresets observed in longitudinal sections (Fig. 45). In the transverse sections, the variation of the dip direction probably reflects the variable plan-form of granule ripple lee faces, and lateral shifts in the points of deposition and erosion along the lee face of the bedforms.

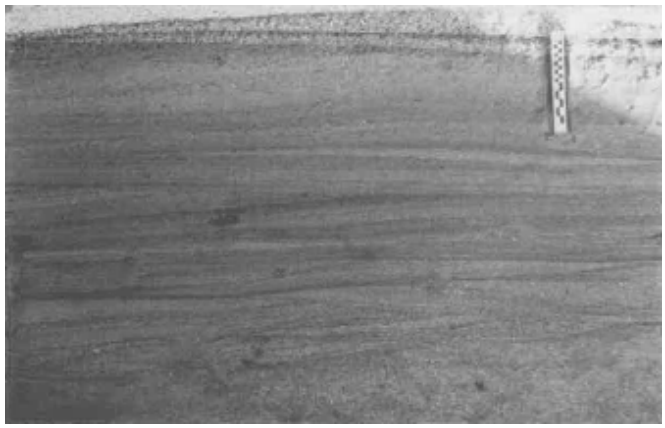

Figure 45. Transverse section through granule ripples showing low-angle stratification. Despite the concentration of granules on the bed there are very few granules in the section which is predominantly sandy. Southerly wind flow out of page. Scale 10 cm.

The internal structure of sequences deposited by granule ripples at Elisabeth Bay (Fig. 46) differs considerably from those described above. The Elizabeth Bay examples are from a sand sheet, and exhibit an internal structure closely resembling the "type-b" interdune deposit of Fryberger *et al*. (1979) and the style of stratification produced by the migration of "small granule ripples" recorded from the northern end of the Namib Sand Sea by Fryberger *et al*. (1992). This style of stratification may therefore be indicative of aeolian systems with somewhat greater sediment supply than characterises the NAEB away from major sediment entry points such as Elisabeth Bay.

Figure 46. Longitudinal section through granule ripples comprising the Elisabeth Bay sand sheet. Also note the underlying aeolian dune bottomsets. Southerly windflow from right to left. Scale in cm

Aeolian Bedload Encroachment Deposits

Bagnold (1941) proposed the term encroachment deposit to describe accumulations of aeolian sediment on the upwind side of obstacles oriented transverse to the dominant transport direction. The progressive approach of the migrating bedload leads to the vertical aggradation of the bed on the upwind side of the obstacle. The orientation of these deposits thus provides further evidence for the dominant influence of the southerly surface-wind regime on the aeolian sediment dispersal system. In longitudinal section, the differences in the structure, as compared with granule ripples, become obvious (Fig. 47). In contrast to granule ripples, encroachment deposits are comprised of low-angle stratification, which approximately mimics the underlying topography.

Due to the nature of encroachment deposits, they probably form over extended periods of time, and the surfaces on which they occur represent stable sites on which aeolian processes have operated uninterruptedly.

The creep bedload commonly exhibits a well-developed imbricate shape-fabric (Fig. 48). This shape-fabric is a stable bed configuration. As Kaiser (1926a) observed, the long axes of particles forming these deposits are commonly aligned parallel to the southerly wind direction. Kaiser (1926a) also noted that many surficial grains exhibit evidence of aeolian corrosion, and bedload particles commonly exhibit the form of small ventifacts. Seeing this, Kaiser (1926a) attributed the orientation and imbrication of the grains to aeolian corrasion. This does not appear to be the case. It is more likely that the imbricate shape-fabric displayed by the surficial grains of encroachment deposits are the result of reptation and/or creep processes.

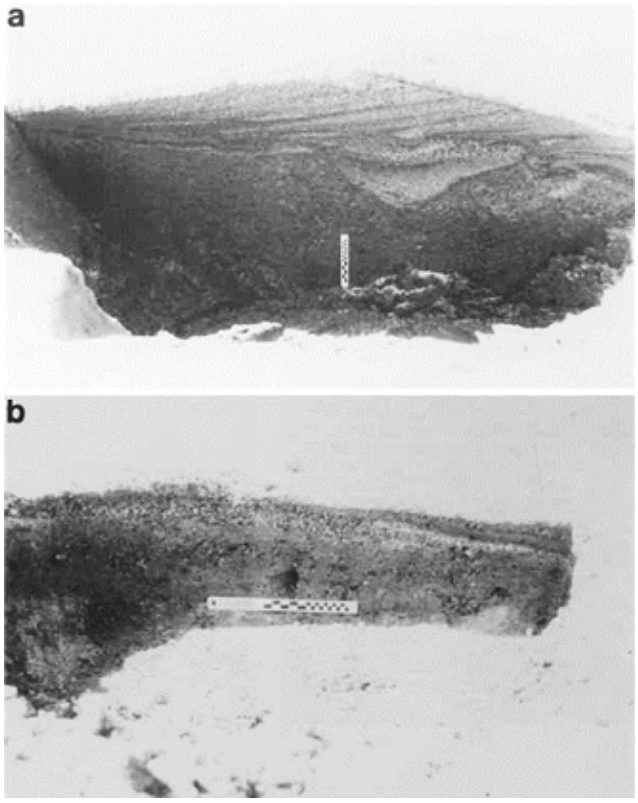

Figure 47. a) Longitudinal section through a granule ripple, showing the north-dipping foresets traversing a small, infilled ephemeral stream scour into the underlying deposit. Southerly wind flow from right to left. Scale 10 cm long, is approximately vertical. b) Longitudinal section through an encroachment deposit showing the absence of north-dipping foresets. Note the domination of the internal structure by low-angle stratification, which mimics the underlying bedrock topography. Southerly wind from right to left. Graduated part of 10 cm long scale is approximately horizontal.

Encroachment deposits develop on a variety of scales depending upon the dimensions of the obstacle. Rough bedrock topography, especially where metaclastics of the Holgat Member of the Gariep Group forms the floor of endorheic basins, is a feature of the NAEB.

Frequently this leads to the existence of small-scale walls, positive and negative steps, and cavities, which are oriented transverse to the southerly surface-wind flow. As Kaiser (1926a) observed, these form effective obstacles to the migration of the creep bedload, and thus provide sites at which encroachment deposits form. Historically (Wagner, 1914; Kaiser, 1926a) encroachment deposits on the upwind side of dykes oriented transverse to the southerly surface-wind have been recognised as potential sites for placer development. Sampling by the author has shown that features formed by quartz veins have a similar effect.

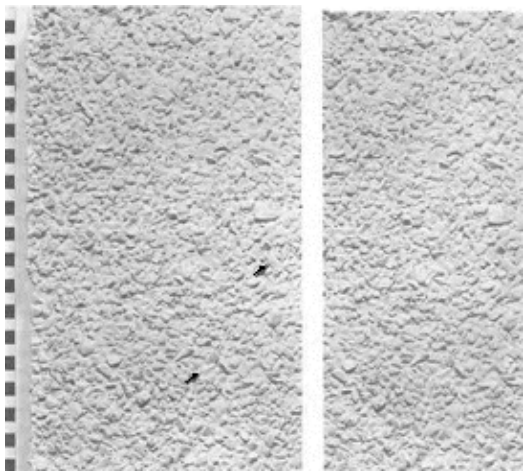

Figure 48. Stereo-pair of a plaster cast of an encroachment deposit taken at the south end of the Idatal. Note the imbricate shape-fabric exhibited by the clasts. Some clasts (arrowed) also show evidence of faceting by aeolian corrasion, and are small ventifacts. Southerly surface-wind flow from bottom to top of frame, scale in cm.

On a basin-scale the south-facing slopes at the northern end of the endorheic basins appear to form obstacles to the migration of the creep bedload. This scenario was identified as being conducive to placer deposit formation during the initial phases of mining (Wagner, 1914; Kaiser, 1926a). The creep bedload is transported up the south-facing slopes by collision impact of the saltating sandflow driven by the southerly surface-wind regime. Many of the examples which were formerly present, have long since been mined-out but in some places, the deposits on south-facing slopes remain intact. The development of encroachment deposits is indicated by the presence of brilliant white patches of quartz granules on the darker sandy substrate (Fig. 48).

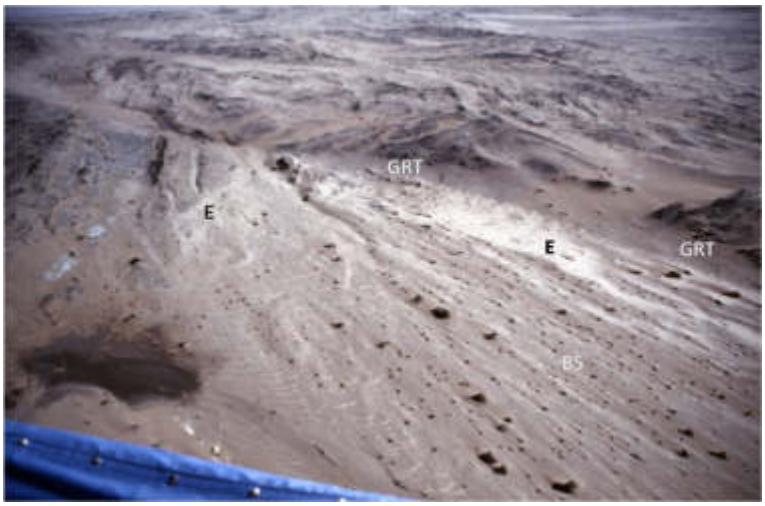

Figure 49. Oblique aerial view of the south-facing slope at the northern end of an endorheic basin about 2 km east of Baker's Bay. Granule ripple trains are migrating to the north, up the south-facing slope towards the encroachment deposit (E) of white quartz granules. Granule ripples are also migrating to the north from the northern margin of this deposit. Note the very clear, wind-aligned, streaks of bedload streaming by reptation and creep particle transport on the bed. Southerly wind flow from bottom right to top left. Ponded water body and ephemeral stream in bottom left.

Heavy Mineral Segregation by Aeolian Bedload Transport

Heavy mineral segregations can be observed in two distinct settings within the aeolian environment:

1) In association with aeolian bedforms;

2) In association with flow transverse obstacles.

A number of early publications drew attention to the existence of low waves or gravel ridges which were attributed to wind action (Merensky, 1909; Krause, 1910; Wagner, 1914). Photographs of the early deposits confirm that these bedforms are analogous to aeolian granule ripples. Merensky (1909) first recorded that diamonds were preferentially concentrated along the crests of these bedforms. This was subsequently confirmed by Krause (1910), who stated that hornblende and garnet are also segregated behind the crests. These observations confirm that at least some of the economic deposits were solely the product of aeolian transport processes operating during bedform migration. Although the examples cited by the earlier workers were largely mined out between 1908 and 1930, some examples of segregation on bedforms have been located during this study. These show that segregation is not restricted to granule ripples, and that aeolian processes during the migration of other bed forms also results in segregation.

A brief account by Wagner (1914) recorded the segregation of heavy minerals at flow transverse obstacles. Kaiser (1926a) documented further examples of this type. The processes leading to heavy mineral segregation under these circumstances are governed by a different set of factors.

Comparatively few studies have been made of heavy mineral segregation in the aeolian environment. Those which have been published more commonly examined segregation arising from the transport of sands by saltation (Willets, 1983; Gerety & Slingerland, 1983). Barchan dunes composed almost solely of heavy mineral sand grains occurring east of Swakopmund (Lat. 23°32'S; Long. 14° 30' 20" E) provide convincing evidence that particle size-density-shape characteristics lead to segregation by aerodynamic forces and saltation under natural conditions.

In the case of bedload creep examples, the reason for segregation is not clear, but the size-density-shape characteristics of the grains must significantly affect the entrainment potential of particles. Chepil (1945a, b) found that the amount of soil removal (q) by the wind could be expressed by:

q = K R Ou (V2-Vl) where:

V1 = volume of non-erodible projections existing at surface prior to exposure to wind;

V2 = volume of projections after soil removal by wind has ceased;

Ou = density of projecting units;

R = ratio of erodible to non-erodible fractions;

K = coefficient depending on the shape of projecting units.

V2 varied widely with wind velocity, and with the size, shape and apparent specific gravity of the erodible and non-erodible fractions. Hence particle density is an important variable. It has been shown above, that aeolian size sorting by bed load creep rapidly alters the grain size distribution of garnet bedload creep tracers. The same processes also affect quartz particles on the bed. Theoretically, if a quartz population and a heavy mineral population with similar grain size distributions are mixed to form a heterogeneous size-density sand which aerodynamic forces alone cannot entrain, size-density sorting by aeolian creep and saltation will modify the original grain size distribution.

Observations made during high-energy surface-winds and consideration of wind tunnel and flume studies of flow over obstacles allow a brief theoretical explanation of some segregations to be attempted. The development of heavy mineral segregations in the natural environment is relatively slow and could not be observed during the study. The processes responsible for their formation

would have to be examined under controlled experimental conditions, where the complex patterns of surface airflow across flow transverse obstacles can be measured directly. The equipment used by D. Zhang *et al*. (2014) could provide an ideal solution to achieving wind-tunnel experiments of coarse bedload transport and heavy mineral segregation in the field.

Segregation Associated with Encroachment Deposits

Minimal evidence of bedform development is generally found on the surface of an encroachment deposit situated on a gently inclined south-facing slope. Examples of segregation on a planar bed are relatively rare in the NAEB today, but they may have been more common prior to mining. They were found at Eisenkieselklippenbake, and on the south-facing slope forming the northern boundary of the Grillental. Another locality at which they occurred lay on the eastern side of the Chameis Bay ATC. In all cases the surfaces observed were being subjected to high sandflow conditions.

Iron oxide and hydroxide particles form patchy, flow transverse segregations on a surface dominated by quartz granules (Fig. 50). The better-developed segregations of heavy minerals define flow-transverse arcuate lines, with their concave margin pointing into the southerly wind. This is the opposite orientation to granule ripples, which generally exhibit convex crests pointing into the southerly wind. Adjacent edges of the arcuate segregations overlap.

Bedforms of similar arcuate form, with concave crests pointing into the southerly wind, occur more extensively within the high wind-energy coastal tract of the NAEB bordering the western margin of the Namib Sand Sea near Meob Bay (Lat. 24°15'50"S; Long. 14°31'25"E) to the north of the Sperrgebiet. Although the bedforms at this locality do occur on sub-horizontal surfaces they are more commonly observed on encroachment deposit surfaces covering south-facing slopes (Fig. 51). Adjacent edges of the arcuate bedforms overlap, and closely resemble the segregations at Eisenkieselklippenbake. In plan view, they surround planar, undisturbed encroachment deposit surfaces elevated a few centimetres above the surrounding bed (Fig. 52).

Figure 50. Heavy mineral segregations forming part of an encroachment deposit comprised predominantly of quartz granules, on a gentle south--facing slope north of the Grillental. Arrow on surface points in the direction of the southerly wind flow. Scale 10 cm.

The bedforms are defined by a south-facing slope which rises to the higher bed elevation immediately downwind (i.e. north). The crest at the top of the south-facing slope, is defined by a ridge of quartz granules a few grain diameters high.

The internal structure of the bedforms resembles that of an encroachment deposit. Low-angle sandy cross-strata dip at the same angle as or at a slightly greater inclination than the sediment surface. Granular material occurs as lens-shaped concentrations along well-defined planes.

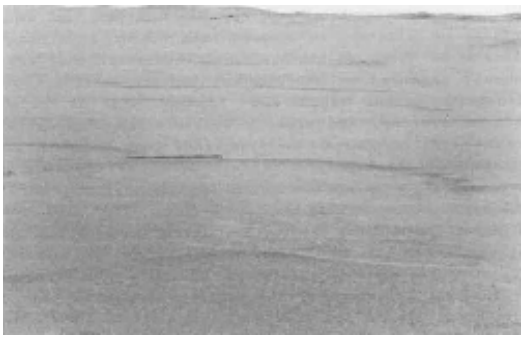

Figure 51. View north, up a south-facing slope near Meob Bay showing small, concave crests of bedforms facing into the southerly wind flow. Scale 1 m long in 10 cm divisions.

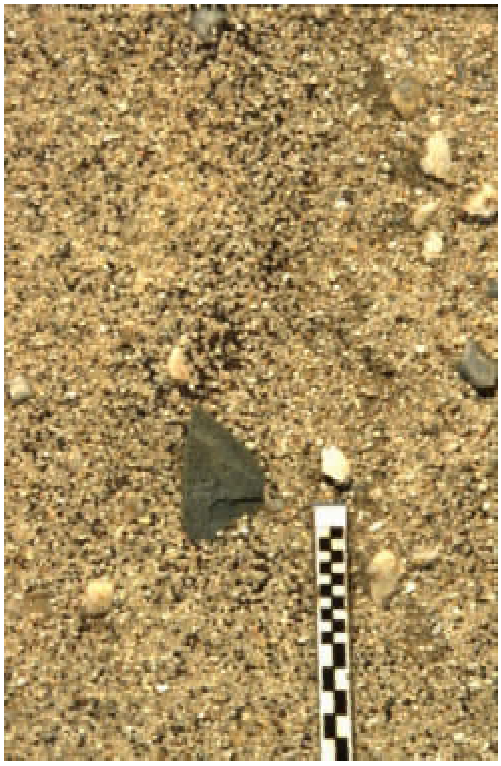

Figure 52. Northern Grillental south-facing slope encroachment deposit. Heavy mineral particle cluster formed in response to the passage of a creep erosion ripple past immobile roughness elements on a stone pavement /planar encroachment surface. Note lack of heavy minerals to right of scale where crest of ripple has already passed. North to left. Scale 10 cm.

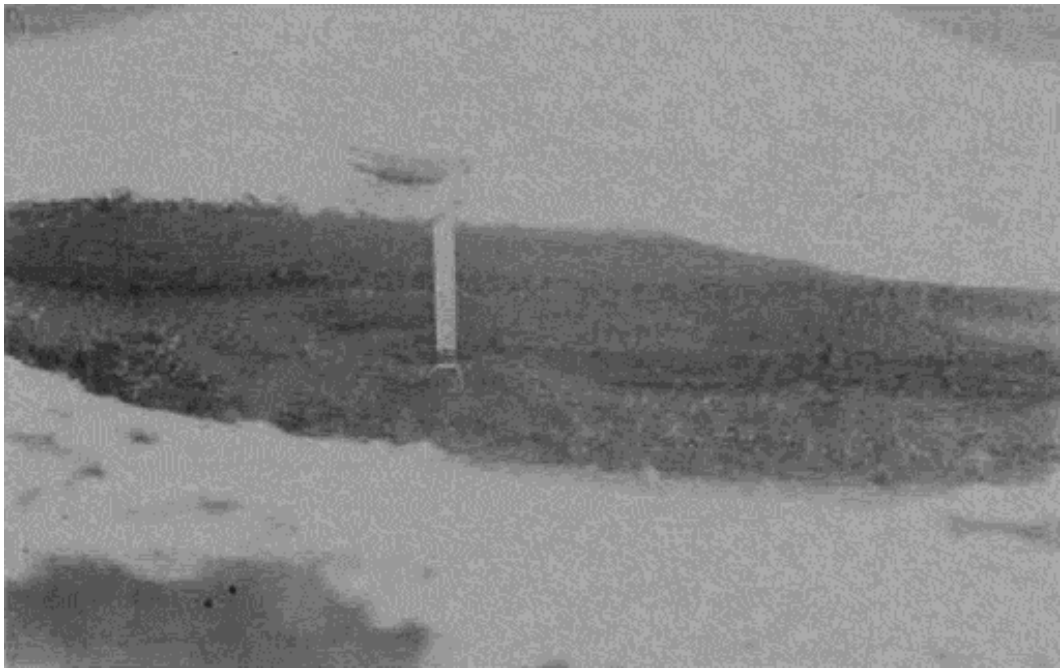

Figure 53. Longitudinal section through the concave crest of a bedform, showing the low-angle stratification of the encroachment deposit, which is mainly composed of quartz sand. Southerly windflow from right to left, scale on face about 5 cm.

The bed upwind of concave crests is coarser-grained than the encroachment deposit surface immediately downwind of the crests (Fig. 53). Angular to sub-rounded, small quartz pebbles are concentrated at the foot of the slope beneath the crest. Garnet granules are segregated along the concave crestal area of the bed forms (Fig. 53). These segregations resemble the plan-form of those at Eisenkieselklippenbake.

The examples shown all occur on aeolian encroachment deposits situated on south-facing slopes. This is confirmed by the internal structure of sediments associated with the bed forms exhibiting concave crests at Meob Bay. Lens-shaped concentrations of granular material along bedding planes observed within longitudinal sections reveal that earlier encroachment deposits are partially preserved in a thin sequence of sediments a few tens of centimetres thick.

Planar, undisturbed encroachment deposit surfaces elevated above the surrounding bed between the concave bedforms are interpreted as evidence of surface lowering, indicating that an earlier encroachment deposit is now being reworked to generate a new sediment surface. The concave bedforms are therefore interpreted as erosional fronts. The coarser grain size of material upwind of the crest (i.e. south) shows that as erosion fronts migrate up the south-facing slope to the north, size sorting is occurring and finer-grained bedload is being eroded. In the process there is a progressive concentration of heavy minerals with segregation occurring along the crests (Fig. 54).

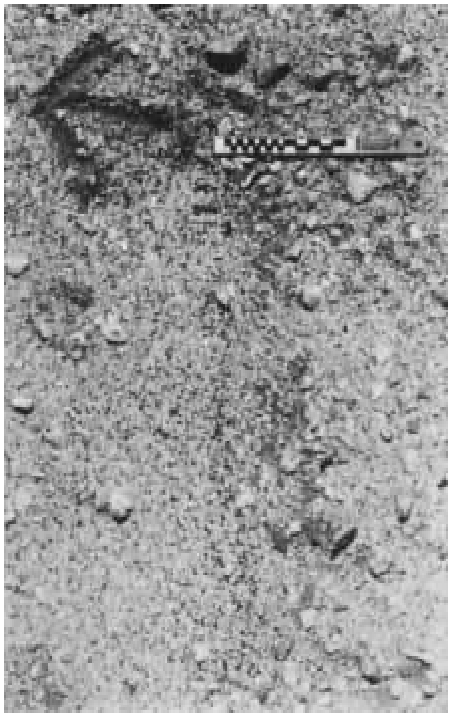

Figure 54. Segregation of garnet grains along the crest of a creep erosion ripple – note that fewer grains are present on the upwind side of the crest. Arrow on bed points in direction of southerly wind flow. Graduated part of scale 10 cm.

These bedforms have been termed "creep erosion ripples" (Corbett 1989). As creep erosion ripples migrate up-slope, the encroachment deposit is reworked to a depth approximately equal to the ripple height. This reintroduces material previously preserved within the sequence back into the aeolian system. It is quite possible that the self-organisation effects of size-density-shape sorting reported by Groh *et al*. (2011) are at play.

Pebble-sized material remains behind to form immobile roughness elements on the new surface together with some of the larger granules. The smaller quartz granules and their entrainment equivalents are apparently incorporated into the advancing ripple crest, and subsequently are removed in the downwind direction by creep. A layer of the encroachment deposit is thus effectively being “peeled back”, as the creep bedload advances north in a series of "waves".

The erosional fronts represented by creep erosion ripples provide sites of optimum reworking of the bed. Newly eroded material from the earlier encroachment deposit continuously supplies garnet and quartz grains to the crest, as the front migrates northwards. The material forming the crest therefore exhibits size-density-shape contrasts. The very coarse sand and small granule fractions are more susceptible to entrainment into saltation and creep. The small pebbles of quartz and feldspar therefore remain behind, and form the new bed. In time, as deflation proceeds, their spatial distribution will alter, and the larger particles become more densely packed. This leads to restabilisation of the bed. Bagnold (1935) considered that larger particles on the bed potentially shield smaller ones from direct saltation impact. The larger quartz grains possibly affect the garnet grains in two ways (Fig. 54):-

1) They potentially shield garnet grains from direct saltation impact;

2) The garnet grains have to overcome a larger pivoting angle than the quartz grains, in order for them to be entrained.

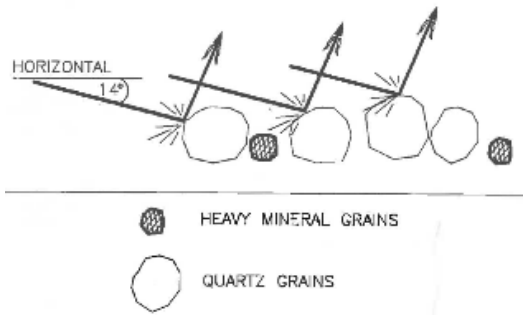

Figure 55. Sketch showing the possible influence of large quartz grains upon the entrainment of smaller heavy mineral grains into reptation and/or creep by saltation.

Bedload Segregation on Granule Ripples

Examples of diamond segregation on granule ripples were first recorded in 1909 by Merensky, shortly after the start of mining operations in the NAEB.

As with the encroachment deposit examples, segregations on the stoss slope of granule ripples form discrete bands of heavy mineral particles oriented transverse to surface-windflow (Fig. 56).

Figure 56. Heavy mineral segregation on the stoss slope of a granule ripple north of the Grillental. Note the distinct line of heavy mineral grains slightly upwind of the crest. Southerly wind flow from right to left, scale 10 cm.

The dynamics of granule ripples in the NAEB was examined during the original study. The net migration direction of the bedforms, according to measurement of their advance and their internal geometry, is to the north. This reflects the dominant influence of the southerly surface-wind flow over the direction of sandflow through the basin. Infrequent high-energy northerly surface-winds temporarily reverse the migration direction. Although the reversals are of comparatively brief duration, a wedge of granules develops rapidly at the top of what under normal conditions, is the lee slope of the bedform. Sections through sequences deposited by granule ripples near Baker's Bay are comprised entirely of the basal part of sandy bottomsets (see Figs 42, 43). Few granules could be seen in any part of the sections excavated, and rare lenses of granules seem likely to indicate former trough positions. The non-preservation of

the upper part of stoss and lee-side slopes confirms that the bed forms migrate by erosion on the stoss slope and deposition on or downwind (i.e. north) of the lee slope. The stoss slope of granule ripple profiles is therefore interpreted as a dynamic area on the bedform on which the coarse-grained fraction is recycled. This is comparable to the situation observed on the stoss slope of barchan dunes recycling bedload as they migrate along ATCs discussed earlier. It also resembles the recycling observed on the stoss slope of subaqueous bed forms (McQuivey & Keefer, 1969). In time, granules from earlier ripples are reworked, providing additional material for the stoss slope. Size-density sorting probably occurs continuously on the stoss slope as material from within the present ripple (together with earlier ones) re-enters the aeolian system through the erosion of the stoss slope.

Detailed observations under controlled conditions are required to observe the size-density sorting process on the stoss slope of the bedforms before definitive statements about segregation can be made. Ultimately, however, heavy mineral segregation on the stoss slope of granule ripples is probably strongly influenced by aeolian size-density sorting. Variation in the susceptibility of particles of differing size and density into saltation and creep are also likely to be influenced by other factors. Observations suggest that the larger quartz granules are theoretically more readily entrained into either saltation or creep by saltation impact of the sand fraction because they protrude a greater height above the bed.

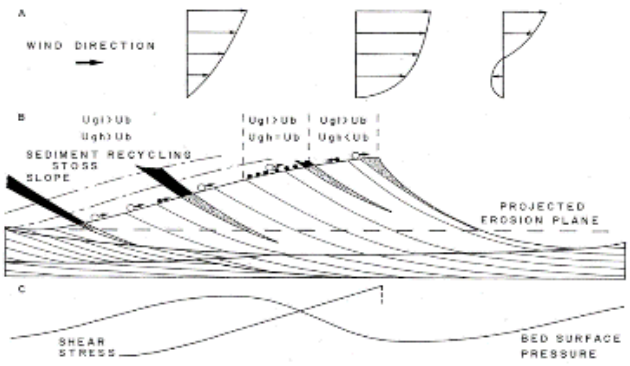

Figure 57. a) The theoretical variation of flow velocity and c) bed pressure across a granule ripple based upon consideration of the pattern across sub aqueous bedforms. b) The distribution of supertractile, subtractile, and equitractile bedload creep populations on the stoss slope of aeolian granule ripples, and the envisaged cyclical pattern of reworking of the coarse-grained component. Ugl = average light particle velocity, Ugh = average heavy mineral particle velocity, Ub = average granule ripple velocity.

Shielding of smaller heavy mineral grains by larger quartz grains from direct saltation bombardment potentially also influences the entrainment potential of grains. In addition, the pivoting angle through which grains have to move is smaller for large grains than it is for the smaller heavy mineral particles in the interstices between them. This highly variable situation is likely to be further complicated by the development of an imbricate shape-fabric by stoss slope surface particles, which also modifies the pivoting angle through which grains must move.

Observations indicate that heavy mineral segregations on aeolian granule ripples are consistently maintained towards the upper part of the stoss slope, slightly upwind of the crest. The segregation of magnetite on sub-aqueous current ripples has been shown to occur preferentially on the stoss slope in response to the surface-flow pattern and the resulting distribution of turbulence intensity and bed shear stress (McQuivey & Keefer, 1969). Grains on the stoss slope of aeolian granule ripples are too large to be entrained

solely by aerodynamic forces. For this reason, the factors governing segregation in the aeolian environment probably differ from that of sub-aqueous examples. Controlled experiments are required to assess the role played by the pattern of surface-flow over aeolian granule ripples on creep bedload dynamics. One possibility, for example, is that the surface-flow influences the frequency of saltation impact with the bed towards the crest of granule ripples, where the flow velocity is predicted to be accelerating (Fig. 56a).

In terms of aeolian size-density sorting, the variation between the creep velocity and the ripple velocity may be an important factor in maintaining segregations on the stoss slope of the bedforms (Fig. 56b).

According to Middleton & Southard (1984) three classes of size-density fraction can exist on a ripple surface based on the average particle velocity « ugi)av) relative to ripple velocity (Ub) (Fig. 56b) :

1) (Ugi) av > Ub everywhere on the ripple profile (supertractile);

2) (Ugi) av < Ub everywhere on the ripple profile (subtractile);

3) (Ugi) av > Ub on the lower part of the ripple profile,

(Ugi) av < Ub on the upper part of the ripple profile, hence

(Ugi) av = Ub at some point on the ripple profile (equitractile).

This study has shown that granules are rapidly size sorted on entering the aeolian system and that different particle sizes travel at different transport rates. If the ripples were supertractile, the surface concentration of size-density fractions would vary monotonically along the profile with minimal development of sharp local concentrations (Middleton & Southard, 1984). This description does not correspond with field observation of granule ripples, which shows that concentrations are locally much greater (and usually situated near the crest).

On subtractile ripples, the heavy mineral grains would ultimately be expected to form a lag concentration in the trough of a ripple (Middleton & Southard 1984). Longitudinal sections through sequences deposited by aeolian granule ripples exhibit no evidence of this type of a lag deposit, which suggests that granule ripples are equitractile. Hypothetically, grains re-introduced to the aeolian system near the base of the granule ripple stoss slope are sorted according to size and density by aeolian processes as they migrate towards the crest. If the condition is met whereby:-

(Ugi) av = Ub

for a particular grain size and density at some point on the profile, the grain will effectively occupy a stable surface position to which like grains will be added. Over a long period of time, repeated addition of heavy mineral grains to this point on the ripple profile will lead to the development of a lag concentration as heavy mineral grains are segregated from the lighter quartz component. This type of segregation would occupy a particular location on the bed forms, which appears to conform more closely both to the early reports on the distribution of diamond on the bedforms and to observations made during the original study.

More recently scaled laboratory models of dune migration in a recirculating flume have revealed that density segregation will result in heavy mineral grains being located in the core of the bedform close to the crest (Groh *et al*. 2011). The observations raise some interesting possibilities that may lead to a better understanding of how heavy mineral segregations develop on aeolian bedforms of different scales.

Aeolian Bedload Segregation at Positive Transverse Steps and Walls

In addition to heavy mineral segregation associated with aeolian bedforms, Wagner (1914) and Kaiser (1926a) recorded examples associated with obstacles oriented perpendicular to the southerly surface-wind flow. As the earlier workers noted, obstacles formed by resistant dykes creating positive topography on the floor of endorheic basins form effective barriers to the transport of diamonds.

Detailed explanation of these concentrations based upon consideration of sedimentary processes has not previously been attempted. The complex form of many of the barriers probably means that the surface-flow over natural examples would be difficult to measure. Observation under controlled experimental conditions would be required to define the pattern fully. Consequently, explanations presented here are primarily based upon field observation during periods of high wind velocity and sandflow. The general surface-flow pattern has been estimated from the consideration of published flume and wind tunnel studies of flow over steps.

Some of the best small-scale examples of segregation at a transverse wall occur towards the eastern end of the Grillental. Obstacles are provided by cobbles of quartzite and phonolite on the surface of a coarse-grained alluvial gravel tentatively correlated with the Gemsboktal Conglomerates. This locality is situated at the northern end of the Baker's Bay ATC which continues along the eastern margin of the Namib Sand Sea prior to entering the depositional basin. Consequently, very high sandflow conditions prevail.

A blade-shaped phonolite cobble ventifact standing on its edge and oriented approximately transverse to the southerly surface-wind was excavated to determine whether heavy mineral segregation was associated with the feature (Fig. 58).

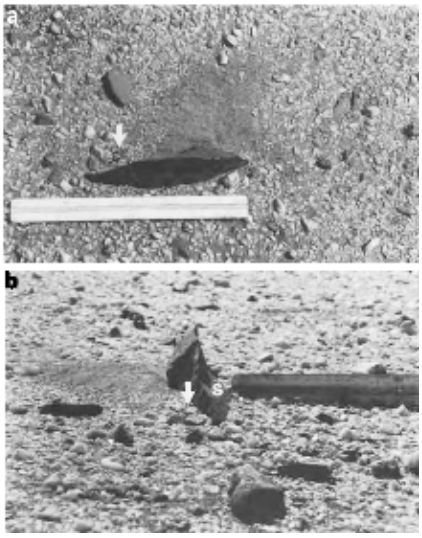

Figure 58. a) Plan-view, showing the phonolite roughness element on the stone pavement surface. Note the aeolian sand current shadow on the north side. The position of the segregated garnet grains is arrowed. Southerly wind flow from bottom to top of frame, scale 30 cm long. b) Longitudinal view, showing the stepped profile of the windward face of the roughness element formed by aeolian corrasion. Note the fluting on the south-facing riser which forms the step (S), and the imbricate shape-fabric displayed by the creep bedload at the base of the windward slope. The location of the segregated garnet grains is arrowed. Southerly wind flow from right to left, scale about 15 cm.

The windward face exhibited a stepped profile when viewed perpendicular to the airflow, with a basal 1 to 2 cm high step rising sharply from the bed to an abrupt junction with an almost vertical face rising to a height of about 6.5 cm above the bed. The step was covered by shallow flutes, whilst the steep face had been polished.

The lee-face of the phonolite cobble showed no development of a stepped profile and its surface was comparatively unpolished. Quartz granules and pebbles were present at the foot of the windward face, and an aeolian current shadow had formed on the lee side.

Immediately west of the current shadow, a surficial concentration of garnet particles extended downwind for 1 to 3 cm from the lee face (Fig. 59). Quartz granules and very coarse sand formed a northward fining tail

along the western edge of the sand current shadow, which extended about 20 cm downwind. When the obstacle was excavated from the surface, garnet grains were found to be abundant in zones about 5 cm wide on both the windward and leeward sides. The maximum concentration was visually estimated to be along the margins of the obstacle.

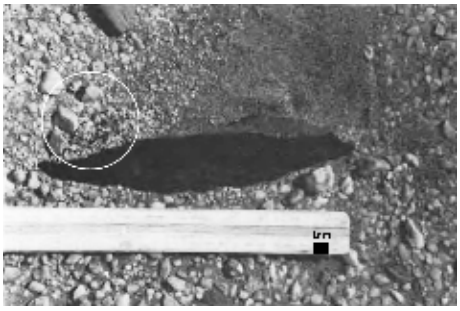

Figure 59. Close-up view showing the patch of segregated garnet grains (outlined by white circle) in the lee of the phonolite roughness element. Southerly windflow from bottom to top.

The inflection point of the stepped profile of the windward face of the phonolite ventifact (Fig. 60) probably indicates the height at which the kinetic-energy flux of the saltation load (sensu Anderson, 1986) declines near the bed.

Much less evidence of aeolian corrasion is seen on the leeward face strongly suggesting once again that the southerly surface-winds govern the development of aeolian corrasion features in the NAEB. Modification of the original roughness element has created a complex shape, which can be viewed more simply as an impermeable vertical wall oriented approximately transverse to flow.

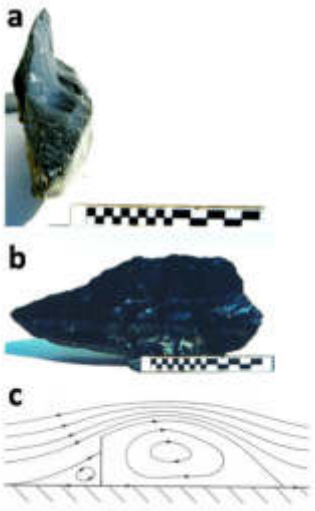

Figure 60. a) Transverse profile of ventifact forming small-scale positive step. b) Longitudinal profile of the ventifact with windward face pointing towards reader. c) Theoretical pattern of surface flow over a transverse wall. Flow lines approximating the cross-sectional form of the ventifact roughness element to show the form of the windward and downwind flow separation bubbles predicted to exist.

The surface-flow over an obstacle of this type is potentially comprised of two separation bubbles (Fig. 60) according to experimental results (Good & Joubert,

1968; Etheridge & Kemp, 1978). The first is encountered at the base of the windward face as observed in the field by placing a ruler transverse to the flow. The second bubble is developed in the lee of the obstacle. Flow passing over the leeward face of a wall is upthrust, so that the crest of the roller is about two wall heights above the flow boundary (AlIen, 1982). For this reason, the roller formed in the lee of the wall is large compared to that on the windward side. This partially accounts for the large size of the current shadow in the lee of the phonolite ventifact.

Bedload encounters an area of increased shear stress along the base of the ventifact's windward face. Placing a ruler approximately transverse to flow, granules and even small pebbles are observed to be transported along the windward edge during high-velocity winds. Hence scour is likely to occur periodically in this region. Size-density sorting of the creep bedload probably occurs under these conditions, with the result that the heavy mineral component of the creep bedload is progressively concentrated along the obstacle's leading edge. Wind scour at the base of the transverse wall could explain the abundance of garnet grains beneath the surface. Scoured hollows potentially provide sites in which heavy minerals would concentrate due to their lower susceptibility to entrainment relative to the quartzitic material (Willetts, 1983). Such scours would probably be infilled once more during reduced wind velocities, burying the heavy minerals. The lee-side concentration of garnet grains is also attributed to the pattern of flow separation.

This study has shown that garnet grains are readily moved by aeolian reptation and creep. Over a long period of time many grains potentially migrate past the fixed point such as that represented by the phonolite ventifact. Experiments by Tsoar (1983) show that for vertical, windward-facing risers, a large separation bubble develops. As the slope of the riser with the horizontal is decreased, the size of the separation bubble at its base diminishes. At angles less than 38° no flow separation occurs. It is potentially significant that at the western end of the transverse wall the riser is not vertical, but inclined at 20° to 30°. Consequently, no separation bubble is anticipated to occur along the windward face at the western end of the ventifact. A notable increase of particles greater than about 2 to 3 mm diameter occurs immediately upwind of the sloping riser, and there is an apparent absence of very coarse sand and small granules. This is seen as evidence that the smaller grains were periodically swept over the riser onto the obstacle's lee-side and incorporated into the western margin of the current shadow. The lee-side pattern of surface-flow at the western end of the obstacle could differ considerably from that at the eastern end where the vertical wall rises about 4 cm higher into the airflow. At the western edge, the riser was only 2 to 3 cm above the bed at its highest point. Consequently, the separation bubble probably extended downwind for a shorter distance. This may be confirmed by the surficial distribution of the garnet grains, which were concentrated in a zone extending from the negative step over a much shorter distance downwind compared to the sandy current shadow. Slightly larger granules marking the northern limit of the surficial garnet concentration may be defining the position of the reattachment line of the separation bubble. Coarse particles on the western margin of the sandy current shadow appear to fine downwind from this point, suggesting that flow to the north resumes at this distance downwind of the step. The surficial segregation of garnet grains in the lee of the transverse negative step is most likely to have resulted from size-density sorting as grains were carried across the sloping riser. In the aeolian environment, where the difference between the density of the air and the garnet is so pronounced, segregation is likely to be very marked.

The zone of garnet concentration beneath the sediment surface along the base of the leeward face possibly developed in a similar manner to that of the windward face. In this instance, however, the scour along the base of the leeward slope is most

likely to have occurred during northerly wind reversals. Under these conditions, what is ordinarily the leeward face briefly becomes the windward one, and significant scour along its base is possible. Segregated garnet from southerly wind conditions is then susceptible to concentration in scour hollows, which are subsequently infilled with the inevitable return to southerly surface-winds.

Heavy mineral segregations associated with ventifacts on the bed provide further evidence of particle cluster development by the mobile bedload on stone pavement surfaces. In addition to quartz granule particle clusters, roughness elements situated in localities experiencing sufficient heavy mineral throughput by creep are capable of generating segregated particle clusters in response to subtle aeolian size-density sorting aided by complex patterns of surface-wind flow. Heavy mineral segregations of this type may provide a useful indicator for the presence of stone pavements in the rock record, especially if the surface wind direction can be shown to be at variance with any alluvial system operating during the formation of the deposit.

Bedload Segregation Associated with Complex Bedrock Topography

Complex bedrock morphology on a variety of scales resulting from differential weathering occurs throughout the NAEB. Small-scale examples of south-facing, sloping risers and transverse negative steps varying in height from 10-15 cm to 50-60 cm are formed by Bogenfels Formation dolomite cropping out about 3 km east of Bogenfels (Fig. 61).

Figure 61. South-facing, dolomite risers which have been polished by aeolian processes, and transverse negative steps which form a complex "riffled", bedrock morphology through which the aeolian creep bedload must migrate. Note the encroachment deposit (E) formed at the base of the first riser. Southerly windflow from right to left, scale 1 m.

These examples are located a few hundred metres west of the Baker's Bay ATC, so they are only subject to low or moderate sandflow conditions under the present aeolian sediment dispersal system.

The south-facing risers are polished and fluted by aeolian corrasion, but the face of

transverse negative steps in their lee are relatively unaffected. Fractures in the dolomite release angular blocks from the edge of the negative steps. In time, sand infiltrates the cracks and the blocks are gradually opened and eventually they fall away from the step. This significantly complicates the bedrock morphology.

Heavy mineral segregations are located both at the base of south-facing risers (Fig. 62) and in the lee of the transverse negative steps (Fig. 63). Segregations are patchily distributed along ridge systems. The heavy mineral component comprised of iron oxide and hydroxide minerals, begins to concentrate upwind of the risers, but the main segregation is packed against their base. Heavy mineral grains smaller than 2 to 3 mm diameter are generally absent from segregations along the windward base of risers.

Figure 62. Heavy mineral segregation at the base of a polished south-facing riser. Close packing of the creep bedload is characteristic in these locations and it commonly exhibits an imbricate shape fabric. The silty soil underlying the encroachment deposit exhibits a vesicular texture when excavated. Southerly wind flow from bottom to top, scale in cm.

Heavy mineral segregation at the foot of the transverse negative steps in the lee of risers prove that some heavy mineral grains are transported over the obstacles. Heavy mineral segregations are best developed where clefts occur in the dolomite ridge. Diamonds have been observed on the floor of scour pit segregations (Fig. 64).

In some instances wind aligned concentrations of large clasts of weathered dolomite also occur. Where present, the segregations occur on the floor of depressions in the lee-side deposit rather than on inclined planar surfaces of lee-side deposits. In contrast to the well-sorted segregations at the base of risers, those in the lee of transverse negative steps are relatively poorly-sorted, and contain a large proportion of sand grade particles.

Summarised experimental data from numerous sources given by AlIen (1982) and work by Tsoar (1983) predict the existence of a separation bubble in the lee of transverse negative steps and the possibility of a less developed bubble at the base of south-facing risers (Fig. 64). The development of the latter is dependent upon the inclination of the riser.

Figure 63. Scoured depression in the lee of a transverse negative step formed by dolomite. The scour is located downwind of a cleft in the step and it is floored by heavy mineral grains. Note the wind-aligned concentration of dolomite fragments in the background at the site of another cleft. Southerly wind flow from right to left, scale in cm.

Figure 64. Small "aeolian" diamond found by John Ward on the floor of a scour pit.

Segregations at the base of risers are characterised by their relatively coarse grain size and very good sorting. The absence of finer-grained heavy mineral particles is interpreted as evidence for the absence or smaller size of the separation bubble formed at the base of the risers. Aerodynamic forces probably entrain finer-grained material as the airflow accelerates up the riser, and grains are almost certainly ejected from the bed by saltation impact and carried over the transverse negative step - probably by reptation. The very coarse sand and granules of heavy minerals are too large to be entrained by aerodynamic forces alone, and are also less readily entrained into saltation proper. These grains are interpreted as part of the reptation and/or creep bedload population, and their segregation at the foot of risers is the result of size-density sorting by creep transport. It is evident from the presence of quartz granules in lee side deposits that some of the creep bedload periodically crosses the transverse negative step. Relatively larger, quartz granules are likely to be more susceptible to being moved onto the riser by creep. Once there, it is possible that the accelerating airflow is capable of blowing the grains up the polished surface of the riser and across the step.

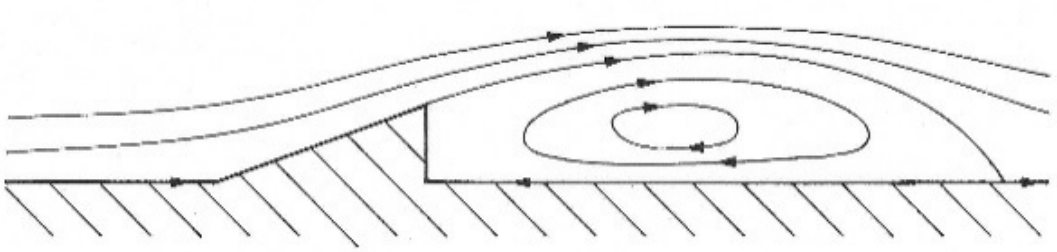

Figure 65. The theoretical pattern of surface flow across transverse negative steps combined with upwind sloping risers based on a summary of experimental work given by Allen (1982) and experiments by Tsoar (1983). Flow lines show the expected pattern of flow separation and reattachment.

Segregations formed in the lee of the transverse negative steps are interpreted as the product of aeolian size-density sorting. Due to their greater settling velocity, heavy mineral grains will be deposited more rapidly in the lee of the step than quartz grains.

Observations show that this only partially accounts for their segregation. The dolomite risers shield the surface of the lee-side deposit from direct saltation bombardment during southerly surface-wind conditions. Hence the segregation of heavy mineral grains beneath the transverse negative steps are considered to result primarily from size-density sorting by aerodynamic forces. During high velocity southerly surface-winds gusting at between 20 to 25 m/sec, evidence of the separation bubble in the lee of the negative step is seen. The movement of sediment within the separation bubble is particularly evident at clefts in the negative steps, where heavy mineral segregation has occurred.

Viewed over several minutes, powerful turbulent eddies along the reattachment line of the separated flow sweep material from the surface of the surrounding lee side deposit into the wind-scoured pit beneath the separation bubble. The more readily entrained light particles are removed from the scour pit by the powerful eddies, leaving the heavy mineral particles slowly migrating around the floor of the pit. These particles remain trapped within the separation bubble. With progressive segregation of more heavy mineral grains in time a densely packed surficial lag forms on the floor of the scour pit. The observed pattern of grain movement within the separation bubble resembles that predicted by Allen's (1968) experiments of low-speed flow separation at three-dimensional negative steps of differing plan form (Fig. 66). Thus the heavy mineral segregation within the scour pit approximately defines the pattern of limiting streamlines for the separated flow, confirming that aerodynamic forces control the development of the lag deposits in the lee of transverse negative steps.

The wind-aligned concentration of angular dolomite fragments on the surface of lee-side deposits is also attributed to aerodynamic forces in the lee of the negative steps. It is suggested that scour by the powerful eddies sweeping the bed within the separation bubbles undermine the margins of the clasts, which subsequently become unstable and slide into the scour pit. As new fragments are weathered from the step, these are added to the debris flooring the pit until a coarse-grained lag deposit develops.

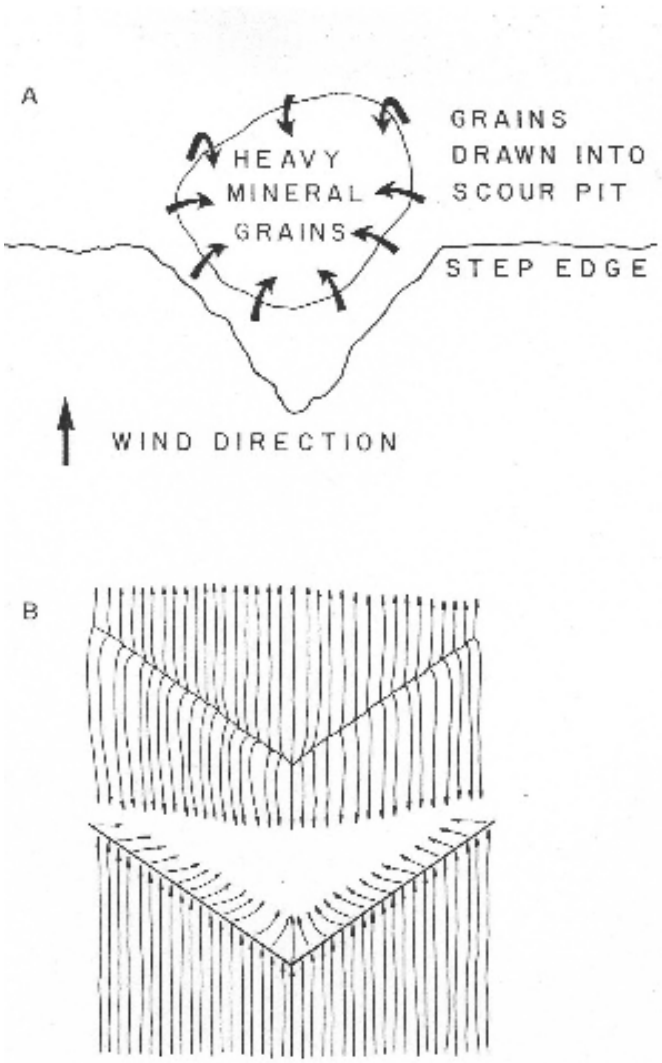

Figure 66. a) The theoretical pattern of limiting streamlines associated with the southerly wind flow across the transverse negative step. Based upon the consideration of flume experiments by AlIen (1968) the observation of the flow pattern across the step in the field during high-velocity southerly winds, and b) the pattern of sediment movement observed on the floor of the scoured pits.

Break-up of the dolomite risers by weathering processes results in more complex bedrock morphologies. Heavy mineral segregations occur at the base of the depressions which approximate to rectangular cavities (Fig. 67). As with segregations at negative steps, these examples are dominated by heavy mineral sands, suggesting that aerodynamic forces play an important part in their development. AlIen (1982) summarises the results of experiments by various researchers examining the pattern of surface-flow across a cavity, and shows that the secondary flow consists of a main vortex together with secondary ones depending upon the Reynolds number and depth of the cavity.

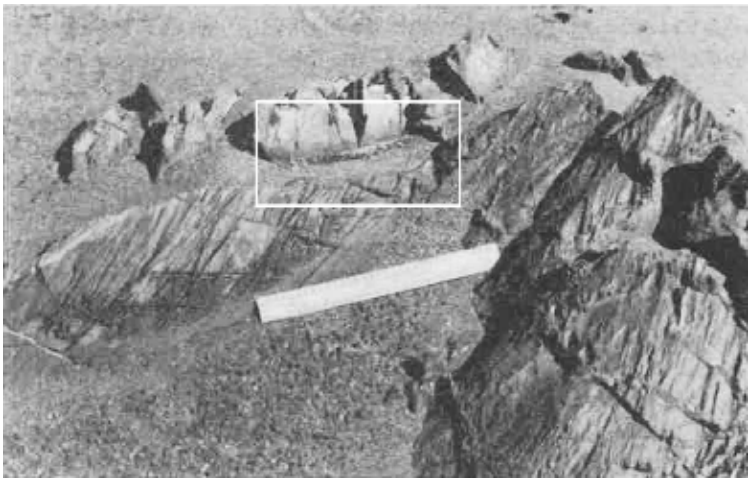

Figure 67. Heavy mineral segregation (in rectangle) in the flow separation bubble at the base of a cavity formed by a weathered block of dolomite separated from the main ridge. The small gap on the bed between the heavy mineral segregation and the downwind margin of the cavity probably indicates the presence of a secondary vortex cell at the base of the cavity. Southerly wind flow from bottom to top, scale 30 cm.

In the example of heavy mineral segregation shown here, a slight gap exists between the northern margin of the heavy mineral grains and the base of the north wall of the cavity. This implies the existence of a secondary vortex located at the base of the northern wall based upon observations by Tsoar (1983) on the development of echo dunes at cliff faces. The segregation of heavy minerals in this setting is therefore interpreted to be the result of size-density sorting in the separated surface-flow. There is little doubt that the larger settling velocity of the heavy mineral grains plays an important part in this process.

From the above discussion of the factors governing the development of heavy mineral segregations, it is clear that lag concentrations can develop by bedload migration by collision-induced reptation and/or creep and/or aerodynamic forces alone. Segregations at the base of south-facing obstacles on the bed prove the dominant influence of the southerly surface-wind flow in maintaining creep transport to the north. Provided that aeolian processes at these sites are not disturbed by ephemeral stream activity or surface run-off to any great extent, surficial lag accumulations of heavy minerals will form.

Significant concentrations of diamonds were located on the windward side of dykes running perpendicular to the prevailing wind direction across the floor of endorheic basins (Fig. 68). Sampling by the author showed that quartz veins forming positive steps produce similar effects.

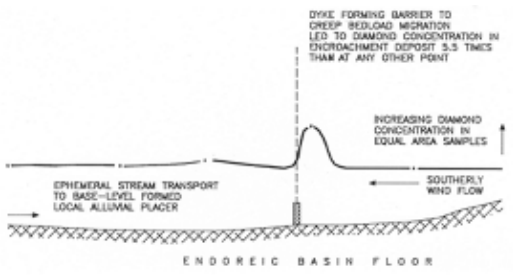

Figure 68. Development of a local diamond placer body associated with an encroachment deposit on the upwind side of a phonolite dyke running east-west across the floor of an endorheic basin. Based upon prospecting data held in Oranjemund by Namdeb.

As Kaiser (1926a) observed, localised concentrations such as these prove that diamonds are transported along the floor of endorheic basins by aeolian processes. They also provide further proof that the palaeowind direction has consistently been dominated by southerly quadrant winds during the development of the placer bodies.

The importance of positive steps is greater still when the bedrock morphology of the fabulously rich endorheic basins such as the Idatal and Hexenkessel is examined more closely. Positive topographic features can halt the progress of the heavy minerals being transported by aeolian processes (Kaiser, 1926a). Those oriented obliquely to the southerly surface-winds locally modify the direction of surface-wind flow, and hence sandflow, which determines the direction and rate of migration of the creep bedload.

Segregation on Dynamic Bedload Stone Pavements

An example of a ventifact forming a positive step on a coarse gravel pavement was discussed earlier in this section on heavy mineral segregation.

The garnet tracer experiment provided an opportunity to observe heavy mineral segregation in action on a dynamic bedload stone pavement.

Based on observations it was immediately apparent that roughness elements play an important role in determining where segregation occurs (Fig. 69). But the patterns are complex and it is difficult to observe changes during high-energy sandflow events to understand how the grains migrate.

Figure 69. Garnet tracers migrating across a dynamic bedload pavement. Note the presence of discrete grain concentrations which suggest the existence of pathways and preferred sites for segregation of heavy mineral particles. Scale 10 cm

Concentrations of garnet grains were seen to form at specific locations on the stone pavement surface, suggesting the existence of preferred pathways between immobile roughness elements and/or sites for segregation leading to clustering of grains.

Immobile roughness elements are also provided by vegetation on pavement surfaces. Current shadows produce complex patterns of flow beneath the saltation load. It is evident that preferred pathways for bedload migration exist between adjacent elements. The leeside eddies formed by separation bubbles associated with current shadows appear to provide sites at which segregation takes place on a micro-scale (Fig. 70).

A pavement was observed during a high-energy wind reversal. These observations showed that sandflow driven by northerly winds plays an important role in dislodging heavy mineral particles from sites that are stable with respect to the southerly wind and sandflow (Fig. 71).

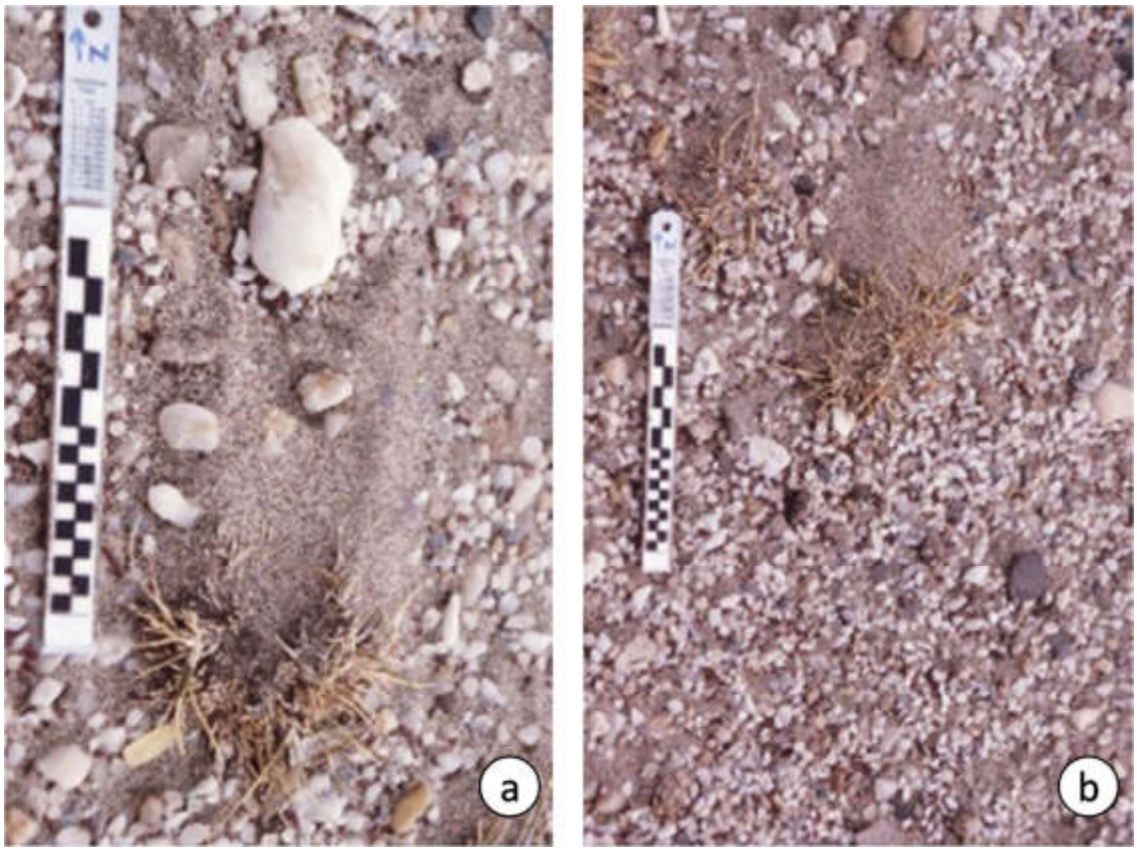

Figure 70. Garnet bedload tracers interacting with immobile roughness elements provided by vegetation. a) Combined effect of a current shadow and leeside eddy plus a quartz clast ; b) two roughness elements with a pathway for bedload migration separating them.

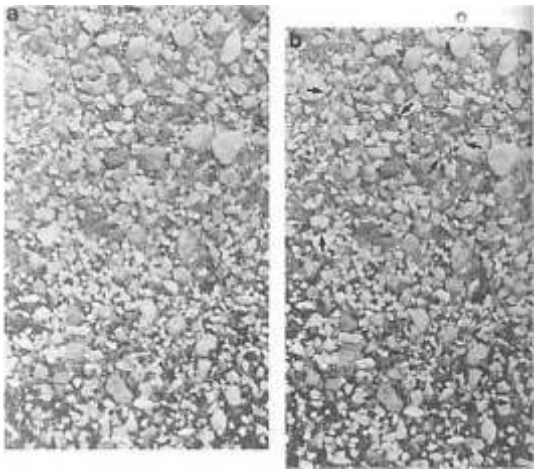

Figure 71. Stereo pair of stone pavement taken during a northerly wind reversal on 22/09/87. (a) was taken about 5 minutes before (b). The arrows highlight the pervasive changes which affected the bed configuration as reptation, creep and possibly saltation proper proceeded to entrain particles. The dark grains are the garnet bedload tracers used in the experiment on the stone pavement near sand trap site c. Note how some of the grains become lodged behind the immobile roughness elements.

The Role of Ephemeral Rainfall in the NAEB
Light Rainfall and Short Duration Run-Off

Rainfall occurs throughout the year within the NAEB, but the heaviest rain tends to fall during the winter months (April to July) (Kaiser, 1926a). Personal observation shows that the generation of surface run-off is enhanced by the presence of exposed bedrock and the sub-surface carapace of silt beneath stone pavements. As in other deserts, the sub-surface carapace tends to reduce infiltration of the run-off (Cooke, 1970) as does the bedrock.

The best catchments are therefore located in areas that are characterised by exposed bedrock and areally extensive stone pavements.

During light rainfall, the generation of surface run-off is principally restricted to areas of exposed bedrock. Slight depressions form localised catchments in which run-off collects before flowing in shallow channels a few centimetres to tens of centimetres wide (Fig. 72).

Figure 72. Aeolian sands partially reworked by a brief period of surface run-off from a bedrock floored catchment. Note the depositional lobes formed by switching of the main channel. Scale 1 m.

These small streams are highly ephemeral. Their transport capacity is limited and they tend to rework aeolian deposits of sand and granules downslope over short distances. The reworked material is commonly redeposited in a series of small lobes, each of which remains active for a short period only, due to infiltration of the run-off. Consequently, the distributary channels frequently switch direction. Where the catchments are slightly larger, or the rainfall persists longer, gullies are rapidly eroded into sandy aeolian substrates and the material is redeposited as small alluvial cones at the base of the slope (Fig. 73).

The main effect of these events on the aeolian system is to reintroduce sediment from aeolian storage sites along the margins of the endorheic basins where it can be eroded by the aeolian system.

Figure 73. Ephemeral run-off reworking a mixture of aeolian sand and granule ripples along the edge of a basin. Note the lobes deposited due to rapid infiltration of the water producing a slurry of sediment. Scale 1 m in 10 cm divisions.

When rainfall ceases the resulting alluvial cones are rapidly reworked by the aeolian dispersal system as the sediments dry out.

A slight increase in the sandflow rate is probably experienced by areas lying downwind (i.e. to the north) until the alluvial deposits have been completely reworked or the sediment surface is stabilised once more.

Heavy Rainfall and Ephemeral Stream Activity

During heavy rainfall events, as occurred on 03/12/85, 11/6/86, 4 to 5/6/87 and 17 to 20/7/87, surface run-off is generated over a much wider area. Catchments floored by exposed bedrock still tend to generate run-off more efficiently than those floored by other substrates (Fig. 74).

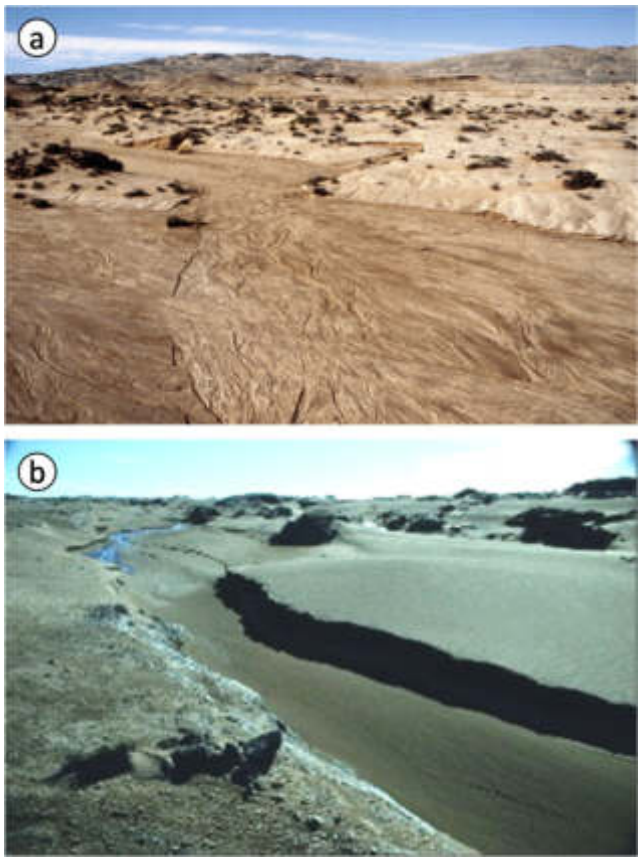

Figure 74. a) Bedrock floored catchment south-east of Baker's Bay, showing the sandy nature of the material transported between 17-20/07/87. Note how the channels coalesce, to redistribute aeolian sand from former current shadows. b) Reactivation of an ephemeral stream channel resulted in the erosion of large quantities of aeolian sand from the channel course. This material was removed from a temporary storage site, and re-introduced to the aeolian system. The channel is about 1 m deep.

Numerous distributary channels from different catchments coalesce to form a braided network which rapidly merges into larger, higher-order channels within the drainage network. As the water flows down from the basin margins, aeolian sands choking old channel courses are rapidly eroded down to bedrock

The run-off from larger catchments is sufficient to re-activate old channel courses that cross relatively flat stone pavements (Fig. 75) and large-scale reworking of sediment comprising the stone pavement occurs.

No matter what form the basin takes, there is a tendency for the ephemeral stream systems to exploit subtle topographic depressions which need only be 2 to 3 m deep at the base-level of the ephemeral stream systems. Centripetal drainage patterns develop at the termination of the system to form ponded water bodies. Kaiser (1926a) termed these sites "gravitational centres" because of the deposition of reworked material around their margins (Fig. 75a).

The ephemeral stream networks within endorheic basins are controlled entirely by basin morphology (Kaiser, 1926a). Typically, the systems consist of dendritic tributary networks which form on the south-facing slopes at the northern ends of basins (Fig. 75b). These slopes act as a natural catchment, which feeds into successively higher-order streams, until a main channel flows south into the ponded water body at base-level.

Interaction of the ephemeral stream networks with the aeolian system takes on a special significance where the basin is

being traversed by active ATCs, as is the case in Figure 75b. In this scenario the dendritic tributary networks rapidly rework large quantities of aeolian sediment, which includes coarse-grained streaming bedload deposits along the valley walls and on the surface of dynamic bedload pavements (Fig. 76).

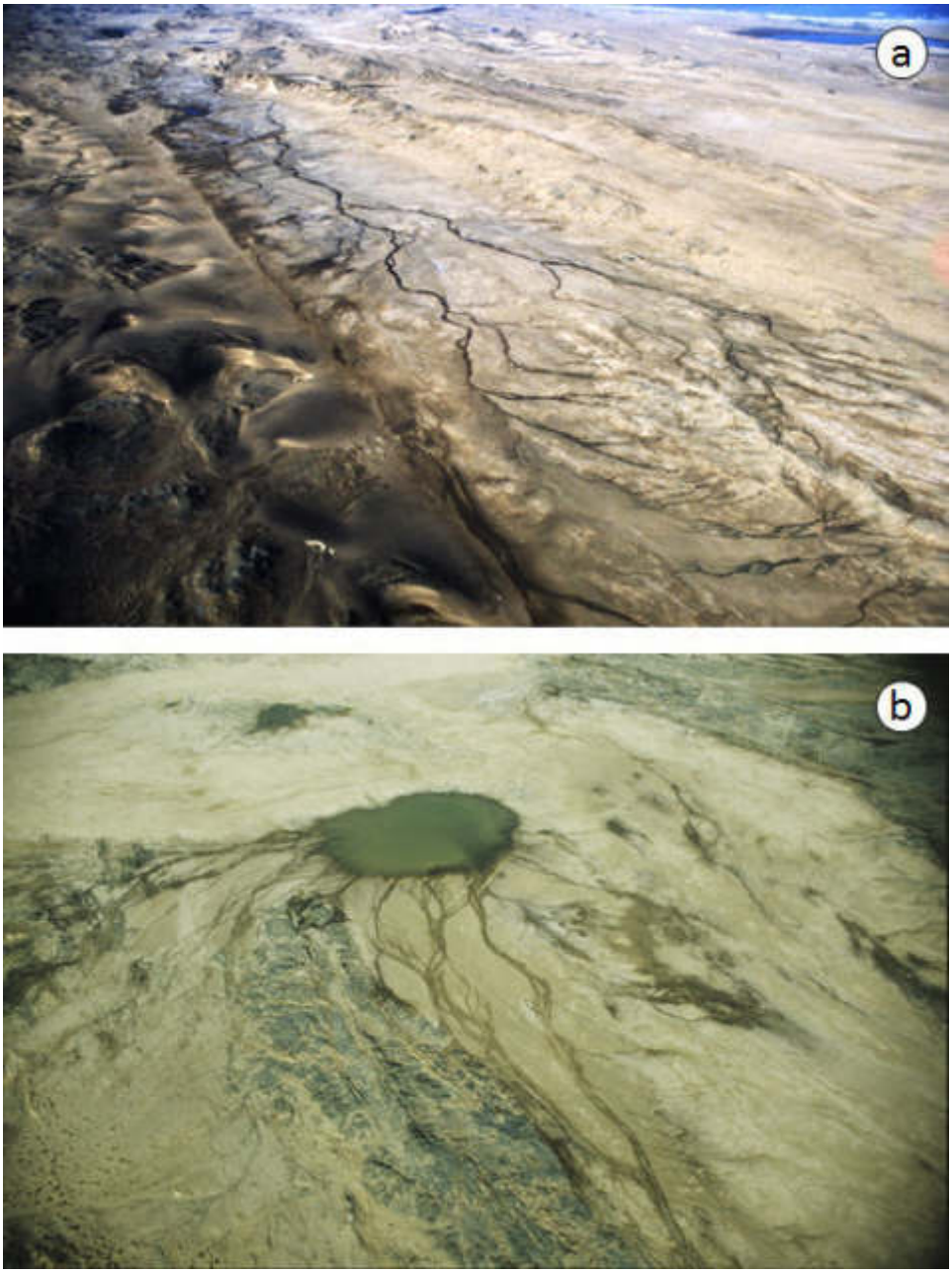

Figure 75. These images capture the essential architecture of ephemeral stream systems in endorheic basins within the NAEB. a) Oblique aerial view south, about 3 km west of the Buntfeldschuh escarpment. The ephemeral stream catchment is situated on the south-facing slope at the northern end of the endorheic basin. The tributary network feeds into a main channel, which enters the ponded water body formed at base-level at the southern end of the basin. Note the western margin of the Chameis Bay aeolian transport corridor in the bottom left corner. Southerly wind flow from top left to bottom right. b) Ponded water body at the distal end of numerous ephemeral stream channels crossing stone pavements flow into a minor bedrock depression south-east of Bogenfels – this is an example of one of Kaiser's (1926a) "gravitational centres".

Aeolian deposits are also reworked along the margins of the basins, and aeolian granule ripples are eroded in many cases (Fig. 77). These sediments are then incorporated into deposits on the ephemeral stream bed. Provided that rainfall is sufficient to maintain the run-off, the reworked aeolian material is transported back towards base-level.

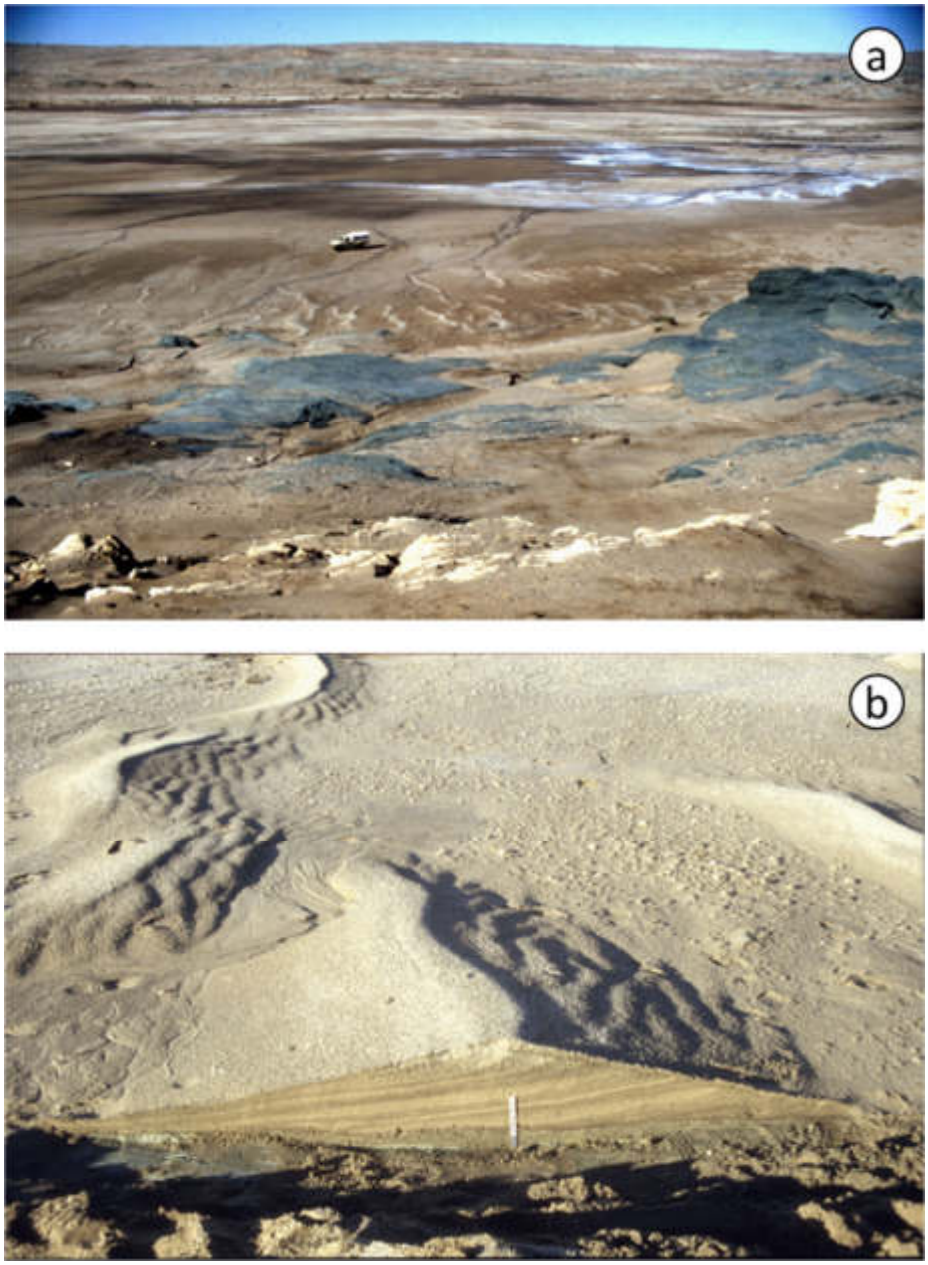

Figure 76. a) Bedrock catchment with granule ripples at the base of the slope being eroded by ephemeral streams. The granule ripples have been reversed by a high-energy northerly wind during the rainstorm. b) Longitudinal section through an aeolian granule ripple, showing crest reversal in response to the northerly wind of 17-20/07/87 – note the relative lack of granules within the predominantly sandy interior, with coarse particles localised close to the crest. A small ephemeral stream channel partially reworked the bedform. Note the very shallow depth of the deposit beneath the granule ripple, which rests on weathered bedrock. Southerly wind flow is from right to left. Scale 10 cm.

Major rainfall events rarely occur within the hyper-arid NAEB, but their role in terms of the regional sediment dynamics cannot be overestimated. In contrast to aeolian bedload transport which is comparatively slow to act, ephemeral stream systems transport large volumes of sediment, including sand and pebbles, in a very short space of time. Like northerly wind reversals, these events fundamentally disrupt the equilibrium of the aeolian system with the southerly surface-windflow. As a consequence they release vast quantities of material from temporary storage sites back into the aeolian sediment dispersal system, creating ideal conditions for peaks in sandflow to occur as the southerly regime dominates once more (Fig. 78).

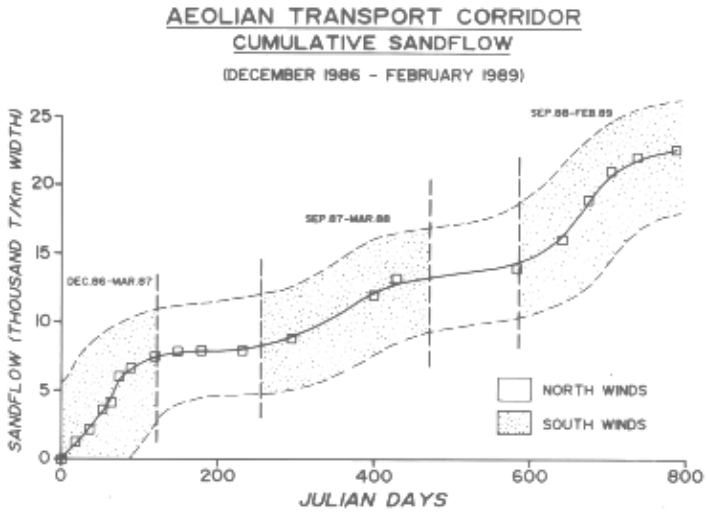

Figure 77. Seasonal variation in sandflow showing the cyclic alternation between destabilisation of southerly wind storage sites by north wind reversals and the peaks in sand flow that occur after them (from Corbett, 1993).

Events like these not only significantly influence the sandflow through the NAEB by creating stream beds which are actively deflated, but also play an important role in periodically accelerating the rate of bedload particle migration as well (see next section on stone pavement dynamics).

Ephemeral Rainfall, Drainage Systems and Aeolian Sandflow

If rainfall is insufficient to generate run-off, the dampening of the ground surface initially reduces the sandflow rate through the basin. The subsequent desiccation proceeds rapidly, and this effect is short-lived. Surface run-off leading to ephemeral stream activity has a much greater effect upon sandflow through the basin.

Ephemeral stream systems potentially erode large quantities of sand from temporary storage sites within the aeolian system. Once redistributed, these sands are initially out of equilibrium with the southerly wind regime. Consequently, the ephemeral stream deposits provide a widespread source of additional material for the aeolian system to erode and disperse. Therefore as desiccation proceeds after an ephemeral rainfall event, an initial increase in the sandflow rate throughout the deflation basin occurs.

The rate at which the floors of ephemeral channels are reworked initially depends upon the quantity of clay that is present in the individual stream systems. When clay is present the deposition of a fine-grained

surficial drape across the sediment surfaces on the floor of channels initially hampers aeolian deflation. Once aeolian abrasion of the drape occurs and desiccation of the clay exposes the underlying material to the aeolian system deflation is rapid.

In some cases the break-up of fine-grained drapes is also promoted by the presence of salt, which forms a crust as desiccation proceeds. The salt crusts further promote the destruction of the fine-grained drapes by causing doming of the sediment surface. This renders the modified surface more prone to abrasion by saltating particles as it is no longer protected by roughness elements provided by gravel. Aeolian deflation then proceeds quickly (Fig. 79).

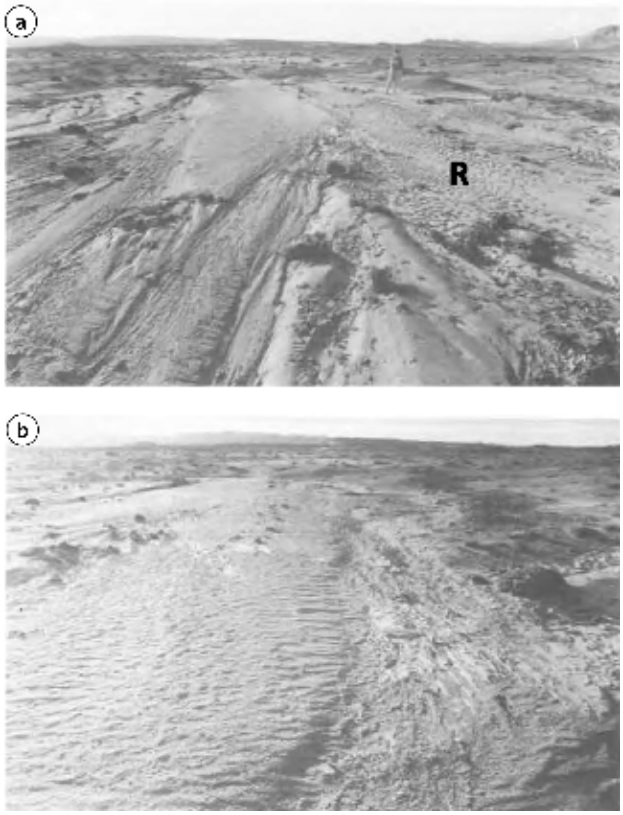

Figure 78. Comparative photographs of an ephemeral stream bed at Bogenfels. a) View north on 11/06/87, after rainfall on 2 and 3/06/87. Note the very shallow nature of the flow, and the large area of bed covered by current ripples (R). Flow towards the reader, person for scale. b) Enlarged view of the bed covered by current ripples on 19/06/86 after the break-up of the original clay/silt drape. Aeolian processes rapidly began to deflate the fine-grained material exposed on the bed once the carapace had been destroyed. As aeolian erosion continued, aeolian size sorting of the material took place. This led to the generation of a coarse-grained creep bedload population and granule ripple formation. The fine-grained carapace continued to be eroded in other places on the bed. Southerly wind flow from bottom to top, scale 30 cm.

Under the influence of high-energy southerly winds, fine-grained sediment is rapidly deflated from the surface of stream beds. This material can then be transported north into the Namib Sand Sea leading to a reduction in the quantity of fine-grained sediment within the NAEB (Kaiser, 1926a). This is the basis of the deflation hypothesis as a mechanism for the lowering of stone pavement surfaces through time.

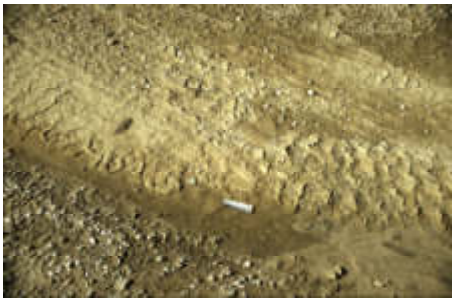

Figure 79. Floor of ephemeral stream bed being distorted by doming of the surface carapace by the growth of a salt crust. Once doming occurs the carapace is prone to abrasion by the saltation load.

The influence of pulses of sandflow on aeolian transport corridors is likely to be less noticeable than in other areas where minimal sandflow usually occurs. Here, sand reworked from storage sites can have a significant influence upon aeolian sediment dynamics.

Ephemeral Rainfall, Drainage Systems and Aeolian Bedload Transport

Kaiser (1926a) realised the importance of the interaction between the aeolian and ephemeral stream sediment dispersal systems. The south-facing slopes at the northern end of endorheic basins provide natural catchments for the ephemeral system. The aeolian current system transports material to the north, but the ephemeral current system redistributes material towards the south. This provides the potential to develop polycyclic reworking of sediment through the interaction of these current systems (Kaiser, 1926a). The ephemeral stream systems transport aeolian material down the south-facing slopes towards the base-level of the systems. As desiccation proceeds high-energy aeolian processes rework this sediment. The material comprising stream beds is then influenced by aeolian size sorting during its transport back up the topographic slope. As shown by the garnet creep tracers, the finer-grained creep bedload will be transported more quickly away from ephemeral stream beds and the coarser material will remain behind forming a lag that will eventually stabilise the bed.

Changes in the sandflow rate through the NAEB will also influence the bedload transport rate, because the frequency of saltation collision will increase. A brief peak in the bedload transport rate is likely to accompany pulses of increased sandflow through the basin.

Observations suggest that periods of ephemeral stream activity may be separated by several years or more. Aeolian processes therefore act uninterruptedly over comparatively long periods of time. Within ATCs considerable redistribution of bedload can take place over this sort of time-scale – by both reptation and creep transport.

The sediment dispersal pattern within endorheic basins should therefore reflect the combined influence of the aeolian and ephemeral stream systems. One or other of the two systems will be dominant, depending upon their ability to redistribute material and the periodicity with which ephemeral rainfall events occur.

Stone Pavements in the NAEB

McFadden *et al*. (1987) presented a model for the evolution of stone pavements that invoked particle generation at surface through:-

- Weathering of surface rocks and rubble,
- The effect of seasonal changes in the underlying vesicular soil horizon

causing displacement of overlying clasts on the pavement surface.

Through this process, an accretionary protective mantle develops, armouring the surface.

Whilst an extensive literature exists on pavements that are predominantly pedogenically influenced, relatively little has been written on the nature of stone pavements that are strongly influenced by aeolian bedload transport. Within the NAEB these occur under conditions of high-energy wind and sandflow. Where ATCs traverse stone pavements they produce extreme conditions for the ejection, entrainment and deposition of coarse aeolian bedload particles. This differentiates the stone pavements found in the Southern Namib from the desert reg or hamada surfaces that characterise other deserts influenced by lower-energy aeolian transport conditions.

Due to the different sedimentological character of the pavements within the NAEB, I have termed them "Dynamic Bedload Pavements" within this section on aeolian bedload transport and deposition. This does not preclude the likelihood that many of the processes first identified by McFadden (1987) also occur in the Namib.

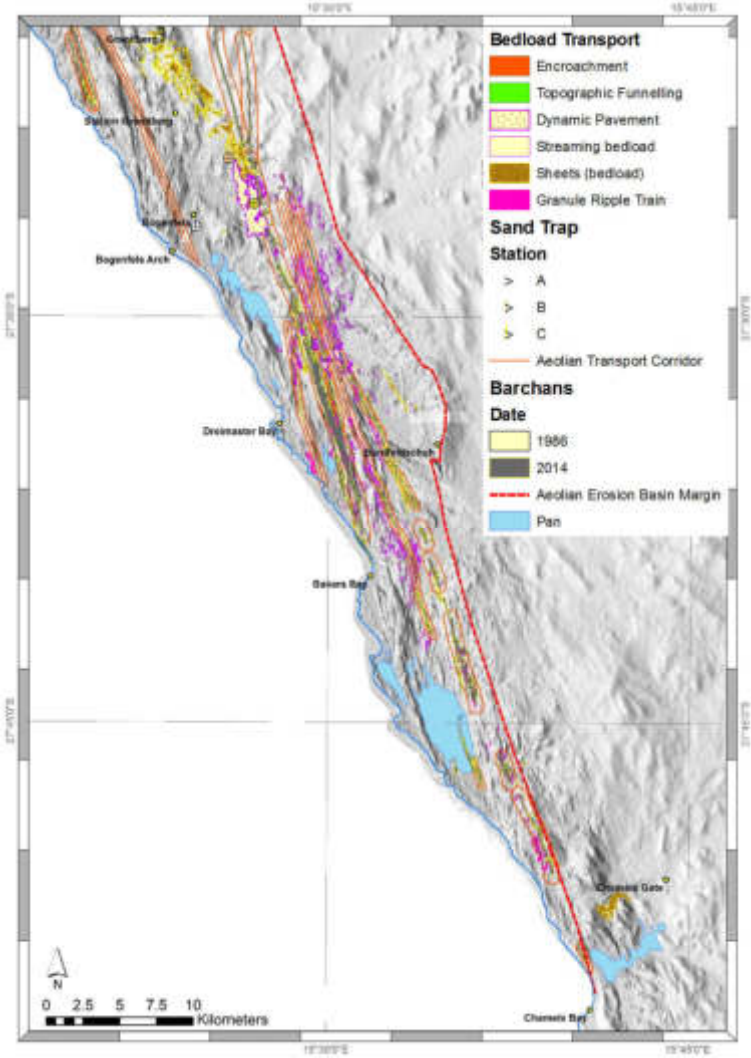

Figure 80. Overview of the pattern of sandflow from the Chameis and Baker's Bay point sources and the distribution of bedload transport within the selected study area described in this section. The distance from Chameis Bay to the northern end of the sheets containing coarse bedload at Granitberg is 73.6 km. Detailed explanations of the different bedload transport-related deposits are provided in the text.

Observation of the recovery of pavements on areas cleared during sampling for diamonds suggest that in all probability similar pedologic processes do occur, as the vesicular soil horizon can be seen to be widely present beneath them. It is thus interesting to note that the ATCs are generated in areas where large salt pans exist creating the potential for aerosol generation.

However, for this paper, the focus is on the surface expression of coarse-grained aeolian bedload transport processes.

Examination of Figure 81 will show the observer that one of the larger areas of dynamic pavement lies immediately to the east of Bogenfels.

Figure 81. Aerial view looking south (upwind) along the Baker's Bay ATC. The barchan was close to the sand trap site "C". Note the large expanse of dynamic pavement characterised by coarse bedload transport to the right of the dune train. The streaks of sand immediately north of the right horn of the barchan delineate the windflow pattern on the pavement surface. Corbett (1989, 1993) interpreted this as evidence of secondary flow retaining sandflow to within the narrowly-defined ATC pathway.

The pavement surface is characterised by quartz-rich gravels that have been produced through the weathering of an alluvial fan sequence called the Blaubok Conglomerate. The alluvial sequence overlies a fine-grained marl that contains the trunks of silicified trees (Pickford, 2015) which have been assigned an Eocene age (Bamford 2003). The Blaubok Conglomerate was deposited during the Oligocene according to Pickford (2015). Unlike low-energy pavement surfaces produced mainly by pedologic processes that characterise many piedmonts in other desert regions (Pelletier *et al*. 2007), the surface of this stone pavement provides much evidence to show that aeolian bedload transport is actively occurring across its surface (Fig. 83).

Figure 82. View of fragmented silicified tree trunk. Note the quartz-dominated bedload encroachment against the windward (south) side through the opening between fragments of the Eocene tree trunk. Sand current shadows have formed in the lee. North to top, scale 1 m in length in 10 cm divisions.

Three types of particle occur on the stone pavement surface:-

- Immobile roughness elements large than -4 Phi (16 mm) diameter;
- Coarse-grained bedload creep and reptation load from 1.0 to -3.5 Phi (2 mm to 12 mm) diameter;
- Sand fractions comprising the saltation load stored within the stone pavement.

Pavements with Regularly-Spaced Immobile Roughness Elements

The surface configuration of stone pavements varies widely. On some stone pavements the roughness elements exhibit a preferred orientation, with the long axes aligned approximately transverse to the surface windflow. On these pavements, roughness elements are observed to form regularly-spaced rows (Fig. 84).

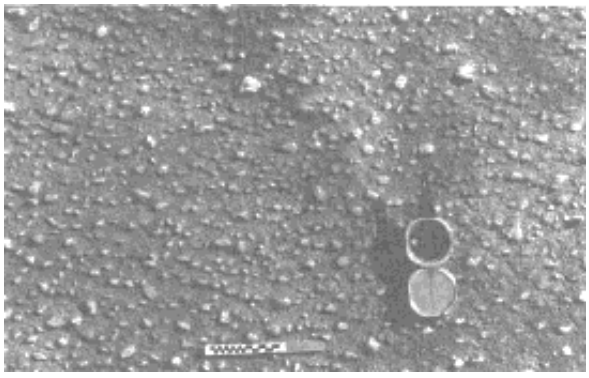

Figure 83. Quartz roughness elements forming a stable stone pavement near Fröhe Hoffnüng, exhibiting preferred orientation with their long axes transverse to the prevailing southerly wind which blows from bottom to top of frame. Note the regular arrangement and spacing of the roughness elements which are separated by a sandy bed. Pitting on the sand surface is due to rain impact and rainsplash erosion. Scale 10 cm, compass pointing north.

In these situations the bed between roughness elements is commonly sandy, with current crescents scoured along the upwind-facing (south) side. Similar observations led Bagnold (1941) and Sharp (1963) to conclude that surface stabilisation by organisation of roughness elements was due to wind scour at their base causing immobile clasts to lean, roll-over and eventually reorientate. This process of vortex generation and scouring has recently been recorded in field-based wind tunnel experiments to investigate aeolian erosion and deposition on gravel beds (W. Zhang *et al*. 2014). Under high wind velocities erosion of the intervening bed continues until the height and spacing of the roughness elements protect them from further bombardment by saltating grains (Chepil, 1945b) and the drag on the intervening bed is too low for entrainment by aerodynamic forces alone (Lyles *et al*. 1974) whereupon deflation ceases.

On ordered surfaces of this kind Chepil (1945a, b) found that the angle from the top of one immobile element to the base of the next varied from 4° to 12° on beds that had stabilised. Stone pavement casts from the southern Idatal exhibited angles of between 4° to 7°. The ratio of roughness element spacing to height varied from 8.4:1 to 11.5:1. The similarity to Chepil's (1945a, b) measurements indicate that the mature surface had reached stability and that impacting saltation load could no longer affect the intervening sand bed.

Dynamic Aeolian Bedload Pavements & the Bedforms that Characterise Them

Natural stone pavements are not featureless. They have subtle undulations and a variety of small-scale bedforms on their surface.

These pavements are characterised by immobile roughness elements separated by a bed that is covered by granules and small pebbles. The clast composition varies depending on the source of the pebbles – surfaces with exotic clast compositions include particles derived from the reworking of sedimentary sequences eroded due to topographic/basin inversion.

Micro-topography occurs in association with immobile roughness elements, which act as barriers to bedload migration, becoming nuclei for particle cluster formation as particles creep and reptate northward (Fig. 85). These bedforms are similar to those formed on the gravel bed of fluvial channels (Dal Cin, 1968; Laronne & Carson, 1976).

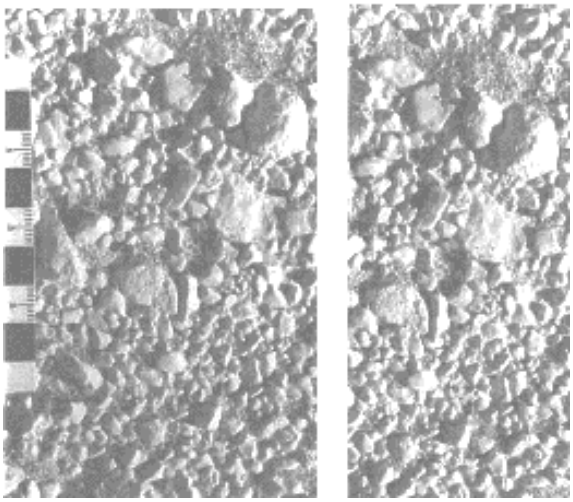

Figure 84. Stereo view of a small, granule covered mound on the upwind side of an immobile roughness element on the stone pavement near sand trap site C, forming a particle cluster. Note the imbricate shape-fabric of some of the creep bedload, some of which are small ventifacts. Southerly wind flow from bottom to top of frame. Scale in cm.

Studies by Allen (1982) and Brayshaw *et al*. (1983) imply that very high bed pressure will develop along the windward edge of roughness elements and along sections of their margins, creating vortices. Particles entering these zones become unstable and can be seen to vibrate under the influence of strong vortices which periodically entrain the grains short distances along the side walls. Selective sorting therefore takes place according to variation in particle size and density. Less mobile grains progressively become lodged along the leading edge of the roughness elements creating bottlenecks and retarding bedload migration, a situation described by kinematic wave theory (see later section).

The windward (south) surface rises fractionally as the roughness element is approached. The resulting mound is covered by granules and small pebbles which form particle clusters exhibiting a well-developed imbricate shape fabric. The clasts are inclined into the southerly surface windflow. Current shadows of medium- to coarse-sand grade form in the lee of roughness elements.

Where a gap oriented transverse to windflow separates two or more roughness elements, the bed between them, comprised of granules and small pebbles, is slightly elevated, and the clasts are frequently imbricated (Fig. 85). A downwind-facing step forms some distance north of the gap. The bed elevation then drops abruptly back to the level of the surrounding bed, and sand deposition occurs in the lee of the step.

Figure 85. Stereo view of plaster cast taken on stone pavement at sand trap site C. Particle clusters can be seen in the gaps between neighbouring roughness elements on the bed (arrowed). In addition, further examples of particle clusters on the upwind side of roughness elements can be seen. Examples of small aeolian current shadows can also be seen in the lee of some of the roughness elements. Note that many of the creep bedload particles are imbricated into the southerly wind flow, which blows from left to right. Scale in cm.

Low, ripple-like bed forms generally less than 2 cm high are a common feature of stone pavement surfaces traversed by ATCs (Fig. 86). Stoss slopes varying from 5 cm to 10 cm wide are covered by imbricated, tightly packed, very coarse sand and granules at their base. The grain size gradually increases towards the crests, which are generally less than 30 cm long. The crests are marked by accumulations of small and medium quartz pebbles which have a tendency to become preferentially oriented with their long axes parallel to the southerly surface-wind. The crest shapes vary from slightly crescentic to relatively straight.

Figure 86. Bogenfels ATC pavement west of main barchan with sand trap site. Detail of surface showing the ripple bedform on the stone pavement. Note the density of packing, grain imbrication with long-axes of particles parallel to prevailing wind and sandflow - this is a stable surface that has reached equilibrium with the prevailing southerly wind and sandflow. North to right. Scale 11.5 cm long

The gently sloping lee face, downwind of the crest, is composed of medium- to coarse-sand, but scattered granules and small pebbles commonly occur on them. Wherever dynamic bedload pavement surfaces are disturbed, patches of tightly packed granules and small pebbles displaying an imbricate fabric are found covering the surface – this differs from low energy pavements, on which sand accumulates in depressions on the surface. Abandoned, or infrequently used game trails provide good examples (Fig. 87).

Figure 87. Rarely used game trail crossing the stone pavement near sand trap site C. Note that the surface is now covered with quartz granules which have been transported into the depression by creep, and exposed by deflation. The streaky appearance of the bed is caused by the distribution of the creep bedload. The streaks are aligned with the southerly wind, which blows from the lower right to upper left corner of the frame. Note also that in the foreground there are numerous aeolian current shadows in the lee of vegetation and large roughness elements on the bed. These are temporary sites of sand storage within the aeolian system. Scale 11.5 cm.

Fieldwork throughout the NAEB showed that the development of an imbricate shape-fabric is a common feature of dynamic bedload pavements. Although the forward movement of grains forming clusters is retarded, saltation bombardment continues to add additional bedload to particle clusters and bed forms on the stone pavement surface. As a result, the creep bedload particles become densely packed, and an imbricate shape-fabric is developed. Observations under controlled conditions in a wind tunnel are required in order to establish the mechanism for this. It has not been possible during this study, but the consideration of observations from flume experiments possibly provides some insight as to what happens.

According to the experimental results of Brayshaw *et al.* (1983) an area of very high bed pressure exists along the leading edge of particles on the bed. Hence wind scour can be anticipated to occur, forming small scour hollows. Provided that scouring continues, the grains will ultimately slide into the hollows, and tilt, so that their upper surfaces face into the southerly surface-wind flow.

Fahnestock & Haushild (1962) observed the initiation of an imbricate shape-fabric by a similar mechanism in flume experiments. Scour at the upstream edge of bedload particles obstructed by an obstacle on the bed created small upstream scour hollows. The particles, which were previously rolling with their long axis transverse to flow, subsequently sank into the hollows, and rotated until their long axes were parallel to the flow, and their upper surfaces were tilted up-current. Once this shape-fabric is developed by the aeolian creep bedload forming encroachment deposits or stone pavements, inclined particle surfaces are exposed to the saltation load. Saltation collisions then possibly become less effective in ejecting particles because:-

- Impacting grains glance off the imbricate grain surface;
- The inclination of the surface alters the horizontal and vertical component of the collision force acting on the stationary grain (Fig. 88);
- Or, once the grains are imbricated, experimental evidence suggests that the pivoting angle is substantially increased relative to those which are not (Li & Komar, 1986).

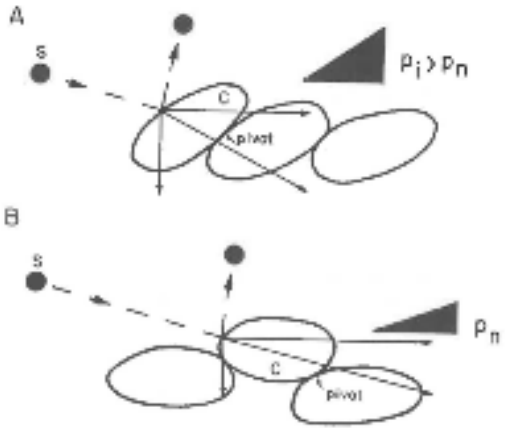

Figure 88. Sketch illustrating the suspected role of the imbricate shape-fabric in modifying the direction in which the impact force acts on a bedload particle on the bed. Note schematic representation of the envisaged difference between the pivoting angle of imbricate grains (pi) and non-imbricate grains (pn).

A reduction in the frequency of ejection and entrainment into reptation and/or creep may then result because a smaller proportion of the saltation load is capable of supplying sufficient collision force to overcome the relative increase in the

pivoting angle. Surfaces exhibiting this high degree of particle orientation become stable, and reach a state of equilibrium with respect to the southerly surface-wind flow.

The turbulent wakes shed from upwind, closely-packed, similarly-sized particles covering the bed, impinge on the inclined surfaces of succeeding particles downwind, and not on the intervening bed (Brayshaw, *et al.* 1983). The increased packing density of the particles thus prohibits any further deflation of the sand fraction which underlies the sediment surface.

In the high-energy aeolian environment of the NAEB, imbrication is probably one of the most stable bed configurations that a stone pavement surface can attain, and erosion by aeolian deflation is reduced to a minimum. However, the garnet creep tracers showed that some creep activity persists across these stabilised surfaces. Hence particles which are not locked into the imbricate shape-fabric continue to move by creep, reptation and periodic saltation until they themselves become trapped in the pavement fabric.

Reptation and creep transport of bedload particles is thus maintained even when pavement surfaces stabilise, and bedload continues to migrate progressively through the NAEB.

During very high sandflow conditions, when large grains might be entrained into saltation, stabilised pavement surfaces are possibly disrupted due to abnormally large saltation impact forces. Imbricate particles may then be dislodged from the stable surface and reintroduced to the creep population. The vacant space on the pavement is then possibly closed-up by modification of the bed configuration or the addition of new particles from upwind may replace the eroded grain to re-establish stability.

The dynamics of the creep bedload moving through the complex micro-topography of stone pavements within the deflation basin appears to resemble the behaviour of unidirectional traffic flow approaching bottlenecks along a road. It thus seems to behave in the manner predicted by kinematic wave theory, as described by Lighthill & Whitham (1955a, b).

Theoretically, provided that the system is not disrupted, the movement of bedload across the stabilised bed will continue until the entire upwind reach of the aeolian transport corridor attains equilibrium with the southerly surface wind regime. If this were to occur, aeolian removal processes would cease completely. In reality, a combination of other aeolian processes, weathering processes and current systems also operate to modify the shape, size and distribution of immobile roughness elements. Viewed over a sufficient time-scale, this limits the degree to which the bed can establish and maintain equilibrium.

Destabilisation by Northerly Wind Reversals

Photography of stone pavement surfaces during high sand flow events is difficult, not only due to the sand in saltation, but also because gusting causes camera shake. A photographer's presence can also dramatically alter the pattern of surface windflow over the bed. In order to try to overcome some of these difficulties the garnet creep tracers were photographed on 22/09/87 during a moderate-energy northerly wind reversal.

The stone pavement surfaces are usually in equilibrium with the southerly surface-windflow. During a northerly wind, the imbricate shape-fabric is less effective in stabilising the surface grains, and some of the bedload creep population is likely to be dislodged from stable positions on the bed (Fig. 89). This results in the partial destruction of equilibrium with the southerly surface-wind.

Northerly winds are therefore instrumental in reintroducing creep grains to the mobile population, and maintaining northbound bedload transport through the basin.

Cooke (1970) noted that wind abrasion features were rare on stone pavements that he studied in the Atacama and Californian deserts, except in exposed coastal zones and in the high Andes where winds are strong and loose abrasive materials are available.

Such conditions are widespread in the NAEB, where ATCs should provide optimal conditions for aeolian abrasion due to the high sandflow over stone pavements. Field observations support this concept. Many roughness elements exhibit evidence of aeolian corrasion. The facets cut into the roughness elements are predictably best developed on south-facing surfaces. The facetted surfaces are either rather flat or fluted (Fig. 90) or are concave-up and smoothly polished (Fig. 91).

On some windward surfaces of immobile roughness elements, a sub-horizontal step can be observed to have been cut just above the ground surface (Fig. 92, 93). The height at which this step is cut probably indicates the height at which the kinetic-energy flux of the saltation load (sensu Anderson, 1986) declines close to the bed.

Ultimately, whatever form of corrasion initially takes place, given sufficient time, it is likely to plane the roughness element almost level with the surrounding bed (Fig. 94). The achievement of the end-point of modification is probably rarely observed because the surfaces are disturbed by other factors. It is probably most frequently attained where relatively soft clasts of pan carbonate (calcite, with minor dolomite) and Bogenfels Formation dolomite occur on surfaces.

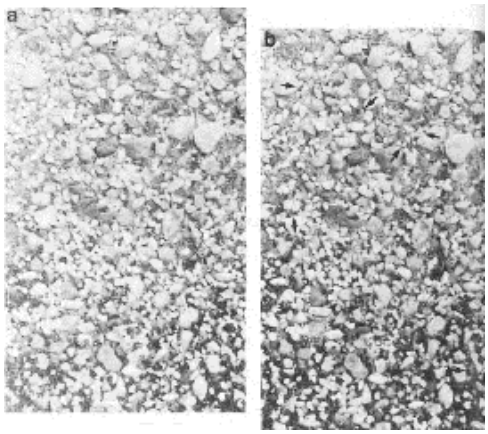

Figure 89. Stereo-pair of stone pavement taken during a northerly wind reversal on 22/09/87. (a) was taken about 5 minutes before (b). The arrows highlight the pervasive changes which effected the bed configuration as reptation and/or creep transport proceeded. The dark grains are the garnet bedload creep tracers used in the experiment on the stone pavement near sand trap site C. Note how some of the grains become lodged behind the immobile roughness elements.

Initially, aeolian corrasion modifies the pattern of wind flow in the vicinity of the roughness element. This is liable to change the pattern of bed shear stress surrounding the roughness element. The configuration of the creep bedload on the stone pavement must readjust if surface stability is to be maintained. The alteration of cross-sectional profiles is also likely to modify the pattern of vortices shed by the roughness element. Thus the points at which the high-velocity vortices impinge on the downwind bed will vary with time, resulting in further readjustment of the bedload. In addition, as the cross-sectional area of the roughness element protruding above the bed is reduced, the extent of the lee-side shadow zone protected from direct

saltation impact during southerly wind flow decreases. Pervasive alteration of the bed configuration over a· wide area downwind of the modified roughness element probably then results. This reflects the extensive sphere of influence which roughness elements impart on the downwind bed configuration.

Figure 90. Cobbles and boulders of silcrete on a stone pavement hosted by an alluvial deposit. The windward faces are severely facetted and fluted, and bedload covers the surface between the immobile roughness elements. The barchan dune in the top right corner (arrowed) shows the site's proximity to the centre of the Baker's Bay ATC. The southern end of the main dolomite yardang field, approximately due east of Pomona, can be seen to the north of the stone pavement.

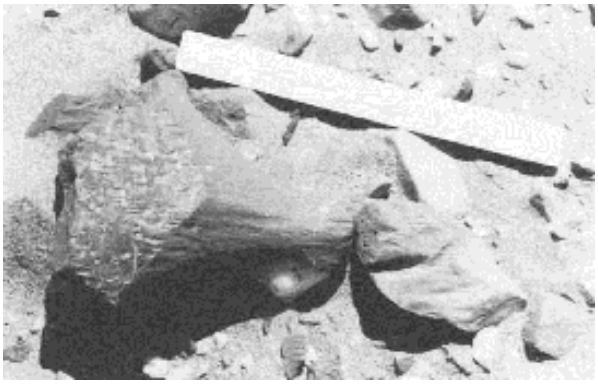

Figure 91. Concave-up facetted surface of a phonolite cobble on an alluvial plain at the eastern margin of the Baker's Bay ATC approximately due east of Bogenfels. Note the fluting on the upper surface, which appears to be initiated where feldspar phenocrysts are exposed. The silcrete clasts on the upwind side have been polished by aeolian processes. Southerly wind from right to left. Scale 30 cm.

Figure 92. Stepped facet cut into a quartzite cobble on a stone pavement surface at the eastern end of the Grillental. The step probably marks the height at which the saltation load's kinetic-energy flux diminishes above the bed. Note the particle cluster on the bed (arrowed) in the lee of the clast. Southerly windflow from left to right, bar on scale 10 cm.

Once a roughness element is planed to the approximate elevation of the surrounding stone pavement, its influence is reduced considerably. Provided that the step, marking the upwind margin is sufficiently elevated above the bed, it will act as a barrier to the migration of the creep bedload (Fig. 95).

Figure 93. Calcrete pebble with a sub-horizontal step cut into the south face. Had this process continued, the entire clast would have eventually been planed at the bed elevation. Note the small knobs and bosses near the top of the windward face, which formed in response to differential corrasion due to the presence of small quartz grains in the calcrete. Scale 10 cm.

Figure 94. Sternsfelder - aeolian corrasion modification of a quartzite cobble. Note adhesion structure at base of cobble on salt crust surface on the floor of an ephemeral stream bed. North to bottom right. Scale 10 cm.

Figure 95. A roughness element of Bogenfels Formation dolomite planed approximately level with the surrounding bed by aeolian corrasion. Note the small knobs and bosses formed due to small patches of quartz in the dolomite. There is a small step along the windward (left) edge, which forms a minor obstruction to the migration of the creep load. A particle cluster is present along this temporary barrier. This clast lies directly in the path of a 28 m high barchan dune within the Baker's Bay ATC, which accounts for the large amount of sand stored on the pavement surface. Scale 10 cm.

Other Processes Destroying Immobile Roughness Elements

Other weathering and erosion processes influence the spacing and density of roughness elements on stone pavement surfaces within ATCs, but evidence of them is destroyed by aeolian corrasion and transport.

Stone pavement surfaces located beyond the influence of ATCs do not exhibit the same degree of surface organisation (Fig. 96) despite the continued, but reduced, influence of the aeolian dispersal system. The cracking / splitting and spalling of clasts appears to be a common feature of pavement surfaces, many of which contain large cobbles and boulders derived from underlying and surrounding alluvial and / or marine deposits.

Figure 96. Example of a stone pavement outside the influence of an active aeolian transport corridor. Note that the surface does not show the same degree of organisation and that there is much less evidence of aeolian bedload moving between immobile roughness elements. A silcrete clast (S) and a dolomite clast (D) have been split. This is a feature of these stone pavements. Quadrant marked in 10 cm divisions, arrow shows the direction of southerly wind flow.

The spalling of successive layers from clast surfaces protruding above the stone pavement surface particularly seems to affect quartzite clasts (Fig. 97).

Figure 97. Quartzite boulder on a stone pavement surface overlying Upper Eocene marine deposits near Bogenfels. Note the spalling of the surface. Fragments have been removed from the south face by aeolian corrasion. Southerly wind flow from right to left. Scale approximately 15 cm.

This form of weathering produces angular, platy fragments and smaller debris as succeeding layers are loosened, reducing the height of the roughness element. Loose flakes are eroded from the south-facing surfaces by aeolian corrasion, whilst the flakes remain attached to downwind surfaces.

Ultimately, evidence of the original roughness element is virtually destroyed by weathering. Pebbles, possibly transported to the site by ephemeral surface run-off, or

brought to the surface by soil-forming processes, or deflation, subsequently occupy the space created on the stone pavement surface (Fig. 98).

Figure 98. A quartzite cobble that has almost been destroyed by spalling. Note that clasts have migrated into the gap produced on the stone pavement surface, masking the presence of the relics of the original clast beneath the surface. Scale in cm.

Cracking or splitting of clasts on stone pavements (Fig. 99) has been widely reported and studied in many deserts (Cooke, 1970). In the NAEB it affects a wide variety of different rock types, including quartz, quartzite, silcrete, phonolite, dolomite, and pan carbonate.

Many of the affected clasts show little evidence of planes of weakness, although the presence of bedding planes within them is frequently exploited.

As with examples of splitting from other desert regions (Cooke, 1970) the fracture orientation relative to the stone pavement surface varies widely, and there is no distinct evidence of chemical alteration.

Figure 99. Split phonolite boulder on a stone pavement formed from an alluvial host. The fragments are close-fitting, and there is little evidence of planes of weakness. Scale 0.75 m.

Excavation revealed that the fractures continue below the stone pavement surface, but they close with depth in some instances (Fig. 100a, 100b). This implies that they have opened at the sediment surface, where the addition of loose granular material progressively infills the opening.

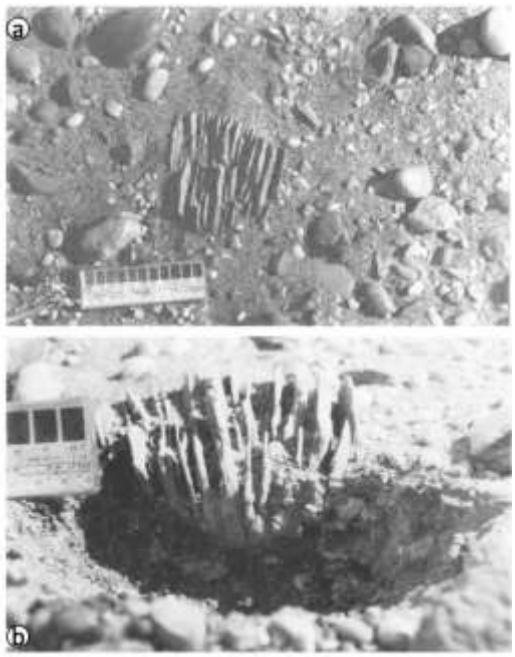

Figure 100. a) Stone pavement surface with a quartzite clast split along bedding planes. The fragments are approximately parallel with the southerly wind flow from bottom to top. Note the absence of quartz granules of creep bedload. Scale 11.5 cm. b) Section along south edge of split clast showing closure of the fractures with depth. Fine-grained sediment infills gaps, possibly by infiltration into the bed during fog or rainfall. Coarser grains between the split fragments were probably transported there by aeolian creep. Scale in mm.

Split clasts on stone pavement surfaces also act as nuclei for creep bedload particle clusters to develop. Splits oriented into the southerly surface-wind provide openings into which the creep bedload can migrate (Fig. 101).

Figure 101. Split and facetted quartzite clast on an alluvial surface in the Grillental. Note that the creep bedload particles have migrated into the south end of the wind-aligned split. This provides a possible mechanism for the maintenance of the split once it is initiated. In this instance it also resulted in the development of a particle cluster on the bed at the leading edge of the roughness element. Quartz granules along the windward edge and eastern side exhibit a poorly developed imbricate shape-fabric. Small particles occupy unstable positions along the leading edge where vortices potentially move them to the margins of the roughness element. Also note the aeolian current shadow on the north side of the roughness element. Southerly wind flow from bottom to top. Scale about 15 cm.

This is one mechanism by which grains enter the crack, allowing the split to be maintained.

The process by which cracks are initiated is a controversial subject. Ollier (1965) proposed the concept of dirt cracking, which Dorn (2011) has shown to occur in response to the wetting and drying of fine-grained sediment fills and/or the precipitation of calcium carbonate into fissures. Both progressively lead to expansion of the cracks. Salt weathering has also been proposed as a mechanism to explain this surface phenomenon in other deserts (Cooke, 1970, 1981; Goudie & Day, 1980).

Kaiser (1926a) (who recorded that rocks cracking sounded like gun shots in the otherwise quiet desert) thought the cracks were due to insolation. This process has also been supported by a number of later studies (McFadden *et al.* 2005; Wells *et al*. 2014). However, research has shown that thermal stress created by the temperature gradient that forms in response to rapid variation in temperature provides a powerful fragmentation mechanism (Hall 1999; Hall & André 2001). Recently the author undertook a detailed programme of research to investigate the effect of thermal gradient/stress on the fragmentation of rocks, and found that it does indeed cause microfractures in crystalline rocks. The Namib, with the strong temperature contrast that accompanies the incoming Benguela Fog presents an almost ideal environment for this phenomenon to occur given that Hall (1999) has shown that thermal contrast of 2° C is enough to initiate fracture.

In light of the above, it seems likely that cracking results from a variety of processes. All of them susceptible to subtle local variations or differing combinations in different geomorphic contexts and climatic settings.

Returning to the morphology of stone pavements, Cooke (1970) demonstrated that an important effect of splitting clasts is to increase the density of roughness elements on stone pavement surfaces through time. In the NAEB the accompanying reduction in the size of the clasts forming roughness elements performs another function, because in this high-energy aeolian dispersal system weathered fragments can be entrained into both the aeolian saltation and the bedload. As a result surfaces can be lowered by the combined effect of aeolian deflation of fine-grained sediment and the bedload transport of significantly coarse particles. Evidence of this is provided by the ALS data in the vicinity of Bogenfels (Fig. 102). Topographic inversion due to the progressive erosion of the Gemsboktal Conglomerates has formed a series of steps from east to west as the surface is lowered. Given the location of this example, there is little doubt that salt weathering due to saline aerosol distribution off the large Bogenfels Salt Pan has also played a role. Given the large embayment formed by the Bogenfels Sub-Basin some influence of marine erosion can also be expected to be present, although no direct evidence has been observed with the exception of the 4 m transgression which encroached into the embayed feature. The beach is in the crescent defined by the small northern pan backed by an inverted surface covered by a thin veneer of the Gemsboktal Conglomerate Formation.

In areas outside aeolian transport corridors, this material might remain on the surface for a long time, until a change in the coastal morphology alters the position of high sandflow zones.

As shown in the Bogenfels example, slope processes, acting in conjunction with ephemeral rainfall (see next section) and surface run-off, also contribute to pavement erosion by redistributing the products of weathering.

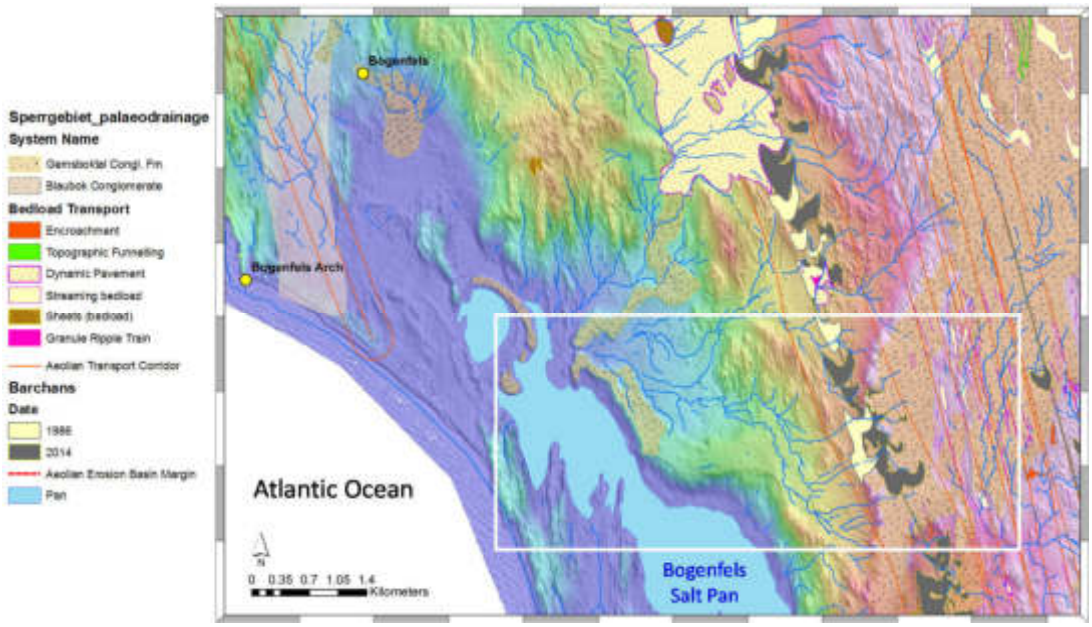

Figure 102. Coloured ALS DEM outlining changes in elevation with example of large-scale topographic inversion taking place south of Bogenfels. Progressive erosion of the Middle to Upper Miocene Gemsboktal Conglomerate Formation is resulting in lowering of the surface elevation - the area inside the white rectangle shows a series of topographic step-downs from east to west. It is highly probable that in the past ATCs passed directly over the area of inversion to the west of the main Baker's Bay ATC defined by the train of barchan dunes. Note the position of the inversion in relation to Bogenfels Salt Pan. Saline aerosols driven off the pan by the prevailing southerly wind regime probably contribute to the ongoing weathering of the alluvial sequence. Simplified modern drainage pattern is shown in blue.

Destabilisation of Dynamic Bedload Pavements by Ephemeral Rainfall and its Effect on Sandflow

Although it has been postulated that raindrops influence stone pavement surface configurations (Cooke, 1970) as far as the author is aware it has not been observed directly.

The link between hyper-aridity and extreme aeolian erosion landscapes has been highlighted by a number of authors (Goudie, 2008). However rare rainfall may, when it does occur, play an important role in sediment dynamics. In the NAEB the incidence of heavy rainfall tends to coincide with high-energy northerly wind reversals. A classic example of such an event occurred between 18/7/87 and 20/7/87. It was linked to the passage of a coastal low air pressure cell moving south down the coast in response to the passage of a cyclone to the south of the continent (Fig. 103).

Atmospheric pressure fluctuated markedly prior to the main event, which resulted in several low-energy wind reversals, typical of the winter months. The atmospheric pressure recorded at Alexander Bay showed a period of deep low pressure between 17/7/87 and 19/7/87, which corresponded with the intense peak in northerly wind-energy that was experienced at Bogenfels, during the main rainfall event.

People witnessing the main period of rainfall stated that it was unusually heavy for the west coast. The rain was accompanied by very high-velocity northerly winds. Evidence of this wind reversal was widespread. Prior to this event, the stone pavement surface to the east of Bogenfels exhibited a high degree of surface organisation, and was effectively in equilibrium with the southerly surface-wind regime. No evidence of this state remained on 20/7/87 (Fig. 103).

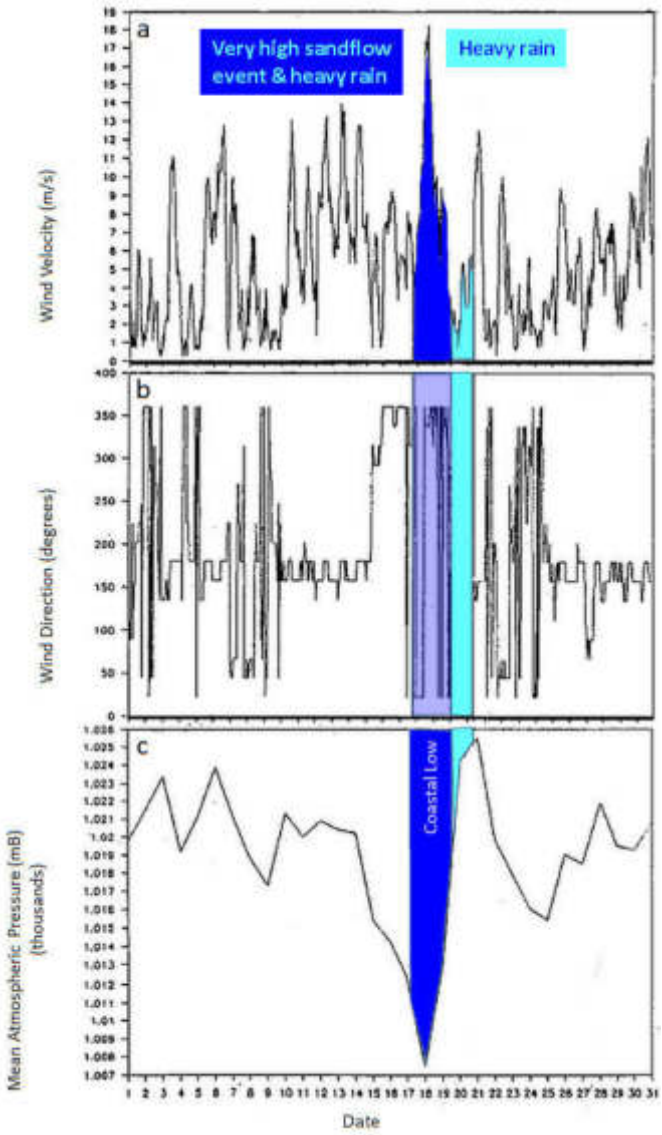

Figure 103. Graphs showing the variation of a) the wind speed, b) the wind direction, and (c) the atmospheric pressure during July 1987. Pressure records are for Alexander Bay. Note that the peak in northerly wind energy clearly corresponds to the sharp reduction in atmospheric pressure, interpreted as a coastal low. The duration of the rainfall event is also shown.

The changes were remarkable. Granules and small pebbles of quartz were reorganized into low ridges resembling ripples, one or two grains high, which were approximately oriented transverse to the northerly wind flow. The 'surface configuration' resembled that observed after an earlier rainfall event in May 1985, which was better developed (Fig. 104). In addition, granules and small pebbles of quartz could be seen piled up on the sediment surface.

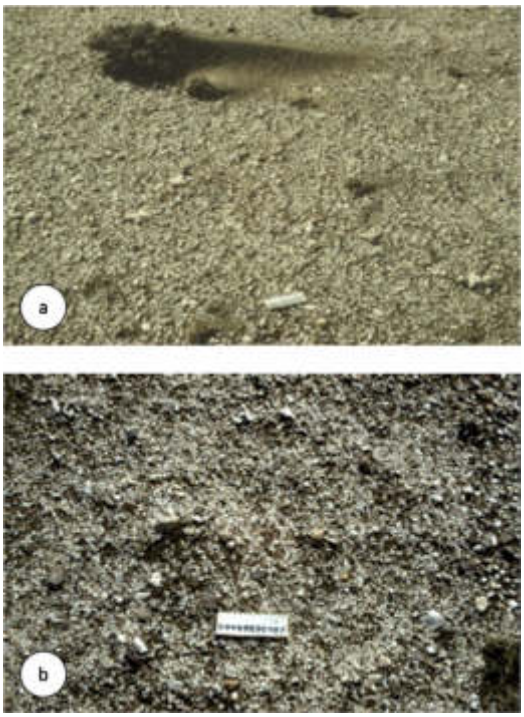

Figure 104. a) Completely reversed aeolian current shadows in the lee of vegetation in response to high-energy wind reversal. Note the disorganised, chaotic appearance of the stone pavement near sand trap site C. Northerly wind flow from left to right. b) The destruction of the imbricate shape-fabric and close packing of the creep bedload by rainsplash erosion. The underlying fine-grained material has been exposed, and eroded deeply by raindrop impact. Northerly windflow from top to bottom. Note that the quartz granules have accumulated in discrete patches. Scale 11.5 cm long.

Some of these particles were imbricated, but their upper surfaces were inclined to the north (i.e. opposite from previous observations), and uneven, deeply eroded pits separated the larger clasts (Fig. 105). Some particles could be seen standing on their edge on the floor of some of these pits.

Prior to 20/07/87, rainfall events observed were not as heavy, and evidence of rainsplash had been limited to rain-impact craters on silt and clay surfaces in ephemeral stream beds and the margins of ponded water bodies, on which a similar ripple-like effect had been observed.

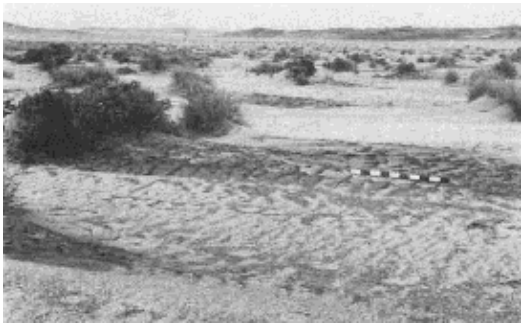

Figure 105. Ridged, sandy surface marking the earlier position of an aeolian current shadow (now reversed), on which rain-impact ripples have formed. Ripple-like, transverse bedforms in the foreground have developed on a previously planar encroachment deposit surface. Northerly wind flow from right to left. Scale l m.

Craters formed in the troughs due to raindrop impact, and ridges a few millimetres high formed rain-impact ripples (sensu Clifton, 1977). Rain-impact craters were absent from the crests, possibly reflecting a tendency for ridges to be flattened by repeated raindrop impact once a certain height related to raindrop size has been attained, as described by AlIen (1982). Raindrop impact also resulted in transverse ridges forming on the surface of aeolian current shadows, with the steeper face inclined into the northerly wind and the falling rain. The surface of the bedload encroachment deposit between the aeolian current shadows was modified into a series of distinct ridges by repeated raindrop impact.

Another form of pavement reorganisation was observed near Marmora Pan, where rain impact left large quartz roughness elements perched on top of sand pedestals between 0.5 to 1 cm high, surrounded by sandy depressions with pitted floors (Fig. 106). Ridges of sand associated with these features were pointing to the south forming scour-remnant ridges in the lee of the roughness elements, which confirmed that raindrop impacts were driven by the northerly wind reversal.

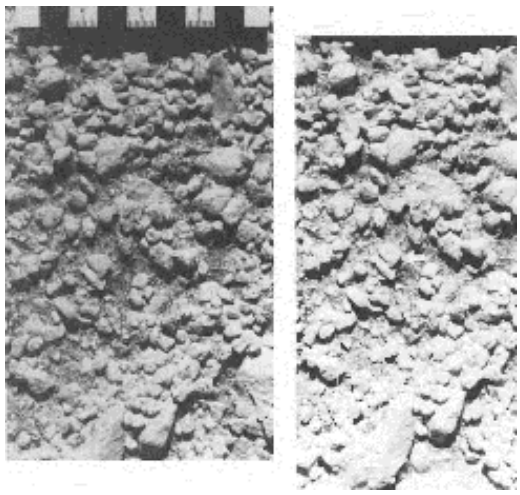

Figure 106. Stereo-pair illustrating the depth of the rain-impact hollows eroded into the fine-grained material exposed between the immobile roughness elements and creep bedload. Note the imbrication of clasts (arrowed), which are oriented for a northerly windflow from top to bottom.

The combination of heavy rainfall, large droplets and a high-velocity northerly wind is capable of greatly modifying the surface configuration of granules and small pebbles on stone pavements. Sustained surface wetting probably softens the underlying soil carapace composed of silt, which reduces its resistance to rainsplash erosion. As the impact of large raindrops alters the surface configuration, the underlying, fine-grained material is then susceptible to rain splash. The sand and silt is thrown up and erosion hollows are formed. The stone pavement is totally destabilised by this activity. During the subsequent return to southerly surface-wind conditions, the stone pavement surface dries out. In places raindrop erosion exposes new roughness elements which were beneath the former surface, and changes in the configuration of immobile roughness elements become possible.

Figure 107. South-pointing, fine-grained scour ridges in the lee of roughness elements raised on pedestals above the surrounding bed, which represent areas which were protected from rainsplash erosion. Northerly wind flow from left to right. Scale 10 cm.

As deflation of the exposed fine-grained sediment proceeds, the pedestals supporting the larger clasts are eroded and the roughness elements are lowered to the new elevation of the bed. This process also changes the surface configuration and provides a potential mechanism for the lowering of stone pavement surfaces in the manner described by Cooke (1970).

From the perspective of bedload transport, the bed is not in a stable surface configuration. Saltating sandflow crossing stone pavements in this state is more likely to entrain granules and even small pebbles more readily than equilibrium conditions allow. It is therefore likely that for a brief period creep and reptation transport rates increase. However, observation showed that evidence of rain-impact modification is very short-lived. Within a few days the erosion hollows are difficult to locate, and the pavement surface begins to readjust. By early January 1988, reorganisation of the creep bedload had advanced considerably, and indications of imbricate shape-fabric being attained were evident. Within a year the stability of the surface had been re-established and the presence of bedforms characteristic of equilibrium with the southerly windflow and sediment flux had clearly developed.

When rain-impact occurs on a sand dominated bed, rainsplash is likely to be an important mechanism whereby roughness elements are brought to the surface. Ephemeral stream beds of the type described below are susceptible to this type of stone pavement development. Examples are found at the southern end of the Idatal, where roughness elements appear to stand noticeably more proud of the intervening sand surface after rain events than they normally do. Surface run-off along with other factors (see below) may also partially account for this.

The evidence presented above shows that within hyper-arid, high-energy aeolian environments such as the NAEB the history of stone pavement development can be complex. The role of raindrop impact erosion in the development and maintenance of stone pavements cannot be overestimated.

Coupled with observation of the role played by bedload creep transport, thermally-induced stress gradients and salt crystallization near the sediment surface in promoting stone pavement formation, it is clear that previous deflation hypotheses (Blake, 1904; Moulden, 1905; Free, 1911; Cooke, 1970) are too simplistic. Especially when processes related to cumulate soil formation are considered as well. It is therefore dangerous to assume that a single process might explain the development of stone pavements, because the climatic and wind conditions under which they occur vary greatly. It is more probable that numerous processes, some of which might only occur rarely, interact to create a stone pavement. Depending upon local conditions one process might completely dominate the others. The role of brief, infrequent events, in creating and maintaining stone pavements should not be underestimated.

Diamond Placers in the NAEB

Introduction to Diamond Placers in the Namib Aeolian Erosion Basin

The entire Namib Aeolian Erosion Basin was systematically prospected following initial diamond discovery and pegging of claims. Prospecting was undertaken using trenches of 1 or 2 m width which were cut across virtually the entire breadth of the Namib Aeolian Erosional Basin. The trenches are oriented perpendicular to the long axis of the valley systems (east-west) typically occur at a 100 m or 200 m interval. In many instances the trenches went up and over the ridges separating adjoining valleys. The trenches were sampled in 25 m long paddocks which were excavated to bedrock. The results provide a summary of the number of diamonds recovered per paddock, and the total carats recovered. The average depth of sediment was also commonly recorded.

The original hand drawn maps recording the prospecting results are held by the Namdeb Mineral Resources Department at Oranjemund. These maps were in the process of being captured digitally at the time the original thesis was written. For this reason the diamond dispersal patterns in the Pomona Claim were the only ones modelled. For this update the Mineral Resources Department has also made the diamond stone data available to the south of the Pomona Claim as far as Buntfeldschuh, which is the southernmost limit of the economic deposits mined.

The combined data sets provide a unique insight into the diamond distribution through the NAEB from the southern limit of the economic deposits to the northern margin which abuts against the active plinth of the Namib Sand Sea some 56 km to the north near the town of Lüderitz.

The mined areas were mapped physically by the author on the ground during the early 1980s using aerial photographs to compile 1:25,000 scale detailed maps for the evaluation of the remaining diamond resource. For this update, the distribution of mined diamond placers (which are defined as economic mineral resources that can be mined profitably) has been mapped throughout the entire Namib Aeolian Erosion Basin from Chameis to Schmidtfeld (north of Lüderitz) using a combination of ALS data and related photographic coverage and Google Earth coverage of those areas not included in ALS acquisition.

The distribution of mining activity has been divided into two phases for the purpose of mapping:-

- German Mining conducted primarily between 1908 and ca 1921;
- Modern Mining principally conducted from 1988 onwards either by Namdeb or sub-contractor teams.

In some instances, such as Elisabeth Bay, recent mining activity has almost completely eliminated evidence of earlier operations which took place in the late 1920s to early 1930s.

The scale and intensity of mining operations within the NAEB define those areas with the greatest economic interest. Four main zones of placer formation can be identified within the main basin (Fig. 108). The smallest areas of placer mining are located in the south in the vicinity of the Buntfeldschuh Escarpment. Two large centres of placer development occur in the central area of economic interest in and around the ghost towns of Bogenfels and Pomona. The most northerly operational area extends northwards from Elisabeth Bay to the active plinth forming the southwestern margin of the present-day Namib Sand Sea.

Papers that discuss the west coast diamond placer system usually refer to the summary of diamond size distribution presented by Hallam (1964). Hallam published a summary of the average diamond size recovered from different points within the overall placer system. Unfortunately, averaged data hides crucial information about the diamond size distribution that provides key insights into the nature of the deposits being examined.

In particular, the marked bimodality of the diamond size distribution within the NAEB is almost completely obscured.

This textural information on the detailed characteristics of the diamond resource should form a crucial element in any study aimed at discussing and understanding the development of this unusual component of the West Coast Diamond Placer System.

The bimodal nature of the diamond population first became apparent to the author when a metal trunk containing the original field books of the prospectors was discovered in Oranjemund in the early 1980s. A brief inspection of the books revealed that diamonds of 30 to 60 carats were surprisingly common in the Bogenfels and Pomona claims.

A short section summarising this background information on the main diamond mining areas and the resources they contained is provided below. This has been made considerably easier with the publication of Gabi Schneider's (2008) book entitled *Treasures of the Diamond Coast* in which rare pictures of some of the largest diamonds produced from the region are reproduced. Much useful information on the sizes of diamonds produced both during prospecting and subsequently by mining operations are also given.

Coupled with the overall spatial distribution of the economic deposits and the geometry of the placer deposits, the stone size data summarised below and knowledge of the areas in which the main concentrations were originally located are fundamental to unravelling the development of these remarkable deposits.

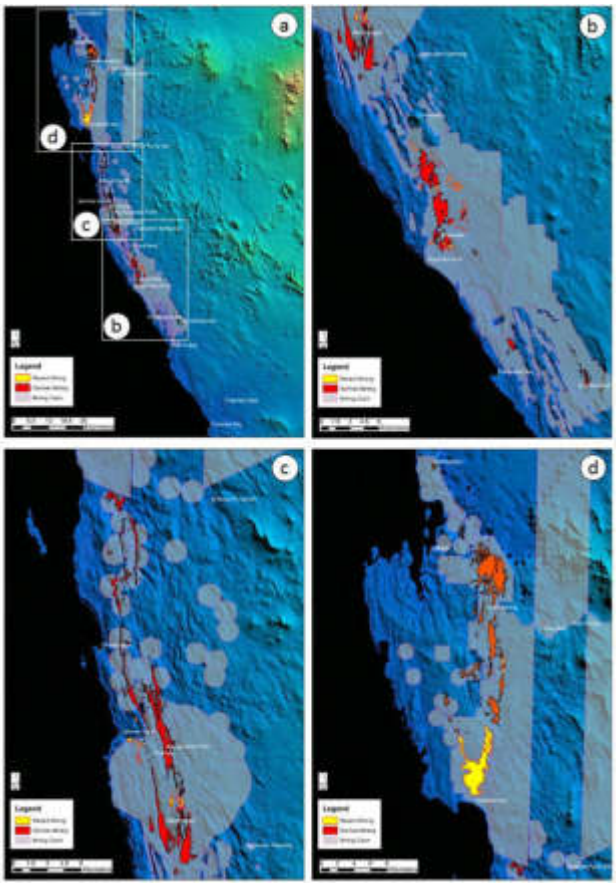

Figure 108. a) The regional distribution of diamond placer mining claims and operations through the Namib Aeolian Erosion Basin. b) Southern diamond mining localities between Buntfeldschuh and Granitberg. c) Central area of mining between Lüderitzfelder and Pomona to Grillental. d) Northern area of mining operations from Elisabeth Bay on the coast to Schmidtfeld on the active plinth of the Namib Sand Sea.

Buntfeldschuh Claim

Mining in the Buntfeldschuh claim area is centred immediately west of the 120 m high Buntfeldschuh Escarpment (Fig. 108b, 109) which forms the eastern margin of the Namib Aeolian Erosion Basin at this locality. Most of the mining activity occurred in the depocentre into which the alluvial systems draining off the escarpment flow. Smaller extensions of mining are located on south-north oriented floors of small valleys immediately downwind of the main centre of mining activity over a length of 5 km, although mining is patchily distributed and tapers rapidly northwards. The width of the mined area at the southern end is approximately 1 km.

Schneider (2008) records that Reuning (unpublished field notes ca 1912) located a rich placer deposit in a small windswept valley called Elsetal, close to Buntfeldschuh, which was characterised by an average diamond size of 1 ct/stone. A stone of 2.5 cts was also recovered later from the Buntfeldschuh claim during mining (Schneider, 2008).

Reuning (unpublished field notes ca 1912) was the first to recognise the possibility that the diamonds had been supplied from the interior of southern Africa. He might have proved this with prospecting trenches in the fluvial terraces had he not been recalled to Lüderitz before the work was completed. According to Schneider (2008) his notebooks show that his study at Buntfeldschuh led him to the conclusion that the Orange River had exited at this locality prior to occupying its present-day exit at Oranjemund, 150 km to the south.

Fröhe Hoffnüng Claim

Mining in the Fröhe Hoffnüng claim to the north west of Buntfeldschuh took place on the floors of two adjacent endorheic valleys. The floor of the main valley was systematically mined over a length of 1.4 km by 0.5 km wide. A smaller area of mining activity is located at the northern end of the adjoining smaller valley. The diamond size characterising these deposits is considerably smaller (0.2 cts/stn) than at Buntfeldschuh, and there are no known records of larger diamonds having been recovered.

Based on the original prospecting results there is little evidence of economic placer formation between the deposits mined at Buntfeldschuh and Fröhe Hoffnüng and Bogenfels to the north, which is the next area in which mining activity has taken place. However, this does not mean that the area between these centres is completely devoid of diamonds. Marine deposits approximately 160 masl at Eisen-kieselklippenbake were originally identified and mapped by Kaiser & Beetz (1926). These deposits were sampled by the author as part of a Namdeb exploration programme in 1987. The relatively small samples consistently produced diamonds. The two largest stones averaged 0.73 cts/stone. This stone size is similar to the diamond size at Buntfeldschuh and it is also close to the average stone size for the offshore Atlantic 1 deposit that is mined by De Beers Marine Namibia.

Schneider (2008) notes that Reuning (unpublished notes ca 1912) recorded the presence of terraces with diamonds as far south as Chameis Bay. However, mining is restricted to a few small, isolated recently mined areas within Kahle Felder. This endorheic system was sampled geologically in the early 1980s, and it was shown that granule ripples on the floor of the valley contain diamonds. The Kahle Felder – Fröhe Hoffnüng endorheic valley systems are discussed in more detail in a later section.

Bogenfels-Granitberg Claims

The main German mining operations between Bogenfels and Granitberg (Fig. 108b) extend about 12 km from south to north and they vary from 1.5 to 2 km in width. The placer deposits in this locality occur in two south to north swathes. The western swathe contains the largest mining areas which broadly form three zones from south to north. These are the deposits on which the town of Bogenfels was founded. A second, smaller south to north swathe of mining activity follows a topographic break in slope between the rugged relief of the basement-floored aeolian erosion basin and the comparatively smooth planar surface of the Terrassen Claim which is located along the eastern margin of the Namib Aeolian Erosion Basin.

Schneider (2008) records that shortly after the initial discovery diamonds of 8 and 17 cts were recovered in the vicinity of Bogenfels, and that subsequent mining operations periodically produced diamonds of about 40 cts. A series of small geological samples were processed from different locations within the Bogenfels claim blocks. A granule ripple crossing the surface of Eocene (Bartonian) marine sediments at approximately 50 masl produced 11 diamonds with an average size of 0.19 cts/stone.

Based upon prospecting data the area of economic interest extends northwards from the northern limit of the Granitberg claim into a narrow valley at the southern end of the Lüderitzfelder claim, in which there is a 1.5 km long area of mining on the valley floor. The main mining area is located within the Langental Valley at Bogenfels and within the area known as Wanderfeld and Station Granitberg.

Smaller areas of German and more recent mining activity are located to the east of the Langental, which contains small remnants of Late Santonian middle shelf and Eocene (Bartonian) nearshore marine sediments.

Lüderitzfelder - Pomona Claim

The placer deposits which begin towards the northern end of Lüderitzfelder in the southernmost part of the Idatal endorheic basin extend approximately 35 km north through a series of valleys. At the southern end three principle valleys called Idatal, Hexenkessel and Scheibetal form the main placer body which spans about a 3 km width from east to west.

Diamonds of 43 cts and 52 cts were recovered during the initial prospecting of the Idatal and later during mining operations a 112 ct diamond was recovered from the same valley (Schneider, 2008). The original prospecting books show that diamonds of 30 to 60 cts were relatively common in the vicinity of the junction between the Idatal and Lüderitzfelder drainage systems – an observation that is reputed to have led August Stauch to invest a large part of his fortune in the pursuit of the source up the Lüderitzfelder system.

The three principle valleys were fabulously rich in diamonds and produced more than 1 million cts in the first 20 months of mining – parts of the valley would eventually be mined seven times. The smaller Hexenkessel valley to the east of the Idatal proved to be an exceptional trapsite in which diamonds collected to the point that even the early prospectors themselves doubted their results. One 1 m-wide 25 m-long trench paddock produced a total of 1,693 diamonds. A parallel trench was cut immediately south of the first to check - the adjoining paddock produced in excess of 900 more diamonds. No wonder that legend has it that August Stauch and Professor Scheibe continued their prospecting of the area in the moonlight when they discovered the deposit. On completion of prospecting it was estimated that the diamond resource within the Pomona Claim was 54 million carats (Schneider, 2008).

Although the southern end of the Idatal is eroded into clastic metasediments, the central and northern part of the valley

which contained the main placer concentration of diamonds is eroded into gneiss bedrock. The Hexenkessel and Scheibetal valley systems are eroded into clastic metasediments and dolomite which consequently exhibits a different structural grain. Hence these two systems follow different paths which eventually merge together into the large endorheic basin called the Kaukausibtal. This endorheic basin extends for approximately 10 km from south to north, with the smaller Kaukausibtal Öst lying parallel to the east of the main Kaukausibtal Valley. The diamond distribution through the three main Pomona valley systems is discussed in detail in a later section.

A 7.5 km gap in mining extends north from Kaukausibtal, before mining operations resume along the floors of tightly constrained, narrow, sub-parallel valley systems which eventually merge together almost 19 km north of the Pomona Claim boundary in the Grillental IV and Grillental V claims. The average diamond size for these more northerly parts of the deposit was 0.167 cts/stn, although production was modest at 300 to 400 cts/month and was not sustained for long (Schneider, 2008).

Elisabeth Bay – Friedlicher Nachbar-Kolmanskop - Charlottental

A large area of mining operations extend for approximately 35 km from the Atlantic coast at Elisabeth Bay to the Friedlicher Nachbar claim which is located on the active plinth of the Namib Sand Sea within the Namib Depositional Basin.

The mining operations are approximately 3 km wide at Elisabeth Bay and extend 9 km northwards (Burger, 2015). From there mining operations extend along a 2 km to 1.2 km-wide system of relatively shallow valleys floored by gneiss before plunging down into a depression which marks the edge of the main depositional basin of the Namib aeolian system. Here, the mining operations fan out and are almost 4 km wide.

At the coast within Elisabeth Bay the average diamond size is 0.25 cts/stn but at the northern end of Elisabeth Bay mining operations, the stone size declines rapidly to 0.14 cts/stone. As of 2015 mining at Elisabeth Bay had produced in excess of 4 million carats (Burger, 2015).

Between Elisabeth Bay and Friedlicher Nachbar the diamond size declines from 0.166 cts/stn in the south to 0.125 cts/stn in the north.

Thick sequences of sediment at Elisabeth Bay and in the northern part of the Kolmanskop area approaching the active plinth of the Namib Sand Sea led to these areas becoming heavily mechanised early in the mining history, and it was not uncommon for the ratio of gravel to sand to vary from 1:3 to 1:7 (Schneider, 2008).

Schmidtfeld

The location of Schmidtfeld along a section of the active plinth of the Namib Sand Sea is the most northerly occurrence of mining included in this study. The location on the plinth also meant that the deposits within this claim were relatively thick (>3m), with a lot of sand present. The average diamond size varied between 0.125 cts/stn and 0.111 cts/stn (Hallam, 1964; Bluck *et al.* 2005).

In summary, several discrete areas contained diamond placers based upon the mapping of mining activity. Mining activity increases significantly from Bogenfels northwards, but depositional gaps in the distribution of economic placer deposits separate the areas.

In summary, mining primarily took place in the following claims (see map in appendices) from south to north:-

1) Buntfeldschuh, Straüchpfütz;
2) Kahle Felder, Fröhe Hoffnüng;
3) Bogenfels, Granitberg, Lüderitzfelder (south);

4) Lüderitzfelder (north), Pomona (Scheibetal/Hexenkessel/Kaukausibtal), Möllerfeld;
5) Pomona (Idatal), Carlstal, Ginnestal;
6) Pomona (Annatal);
7) Liebestal, Sudstern I & II, Grillental V & IV;
8) Liebestal, Merkurtal, Claratal, Grillental V;
9) Elisabeth Bay, Friedlicher Nachbar;
10) Kolmanskop, Charlottental;
11) Schmidtfeld.

The mining claims were defined using the regional coverage provided by prospecting trenches. The distribution of mining therefore provides a clear indication of those areas in which economic diamond deposits existed.

Diamond Introduction

Although in-depth discussion of the diamond supply to the West Coast of southern Africa is beyond the scope of this paper it is necessary to set the context to examine placer development within the NAEB.

The nature of the material entrained into transport by aeolian processes is determined by the lithology of the substrate across which an ATC passes at any one time. Numerous palaeoshorelines ranging in age from Cretaceous (Late Santonian/ Cenomanian) to Late Holocene are variably preserved within the onshore Bogenfels-Buntfeldschuh Basin.

The earliest evidence of diamond introduction to the continental margin north of the Orange River is provided by a marine sequence at Buntfeldschuh and more localised remnants in the Bogenfels-Langental area (Kaiser, 1926a). The only other marine sequences known onshore within the NAEB are the so-called Pocket Beaches preserved at between 10 mbsl to 18 mbsl which are of Eemian to Holocene age and the Holocene raised beach at 4 masl (see Fig. 102). Geological sampling and subsequent mining operations have shown both to be well-mineralised.

The main beach diamond placers that made the southern Namibia coastline world famous and have sustained onshore mining operations for almost a century occurred in marine terraces preserved to the south of Chameis Bay (see Fig. 1). They extend over a distance of about 100 km between the Orange River mouth and the log-spiral embayment at Chameis, where the present-day deflation basin originates. These beach deposits are predominantly of Late Pliocene to Early Pleistocene age and younger (Carrington & Kensley, 1969; Pether *et al.* 2000) .

In total, palaeoshorelines occurring at elevations ranging from -135 mbsl to about 170 masl have been shown by onshore and offshore exploration and mining, to contain placers with exceptional concentrations of predominantly gem quality diamonds.

Release of Diamonds from Palaeoshorelines

The raised palaeoshorelines within the NAEB and those exposed on the shelf during regressions have been subjected to extensive arid zone weathering processes. Early reports of loud cracking noises heard by German geologists working in the Namib were attributed to the process of insolation. More recent studies of weathering have highlighted the important role that thermal shock plays in the natural fragmentation of rock (Hall & André 2001). Given the frequent surface cooling by the Benguela Fog, the Namib may well be a particularly effective environment for this mechanism. Once fractured by thermal fatigue, salt weathering vigorously attacks clasts comprising the diamondiferous palaeoshorelines and ephemeral stream diamond placers within the deflation basin. Together with the effects of insolation (Kaiser, 1926a) these processes break down the material comprising deposits through

splitting, spalling and inter-granular disintegration.

Due to the extreme nature of the erosional environment described in earlier sections, extensive topographic inversion is taking place within the NAEB. The full extent to which this is occurring is only now starting to become clear with detailed palaeontological research (Pickford, 2015). Through this process (and probably aided by extensive early diamond mining activities) this region contains the only known onshore sequences of Cretaceous (Late Santonian) and Eocene (Bartonian/ Priabonian) marine sediments along the margin of Namibia and the west coast of South Africa.

The marine sediments, in the most part are exposed as small, localised remnants. However, a laterally extensive sequence is exposed over a 5 km length as a 120 m high scarp/ cliff section at Buntfeldschuh (Fig. 109). The deposits were studied during the early 1900s by a number of German geologists and extensively documented in Kaiser (1926a).

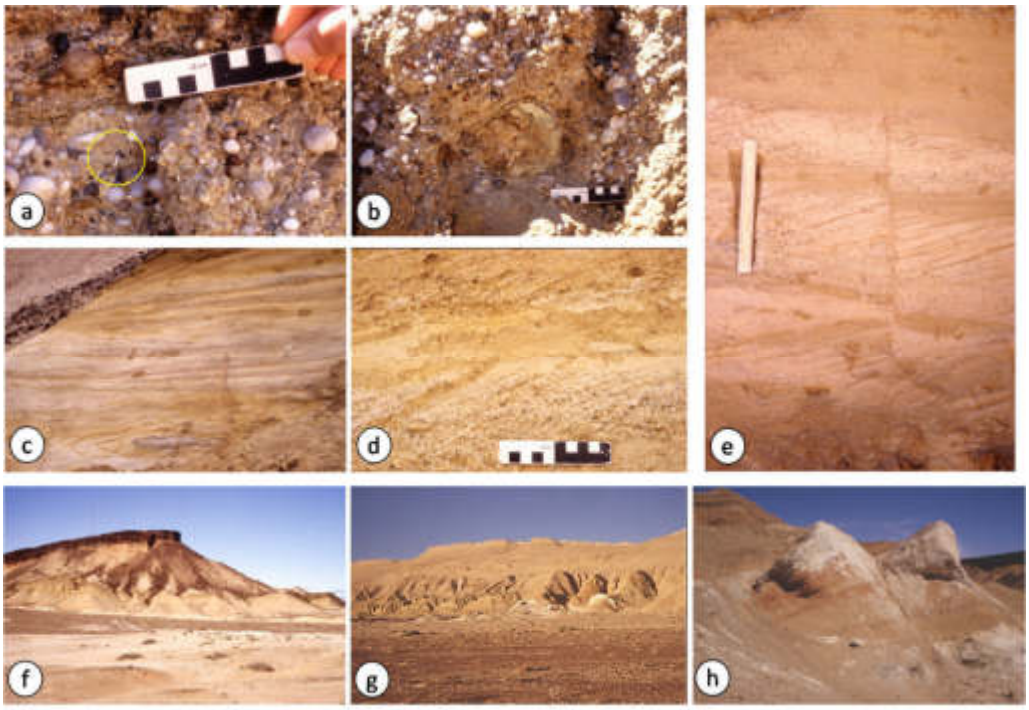

Figure 109. Photographs a - e showing different aspects of the upper Buntfeldschuh Bartonian marine section. a) Small Eocene shark tooth in pebble lag. b) Weathered, well rounded phonolite clast in pebble lag. c) Gravel waves. d) Nearshore trace fossil in fine-grained sand unit between cross-bedded grit facies. e) Fault indicating possible seismite evidence in nearshore gravel and grit-dominated longshore bedforms. f) Kakaoberg at the southern end of the Buntfeldschuh escarpment showing the "saucer-shaped" geometry of the lower section comprised of marine sediments. g) Section of the escarpment showing the full sequence. Note the light-coloured units at the base of the sequence which are shown in more detail in picture (h). The coarser-grained Bartonian nearshore marine sediments are located above the basal sand unit. The upper part of the sequence consists of an aeolianite which is capped by calcrete to the north of Kakaoberg which is capped by ferruginised sand and the Namib 1 Calc-crust. h) The toe of rotated fault blocks in the undated basal sand unit.

Siesser & Salmon (1979) subsequently re-examined the sequences between Buntfeldschuh and Bogenfels and recognised that they are significantly different in terms of their textural characteristics. Based on the fossiliferous exposures between 50 masl to 90 masl in the Langental and Bogenfels area (Fig. 110) Siesser and Salmon assigned them to the Priabonian (37.5-39.5 Ma). They also

considered that the basal unfossiliferous Buntfeldschuh Beds, which are topographically higher, might be Palaeocene to lower Eocene in age.

Offshore, the Eocene sequence, which shows evidence of having been folded, has been extensively studied (McMillan & Dale, 2002). Micropalaeontology has been used to provide detailed biostratigraphic control to aid seismic interpretation. Shoreward projection of the Bartonian reflectors intersect the marine sequences in the Langental and at Buntfeldschuh. Marker foraminiferal species from samples of the Langental Beds confirm the early Bartonian age. McMillan & Dale (2002) concluded that the abundance of *Lobatula* sp. indicated that the sediments were deposited in close proximity to, or within the wave breaker zone. This is consistent with the abundance of *Turritella* sp. and the presence of oysters in some of the Langental exposures (McMillan & Dale, 2002). These observations are supported by the presence of gravel waves in the upper marine unit of the Buntfeldschuh section, which observation using the Jago submersible have shown to be produced by northbound longshore transport along the present-day coast near Lüderitz in water depths of 30 to 50 m (Spaggiari, 2011).

Given the recent identification of widespread onshore evidence for a Lutetian – Bartonian - Priabonian aged Sperrgebiet silicification event by Pickford (2015), it is interesting to note that offshore evidence of this event was recorded by McMillan & Dale (2002), who also linked the distinctive diagenesis event to flushing of the sediments by silica-rich hydrothermal fluids produced during the emplacement of the Klinghardt intrusive complex.

Detailed mapping by Mike Shaw (2002) has also shown that the emplacement of the volcanics offshore of Chameis occurred during the middle-late Bartonian. High resolution seismic data provides clear evidence of tectonic instability of the shelf at that time which, based on McMillan & Dale's (2002) research, ultimately led to a major offshore retreat in sea-level 45 km to the west – driven by tectonic uplift and not driven by global sea-level change caused by early polar glaciation episodes. Active tectonism during the Bartonian and the resulting uplift almost certainly resulted in a flush of diamonds to the west coast of southern Africa, setting the scene for the subsequent development of the world's greatest gem diamond placer discovered to date.

On the basis of the micropalaeontological correlations across the shelf and onshore, the slightly younger Priabonian age for the Langental and Buntfeldschuh Beds advocated by Siesser & Salmon (1979) and more recently Pickford (2015) is unlikely to be correct.

Although a detailed discussion of the relationship between onshore tectonics and the offshore structure of the shelf is beyond the scope of this study, the apparent structural control of the shelf morphology outlined by the shoreward inflection of the Eocene sequence exposed on the shelf (Fig. 110) is important to note. This feature is intersected by a set of SSW to NNE oriented faults that come onshore in the vicinity of Bogenfels and the Kudu Lineament identified by Corner (2008) whose map suggests that significant left-lateral displacement can be mapped based on fault offsets further offshore in the Orange Basin. The Kudu Lineament runs to the south of the Buntfeldschuh Escarpment. Interestingly the Chameis volcanics occur just south of the Kudu Lineament close to its intersection point with a fault (possibly a reactivated Gariep thrust fault) that runs sub-parallel to the modern coastline. Detailed micropalaeontological studies (McMillan & Dale, 2002) show that to the south of the Kudu Lineament the Bartonian (42.5 Ma) Eocene sequence was deposited in a nearshore environment. However to the north of the lineament the micropalaeontological assemblage indicates a deep-water shelf to upper slope environment. It is postulated here that the Buntfeldschuh - Bogenfels sequences represent the laterally displaced and uplifted inshore / shoreline deposits that are associated with the deep-water facies exposed on the shelf north of the Kudu Lineament.

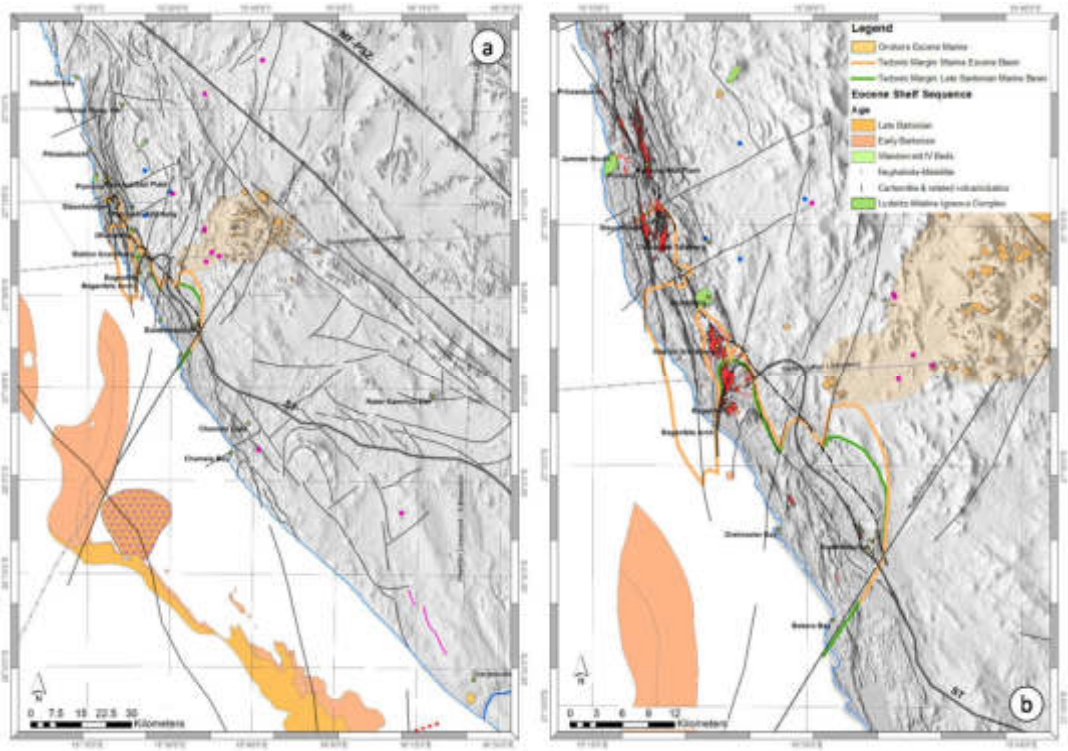

Figure 110. a) Map showing the distribution of Bartonian sediments on the Namibian continental shelf based on the work of Pegler (1998), McMillan & Dale (2002) and Stevenson (pers. comm. 2015). The Kudu Lineament and a series of faults running sub-parallel to it form a significant structural boundary that strongly influences the morphology of the continental shelf. b) Closer view of the Buntfeldschuh-Bogenfels area showing the distribution of diamond mining with respect to the exposures of Eocene marine sediments. The dashed black line marks the position of the "Eocene shoreline" as defined in Kaiser (1926a). The postulated tectonically controlled margin of the Late Santonian basin is shown by the thick green line. The tectonically-controlled onshore extension of the Eocene basin is shown by the thick beige line – the complex shape is defined on the basis of the spatial distribution of diamond deposits with a strongly bimodal size distribution (see more detailed explanation in the section on diamond dispersal patterns). Pickford *et al*. (2013) estimate that basement rocks in the Klinghardt Mountain dome were uplifted by 300 m. The nearshore and coastal sediments at Buntfeldschuh and Eisenkieselklippenbake several kilometres to the north lie between 186 to 168 masl, whereas the age equivalent sequences in the Langental-Bogenfels area lie between 50 masl to 90 masl.

Importantly, from a diamond placer perspective, geological sampling by the author has confirmed that the early Bartonian sediments exposed onshore at Bogenfels contain diamonds (see later section). These sediments and the residual coarse clastic lag gravels associated with them were mined extensively following their discovery – these are discussed in more detail in the next section on diamond dispersal patterns.

Faulting has long been recognised within the sedimentary sequence exposed along the Buntfeldschuh Escarpment (Siesser & Salmon, 1979) which forms a 120 m high topographic edge to the Namib Aeolian Erosion Basin at this locality. Faulting is particularly noticeable in the basal fine- to medium-grained green sand unit below the planar erosional surface at the base of the upper coarse-grained nearshore marine sequence that occurs approximately 160 masl. Bluck *et al*. (2007) recorded the presence of these faults in the lowermost part of the Buntfeldschuh section and interpreted them as evidence that this is a down-faulted section. However, the significance of the fault geometry, and the

rotated blocks in particular, as recorded in Figure 3a of Bluck *et al.* (2007) who note that "slices of highly weathered basement thrust into sands" along rotational glide / shear planes (Fig. 108) has not previously been fully appreciated.

The upper unit contains fossil shark and fish teeth which closely resemble those recovered from the Eocene (Bartonian based on micropalaeontology) nearshore to shoreface clastic sediments containing diamonds between 50 masl to 90 masl in the vicinity of Bogenfels and further north up the Langental valley. Siesser & Salmon (1979) originally questioned whether the basal marine sequence at Buntfeldschuh, which they observed to be texturally quite different to the dated Bartonian nearshore sequences at Bogenfels form part of the same stratigraphic unit. Corbett (1989) also recognised a lower and an upper unit, noting that the lower section is comprised of largely structureless fine-grained sands with a hint of large-scale cross stratification in places and considered it to be diagenetically distinct due to the presence of large ferruginous concretions up to a metre in diameter. The concretions do not occur in the upper unit which contains gravel bedforms diagnostic of a shallow, nearshore high-energy environment characterised by gravel transport by a dominant northbound longshore transport system (Corbett, 1989; Bluck *et al.* 2007). Small-scale faulting is present in the Bartonian marine section on scales similar to those observed by the author in Plio-Pleistocene marine section exposed by the De Beers Namaqualand Mines operation, where throws of up to a metre are not uncommon. Sections containing these features together with soft-sediment deformation structures have recently been reported by de Beer (2012).

Within the Wanderfeld IV claim, well-dated Late Santonian marine sediments (Klinger, 1977; McMillan & Dale, 2002) appear to underlie thin surficial remnants of the diamondiferous Bartonian nearshore marine succession within the Langental, north of Bogenfels. Although Pickford (2015) determined that the sediments are not *in situ*, their presence here is important. Their micropalaeontology indicates that this sequence was laid down in a mid-shelf environment in a water depth of 60 m to 70 m (pers. comm. Ian McMillan, 2014).

More recently evidence of an Early Santonian marine sequence was located offshore of Bogenfels which has been dated on the basis of pyritised ammonite nuclei and micropalaeontology (Klinger & McMillan 2007). Unfortunately, despite repeated attempts to date the lower Buntfeldschuh sequence, carbonate or siliceous microfossils appear to have been largely flushed out of the sandstone. The only fossil recovered to date is a single, poorly preserved *Lingula* shell found by the author, which was insufficiently diagnostic to be useful.

The style and orientation of the faulting in the basal unit is distinctive, and may provide a clue to the origin of the lower sequence. Bluck *et al.* (2007) probably correctly interpreted the basal faults to be the product of extensional tectonics. However, the orientation of the fault blocks with the toes of the faults dipping landwards may be providing evidence of deep-water thrust belt development which has been identified in seismic data from the Orange Basin (de Vera *et al.* 2010; Butler & Paton 2010) The basal rotated fault blocks in the lower part of the Buntfeldschuh succession resemble the style of faulting that is characteristic of the contractional domain within large-scale deep-water thrust belts (Fig. 111). If true, the sand-dominated basal unit is most likely to represent an outer shelf / upper slope to mid-shelf facies, rather than a marine reworked aeolian sedimentary package as suggested by Corbett (1989). A late Santonian or earlier age for the sequence would then be likely based on the timing of the deep-water thrust belt identified offshore by de Vera *et al.* 2010.

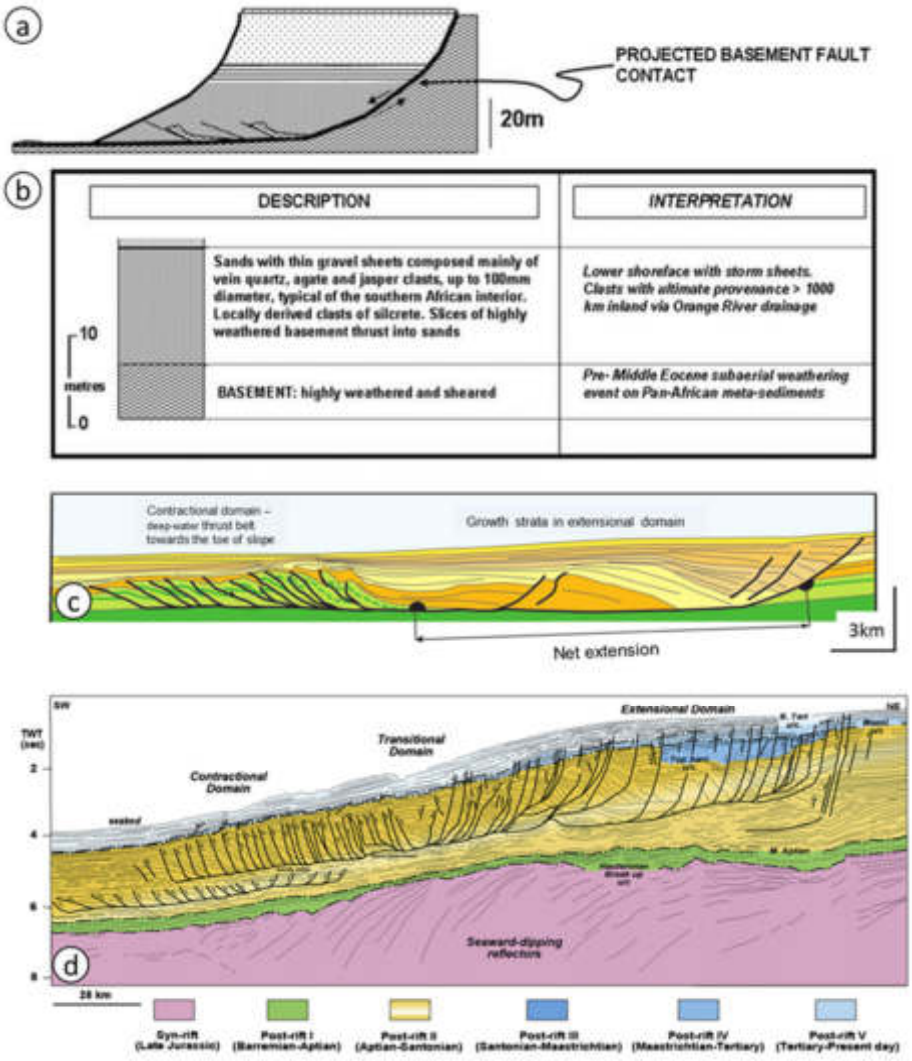

Figure 111. a) and b) Sketch section of sequence illustrating the geometry of the faulting in the lower sand unit at Buntfeldschuh (Bluck *et al.* 2007). b) Description and interpretation of faulted lower unit (from Bluck *et al.* 2007). c) Architecture of gravity-driven thrust systems, based on the Pará-Maranhão Basin, offshore Brazil (Zalan, 2005); (d) Geoseismic section showing the main depositional mega-sequences and the Late Cretaceous gravity-driven slide system in the Orange Basin (modified from Granado *et al.* 2009).

In this scenario, the erosional base of the upper marine unit would then mark a significant event - the development of a major Eocene transgressive erosion surface overlain by diamondiferous early to middle Bartonian nearshore/coastal sediments. Such a scenario would be consistent with the offshore unconformity mapped across the Namibian shelf by McMillan & Dale (2002). It is also possible that the gravity-slide that led to the deep-water thrust was triggered by movement on the Kudu Lineament and/or the SSW-NNE oriented faults.

The onshore Bartonian nearshore marine sediments occur at elevations ranging from 160 masl at Buntfeldschuh to 50 masl in the vicinity of Bogenfels. As can be seen in Figure 112, the marine sequences occur on different basement blocks bounded by major faults and lineaments - changes in elevation therefore suggest differential movement.

Given the prevalence of volcanism at the time and the evidence for 300 m of uplift

related to emplacement of the Klinghardt phonolites between 46 Ma to 37 Ma (Pickford *et al*. 2013) it is suggested that the variation in elevation of the Bartonian marine sequences is evidence for differential uplift of blocks bounded by the NNW-SSE trending faults which run sub-parallel to the Kudu Lineament.

Consideration will now be given to the implications that the preceding section on the influence of tectonics on the distribution and preservation of Palaeocene to Eocene marine sequences with respect to development of diamond placers within the NAEB.

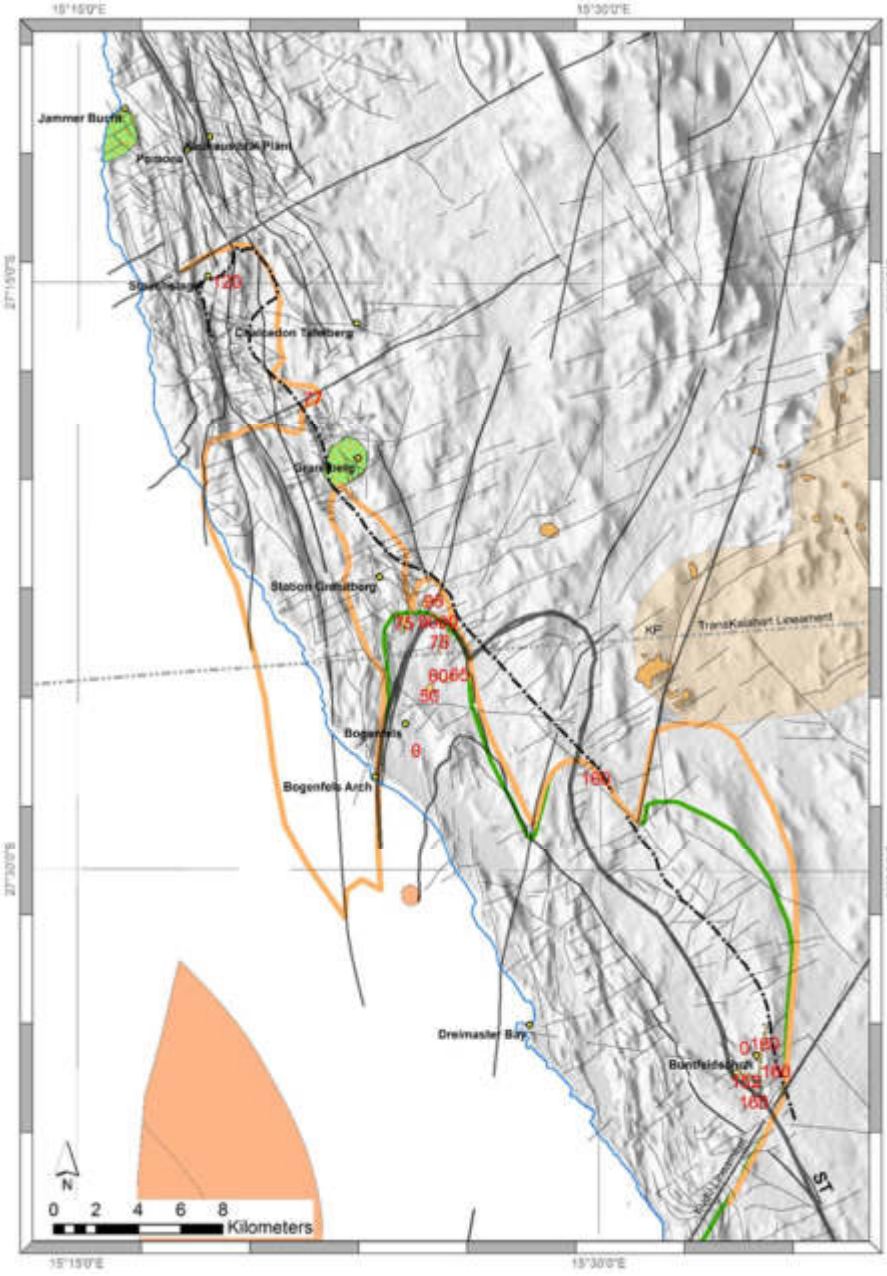

Figure 112. Map summarising the elevation changes in the known exposures of Bartonian nearshore marine sediments at Buntfeldschuh and Bogenfels. Two sites are shown north of Granitberg. The southern site is Lüderitz Krater where sediments derived from local reworking of probable Eocene marine sediments are preserved. The northern locality lies on top of Elfert's Tafelberg, where medium to large pebbles of jasper and agate also indicate that local reworking of probable Eocene marine sediments took place. The changes in elevation can be seen to occur across faults. Null values represent no data.

Diamond Dispersal Patterns

Diamond dispersal patterns from endorheic basins have not previously been described in detail. Wagner (1914) noted that the payable ground was located along the lowermost parts of basins and on south-facing slopes. He also observed that the diamond concentration was characterised by rapid variation in grade.

Kaiser (1926a) provided more detail but was not permitted to publish supporting data. He did, however, make a series of insightful comments:-

1) Diamonds were concentrated in south-north oriented zones;

2) Discrete concentrations were located in southern locations, from which northward tails of diamonds were present;

3) Diamond size declines from south to north;

4) Some basins showed a greater concentration along their western margin;

5) Diamonds were not generally present on the divides between succeeding basins;

6) Diamond concentration did not occur immediately north of basin divides, but some distance down the north-facing topographic slope.

The data used for the examination of the diamond dispersal patterns described by Corbett (1989) were extracted from the original prospecting plans from the Pomona Claim (ca 1912). Prospecting was undertaken using 1m-wide east-west oriented trenches perpendicular to the south-north basin axes. The trenches were excavated in 20 m long sections that were individually treated to recover diamonds. The number of diamonds recovered and the total weight of the diamonds per sample was recorded by hand on the plans. Unfortunately details of the size-frequency distributions of diamonds from samples no longer exist. These data were modelled using Vulcan software. Diamond dispersal patterns were modelled based upon the number of stones and the average size of the stones recovered from each sample. Their position was related to the bedrock topography.

For this study, thanks to the support of Dr J. Jacob at Namdeb (Pty) Ltd, the original diamond dataset has been supplemented by additional digital prospecting data covering the area between Chameis and Grillental. The author also mapped the distribution of mining in detail from Chameis to the southern part of the Namib Sand Sea using the ALS dataset supplemented by Google Earth imagery.

Collectively, the additional datasets provide the basis for the first comprehensive review of the NAEB diamond placers and the sedimentary systems that formed them to be published. The pattern of drainage networks and catchments has been modelled using the ALS DEM data available for this study. This unusual dataset spans virtually the entire NAEB from Chameis to the Grillental. The hydrologic terrain analysis was done using the TauDEM 5.1 (Terrain Analysis Using Digital Elevation Models) software developed by Prof. David Tarboton at the Utah State University. I am indebted to Prof. Tarboton for his assistance in introducing me to the software and helping me run the model.

A broad overview of some of the characteristics of the diamond deposits was provided at the start of this paper. These aspects will be contextualised and the implications of them explored in this section of the paper. As the most comprehensive diamond dataset is available for the Pomona Claim this section will start with the Pomona-Grillental Placer Domain, which first brought the region to the attention of the world.

The distribution of mining in this domain is shown in Fig. 113. The orientation parallel with the unimodal southerly winds is immediately evident.

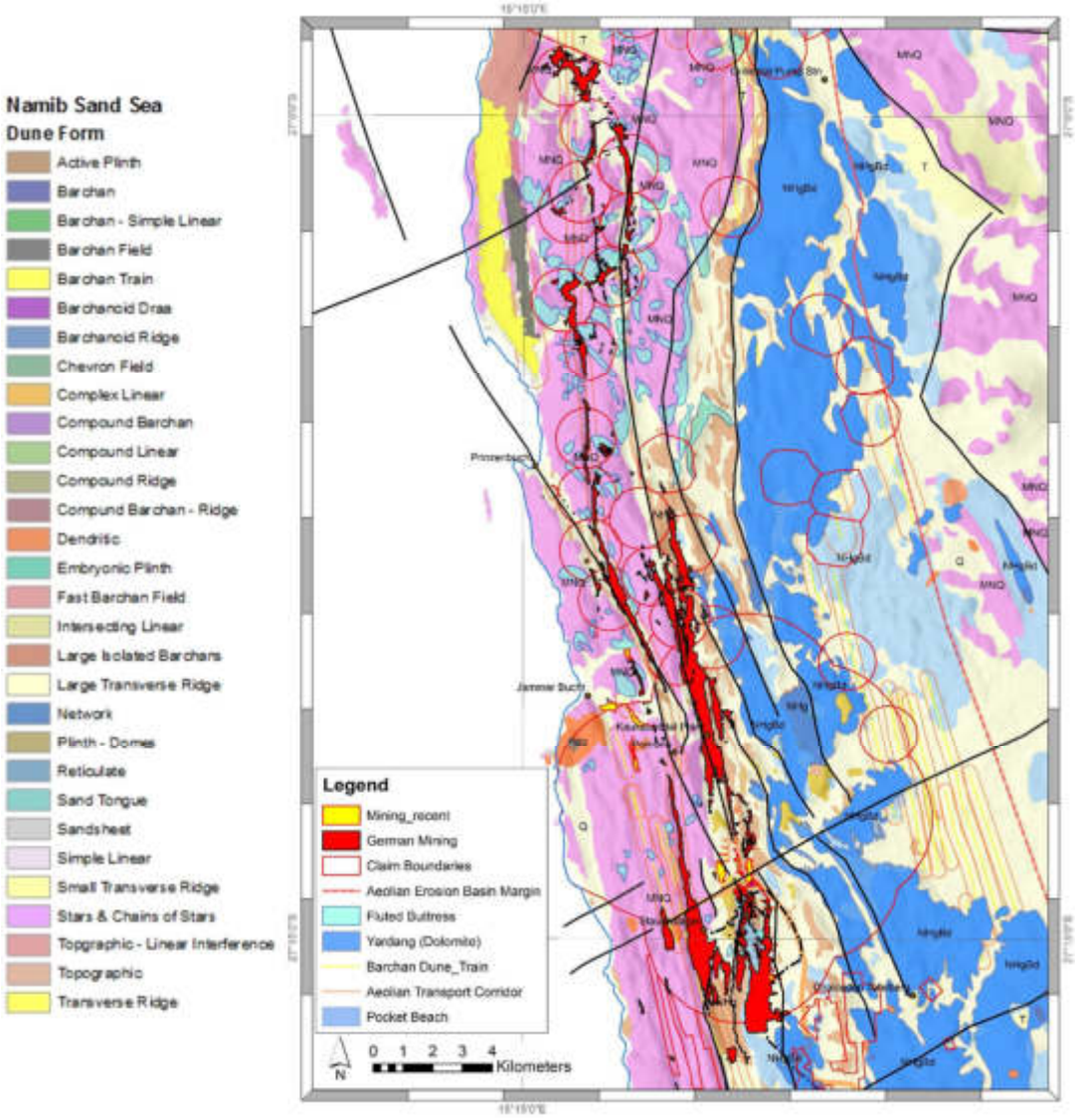

Figure 113. The distribution of mining within the Lüderitzfelder-Pomona-Grillental Diamond Placer Domain in relation to the erosional architecture of the NAEB and the present-day distribution of ATCs. Legend for bedrock geology can be found in Fig. 16. The legend for dune forms in the southernmost part of the Namib Sand Sea (top left in image) is provided.

It is also apparent that the deposits taper from south to north, and that areas of mining are separated by short gaps in which limited or no mining activity took place. These dispersal patterns provide important evidence about the nature of these deposits. Together with modelling of the prospecting data there is unequivocal evidence of diamond transport by arid zone transport systems (Fig. 110) including aeolian bedload transport and ephemeral streams.

Significantly, the most southerly basin contains the largest diamond sizes, and successive basins to the north contain smaller diamonds. This indicates that the

diamonds have been transported northwards from a source area located in the south.

The Pomona Claim produced the largest diamond (112 cts) recovered from the NAEB placers together with a number of stones that ranged between 40 to 60 cts. Sampling by the author and personal observations from early prospecting results show that diamonds transported as aeolian bedload typically range from 0.5 cts/stone downwards. As far as is known, no primary kimberlite deposits occur within the Sperrgebiet. The supply of such large diamonds must therefore either be due to proximity to a fluvial entry point or to nearshore transport by the marine system. Kaiser (1926a) suggested that a palaeoshoreline which we now know to be Bartonian in age extended north of Bogenfels. The previous section, however, presented new information on tectonics that suggests that the distribution of remnants of Bartonian marine sediments is tectonically controlled within a basin extension.

Stauch, who discovered the deposits and later mined them in the southern part of the Pomona Claim believed that these large stones had entered the basin via Lüderitzfelder. A proven prospector of note, we need to take cognisance of this in the context of new evidence from Pickford (2015) that suggests the Idatal valley was in place in the Miocene (and possibly even earlier based on the relief of the Katchen Plateau Formation silcretes).

The Buntfeldschuh sequence has commonly been promoted as evidence that a fluvial entry point for the palaeo-Orange River existed at this locality (Bluck *et al.* 2007; Pickford, 2015). An alternative explanation for the presence of an "Orange River Suite" of exotic clasts could also be that northbound longshore transport was both established and of sufficient energy in the Eocene to transport large to very large pebbles. Observations made from the Jago submersible by Ward during 1999 (cited by Spaggiari, 2011) proved that 300 km north of the Orange River in 60 m water-depth gravel waves are migrating northwards sub-parallel to the Lüderitz coast. According to Spaggiari (2011) these bedforms possibly migrate shoreward, towards the present-day coastline. According to Harry Swart (pers. comm. 1986) during extensive coastal engineering studies by the CSIR to determine present-day longshore transport rates it became clear that pebbles of 32 to 64 mm diameter are today very mobile in the surf zone. Swart considered that transport along the Sperrgebiet coastline was simply a question of time.

Based on the above and research for this paper, two possibilities exist to explain the presence of the large diamonds in the Pomona Claim:-

1) The nearshore margin of the marine basin lay further to the east of the known residual lag gravels containing exotic clasts typically associated with Eocene sequences. Subsequently, or even contemporaneously, uplift associated with the emplacement of the Ystervark Carbonatites and/or the Klinghardt phonolites led to local erosion and transport of these marine deposits in proto-valleys which later came to lie within the NAEB;

2) Topographic inversion in the Pomona area within the NAEB advanced further and commenced earlier than it did in Bogenfels, resulting in the almost complete destruction of evidence for marine sediments having been present.

In both instances the large diamonds would ultimately be the last remaining residual evidence for the former presence of a Palaeocene and/or Eocene marine placer source.

The Idatal Endorheic Basin

The Idatal endorheic basin (Fig. 114) is located to the north of the Bogenfels Basin, from which it is separated by Daheimtal, another endorheic basin. The Idatal, like the other endorheic basins, has formed by a combination of salt weathering, aeolian deflation and aeolian corrasion. The basin is a linear south-north oriented feature, with the minimum base-level of -1 mbsl situated near its southern end. From this point, the

basin floor rises gradually to form a south-facing slope which tapers to an apex in the north near Pomona. The Idatal has a stepped longitudinal profile and a number of sub-basins exist within it.

The dispersal pattern forms a linear feature running along the floor of the Idatal basin. The average diamond size data (Fig. 115a) is clearly zoned spatially. The largest diamonds were located at base-level along the western margin of the basin. A series of concentric bands on the northern side of the zone containing the largest stones show that there is a reduction of diamond size to the north, up the topographic south-facing slope.

Figure 114. Oblique aerial view to North West showing the central Idatal and the famous Hexenkessel. The western margin of Scheibetal is also visible.

The zones representing the large and medium average diamond sizes are relatively narrow, compared to those of the smaller average diamond sizes, which extend greater distances to the north.

The maximum number of diamonds was located towards base-level (Fig. 115b). The number of diamonds declines rapidly to the north of the main concentration. A smaller secondary peak occurred north of the main one. This marks the position of a smaller bedrock depression forming a local base-level lying above that in the south. Thus a smaller endorheic feature is present within the main basin. The peak in the number of diamonds coincides with the location of the zones representing large and medium average diamond sizes. Hence peaks in the concentration of diamonds do not correspond with zones containing small diamonds.

In terms of the present-day sedimentary environment two dispersal systems influence terrigenous sediment dispersal (Kaiser, 1926a). These are the aeolian and the ephemeral stream systems, which operate independently of each other.

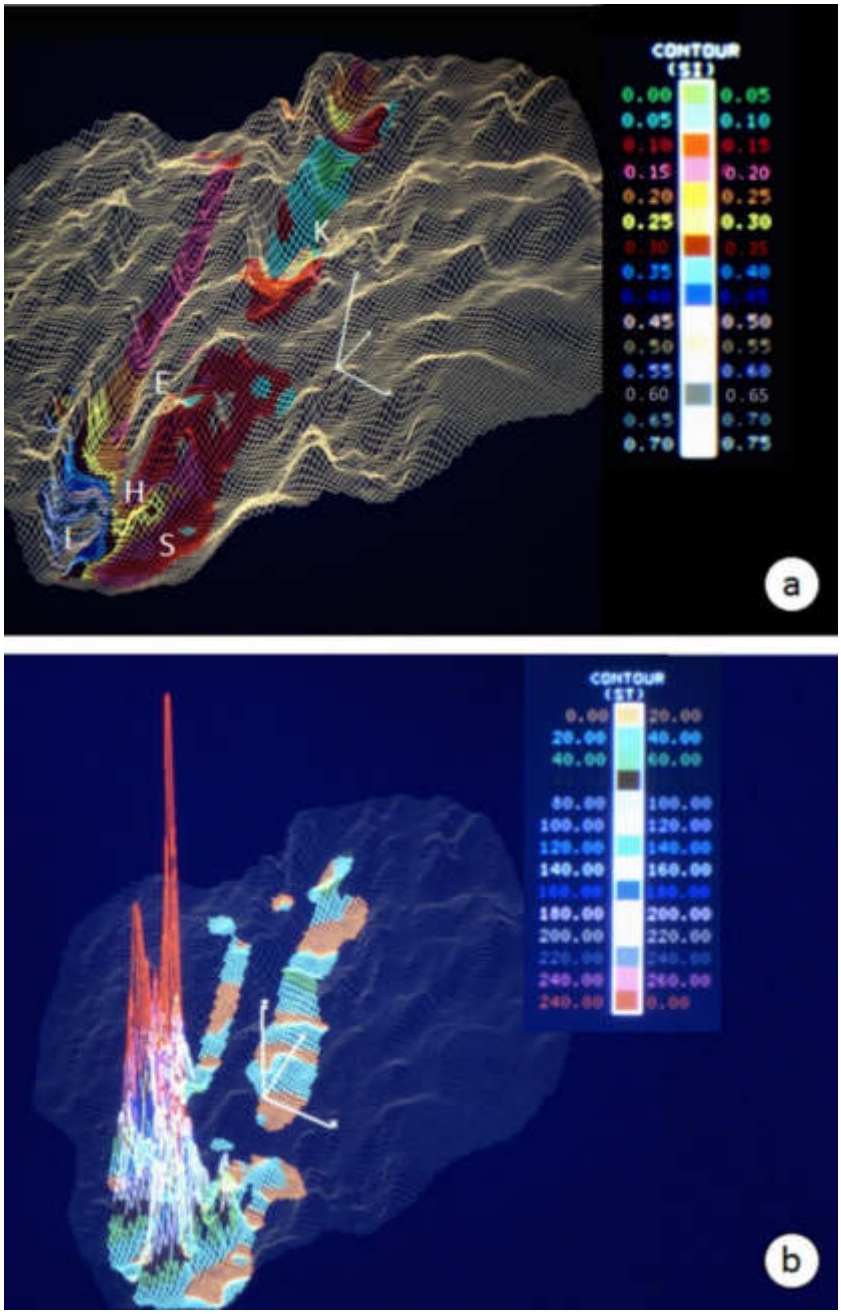

Figure 115. a) Diamond dispersal pattern shown by the variation of average diamond size in the southern part of the Pomona claim. The colours denoting the different class intervals are given in the legend. In the text describing the dispersal pattern, the term small refers to values of 0.05 to 0.2 cts/stone, medium to values of 0.25 to 0.4 cts/stone and large to values of 0.4 to 0.75 cts/stn. The endorheic basins in which the placer bodies were situated are: Idatal (I), Hexenkessel (H), Scheibetal (S), and the Kaukausibtal (K). The topographic residual known as Elfert's Tafelberg (E) separates the Hexenkessel from the Scheibetal. Note the concentric zones of decreasing diamond size extending to the north along the Idatal endorheic basin. b) Diamond dispersal pattern shown by the variation of diamond concentration in the southern part of the Pomona claim. The variation of concentration is shown graphically, with peaks corresponding to high diamond concentrations. Colour coding of the diamond concentration contours are, shades of: red, pink, and grey = high concentration; blue, and white = medium concentration; brown, green, and orange ~ low concentration. The massive peak in the diamond concentration is located within the Hexenkessel. The smaller peak to the west, near the base-level of the Idatal endorheic basin, approximately corresponds with the position of the zones of large and medium average diamond sizes.

According to Sternberg's (1876) Law in any alluvial system, sediment transport will result in the downslope reduction of particle size. Examination of the spatial variation of average diamond size data shows that this does not occur within the Idatal. The dispersal pattern clearly shows that the average diamond size fines to the north, up the south-facing topographic slope. This diamond dispersal pattern cannot therefore solely be the result of alluvial transport.

Garnet tracers deployed during this study prove that the dominant migration direction for both the bedload and saltation modes of aeolian transport is to the north. These are the only present-day transport processes operating in the region which are able to account for the up-slope decline in diamond size as Kaiser (1926a) realised. Observations during the original research strongly suggested that the small to medium diamonds are periodically entrained into saltation proper. The largest diamond recovered from the Pliocene Fiskus Sandstone Beds during prospecting work at Elisabeth Bay weighed 1.2 carats. This diamond would have been transported across a soft dune sand substrate prior to its deposition. The creep transport capacity across the hard substrate of the stone pavements which floored the Idatal endorheic basin would be greater because of reduced dissipation of saltation grain kinetic energy on rebound. The majority of diamonds weighing less than 1 ct recovered from the Idatal would therefore have been susceptible to aeolian bedload transport by reptation and/or creep. This confirms Kaiser's (1926a) conclusion that diamonds were transported northwards, up the south-facing slopes of the valleys by aeolian processes.

The concentrically zoned pattern of progressively smaller diamond size that fines to the north had not been documented previously. The pattern is interpreted as evidence for differential aeolian transport rates resulting in size sorting. The process has been modelled using the garnet tracers, but the Idatal diamond dispersal pattern exemplifies the subtlety with which it occurs. The garnet tracers also confirm that small diamonds should be more frequently entrained into saltation proper and/or reptation as well as creep. As a result the small diamonds migrate more rapidly than larger diamonds. This accounts for the extreme downwind extension of the fine-grained diamond dispersal tail which ultimately extended to the Grillental.

The decrease in both diamond concentration and the average diamond size to the north is not seen as evidence for a deficit of small diamonds in the original size-frequency distribution. This feature of the diamond dispersal pattern is attributed to the differential transport rate of the particles according to their size. The faster transport rate of small diamonds means that if diamond supply to the endorheic basin system occurred in pulses the quantity of small diamonds left will progressively diminish as a function of time spent in the high-energy aeolian environment.

The progressive deepening of base-level due to the continued excavation of the endorheic basin would periodically rejuvenate the ephemeral stream systems within it. The points at which the aeolian placer bodies on the south-facing slope are reworked by the streams therefore alters with time. Sampling during the course of this study, and the consideration of experimental flume work by Mosley & Schumm (1977) and Best & Brayshaw (1985) demonstrates that channel junctions within dendritic tributary networks provide sites for the local generation of alluvial placer bodies. This process substantially modifies the aeolian sediment dispersal pattern. Comparative photography of sites in the Idatal proves that the alluvially redistributed granule-sized material is not locked in the stream bed beyond the influence of the aeolian system. Kaiser (1926a) observed aeolian deflation of the ephemeral stream beds. This study shows that aeolian reworking commences with deflation shortly after the flood event even before the stream bed is dry. The time required for the coarse-grained, re-released alluvial material to generate a new stone

pavement surface, and the periodicity of rainfall then determines the extent of deflation. The previous aeolian dispersal pattern is partially destroyed by the alluvial activity. Progressive size-density-shape sorting of the material forming the ephemeral stream beds leads to the removal of the smaller diamonds. Provided that the diamonds remaining on the ephemeral stream bed are too large to be entrained into aeolian creep transport, a lag placer body is then generated.

The floor of the Idatal endorheic basin is not smooth. Complex bedrock morphology influences the ephemeral stream systems. The basin floor slopes to the west, descending in a series of steps. The rapid breaks in slope create localised areas of reduced flow velocity where rapid deposition of ephemeral stream sediment occurs. These deposits are also reworked by aeolian processes as desiccation proceeds, and banks of coarse-grained material form encroachment deposits and granule ripples. As discussed previously, the bedrock morphology controls the migration direction of granule ripples. In the case of the Idatal the material was progressively transported west towards the base-level of the system within the Pomona Claim boundary.

The continued transport of material into this part of the basin is a pre-requisite for the generation of the placer deposit. If polycyclic reworking had continuously removed diamonds to the north and no new material entered the basin, the placer body would have diminished through time as diamonds left the basin. Infrequent rainfall events and the continued influence of sandflow driven by the high-energy aeolian system would have continued size sorting the remaining sediment to re-establish the aeolian dispersal pattern comprised of progressively coarser diamonds.

Ultimately Kaiser (1926a) concluded that the diamonds concentrated within endorheic basins represented polycyclic lag placers that evolved through interaction of the aeolian and ephemeral stream sediment dispersal systems (Fig. 116).

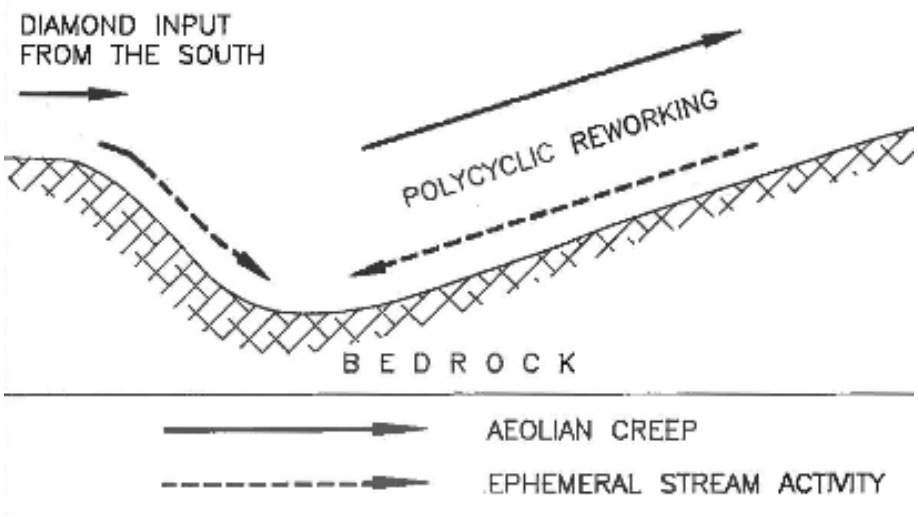

Figure 116. Sketch illustrating the polycyclic nature of the diamond placer deposits located within endorheic basins in the vicinity of Pomona. Based upon observations by Kaiser (1926a) and this study.

Kaiser (1926a) considered that the deflation of a pre-existing sediment pile resulting in the progressive concentration of diamonds on the basin floor through a process of surface lowering accounted for the placers. The bimodality of the diamond population (which is masked by average diamond size data) and the location of the main diamond placer body containing the larger diamonds near the Idatal's base-level support his deflation lag theory. However, this concept implies that a finite diamond

resource held in a sediment pile ultimately accounted for the placers. We now know that diamonds supplied to the margin during the Cenozoic arrived in a series of pulses – the evidence for this had not been discovered when Kaiser and his colleagues studied the region. The deflation lag concept can therefore provide only a partial explanation.

Coupled with ongoing diamond supply, the mobility of the bedload population and the diamonds it contains presents an alternative hypothesis. In this case, diamonds were supplied to the NAEB from a variety of sources over time leading to the progressive development of placers. Pathways defined by Aeolian Transport Corridors enabled diamond transport into successive endorheic sub-basins.

Although diamonds of large to medium average size would be less readily entrained into bedload transport, many were less than 1 ct/stone. These diamonds potentially formed part of the mobile aeolian bedload population. Differential transport rates would mean that larger diamonds would remain within the endorheic basin for a much longer period than the smaller diamonds, which could migrate at a faster rate. Provided that sufficient sandflow passed through an endorheic basin, given time, bedload transport would ultimately transport a substantial percentage of the larger diamonds in the mobile bedload up the south-facing slope at the northern end of a basin. There, they would become susceptible to reworking by ephemeral streams back towards the base-level (Kaiser's gravitational centres).

Evidence supporting this scenario is described in the next section.

Idatal-Hexenkessel-Scheibetal Endorheic Basins

A series of mature endorheic basins characterise the geomorphology of the Pomona Claim. They extend north from a common origin in Lüderitzfelder. Rich placer deposits floored the Idatal, Hexenkessel, Kaukausibtal and Scheibetal sub-basins. The Idatal is the largest sub-basin on the western side of the Claim, whilst the Hexenkessel is situated centrally, to the south of the Kaukausibtal. The Scheibetal is a large endorheic sub-basin on the eastern side of the Claim (Fig. 117). As in the Idatal, base-level in the Kaukausibtal and Scheibetal is along the western margin. Pervasive silicification associated with carbonatite volcanism aided the development of uneven bedrock topography on the floor of these basins.

A re-evaluation of the duricrusts present within the Sperrgebiet by Pickford (2015) and Pickford & Senut (2016) is providing the basis for a fundamental change in understanding of the topographic evolution of the NAEB. These researchers have concluded that the silicified rocks which were originally included in the Pomona Schichten by German geologists and later called the Kätchen Plateau Formation by Miller (2008) in fact represent silicification of a marine sandstone containing leben-spurren and silicification of limestones of the Ystervark Formation (of carbonatitic affinities). Pickford (2015) considered that the main period of silicification ocurred during the Lutetian-Priabonian, related to geothermal waters emanating from the Klinghart Phonolite Cluster. This silicification is not to be confused with the much slighter silicifcation that has affected the Namib 1 Calc-crust of Middle Miocene age (pers. comm. M. Pickford, 2016).

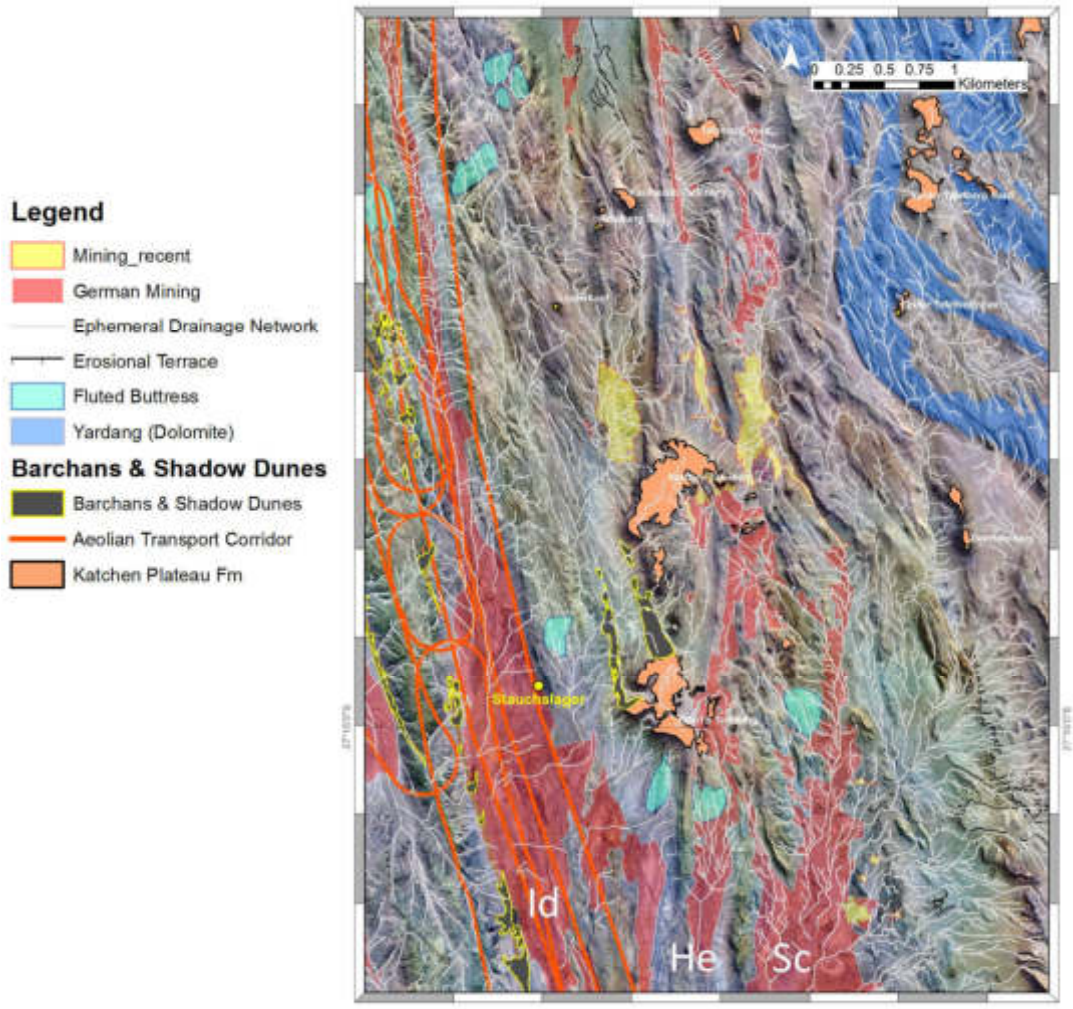

Figure 117. ALS DEM showing three of the most famous endorheic basins that contained diamond placers in the Namib Aeolian Erosion Basin. Id =Idatal, He = Hexenkessel, Sc = Scheibetal. The ephemeral drainage networks exhibit the classic form described by Kaiser (1926a). In the south-eastern corner headward retreat by ephemeral streams has cut an erosional terrace.

The diamond dispersal pattern of the Hexenkessel closely resembles that of the Idatal (see Fig. 115), with a clear reduction in the average diamond size from south to north. A slight increase in the diamond size is evident on Elfert's Tafelberg at the northern end of the south-facing slope.

The diamond dispersal pattern within the Scheibetal also shows a general decrease in average size from south to north. There is also a noticeable reduction in the average diamond size from west to east across the Idatal, Hexenkessel and Scheibetal.

The Kaukausibtal diamond dispersal pattern is particularly interesting when viewed in conjunction with the data from the Hexenkessel and Scheibetal. Whilst there is a general south-north trending reduction of the average diamond size within these basins, when it is viewed in detail several deviations from this trend are observed within the Kaukausibtal (Fig. 115, 118).

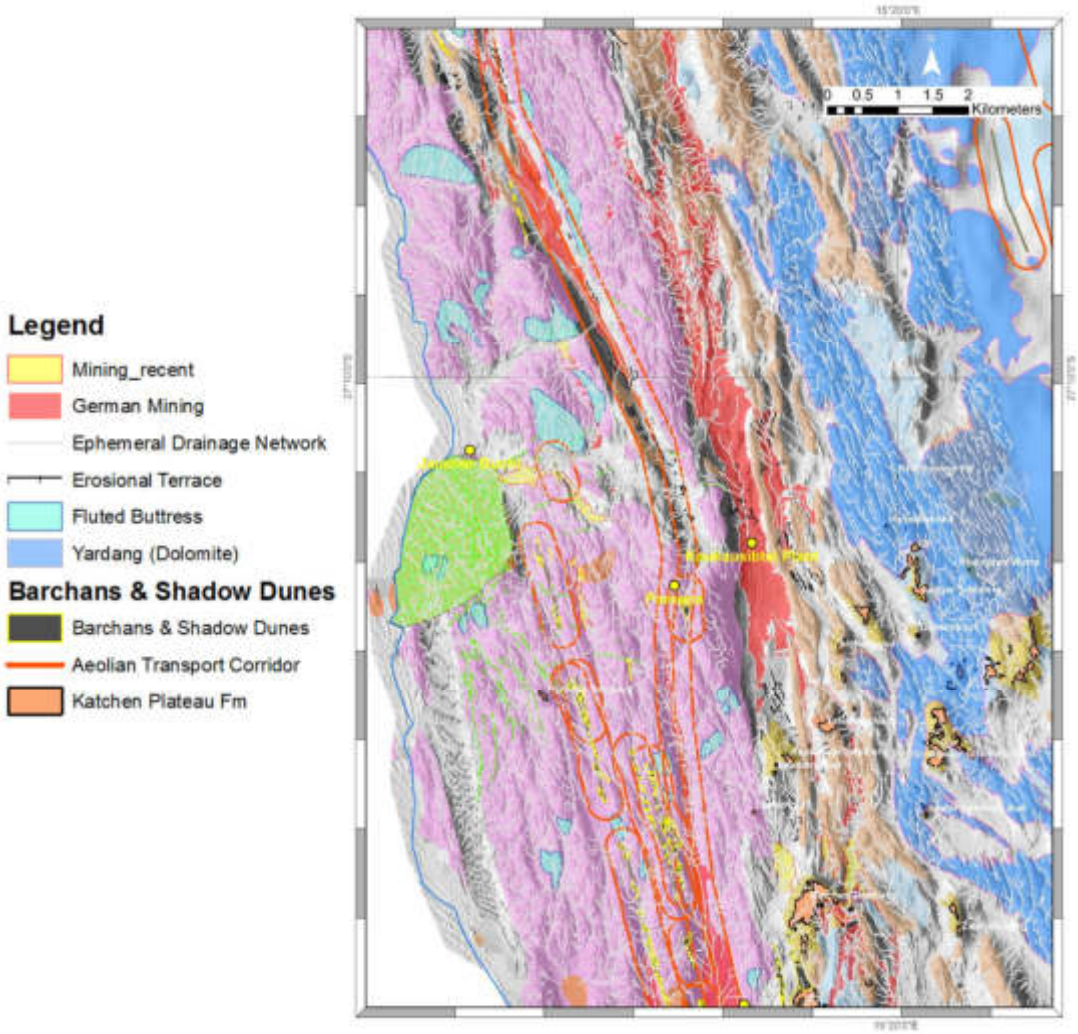

Figure 118. ALS DEM with bedrock drape showing the location of the Kaukausibtal sub-basin and the smaller Kaukausibtal Öst. The mining operations in Kaukausibtal were extensive. Note the presence of erosional terraces through the area related to the development of the drainage network – these are located along the eastern sides of the endorheic sub-basins. The northern Idatal extends up to Pomona. The valley immediately north of Pomona is the Windhuktal.

Within Kaukausibtal, the larger diamonds were concentrated along the western side of the valley at the base-level of the system. Slightly smaller diamonds were located at the extreme southern margin on the watershed. Hence on the north-facing slope at the southern end of the basin, there is evidence of a downslope increase in diamond size. North of the sub-basin's base-level, an elongate tail of small diamonds extends along the gently inclined floor of the south-facing slope. At the northern end, as the south-facing slope steepens the average diamond size increases slightly. Another small increase in the average diamond size also occurs at the base-level of the next endorheic basin to the north. A series of northward-fining zones of average diamond size extend north in narrow elongate zones from this point.

Viewed as separate entities, each endorheic basin exhibits a classic dispersal pattern which is beautifully demonstrated by the Hexenkessel where fabulously rich deposits found at a local base-level yielded 1,693 diamonds from one 20 m trench sample. The concentration tailed off abruptly both to the south and the north. Within each basin east-west oriented bands of greater diamond concentration are found where the gradient of south-facing slopes increases. The overall trend in average

diamond size showing a progressive reduction from south to north is interpreted as further evidence of diamond transport in the mobile aeolian bedload population. The dispersal pattern exhibited by the Idatal effectively repeats downwind in successive basins in response to aeolian size sorting.

In the aeolian system, sorting occurs in response to variation of the entrainment potential of particles on the basis of their shape, size and density. Although smaller diamonds are theoretically shielded from direct saltation bombardment by larger grains, they appear to have remained more susceptible to entrainment than diamonds of medium to large size which are entrained by comparatively rare collision of larger particles with the bed. Based on observations by Dong *et al.* (2004) the mobility of the smaller diamonds despite the presence of immobile roughness elements could reflect the effect of near-bed inter-particle collision in the sand cloud blowing over gravel beds which could reduce shielding of the bed between immobile roughness elements.

Nevertheless, the presence of obstacles on the floor of endorheic sub-basins ranging from micro- to macro-scale would undoubtedly also influence diamond migration rate as part of the aeolian bedload. The diamond dispersal pattern within Kaukausibtal and succeeding sub-basins to the north provide conclusive evidence of northbound migration, which terminates finally at Wüstenkönig in the western end of the Grillental (Fig. 119). Looking north from the Scheibetal, the smaller average diamond sizes seem to have been unstable on the divide between the sub-basins, and only small to medium average diamond sizes are represented. It is possible that this is related to accelerating airflow over the watershed resulting in aeolian size sorting. The slight increase in diamond size at base-level is probably the result of alluvial transport down both the south- and north-facing slopes together with progressive removal of smaller diamonds due to aeolian size sorting. On reaching the northern end of the basin, the increased complexity of the bedrock morphology together with the presence of a steeper south-facing slope caused a change in transport potential and the deposition of a slightly coarser population of diamonds as size sorting continued.

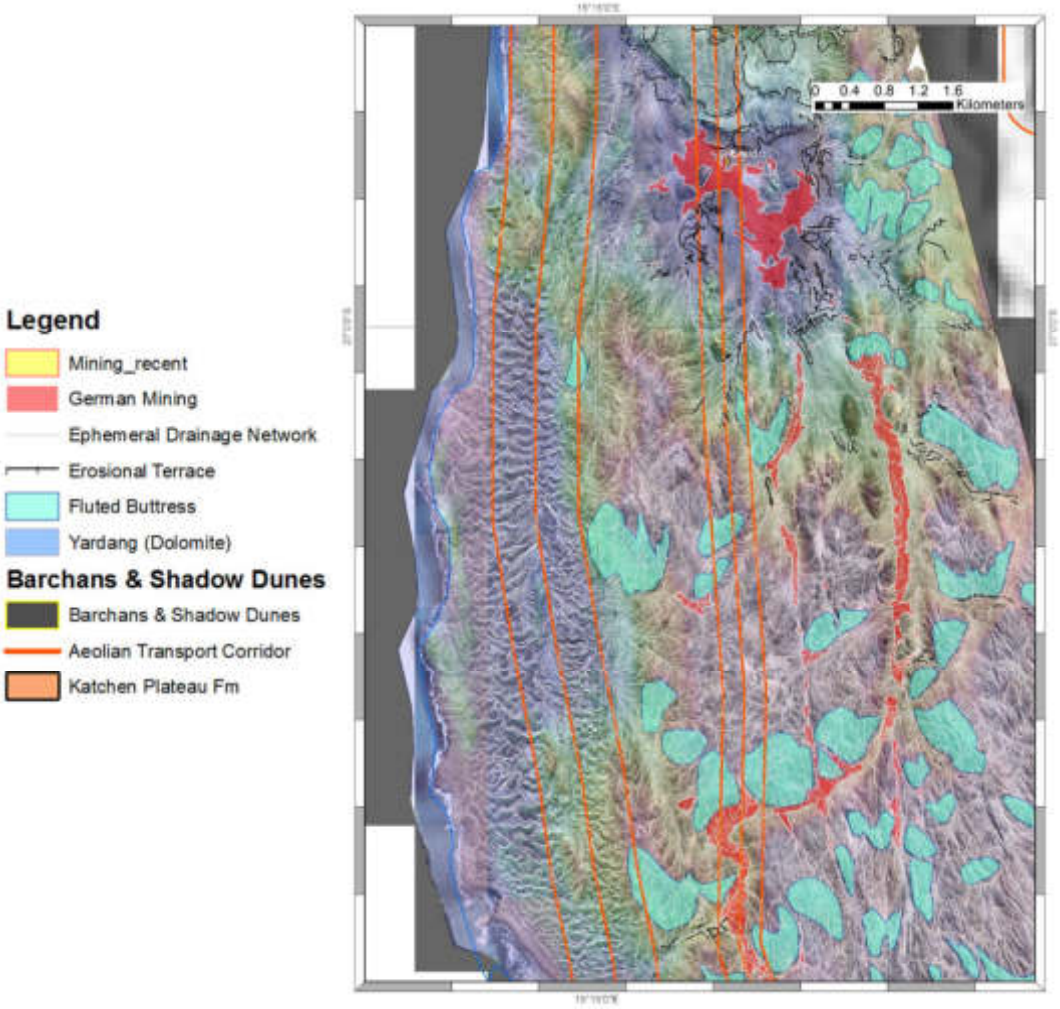

Figure 119. The diamond placers to the north of the Idatal-Hexenkessel-Scheibetal-Kaukausibtal endorheic sub-basins are characterised by fast-moving diamonds of small average size. Some spectacularly well-developed sites at which diamonds formed part of the streaming aeolian bedload can be identified within this part of the domain. In terms of the erosional architecture, fluted buttresses are characteristic of this gneiss-floored area of the NAEB. Although ATCs are present, the system remains under-saturated with respect to sandflow, so no barchan dunes occur in this area in which airflow is topographically funnelled. Transverse dunes characterise the headland bypass system that originated at Prinzenbücht.

Kaiser (1926a) recognised that diamonds had been transported from one basin to another, but was indefinite about the extent to which it had occurred. This becomes more apparent when the patterns of mining activity are examined. One of the best examples of topographic funnelling resulting in streaming aeolian bedload transporting diamonds north is observed to the north of the Hexenkessel (Fig. 120). Diamonds were transported up and over the plateau of Elfert's Tafelberg and around the eastern side of the feature produced by topographic inversion to form a series of narrow endorheic sub-basins. Further evidence of diamonds being incorporated into streaming aeolian bedload can be seen to the north of Windhuktal (Fig. 121). A narrow valley system produced by aeolian erosion extending north contains a series of circular claims that produced small quantities of diamonds. Interestingly within the Pusstal Claim the valley displays a clear structural offset which is picked out by the pattern of diamond mining.

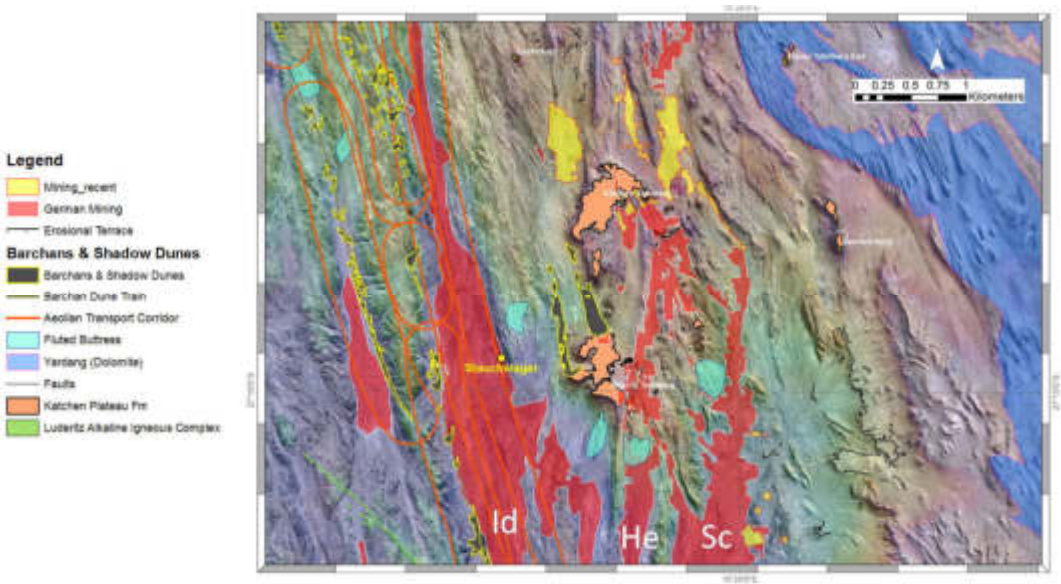

Figure 120. Evidence of diamond transport as part of the streaming aeolian bedload migrating through complex topography produced by topographic inversion. Note the flaring pattern along the western margin of Scheibetal with streamers of bedload extending up narrow valleys that topographically funnel the surface windflow and saltation load. Id = Idatal, He = Hexenkessel, Sc = Scheibetal. Dykes associated with Lüderitz Alkaline Igneous Complex in green.

Aeolian bedload deposition on south-facing slopes outside areas of mining activity shows that these slopes provide ideal conditions for encroachment deposits to develop (Fig. 122). Kaiser (1926a) observed that diamonds were situated amongst neatly placed, spindle-shaped, consistently oriented grains on the surface of deposits. He attributed the shape and orientation of these grains to aeolian corrasion. Whilst aeolian corrasion does produce small ventifacts amongst the bedload population, Kaiser (1926a) was probably referring to the imbricate shape-fabric exhibited by aeolian bedload. Once surfaces are stabilised by the imbricate fabric the probability of diamond entrainment would decrease. Increasing the gradient that a south-facing slope presents to the saltation load would theoretically have a similar effect in reducing the probability of diamond entrainment. As shown by the distribution of diamonds within the Hexenkessel, if the south-facing slope is sufficiently steep it becomes a barrier to the migration of the aeolian bedload by reptation and creep. If transport of the lighter quartzitic material is maintained then segregation by size-density sorting will be enhanced, increasing the concentration of diamonds - this pattern is seen in Figures 120 to 122.

Diamonds that did migrate up the south-facing slope would have periodically been reworked by ephemeral streams and redeposited at the base-level of the system. This explains why the steep part of the slope, leading north from the Hexenkessel was characterised by particularly small diamonds with a higher probability of entrainment. Inevitably some diamonds, migrating at slower rates would be unaffected by ephemeral stream activity, and would eventually cross the watershed into the Kaukausibtal. This may explain the presence of diamonds of increased average size on the basin floor and south-facing slope at the northern end of the Kaukausibtal Basin.

Provided the throughput of diamonds by aeolian processes was maintained at a sufficient rate, progressive segregation by aeolian size sorting would account for the multi-basin diamond dispersal pattern exhibited by average diamond size data.

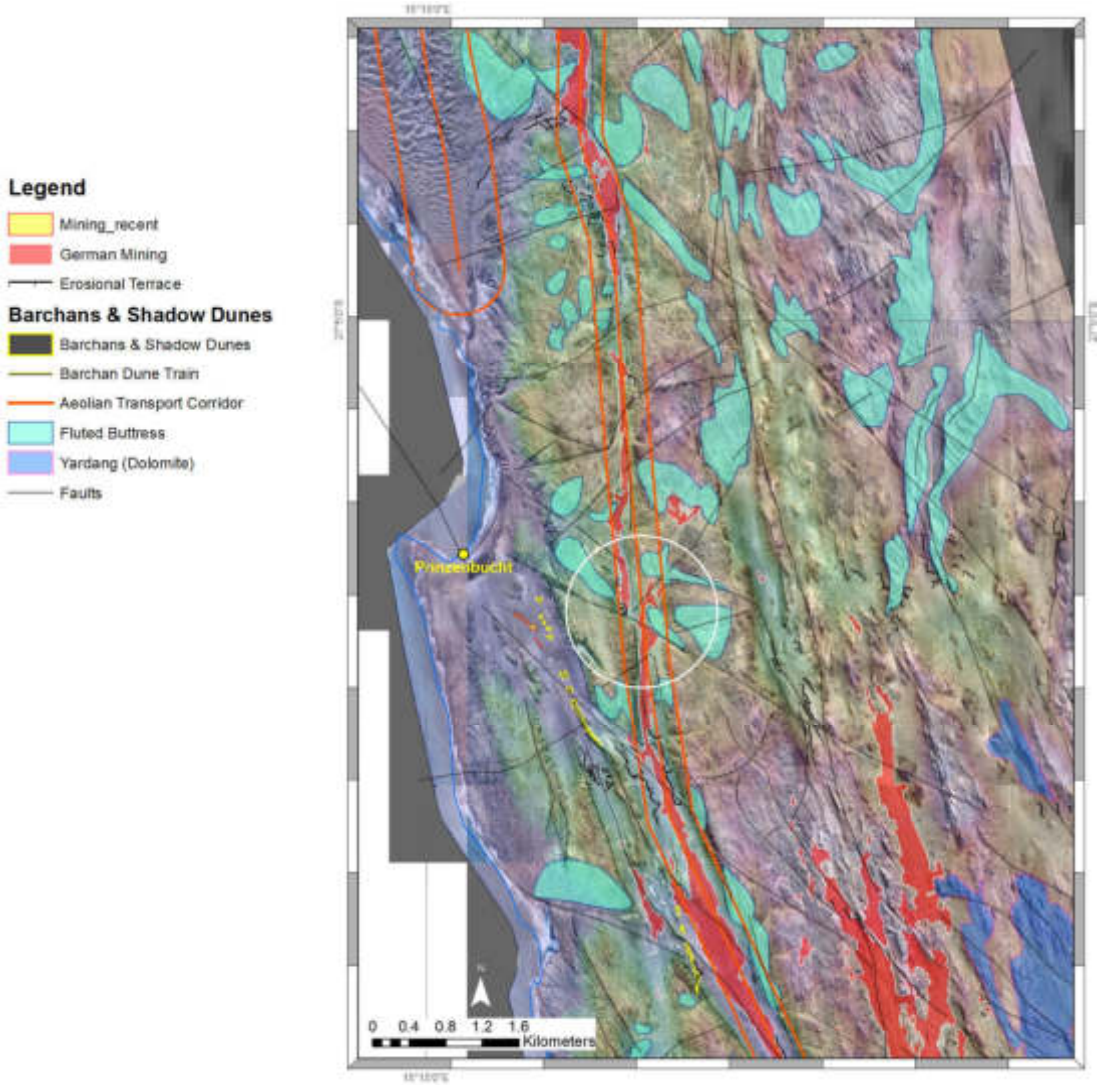

Figure 121. Aeolian bedload tail of small diamonds extending northwards from Windhuktal. White circle highlighting structural neotectonic (?) offset in deflation valley in the Pusstal Claim to the east of Prinzenbücht. Less-developed bedload streaming is seen to the north of Kaukausibtal – this may be a function of placer maturity. Kaukausibtal contained a thick alluvial placer sequence suggesting that the deflation process along the eastern margin of this placer domain was less advanced. Note the yardang field in the top right eroded in gneiss of the Namaqua Metamorphic Complex

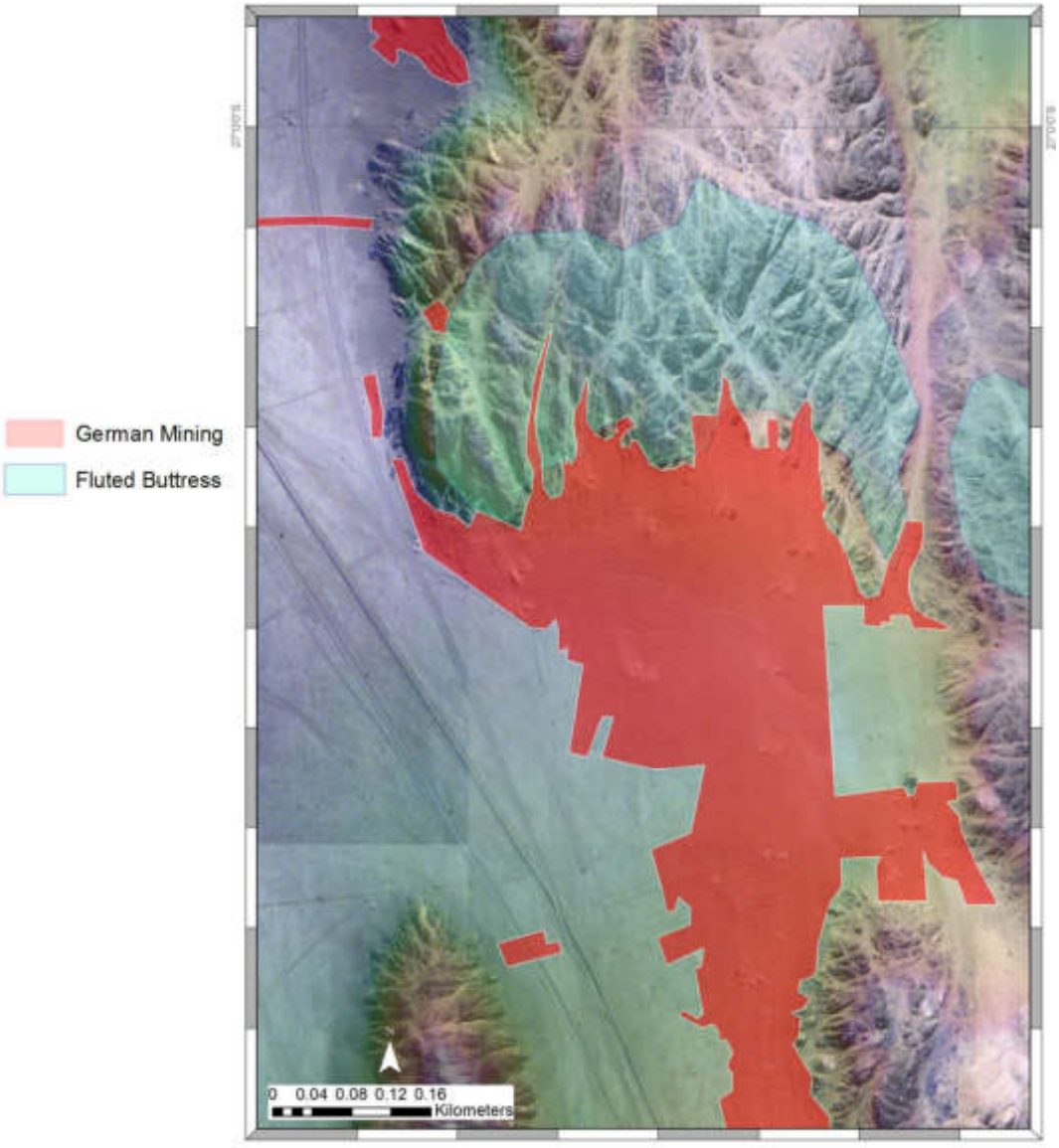

Figure 122. Encroachment deposit forming the northern end of an elongate placer body with streaming bedload containing diamonds extending up south-facing slopes of a fluted gneiss buttress situated at the entrance to Grillental. Note some bedload streaming forming placer extensions bypassing both flanks of the topographic barrier.

Whilst ephemeral streams have influenced the dispersal pattern, the overall distribution of diamonds within this domain is one of aeolian diamond dispersal driven by the unimodal southerly wind regime.

Bedload Transport as Kinematic Waves

Langbein & Leopold (1968) described a kinematic wave as "a group of moving objects in a zone along a flow path through which the objects pass. These concentrations may be characterised by a simple relationship between the speed of the moving objects and their spacing as a result of interaction between them". Lighthill & Whitham (1955a, 1955b) used kinematic theory to describe flood movement in long rivers, and the flow of traffic along crowded roads which appears to bear close analogy to the behaviour of grains during their transport by aeolian

creep. Lighthill & Whitham (1955b) were able to show that the movement of cars along a single-lane road can be expressed using a flow-concentration curve, where flow is the number of cars passing a particular point on the road per unit time and concentration is the average number of cars per unit distance of road. When cars are spaced far apart the linear concentration is zero and the curve passes through the origin, but as concentration increases the point is reached where the vehicles are nose to tail and the flow is then zero. The ascending limb of a flow-concentration curve is stable, and the road is in an uncrowded state, but the descending limb is unstable and the road is crowded. As traffic flows along a road, local concentrations bounded both front and back by a zone of lower concentration occur. This variation represents a kinematic wave.

The velocity of a kinematic wave at any point along a road is given by the slope of the flow-concentration curve for that particular point. On the rising limb the kinematic wave travels more slowly than the cars on the road, but in the same direction. A tangent drawn on the descending limb has a negative slope, and hence the kinematic wave will travel backwards, towards the approaching traffic. When this occurs the wave is termed a "shock" wave, and it results in traffic being denser in front than it is behind. As a consequence oncoming cars entering this wave experience a very rapid reduction of speed. If the flow capacity of a road varies along its length, potential exists for bottleneck development, whereby the maximum flow past a particular point on the road drops below the flow capacity of the main road. Provided the incoming flow rate towards the bottleneck does not exceed its capacity the vehicles only experience a temporary reduction of speed as they pass through. If, as time goes on, the incoming flow exceeds the bottleneck capacity, kinematic waves begin to travel backwards and a shock wave develops, forcing the vehicles to pile up at the entrance to the bottleneck. Continued influence of the shock wave results in the vehicles approaching the bottleneck being reduced to a crawl. Once the incoming flow is reduced to less than the capacity of the bottleneck, the shock wave commences to travel in the downstream direction and eventually passes through the bottleneck.

Bagnold (1935) perceived that the larger grains on a bed subjected to saltation shield those lying immediately downwind from saltation impact by varying degrees, depending upon the variation of grain size. Grains downwind of others therefore migrate more slowly and, in turn, retard the advance of others situated immediately upwind. Bagnold thus envisaged that there were "among the bigger grains alternate traffic blocks and empty spaces" which implies that ballistic ripples can be treated as kinematic waves, a concept later supported by Miller (1983). Observation of a planar bar surface on the floor of an ephemeral stream bed appear to support the above concept (Corbett, 1989). Over a period of time the initially planar bed was modified to form a series of flow-transverse ridges of variable amplitude, increasing in height from south to north, with the propagation of the ridges commencing initially at the northern end (Fig. 115). The ridges eventually formed granule ripples at the northern end of the modified bar surface.

A distinct pattern of grain size variation could be seen across the bed upwind of the fully developed granule ripples. Grains comprising the lee slope are particularly well-sorted compared to those lying on the stoss slope or troughs of the bed forms. A wide range of grain sizes are present in the troughs between the ripples, including the largest grains. The interstices between these particles contain the smaller particles, which corresponds to Bagnold's (1935) "traffic blocks and empty spaces". Although not measured, visual comparison showed that the sorting of the surficial grains noticeably improved up the stoss slope, where fewer large grains are present, and the concentration of particles of similar size increases.

The smaller ridges at the southern end of the bar which underwent modification by

aeolian processes also resulted from the concentration of similar-sized particles. These low ridges are bordered both upwind and downwind by zones of lower concentration, with larger quantities of coarse grains being present in the troughs. The lee slope of the ridges was difficult to see, but its position is clearly marked by a flow-transverse band of better-sorted granules. Therefore, as with the garnet experiment a heterogeneous size-shape-density mixture of grains was modified due to variation in their entrainment potential. Theoretically those grains which are more readily entrained will migrate more rapidly, so that they will approach slower moving grains ahead. As the distance separating the grains is reduced a point is reached when they begin to interfere with one another and the shielding effect of larger grains further retards the migration of particles below a critical size. By analogy with Lighthill & Witham's (1955a, 1955b) explanation of traffic flow, a shock wave is developed, which results in grains entering the "hump" experiencing a dramatic reduction of speed. As observed on the bar, as aeolian modification proceeded, the region of increased concentration spreads backwards in the upwind direction.

Similarly, the influence of obstacles of varying scales on the migration of the bedload creep population can apparently be explained by kinematic wave theory as all obstacles have one effect in common, which is to reduce the transport capacity of the aeolian system. Hence the obstacles appear to act as bottlenecks in which kinematic shock waves are generated leading to discrete concentrations of diamonds forming between roughness elements on stone pavements.

To examine the aeolian system using kinematic wave theory, it is necessary to simplify the sediment dispersal system. Whilst the creep bedload does essentially migrate through the region under the influence of a unidirectional aeolian system, ephemeral stream systems also operate. Polycyclic reworking of ephemeral stream deposits on the south-facing slopes of endorheic basins partially destroys the kinematic waves composed of the aeolian creep bedload. Thus, as the material transported towards the base-level of the endorheic basin systems by ephemeral streams is reworked by aeolian processes, new kinematic waves are developed. Complex interaction between the systems therefore takes place.

The distinct, northward-fining tail of diamonds indicates that the aeolian system governs the overall diamond dispersal pattern at the present time. The interpretation of the placer bodies within endorheic basins using kinematic wave theory applied to the creep bedload, therefore appears to be justified. In this respect the flow-perpendicular bands exhibited by the diamond dispersal pattern based upon the number of stones, is particularly interesting. The bands define alternating zones of slightly lower and higher concentration. Provided that the diamonds enter the aeolian dispersal system at its southern end, the variation of entrainment potential theoretically results in bunches of like grains composing kinematic waves travelling at variable speeds along the transport path. These bands possibly provide evidence for kinematic waves.

Unfortunately the absence of detailed diamond size-frequency data prevents this hypothesis from being tested, and it is impossible to determine whether this pattern is an artefact of the prospecting technique used or not.

The Elisabeth Bay – Schmidtfeld Placer Domain

The second placer domain examined in detail extends from the present-day coast at Elisabeth Bay to the Schmidtfeld Plant which was located to the north of the town of Lüderitz between the coast and the active plinth of the modern Namib Sand Sea (Fig. 123).

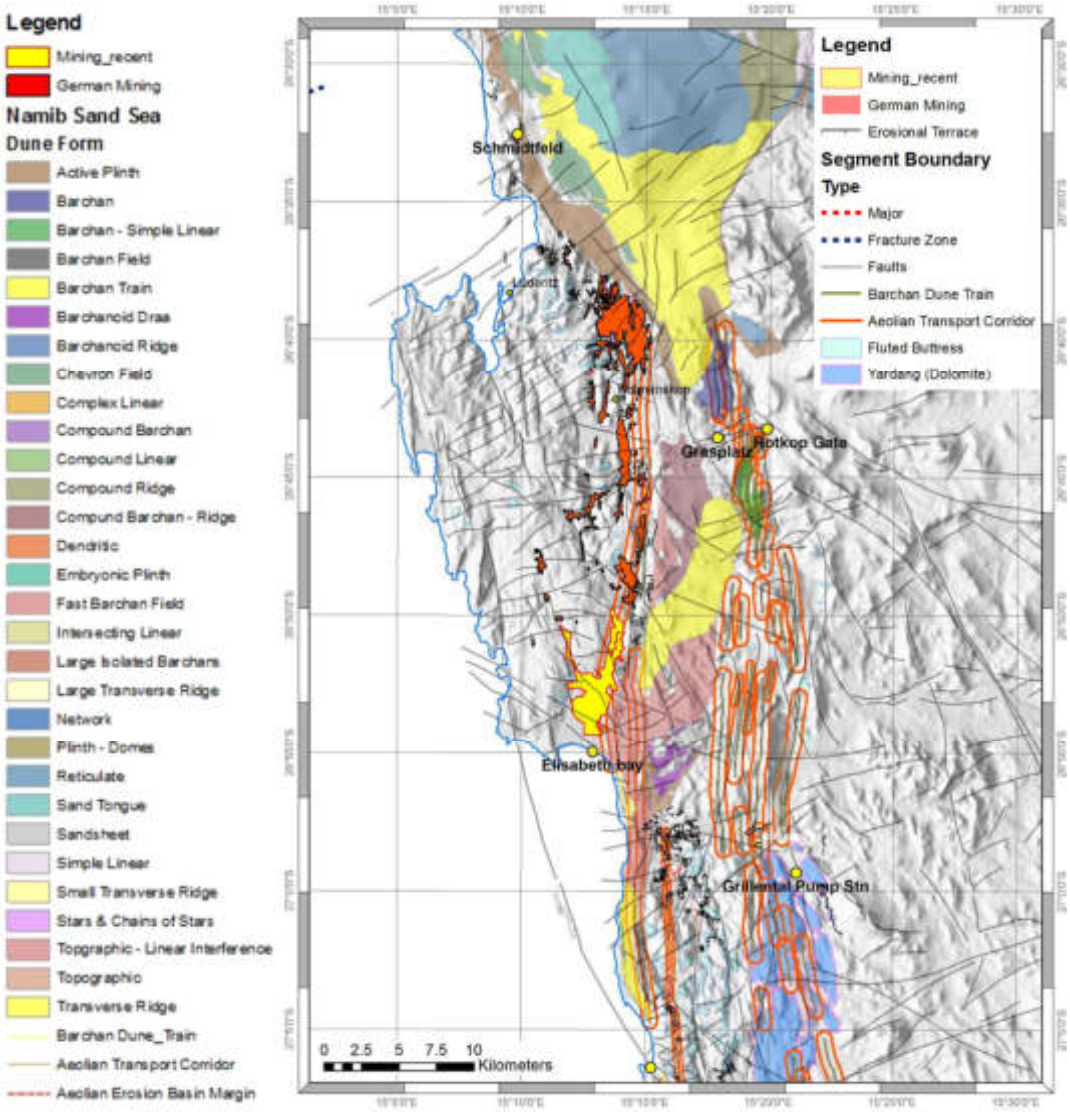

Figure 123. The Elisabeth Bay-Schmidtfeld ATC. Mining originally commenced at Elisabeth Bay around 1929, but the workings have largely been obscured by more recent mining activity. Located immediately to the west of the southernmost extent of the Namib Sand Sea, the development of this placer domain is situated within the transition zone between the Namib Aeolian Erosion Basin and the Namib Depositional Basin. Faults mapped as part of this study are shown. The yellow dot in the south on the coastline marks Prinzenbücht. Dune form distribution is modified after Livingstone *et al.* (2010).

This domain contains some of the most important Miocene vertebrate localities which were worked on extensively by early German researchers and subsequently by the Namibia Palaeontology Expedition. These deposits are characterised by thick sequences of fine- to coarse-grained sediment.

It is possible that the depressions in which they occur may turn out to be fault-controlled basins similar to those located in Namaqualand. Whatever their origin, this domain has been subjected to repeated topographic inversion through the combined effect of weathering and the interaction of the aeolian and ephemeral stream systems as well as episodic marine transgression (Burger 2015).

The depressions containing the Miocene alluvial sequences also preserve important aeolian sequences, some of which are economic placers. An unusual biostratigraphy based on avian eggshells (Pickford *et al.* 1995) allow precursors to

the modern Namib Sand Sea to be differentiated in the Namib Depositional Basin and further south at Rooilepel, close to the Orange River. It is likely that these systems have operated over at least the last 18 m.y.

With the exception of the depressions in which Miocene sequences are preserved, this domain is floored by gneisses of the Namaqua Metamorphic Complex. As a result, the relief is significantly more subdued than it is further south in the Lüderitzfelder-Pomona-Grillental domain (Fig. 124).

Extensive mining took place early on within this domain. Innovations such as the first bucket-wheel excavators were introduced here along the lower part of the active plinth of the Namib Sand Sea at Charlottental. Consequently large areas of ground have been substantially disturbed, making observation of pristine bedforms and sedimentary sequences difficult to achieve with certainty.

The diamond dispersal pattern in this domain is a simple linear ribbon extending from the coast inland to the active plinth. Exploration by Namdeb located a high-grade pocket beach preserved in the eastern corner of the embayment between 10 mbsl to 18 mbsl (Burger 2015).

Figure 124. Oblique view across a relatively subdued erosional aeolian landscape looking south west towards the active plinth of the Namib Sand Sea north of Lüderitz Airport. Note that the southern end of the depositional basin is located within a depression which may be fault-controlled. North to the left.

Based on the limited information available about diamonds from the region only generalised comments are possible. The diamond size declines north from the Elisabeth Bay coast where the average stone size is 0.25 cts/stn to 0.14 cts/stn (Burger, 2015) on the watershed at the northern end of the Elisabeth Bay mine area. At Charlottental, the average diamond size was between 0.25 to 0.2 cts/stn (Schneider, 2008) although it probably declined rapidly up the active plinth where bedforms indicate that migration rate declined and deposition took place (Fig. 125).

Development of the Elizabeth Bay Mine by Namdeb since the 1990s and mapping of the mine geology has shown that a number of aeolian systems contributed to the formation of the sequence that contains the placer deposit(s) above the erosional unconformity with the Lower Miocene clays dated at 18 Ma by the Namibia Palaeontology Expedition (Burger, 2015). Some of these aeolian systems undoubtedly transported material from the exposed continental shelf during regression(s). One of the more novel lines of evidence supporting this comes from Apollus (cited in Spaggiari, 2011) who observed aeolian fluting on bedrock exposed on the shelf in water depths of 60 m to 70 m during a Jago submersible dive in 1999.

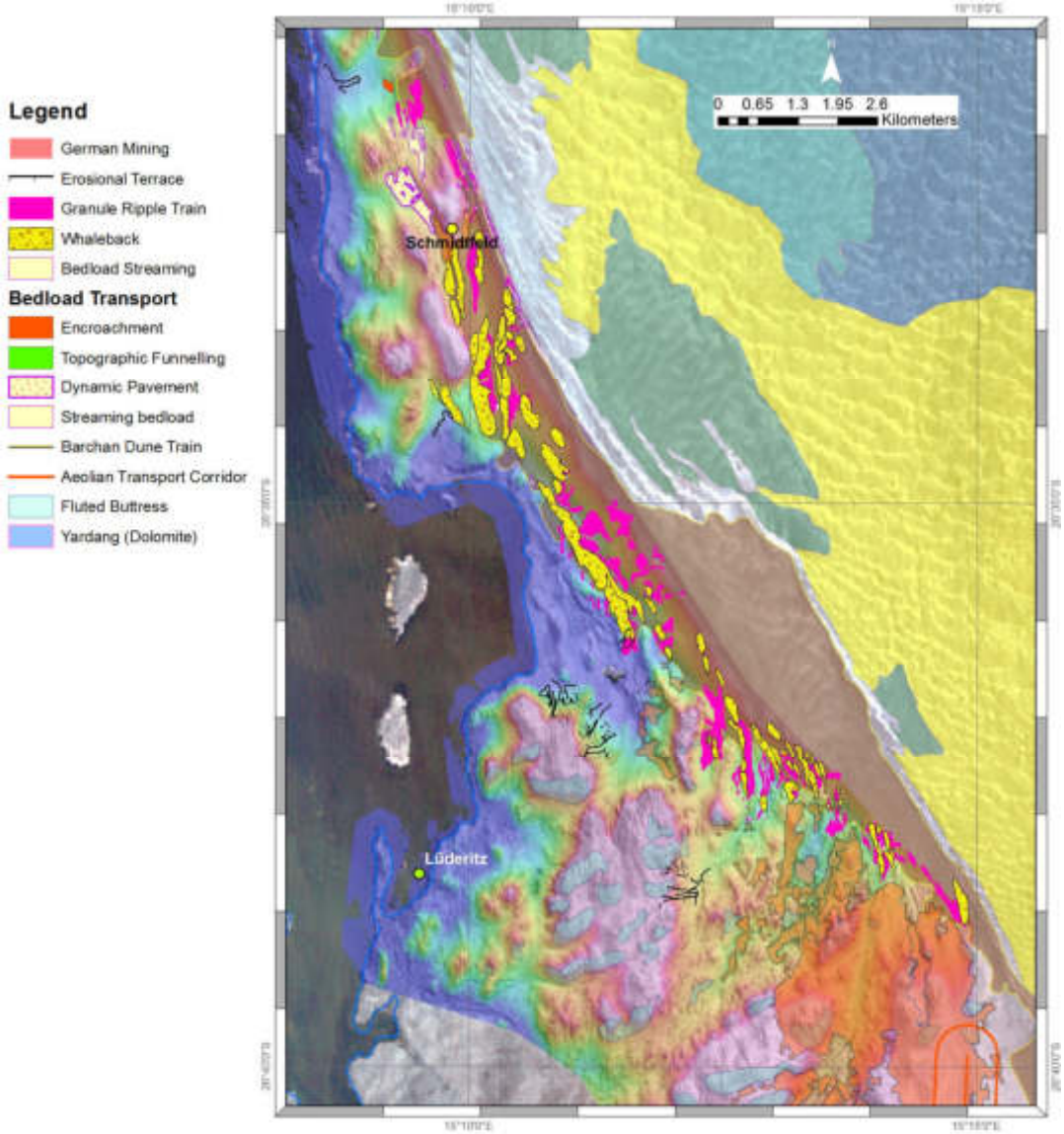

Figure 125. ALS DEM and Landsat image of the Namib Sand Sea with bedforms and deposits attributed to aeolian bedload transport and deposition superimposed along the length of the active plinth. Mining took place along the plinth, but the location of the early activity is difficult to identify. The distribution of dynamic pavement was probably much greater but surface disturbance due to mining prevents recognition. Whilst well-developed yardangs are absent, there is some evidence of fluted buttress formation. Ephemeral streams and ponded water-bodies are active within this region after rainfall. Dune form distribution modified after Livingstone *et al*. (2010).

Coupled with the observation of gravel waves migrating northwards and shoreward at these water depths by Apollus there is no doubt that marine shelf placers will have been reworked and the product incorporated into the aeolian bedload migrating northwards along the Elisabeth Bay ATC over a period of several million years.

The ALS data reveals that a series of large aeolian bedforms termed "whale-backs" during prospecting operations occur along the active plinth of the Namib Sand Sea. The whalebacks are large sheet-like bedforms elongated in the direction of the southerly surface windflow – hence they curve westwards along the plinth. They typically have the surface curvature of a whale's back breaking water. The bedforms consist of sheets of interbedded sand and grit with limited or no vegetation present –

the grits are most likely to be the result of encroachment and ripple train migration. The upwind (southern) margins of the bedforms are often sites for the development of encroachment deposits around their apron. Some of these features, together with granule ripple trains, may be artefacts of early mining operations. Photographs of early mining operations (see Schneider, 2008) into thick encroachment deposits flanking the active plinth would subsequently have been reworked by the high-energy sandflow conditions that prevail along it. Topographic funnelling of the surface windflow is indicated by the orientation of the granule ripple trains climbing north up the plinth.

In conclusion the diamond dispersal pattern in this domain is dominated by evidence of northbound aeolian bedload transport. There is clear evidence that ephemeral stream activity played an important role in developing the placers as well. Locally derived angular sheetflood gravels containing economic concentrations of diamonds are interbedded with the aeolian placers in the Elisabeth Bay (Burger, 2015). Ephemeral streams also played an important role in the development of the placers associated with stone pavements flooring the shallow valleys that descend into the depression in which the Namib Depositional Basin is located (Fig. 126).

Figure 126. Ephemeral stream activity within a mined area to the south of Kolmanskop. Note the relatively subdued relief and the example of a positive step formed by a dyke. Southerly wind from right to left.

Buntfeldschuh-Bogenfels-Granitberg Domain

This domain contains the majority of the Bartonian marine sediments and it also has a complex alluvial history represented by a number of sequences of different ages. As with Elisabeth Bay the domain contains important localities of Miocene vertebrate fossils. These sequences were initially studied by the German palaeontologists brought into the region by Kaiser.

More recently the Namibia Palaeontology Expedition has studied the alluvial sequences throughout this domain and some important new findings have been summarised in a publication by Pickford (2015).

Before discussing the diamond dispersal pattern within this domain it is important to examines the possibility that post-rift tectonic reactivation of old structures might have influenced the development of large alluvial systems within the eastern Sperrgebiet.

The GIS dataset compiled for this study integrates information from numerous sources to build extensively on what was known in the late 1980s. One of the lessons to have emerged during my long acquaintance with the west coast is that when you want to tackle a difficult environment, bringing in the right expertise is essential – this has proved to be the case for palaeontology. Publications by Martin Pickford and his co-workers on the Namibia Palaeontology Expedition have made a particularly significant contribution to developing a new level of understanding both through their palaeontological discoveries as well as by unravelling stratigraphic contradictions and inconsistencies arising from previous publications and reports. Mapping by Namdeb geologists has also been incorporated to produce as comprehensive a dataset as possible.

However, it is when the alluvial dataset is examined in the context of the regional structural trends that key relationships start to become apparent (Fig. 127). The structural mapping undertaken for this paper has revealed that Bogenfels is located at a complex structural junction. The toe of the Schakalsberge Thrust is intersected by a set of converging SSW-NNE faults that run down the northern side of the Klinghardt Phonolite Dome. These faults appear to border the exposures of Blaubok Conglomerate (terminology of Pickford, 2015). The younger Glastal alluvial system also follows this structural trend. Further to the south east, faults with this orientation are recognised to have controlled the development of the Fish River Graben (Mvondo *et al*. 2011) who infer that the Fish River Graben developed during the Eocene – a little earlier than Pickford's suggested Oligocene age for the Blaubok sequence.

The development of the Gemsboktal system on the southern side of the Klinghardt Dome appears to have been influenced by movement of a series of SW-NE trending faults.

A strong SSE-NNW structural trend is evident as well. This trend is a well-documented tectonic fabric that is related to the development of the Namaqua Metamorphic Province (Clemson *et al.* 1997; Raith *et al.* 2003; Viola *et al.* 2012; Frimmel *et al.* 2013) and the collapse of the Namaqualand orogenic belt (Dewey *et al.* 2006). This fabric is increasingly being recognised to have undergone tectonic reactivation in the middle-Late Cretaceous (Raab *et al.* 2002 ; Tinker *et al.* 2008; Kounov *et al.* 2009; Wildman *et al.* 2015). The elongate depression called the Langental, in which lower Miocene alluvial sediments are preserved, follows this structural trend. The exposures of diamondiferous Bartonian marine sediments within the same feature also follow the same trend. The presence of the late Santonian Wanderfeld IV Beds within the Langental feature suggest that it has had a long history as a depocentre.

It is suggested that reactivation of this fault pre-dated movement on the SSW-NNE faults which led to graben formation. Graben development then probably commenced in the Eocene, creating accommodation space which enabled preservation of the Blaubok Conglomerate. It seems likely that this phase of tectonic instability was associated with widespread volcanism on the margin to a greater extent than was previously recognised based on research by Shaw (2006) and Pickford (2015). The Klinghardt Dome was subsequently uplifted by some 300 m (Pickford *et al.* 2014). The combined influence of fault scarp development and initiation of uplift in the vicinity of the Klinghardt Dome probably contributed to the deposition of an extensive Blaubok fan system towards the west. The observation by Kaiser (cited by Pickford, 2015) that the western margin of the Blaubok system interfaced with the Bartonian shoreline is therefore quite plausible, however, it is concluded that this took place within a tectonically-controlled basin setting.

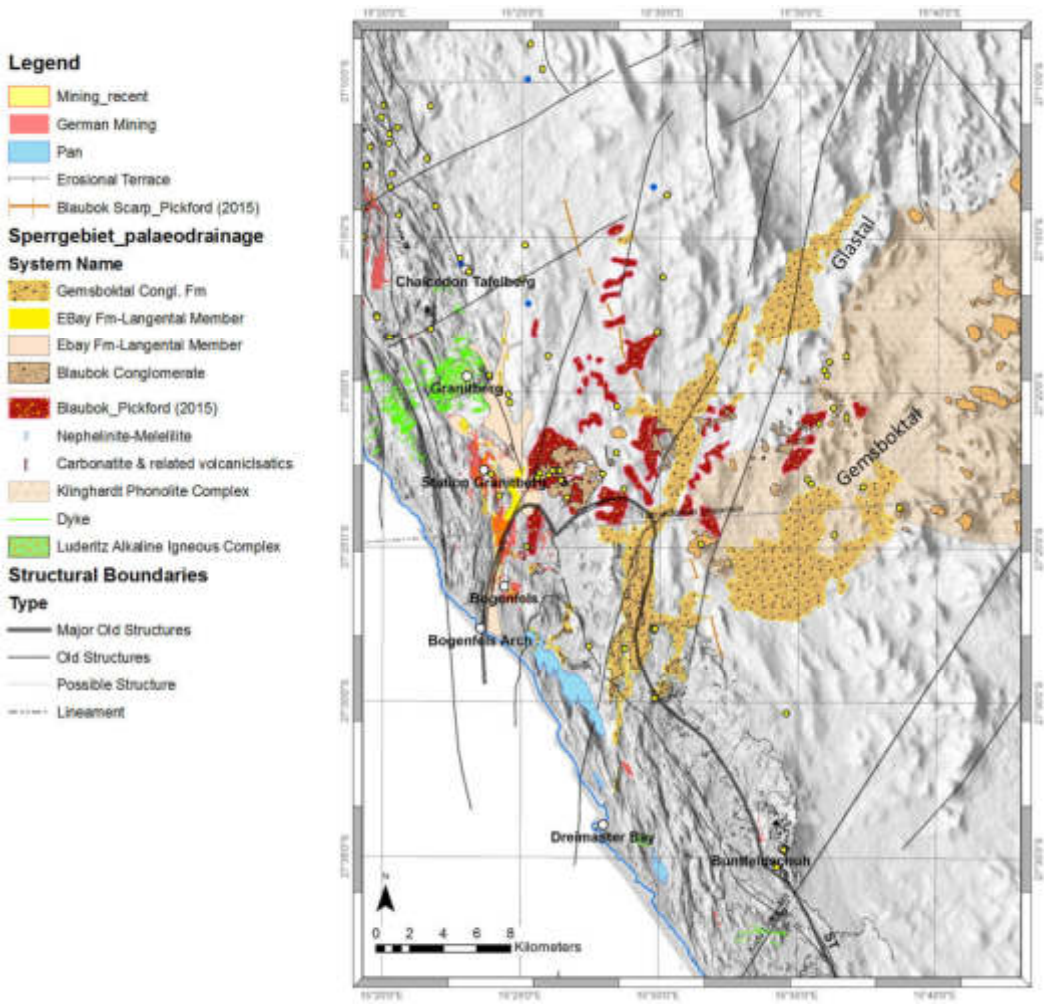

Figure 127. Map showing the distribution of sequences deposited by large alluvial systems between Bogenfels and the Plain Namib in relation to the main structural features identified in this study and the uplifted dome of the Klinghardt Phonolite Complex. Within the NAEB the coarse-gravel alluvial sequences are actively undergoing topographic inversion. The same processes are inverting the tectonically-controlled onshore basin containing the diamondiferous Bartonian nearshore marine sediments for which this area is famous. Note that the SSW-NNE trending faults appear to border the Blaubok and Gemsboktal alluvial systems within a graben-like feature that intersects the toe of the Schakalsberge Thrust. The Langental follows the prominent SSE-NNW structural trend associated with the Gariep orogeny. In Namaqualand, tectonic reactivation of faults with this orientation resulted in the formation of narrow onshore basins, some of which are over 200 m deep, containing stratigraphically complex infills. The small yellow dots show the location of palaeontological sites recorded by Pickford (2015).

Viewed in a broader regional tectonic context (Fig. 128) the relationship between the geographically dispersed alluvial systems within the Sperrgebiet, that are broadly grouped as "Gemsboktal Conglomerates" (following terminology of Pickford, 2015) and the major structural features suggests that these systems also developed in response to tectonic reactivation and the formation of regionally extensive fault scarps. The southern system to the east of Chameis is mappable from a DEM produced from SRTM data. The fan geometry is distinctive, and a clear fan head source area is defined where a SSW-NNE trending fault intersects a major SE-NW trending structural feature.

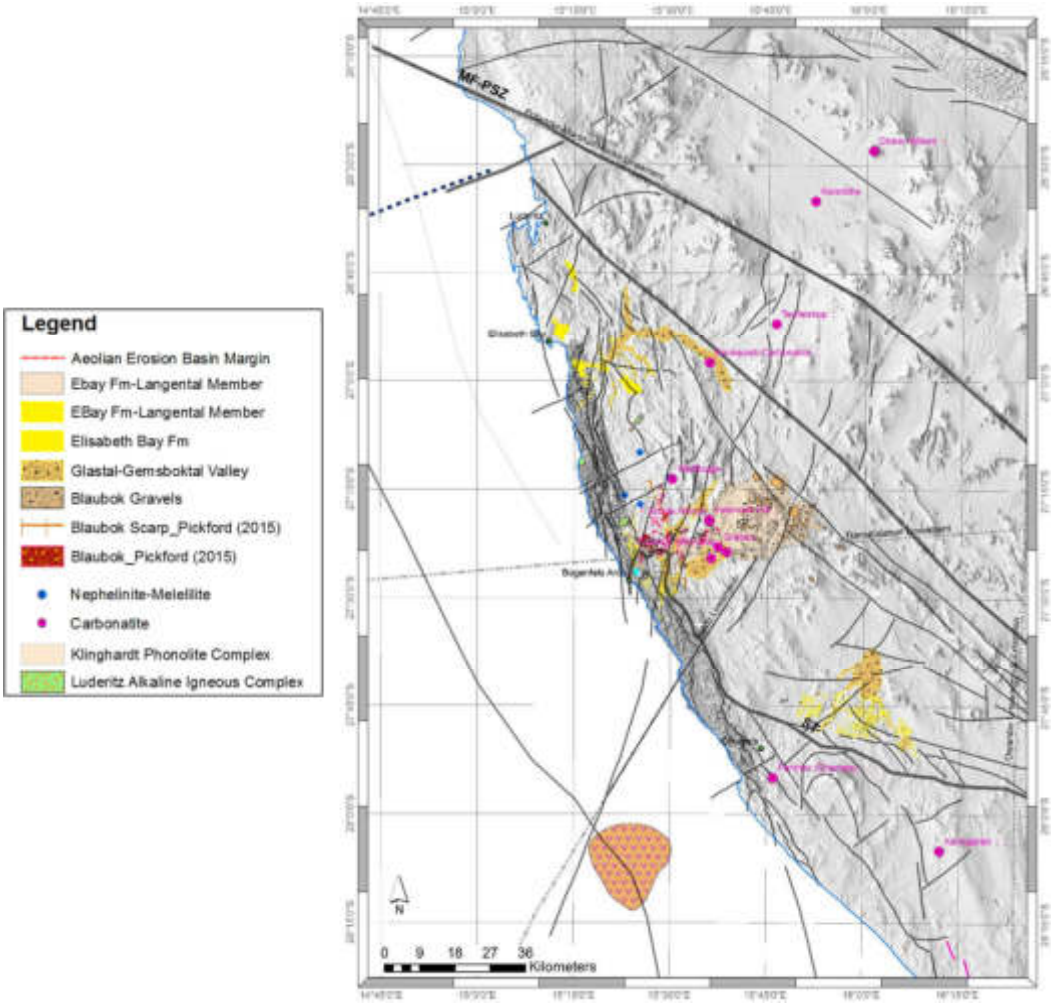

Figure 128. The distribution of large alluvial systems between Chameis and Lüderitz showing the architecture of the systems and their spatial distribution in relation to the major structural features within the region. It is postulated that episodic tectonic reactivation of the faults (extensional tectonics?) led to the development of large fault-scarp controlled alluvial fan systems that flowed broadly westward. The Blaubok and Glastal systems were further influenced by graben development controlled by SSW-NNE faults, which also clearly influenced the distribution of carbonatite volcanism in the interior of Namibia. There are similarities between this graben feature and the larger Lucapa Graben described by Sykes, (1978) who built on an earlier concept proposed by Marsh (1973). Based on palaeontological research in Namaqualand, tectonic reactivation occurred episodically but repeatedly through the late Cretaceous into the Cainozoic. Reactivation in the Cainozoic probably occurred during the Bartonian, Oligocene and the Miocene and later events in the Plio-Pleistocene might well have taken place.

Again, this structural trend is similar to that identified by Mvondo *et al.* (2011) to have controlled the development of the Fish River Graben, providing evidence for widespread development of this fault trend throughout the region. Namdeb geologists mapped a small remnant of what is considered to be an earlier quartz gravel alluvial system (locally termed the Eissenküppe Gravels) which might have been coeval with the Blaubok system at Bogenfels.

The northern Grillental alluvial system also appears to have been constrained by and to have flowed along a major SE-NW trending structural feature before swinging west into the Grillental, the location of which is possibly also influenced by activity on the same SSW-NNE trend.

The scale and distribution of the alluvial systems described in this section is of interest both from a systems and economic perspective. None of the "Gemsboktal" systems, as far as the author is aware, contributed diamonds to the placer deposits within the NAEB. The possibility that the Buntfeldschuh area was once the exit point of the Orange River has long been considered a possibility. Bluck *et al.* (2007) recorded the presence of clasts sourced in the Richtersveld. If this is the case, it is suggested here that the Buntfeldschuh nearshore sediments record terrigenous supply from fluvial incision that initiated what would become a radial drainage pattern with the Orange River flowing around the back of the unroofed Richtersveld Mountains (Fig. 129).

A number of deep "channels", with a similar SE-NW orientation were recorded on the continental shelf by Day *et al.* (1992). If the Buntfeldschuh entry point did exist, it might have been associated with a similarly oriented channel, like the southern limb of the younger Grillental "Gemsboktal-related" system. Pickford (2015) identified a scarp slope associated with the Blaubok system with a similar orientation. These observations once again point to the repeated influence of the SE-NW lineaments on the development of the river systems and in particular, suggest that their reactivation might have resulted in large-scale fluvial diversions. In the case of the Orange, such a diversion would have had to occur prior to 42.5 Ma based on extensive micropalaeontological evidence. As discussed in the section on diamond supply, if this fluvial exit did not exist it implies that high-energy northbound longshore transport must have existed during the Eocene in order to explain the diamond distribution that is recorded from the NAEB.

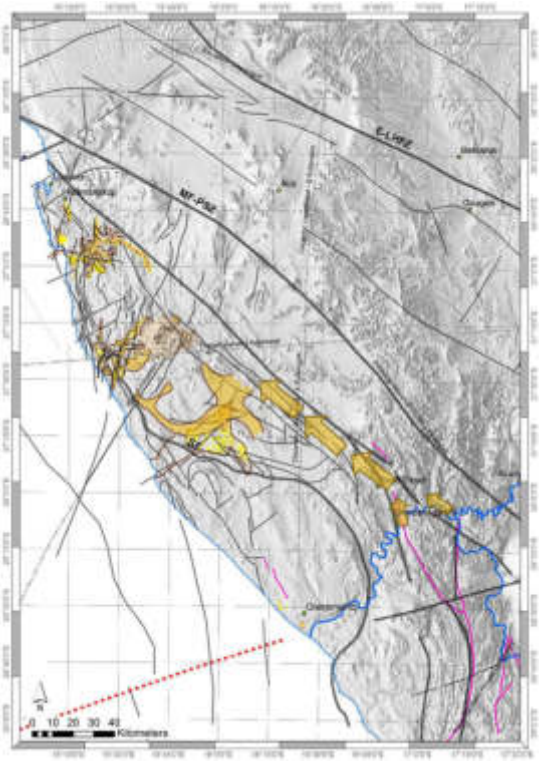

Figure 129. Building on the suggestion by Bluck *et al*, 2007 and Pickford, 2015, this map shows faults in pink that researchers have shown to have been influenced by neotectonic activity. It is tempting to speculate that the Orange River was tectonically diverted resulting in a shift in the entry point for diamonds to the margin.

The possibility of tectonic diversion of the Orange River presents a hitherto unconsidered alternative outlook that could also explain the apparent contradiction observed in the onshore and offshore record of sedimentation in the late Oligocene-earliest Miocene. McMillan & Dale (2002) could find no clear evidence of freshwater input to the shelf off Oranjemund in the Burdigalian based on extensive examination of the micro-faunas in predominantly carbonate sediments. However, extensive evidence of terrigenous input is observed offshore on the shelf further north (McMillan pers. com., 2014). It is possible that a similar tectonic diversion of the Orange River could have taken place due to reactivation of these ancient structures in the late Oligocene/Burdigalian, supporting the establishment of fluvial systems in the vicinity of Bogenfels (Langental) and the Grillental.

Returning to discussion of the diamond dispersal pattern, this basin is today undergoing topographic inversion – the Bartonian marine sediment and the Blaubok and Gemsboktal Conglomerate sequences are progressively being stripped out by erosion (Fig. 130).

As with all of the other examples in which inversion is taking place, the base-level is located in the west – an observation first made by Kaiser (1926a) where inversion (possibly aided by tectonic reactivation) has advanced furthest.

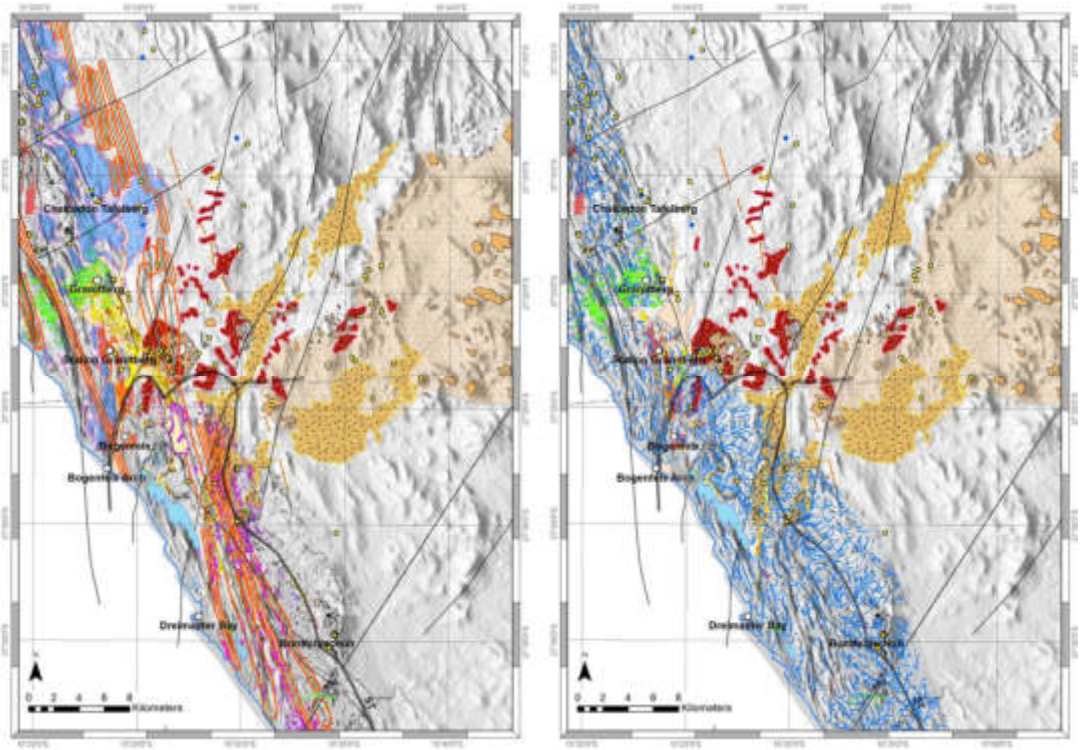

Figure 130. Map summaries of the two principal transport systems responsible for erosion resulting in topographic inversion within the Bogenfels-Buntfeldschuh Basin. The left-hand map shows the convergence of ATCs to the south east of Bogenfels where Gemsboktal Conglomerate exposures are currently being topographically inverted. Deflation of fine-grained weathering products within this zone of extreme sandflow occurs rapidly – but so too does bedload migration as shown by the incidence of granule ripple trains along ATCs which remove bedload consisting of grit and small pebble-sized material. The right-hand map shows the pattern of ephemeral stream networks – note the predominant orientation of networks flowing towards the west. These systems rapidly transport finer-grained sediment to the west promoting further deflation.

This pattern, with greater erosion being localised in the west, repeats throughout the sub-basins within the NAEB. It has produced relief that exerts a strong influence over diamond placer development. However, at Bogenfels the basin is not endorheic, and it has clear connectivity to the shelf. As a result diamonds have periodically been flushed back out onto the continental shelf during regression(s) (Fig. 131).

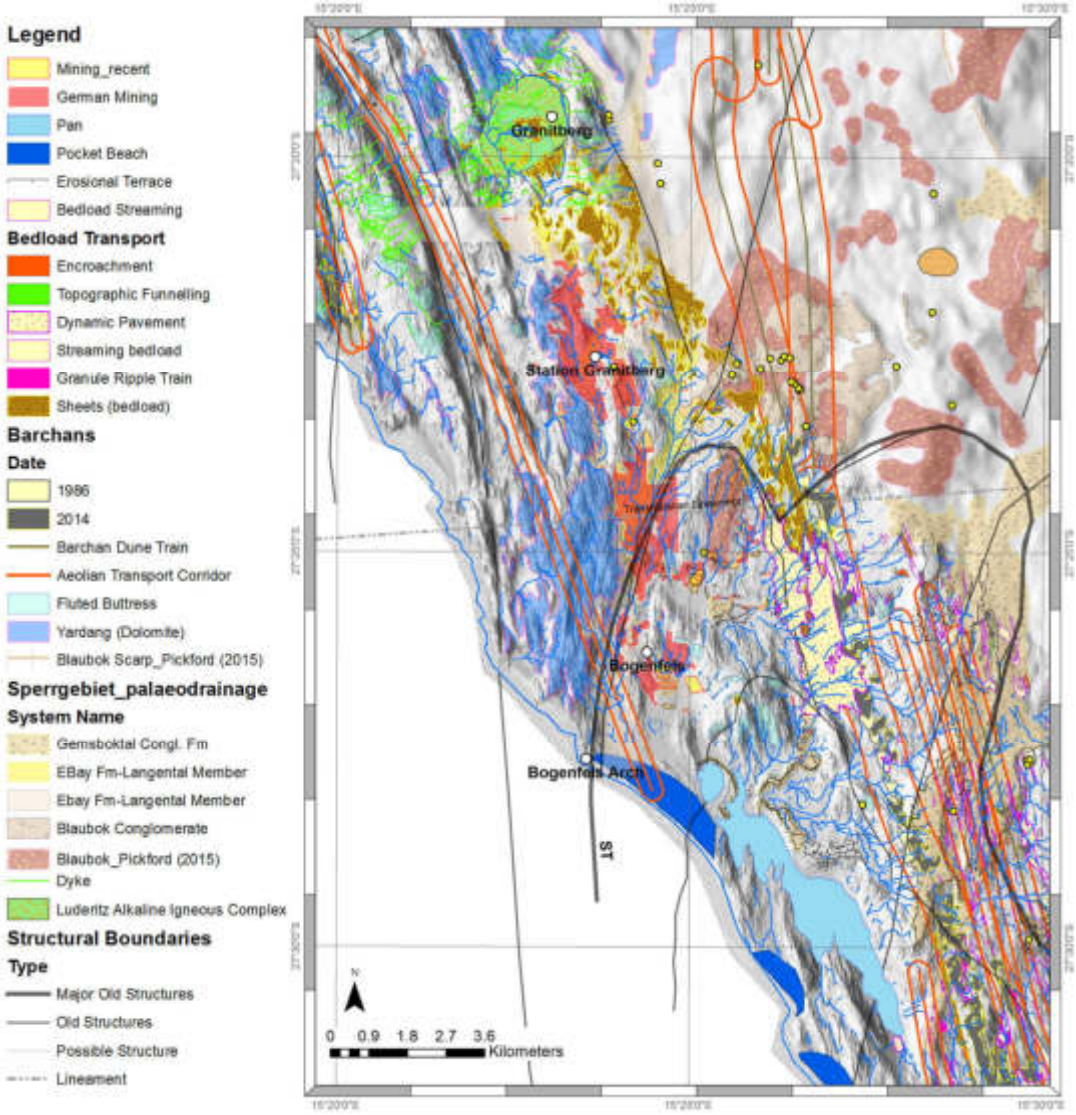

Figure 131. Detailed map illustrating the concentration of mining that leads north from Bogenfels up into the Langental and then across the watershed into the Granitberg claim areas. Whilst there is no doubt that the Eocene (and probably younger) marine beach deposits within the embayed coast accounted for a large percentage of the diamonds that were extracted from this domain the reader's attention is drawn to the main ATC located to the east of Bogenfels. The aeolian system, and its interaction with the ephemeral stream networks in association with the ATC generated placer concentrations of diamonds. The arcuate crescents shaded darker blue along the coast represent pocket beach deposits along the modern coast. Like Elisabeth Bay these beach placers constrained by rocky headlands were preserved between 10 mbsl to 18 mbsl - in some instances the beach placers and exposed shelf areas supplied diamonds back to the aeolian system during regression(s).

Geological sampling at the time of the original research proved that Kaiser's (1926a) deflation hypothesis definitely applies to this domain. Remnants of Bartonian beach sediments are exposed within the immediate vicinity of Bogenfels and extend north along the Langental depression (Fig. 133). The fine-grained siliceous clasts incorporated into stone pavements that form by deflation of these marine sediments produce a stunning suite of small to medium pebble-sized ventifacts which confirm Kaiser's (1926a) observation that abrasion affects clasts on stone pavements (Fig. 132). Agates observed on the surface of stone pavements are often seen to break down, peeling in layers. Oysters together with sharks teeth can be found on the pavement surfaces, although they are unlikely to survive for long once exposed.

Figure 132. Bogenfels 60 m Eocene shoreline (Bartonian) – a thin basal lag undergoing weathering and deflation overlying weathered phyllite. North to right. Scale 1 m in 10 cm divisions.

A granule ripple crossing the surface of the 50 m Bartonian shoreline slightly north of Bogenfels produced 11 diamonds weighing 2.09 cts. The 0.19 cts/stn average size is typical of diamonds in the aeolian bedload. A granule ripple sample adjacent to a dolomite yardang on the watershed with the next sub-basin to the north proved that diamonds are migrating out of the Bogenfels Basin in the aeolian bedload. Eleven stones weighing a total of 0.91 cts showed that aeolian size sorting occurs, with smaller diamonds with an average size of 0.08 cts/stn migrating north up a topographic slope out of the main Bogenfels Basin.

Placers further to the east within the influence of the Baker's Bay ATC have a different origin. These placers are located along the break in slope that effectively marks the eastern boundary of the NAEB where bedrock has been exposed. Above this elevation the floor of the NAEB is characterised by subdued, almost planar, relief provided by the presence of a veneer of the alluvial Blaubok Conglomerate.

The ATC path swings gently east along this slope to climb onto the surface provided by the Blaubok Conglomerate. Aeolian bedload features characterise the western flank of the ATC as it climbs up the slope. The ALS data reveals the development of fields of large rhomboid bedforms (Fig. 133). The individual bedforms are 250 to 500 m in length, often with horns extending north in the direction of the southerly windflow and they vary from 130 to 250 m in width. They are 1 m to 2 m thick. The internal structure of the bedforms, which are commonly vegetated, resembles the deposit at Elisabeth Bay. Thin lenses of granular particles are interbedded with sandier layers. Ribbons of streaming aeolian bedload extend onto the

surfaces in the direction of the prevailing southerly windflow, and in places granule ripple trains form. In some sections excavated into the bedforms, sandy units contain granules scattered through them – whether this reflects bioturbation of the sediment or whether it is depositional in origin is unknown. The sands could represent the remnants of current shadows formed in the lee of vegetation, for example.

Sampling showed that these bedforms commonly contain diamonds. One sample recovered 36 diamonds from one of the isolated bedforms weighing a total of 5.62 cts. The average stone size of 0.16 cts/stn confirms that the diamonds were in the size fraction that typically migrates with the aeolian bedload. These were quite surprisingly positive results. The origin of the diamond concentrations is poorly understood, but it may reflect differential rates of transport with the bedforms progressively capturing diamonds migrating with the bedload or perhaps at times even as part of the saltation load.

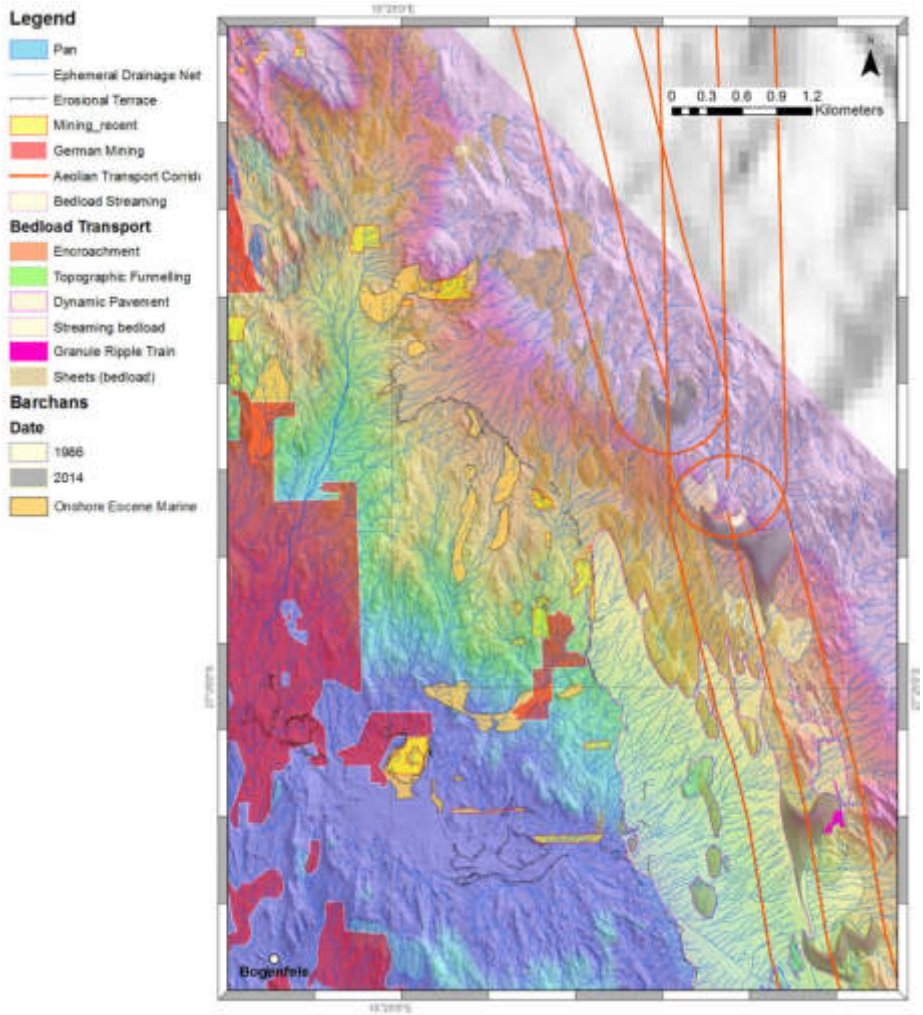

Figure 133. The western margin of the Baker's Bay ATC is characterised by the development of large-scale rhomboid mixed aeolian sand and bedload sheets. Isolated bedforms exist on the dynamic pavement surface to the south of the main area of deposition. Encroachment deposits form an apron around their upwind (southern) margins. The rhomboid geometry and packing of the bedforms up onto the slope indicates that they are migrating northwards – possibly at different rates. As shown in Figure 130 they extend as far north as the south-facing slope of Granitberg. Topographic inversion is clearly shown along the margin of the alluvial plain provided by Blaubok and Gemsboktal Conglomerate sequences, with the exposure of remnants of Bartonian nearshore and beach sediments which are then attacked by the aeolian system.

Figure 133 also shows the dense ephemeral stream networks that have developed along the topographic slope that in essence defines the eastern limit of topographic inversion that has progressed to bedrock within this part of the NAEB. The stream networks provide an effective system for recycling bedload migrating upslope along this margin back down onto the dynamic pavement surface or directly to the base-level, from which it can once again be entrained into the aeolian bedload population. This is another pathway by which diamonds can arrive on the rhomboid sheet bedforms described within this domain.

The importance of ephemeral streams in forming diamond placers in their own right was recognised by Kaiser (1926a). Geological sampling to evaluate the remaining economic potential of the diamond resource at Bogenfels confirmed their importance (Fig. 134).

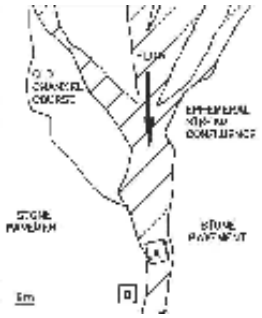

Figure 134. Sample sites about 2 km east of Bogenfels. 20 diamonds were recovered from a sample located downstream of the channel confluence. The stone pavement sample at site B only yielded two diamonds. The difference in diamond concentration is attributed to the dendritic tributary network reworking diamonds from a wide area. These diamonds were then concentrated in a site downstream of the ephemeral stream channel confluence.

A prospecting map from c.1908 held by the Mineral Resources Department at Namdeb (Pty) Ltd revealed a similar dispersal pattern that probably records the diamond distribution in a network of braided ephemeral stream channels in the Langental drainage system where it broadens across a flat basin floor about a kilometre to the north of Bogenfels Basin (Fig. 135).

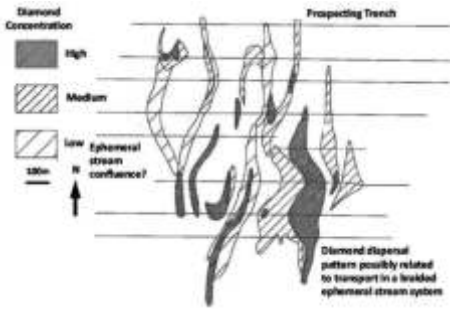

Figure 135. Possible record of a diamond placer formed in a braided network of ephemeral streams in the Langental near Bogenfels.

Mining activity declines rapidly to the south of Bogenfels. Fröhe Hoffnüng is one of the few endorheic basins in which mining did take place. This small basin provides a beautiful example of an endorheic ephemeral system interacting with the aeolian system (Fig. 136). The valley is today completely isolated from

any Eocene diamond source. It is, however, directly downwind from known pocket beach sites. These, together with areas in which marine placers were present on the Atlantic shelf during regression(s) are the most likely source of the diamonds found in this placer. In this part of the NAEB the erosional architecture plays an important role in directing the surface windflow and therefore the sandflow – with multiple ATCs streaming bedload features with the development of long granule ripple trains extending as much as a kilometre along the tightly confined floors of the endorheic basins. Consequently encroachment deposits are well-developed providing ideal sites for the concentration of diamonds as recorded by Kaiser (1926a).

Several valleys have been flooded and pocket beach placers developed between the headlands. These together with marine placer bodies exposed on the shelf during regression(s) probably supplied diamonds to the aeolian system thereby accounting for the deposit located in Fröhe Hoffnüng.

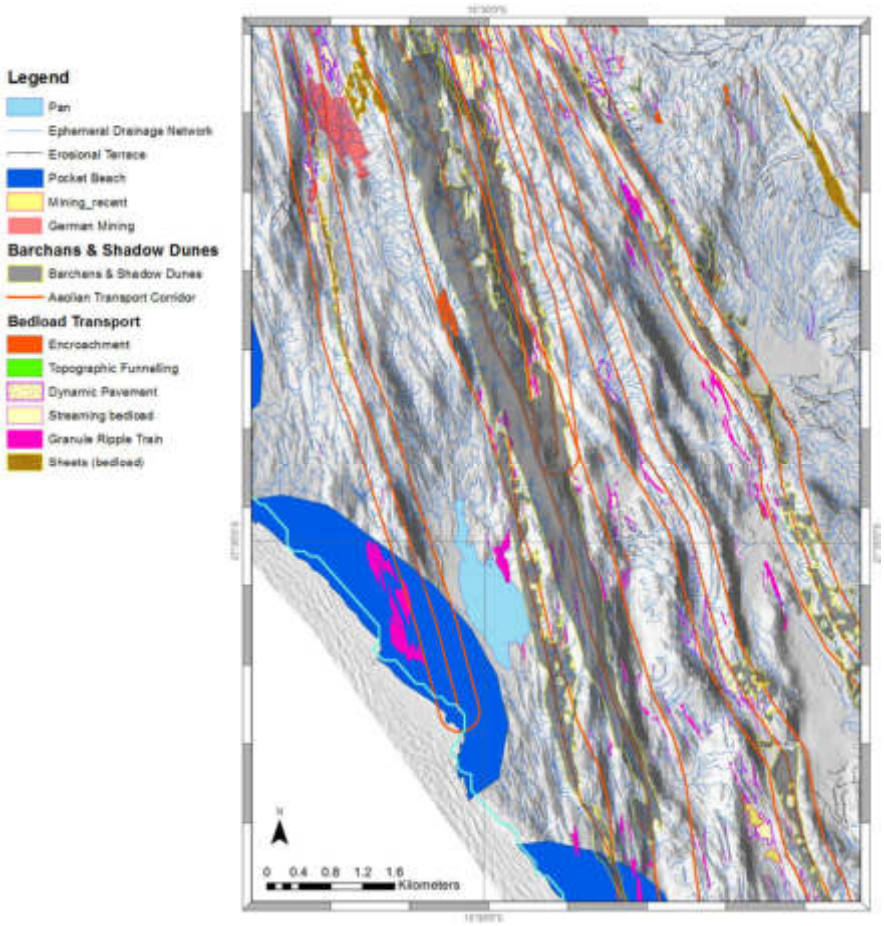

Figure 136. Mining at Fröhe Hoffnüng in the top left-hand corner of the map lies immediately downwind of a number of pocket beach placer bodies located at the southern end of the valleys carved in the aeolian erosion landscape. Fröhe Hoffnüng provides an excellent example of a placer within an endorheic basin. This part of the domain is traversed by a number of ATCs, including the main Baker's Bay corridor. Note the streaming bedload features sweeping north along the ATCs with long granule ripple trains and the development of elongate ribbon-shaped aeolian bedforms along the floors of the valleys. Fröhe Hoffnüng exhibits a classic south-facing slope with a well-developed south-flowing dendritic stream network. South of the valley another endorheic basin is characterised by westward-flowing dendritic ephemeral stream networks which periodically transport sediment being transported as aeolian bedload towards base-level. Once there, active deflation takes place together with entrainment into the streaming aeolian bedload.

The last area in which mining took place that is reviewed in this paper lies at the foot of the Buntfeldschuh Escarpment (Fig. 137). Limited information is available on the diamond sizes but Reuning's discovery of a small valley containing a deposit with an average size of 1ct/stn in the area (Schneider, 2008) confirms the presence of a non-aeolian diamond population. If this was a significant diamond entry point to the margin it is puzzling that so few diamonds were recovered. Given the architecture of the ephemeral stream network it can be concluded that had they been present in quantity the early prospectors would have located them. Later sampling also proved to be disappointing despite the presence of exotic clasts which have been used as an indicator of Orange River sediment supply.

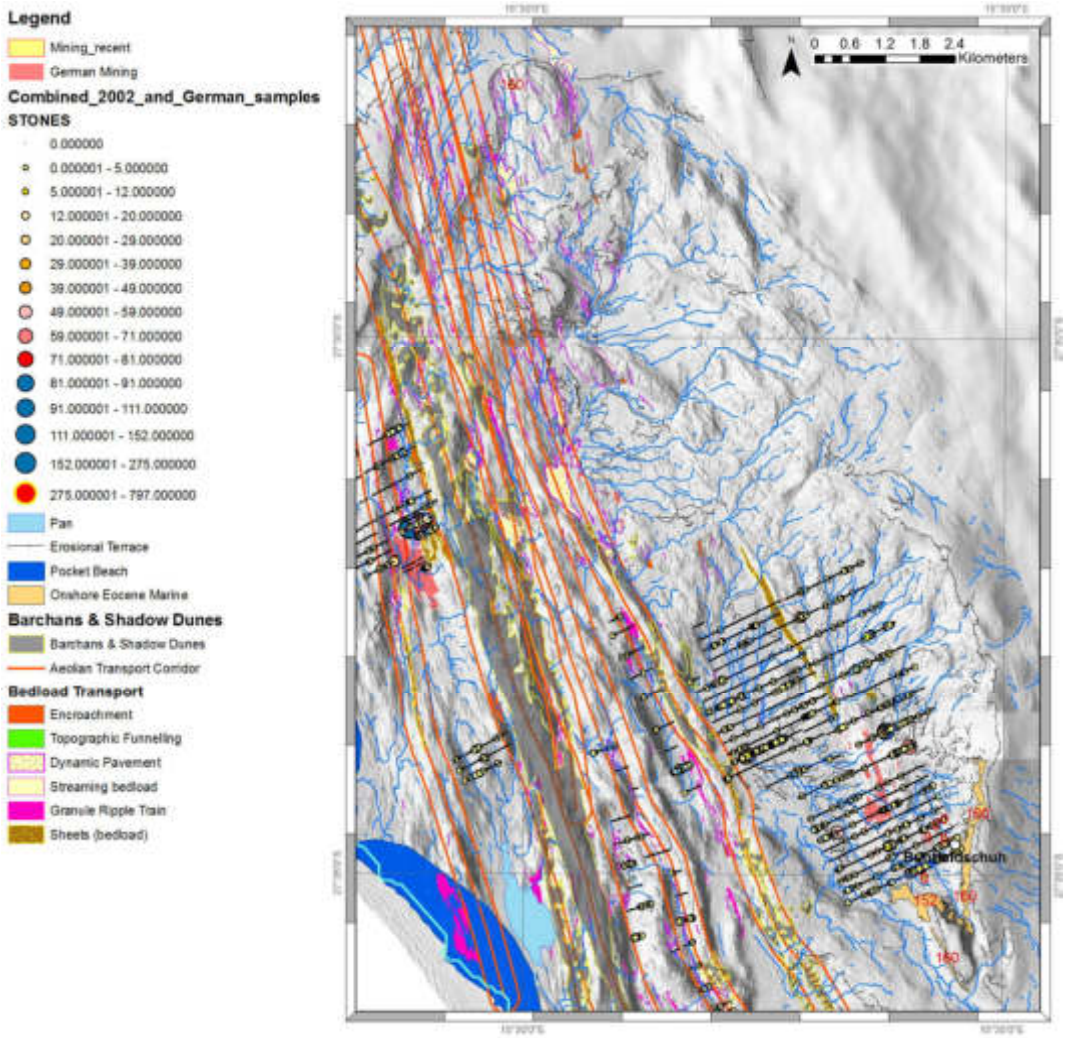

Figure 137. Map showing the distribution of mining activity at the foot of the Buntfeldschuh Escarpment and the spatial distribution of diamonds recovered in prospecting trenches.

A number of possibilities exists to explain the apparent scarcity of diamonds in the sediments derived from the Buntfeldschuh Escarpment:-

1. The nearshore sequence containing diamonds lies to the east of the Buntfeldschuh Escarpment beneath sand cover of what Kaiser & Beetz (1926) termed the "Plain Namib";

2. The Buntfeldschuh nearshore sediments in the upper marine unit pre-date the main supply of diamonds to the margin

which is known to have taken place by the Bartonian;

3. Aeolian deflation and bedload transport have depleted the area in diamonds leaving only a residue of diamonds too large to remove by these means,

Little information is readily available on the production from the Buntfeldschuh Claims – although Schneider (2008) could confirm the presence of diamonds in the 1 to 2 carat size fraction, there is no record confirming the presence of the +40 ct diamond population at this locality, despite its proximity to the Bogenfels Basin in which diamonds of this size were relatively common. The scale of mining is also trivial compared to the main production areas to the north.

In terms of the aeolian reworking hypothesis, the absence of evidence of a well-defined northward-fining tail of bedload having been transported from the Buntfeldschuh renders this is unlikely to be correct.

On this basis we have to conclude that either point (1) or point (2) is correct. Siesser & Salmon (1979) considered that there were differences between the Buntfeldschuh marine sediments and those present in the Bogenfels-Langental area. The relative lack of diamonds in the Buntfeldschuh Claims tends to support this conclusion, irrespective of whether the sediments were supplied by a fluvial system or whether they record early longshore transport from an entry point further south.

On the basis of this review, and particularly of the compilation of the GIS data set, it has to be concluded that an entry point did exist at some point. However, the diamond distribution, and in particular the distribution of large diamonds of +40 cts/stn implies that the main entry point was a little further north than Buntfeldschuh. Probably in the area between Bogenfels and Lüderitzfelder – as August Stauch concluded, although he was convinced an undiscovered kimberlite was the source.

Summary of Placer Formation in the Namib Aeolian Basin

Early Concepts

Beetz (1926) proved the presence of diamonds in the marine deposits at Eisenkieselklippenbake, 145 masl. The inferred age of these sediments based on the presence of exotic clasts of agate, chalcedony, jasper and chrysoprase is Upper Palaeocene to Lower Eocene (Siesser & Salmon, 1979). However the recovery of weathered, discoidal phonolite clasts during geological sampling show that they post-date Klinghardt volcanism.

According to Beetz (1926) Reuning recovered a 2.5 ct diamond from the marine sequence at Buntfeldschuh – this sequence was tentatively correlated with the Eisenkieselklippenbake deposit by Siesser & Salmon (1979). The association of exotic clasts of agate, chalcedony, jasper and chrysoprase with placer deposits led to the concept that many of the diamonds within the region were derived from the reworking of these palaeo-shorelines (Lotz, 1909 (cited by Krause, 1910); Range, 1909 (cited by Krause, 1910); Kaiser, 1926b).

Kaiser (1926b) also considered it likely that diamonds had been introduced during the deposition of the Pomona Beds, which he interpreted as a silicified quartz pebble conglomerate pre-dating the Chalcedon Tafelberg Silcrete Formation (sensu SACS, 1980). Prospecting at the time failed to prove this. In addition, diamonds were recovered from the surface of extensive, coarse-grained alluvial braidplain deposits represented by the Gemsboktal and Blaubok Gravels.

The initial theory that longshore drift within the nearshore marine environment had played an important role in the generation of the placer bodies along the west coast to the north of the Orange River evolved shortly after initial discovery (Merensky, 1909; Lotz, 1909).

Information that became available after Kaiser had completed his work in 1926

considerably altered the interpretation of the deposits. Of primary importance were the discoveries of the beach and nearshore marine placer bodies at Alexander Bay, Oranjemund and Kleinzee in the late 1920's. These deposits proved that Kaiser had been incorrect in concluding that diamond input had only occurred during the Eocene.

The conclusion that diamond supply by one or more palaeo-fluvial systems to the margin introduced the diamonds to the NAEB (Lotz, 1909; Range, 1909) is correct.

Early researchers of desert environments such as Blake (1904) concluded that the removal of fine-grained sediment by aeolian processes (deflation) resulted in surface lowering. Bruggen (1951, cited by Cooke, 1970) summarised this concept (Fig. 138), which leads to stone pavement formation by the progressive accumulation of immobile roughness elements at the surface of the bed. This study has confirmed that surfaces of this type are present within the NAEB.

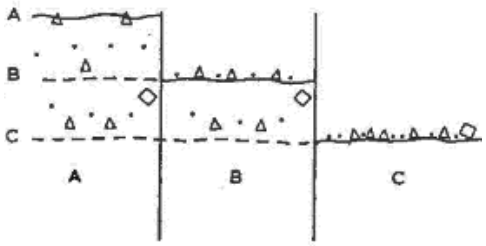

Figure 138. Schematic summary of the concept of residual lag stone pavement resulting from the deflation of fine-grained material. After Brüggen (1951).

Merensky (1909) originally expressed the view that these diamond placers were deflation residues primarily derived from Cretaceous marine deposits, but Kaiser (1926a) noted that this conclusion was not substantiated by thorough investigation.

Kaiser (1926a) concluded that the Eocene marine sediments, and the Miocene alluvial gravels once completely infilled the area comprised of endorheic basins within the NAEB. He refined the "residual lag" theory, and determined that cyclical reworking by aeolian and ephemeral stream current systems was responsible for the formation of the placer diamond concentrations within endorheic basins. Although he realised that aeolian processes had transported, and continue to transport, diamonds northwards from one basin to another, he retained the initial concept of surface lowering by deflation (Fig. 139).

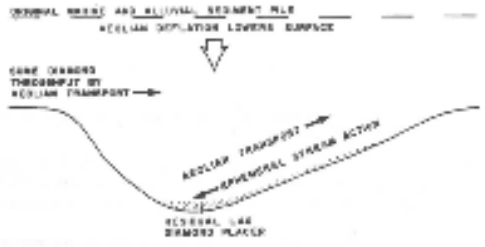

Figure 139. Schematic summary of Kaiser's (1926a) concept of placer development.

More recently, Sutherland (1985) has reiterated that the placer bodies within the deflation basin were of a residual or lag nature.

This opinion was based on MacDonald's (1983) concept that aeolian processes are less efficient than sub-aqueous processes in the sorting of sediment.

The research presented in this paper does not support this concept. Within the coastal aeolian environment of the Namib Desert, barchan dunes composed entirely of heavy mineral grains can be seen. Excellent examples of heavy mineral segregation on aeolian bedforms associated with bedload transport are also found. These observations lead to the conclusion that the aeolian system is perfectly capable of subtle, but very effective size-density-shape sorting as proved by the garnet tracer experiment

Significantly, to the north of Bogenfels, there is little evidence of any correlation between the presence of exotic clasts and the distribution of mining. This field evidence was confirmed by Kaiser (1926a) who recorded that a number of the larger placer bodies did not contain agate, chalcedony, jasper and chrysoprase clasts commonly referred to as the "Eocene suite". This contradicts the theory that all of the placer bodies represented residual deflation lags of material derived from the Eocene transgressive sequences. If this interpretation were correct, the main placer bodies should have been located in the vicinity of the Buntfeldschuh and/or Bogenfels. Prospecting data presented in this paper confirms that minimal economic potential existed in the vicinity of the Buntfeldschuh. Placer deposits were associated with remnants of the Eocene shorelines at Bogenfels, within the re-entrant embayment, and in ephemeral drainage tracts. Rich though these were, they were not as well-developed as those discovered in the endorheic basins in the Pomona Claim.

A New Concept for Diamond Placer Formation in Endorheic Basins within the NAEB

This study has focused on the arid zone processes that exist within the NAEB, and the influence they have had on the formation of some of the highest-grade diamond placers ever to have been discovered.

Kaiser (1926a) noted that a significant increase in diamond concentration occurred in the vicinity of aeolian barchan dunes. The examination of the regional diamond dispersal pattern using the concept of Aeolian Transport Corridors (ATC), provides the basis for a new placer model.

Empirical sandflow data collected using sand traps, proves that barchan dune trains define the maximum areal concentration of sandflow within ATCs. As a result, the aeolian bedload transport rate driven by the collision of saltating grains with the bed is also greater within these linear zones extending through the length of the NAEB. ATCs are therefore highly dynamic tracts along which aeolian processes transport sediment from its coastal generation point to the southern margin of the Namib Depositional Basin.

Corbett (1989) documented evidence of Plio-Pleistocene transgressive deposits at Wüstenkönig, at the coastal end of the Grillental. Backshore, tidally influenced interbedded pan and aeolian dune facies (Fiskus Sandstone Beds) prove the presence of a 30 m transgression. Others may have occurred but have gone unrecognised due to the extremely erosional environment that exists within the NAEB.

The present-day location of ATCs within the NAEB is dependent upon the spatial distribution of log-spiral and south-facing re-entrant embayments along the coast. This distribution changes in response to sea-level movement and modification of the coastline. Palaeo-yardangs to the west of Bogenfels prove that the western margin of the south-facing Bogenfels re-entrant embayment was traversed by an ATC during marine regression(s). Computer modelling shows that this re-entrant would also provide ideal conditions for the generation of a major ATC during transgression(s) (Fig. 140).

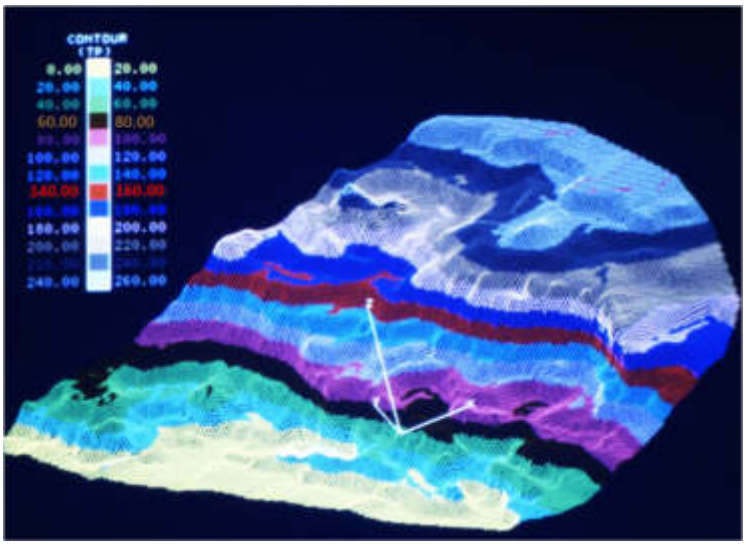

Figure 140. Vulcan 3D net showing the large re-entrant embayment that would characterise Bogenfels during transgression to 100 masl providing ideal sites for the generation of Aeolian Transport Corridors.

It is postulated that one or more ATCs have repeatedly been generated from an embayed coastline at Bogenfels. The main ATC would have traversed Daheimtal and Granitberg prior to entering the Idatal-Hexenkessel-Scheibetal sub-basins before continuing north to the depositional basin. Such an ATC pathway for sandflow would account for the extreme aeolian erosion landscape that characterises the area within and to the north of the Pomona Claim. Its path is recorded by the extensive development of fluted buttresses on the south-facing ramparts of gneiss hills throughout the area.

Topographic inversion and the breakdown of exhumed diamondiferous near-shore sediments within the Bogenfels – Langental Basin by arid zone processes would have released the weathering products of the coarse-grained marine clastics containing diamonds. Weathered fragments would have been removed by both aeolian saltation and bedload transport. Diamonds released into the aeolian bedload would have migrated north together with smaller diamonds which travelled faster as part of the saltation load.

Evidence from submersible observations on the shelf prove that the high-energy aeolian regime operated there during regression(s). At these times, arid zone weathering and subsequent aeolian bedload transport up the exposed shelf would have supplied diamonds released from marine placers into the onshore system.

Theoretically, during regressions the pathways defined by ATCs would have been generated by different coastal configurations causing changes in the spatial distribution of high-energy sandflow through the NAEB, which would have extended further west onto the subaerially exposed shelf.

Mining of aeolian sequences representing palaeo-aeolian systems at Elisabeth Bay and Kolmanskop (Corbett, 1989) confirm that this scenario took place. The coarser-grained nature of the Pliocene Fiskus Sandstone Beds imply that palaeowind conditions were significantly higher-energy than today. Potentially this enabled larger bedload particles (including larger diamonds) to be entrained more frequently.

Kaiser (1926b) realised that the placer bodies within the endorheic basins at least partially resulted from aeolian transport, and that diamonds have been transported from one basin to another by aeolian processes. However given what has been discovered subsequently, he could not have appreciated the full extent to which this has occurred.

Modelling of the diamond dispersal pattern within the Pomona Claim highlights the effects of aeolian size-sorting as

transport occurs between succeeding endorheic basins. The identification of ATCs as linear zones characterised by very high rates of bedload transport may also explain Kaiser's (1926a) observation that diamond concentration was associated with barchan dunes within which size-density sorting takes place.

Present-day migration rates for barchans and bedforms associated with aeolian bedload streaming would, though time, provide ongoing diamond transport through the NAEB – possibly behaving as kinematic waves progressing through endorheic basins.

During pulses of increased sandflow, when aeolian bedload transport rates increased, diamonds migrating with the bedload would be subjected to further aeolian size-shape sorting. Kinematic wave theory suggests that slightly different size fractions of the population would become incorporated into kinematic waves travelling at different speeds. Any increase or decrease in the sandflow rate in response to changes in coastal morphology, would probably modify the speed with which the kinematic waves progressed northwards through the endorheic systems. In the event that coastal morphology caused an ATC to cease traversing a particular path, any kinematic waves with diamonds migrating in them would effectively be "frozen" until the next time an ATC traversed that area and migration could resume.

Bottlenecks of various scales and forms potentially create sites at which kinematic shock waves would retard the progress of kinematic waves through an endorheic basin system. Stone pavements within ATCs are not comprised of immobile particles forming residual lag accumulation on the bed. Roughness elements provide nuclei for the development of particle clusters by the aeolian bedload. Observation of these surfaces shows that, provided the transport of the heavy mineral component in the bedload is maintained past these nuclei, particle clusters dominated by heavy mineral grains will result. Stone pavement surface micro-topography also creates small-scale bottlenecks in the gaps between roughness elements on these dynamic substrates traversed by ATCs. Diamonds in the bedload would also be concentrated within these particle clusters.

As previous workers noted, granule ripples also provide sites for heavy mineral segregation by aeolian processes. How these occur is relatively poorly understood. However, repeated cycling of the bedload component associated with granule ripples has been shown to provide one mechanism by which the segregation of heavy minerals can occur on the stoss slope. This is probably in response to size-density-shape sorting as the bedforms migrate.

The south-facing slopes at the northern end of the endorheic basins appear to act as large-scale bottlenecks to kinematic waves. The advance of the aeolian bedload on reaching these topographic obstacles appears to decrease, resulting in the formation of encroachment deposits in which surficial grains exhibit an imbricate shape-fabric. Kaiser (1926a) recorded that diamonds were recovered from stone pavements of this type. Changes in the pivoting angle, and the direction in which the collision force due to saltation impact acts on particles theoretically increases bed stability and reduces entrainment potential from these surfaces. With continued addition of diamonds to such surfaces, the relative concentration would increase in response to aeolian size-density-shape sorting. Once incorporated into the imbricate shape-fabric, diamonds would assume stable positions and the potential for their entrainment would decrease. This potentially explains the frequent occurrence of diamond placers on the south-facing slopes of endorheic basins.

The extent to which palaeoclimatic changes resulting in increased rainfall and more frequent alluvial activity, influenced placer formation once the endorheic basin system had fully developed is difficult to assess. Photographs of Kaukausibtal reproduced by Schneider (2008) suggest that these conditions diluted grade. However, where stream networks extended between basins they also had potential to

move large volumes of material to the base-level of the system. Once there, resurgence of the aeolian regime and consequent deflation could then act to produce extremely rich concentrations of diamonds.

The erosional architecture of the NAEB ultimately played a crucial role in determining how and where the diamond placers would form (Fig. 141). These features of the erosional architecture fundamentally control the way in which the core arid zone processes of a high-energy southerly wind system interacts with ephemeral stream networks. At a smaller scale, the complex relief subtly influences aeolian bedload transport and the localities at which aeolian size-density sorting can act on streaming bedload migrating through them.

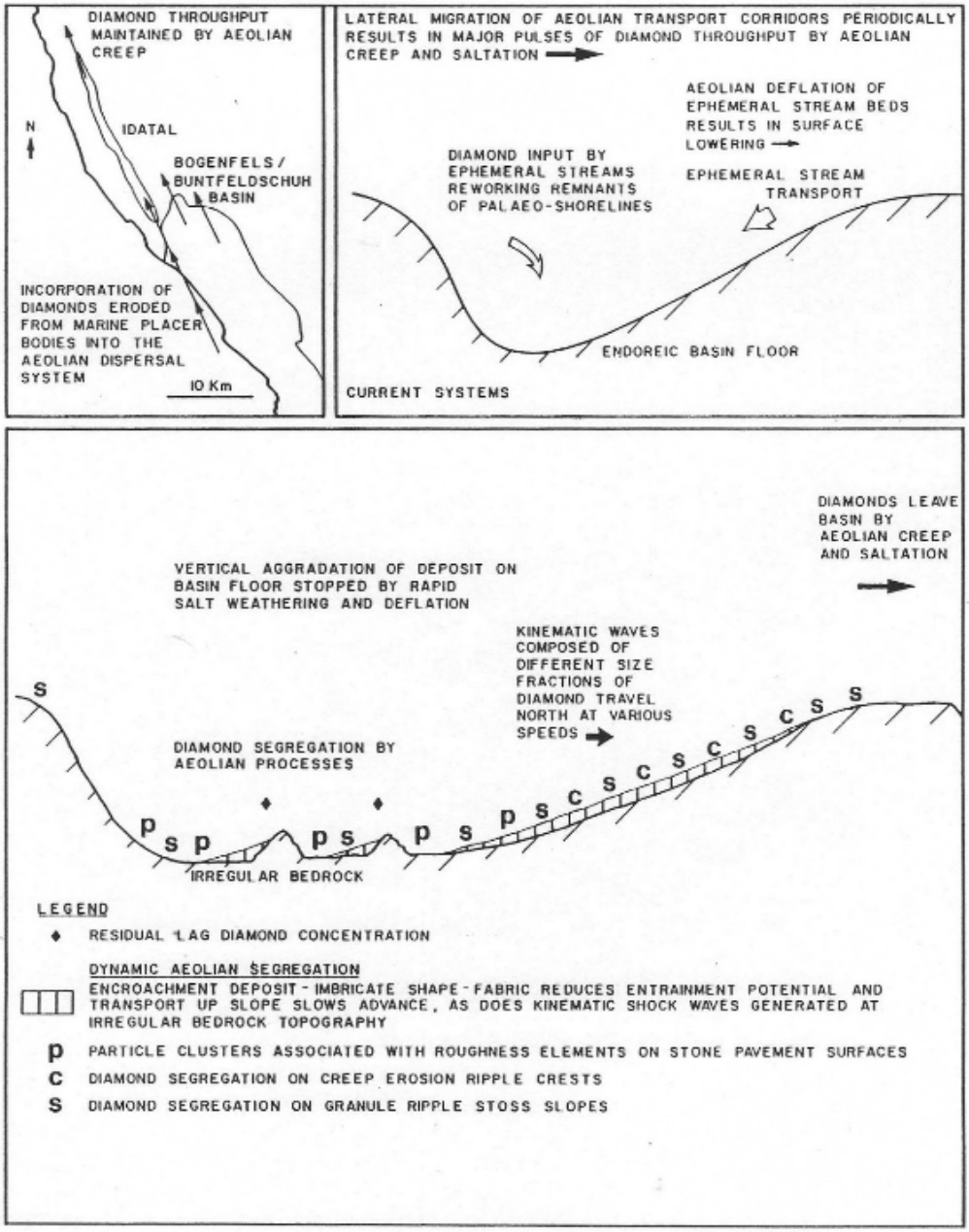

Figure 141. Conceptualised summary of diamond placer development within endorheic basins by aeolian transport processes influencing the bed.

With the global focus on climate change and the availability of new dating techniques there is a growing interest in understanding the long-term controls on the development of sand seas and how they change through time.

Key issues that have been identified by the Sand Seas and Dune Fields Working Group of the British Geomorphological Society for understanding sand seas include:-

- Boundary conditions for sand sea development;
- Identification of sand sources and transport pathways;
- Factors that control distribution of dunes of different size and morphology;
- Role of changes in boundary conditions (Lancaster, 2010).

This section explores the implications of observations derived from the research reported in this paper within the context of these main themes.

An appreciation of changes in observational scale and the ability to identify interdependencies which otherwise remain hidden represents one of the key developments in mineral exploration.

This outlook has emerged through the translation of exploration strategies originally employed in oil and gas exploration into the Mineral System concept enabling spatially-predictive targeting of other minerals (Hronsky & Groves, 2008; Hronsky *et al.* 2012; McCuaig *et al.* 2010). Underlying the power of the approach is the ability to place detailed observations into a systemic context to test and develop understanding.

The data and tools available for updating this research into the aeolian system that operated in the southern Namib to form diamond placers, provides such an opportunity. Given the emphasis of this research on understanding transport pathways in relation to the transport of diamonds within aeolian bedload, the discussion begins there. Consideration is then given to the other factors.

Namib Transport Pathways: Evidence of Palaeo-systems

Remote sensing techniques are enabling transport pathways to be defined over broad areas. This research provides an opportunity to compare empirical data with a regional study conducted using ASTER data and COSI-corr analysis by (Scheidt 2012; Scheidt & Lancaster 2013). The regional transport pathways supplying sediment to the Namib Depositional Basin are immediately evident (Fig. 142).

The point was made earlier that exploration activities south of the Orange River have shown that aeolian systems are sensitive indicators of surface relief influenced by underlying tectonic structure. Few studies of which the author is aware, have examined modern aeolian system dynamics with respect to regional tectonic frameworks, and none have done so in the Namib.

The data presented by Scheidt (2012) is especially interesting because it extends to the east of the NAEB and defines a transport pathway lying well outside the system as it is normally viewed. The transport corridor that has been defined to the north of the Schakalsberge Thrust exhibits several sites along its length where offsets across faults are apparent and/or increases in sand deposition are observed. This begs the question whether the routes that transport pathways take, and the location of depocentres along them, are being controlled by surface relief that is influenced by underlying neotectonic reactivation of old structures.

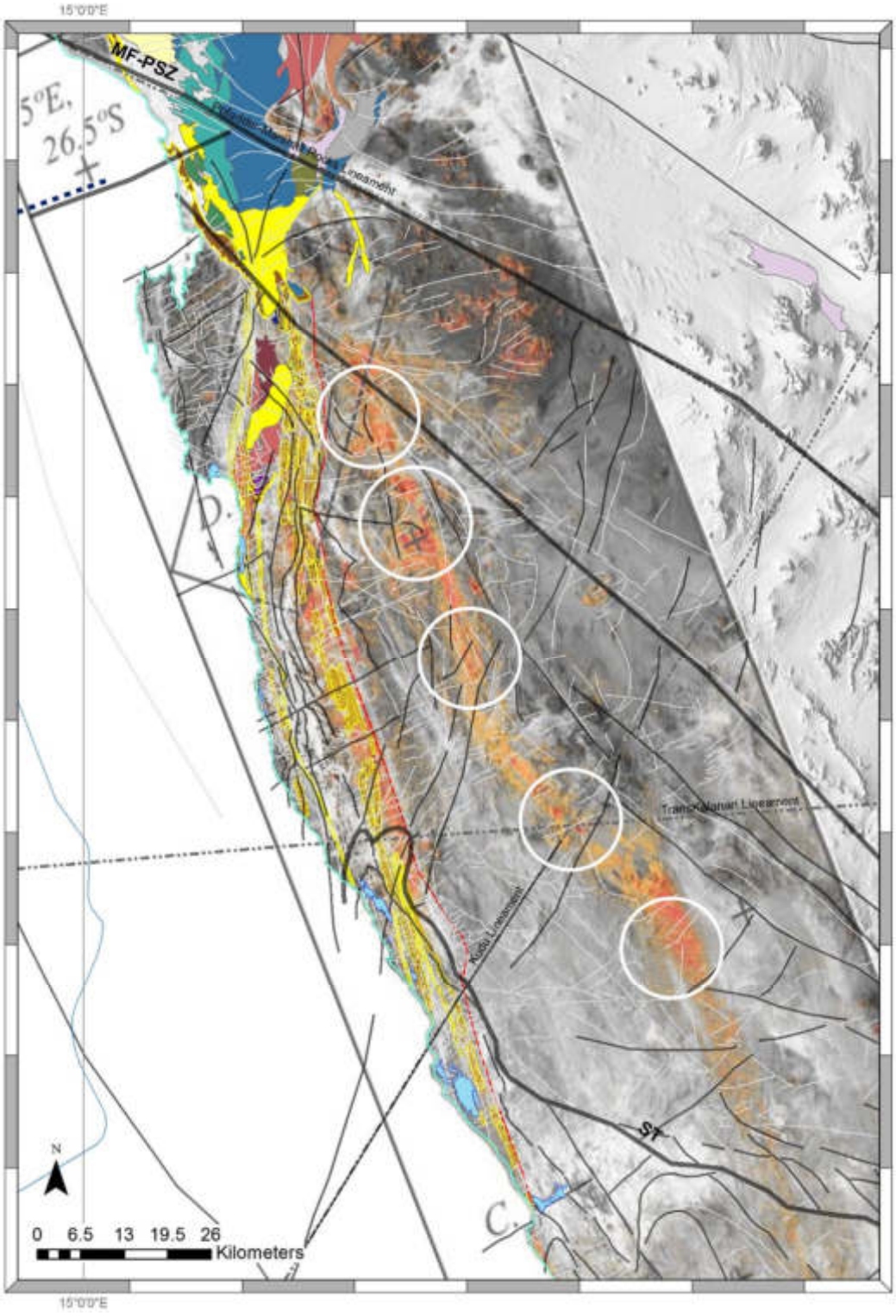

Figure 142. Overview of the transport pathways defined empirically (yellow lines) within the NAEB with basin edge shown by dashed red line and orange and red shading produced by the analysis of ASTER data by Scheidt (2012). White circles highlight some of the potential offsets associated with faults and/or changes in deposition across faults. Black lines define main structural trends, with other faults shown by light grey lines. Sand Sea dune forms legend in Figure 144.

The transport pathways are presented within a regional geological context in Figure 143. It can be seen that increased concentrations of Scheidt's (2012) "dark sands" correspond to the locations of the large alluvial fan systems preserved within the Sperrgebiet. According to Pickford (2015) these fans were active during the Oligocene and the Miocene. The aeolian system within the NAEB is aggressively eroding the alluvial sequences which are undergoing extensive topographic inversion. The pattern mapped by Scheidt (2012) suggests that the eastern pathway has also incorporated material reworked from the southern fan system and possibly also from the Gemsboktal / Glastal fan systems associated with the uplifted Klinghardt Dome discussed in an earlier section.

The map shows the distribution of aeolianite sequences throughout the southern Namib as well. The sequences have been mapped in some detail by a number of researchers (Greenman, 1966; Ward, 1984, 1987; Corbett, 1989; Ward & Corbett, 1990). A biostratigraphy based on avian eggshells has been established by Pickford *et al.* (1995). These dated sequences span a time period of about 20 m.y. from the earliest Miocene. The age of the Buntfeldschuh aeolianite remains uncertain. Ward & Corbett (1990) considered it to represent an early precursor to the Namib Sand Sea that formed during the Palaeogene. Pickford (2015) recently challenged that interpretation, concluding that it is too geographically limited to represent the development of a major erg, preferring to interpret it as a coastal dune sequence.

Given the tectonics described in this paper and the evidence of a major regression at the end of the Eocene based on McMillan and Dale's (2002) offshore research it could still represent the eastern margin of an erg developed during widespread shelf exposure. In terms of the present-day aeolian transport pathways, it is a minor contributor to the Chameis Bay corridor.

There are two main areas in which the erosion of aeolianites linked to topographic inversion is presently contributing to transport pathways feeding into the Namib Aeolian System. The main locality in the south is at Rooilepel, where some of the oldest aeolianite sequences in the Namib are preserved at the base of a 100 m thick sequence to the north of the Orange River. It is possible that tectonic reactivation has provided accommodation space for deposition and preservation of this sequence.

The corridor extending from Elisabeth Bay northwards through Kolmanskop forms the second - here the aeolianites are Pliocene in age, and they have been proven to contain diamonds.

The pattern mapped by Scheidt (2012) at the northern end of the NAEB (Fig. 144) provides interesting evidence confirming that the transport pathways diverge either side of the large barchanoid draas that form a tongue-shaped body of sand extending to the south of the main depositional basin.

Although the Orange River has undoubtedly acted as the primary source (Rogers, 1977; Garzanti *et al.* 2012, 2015) in terms of aeolian sediment dynamics, the pattern is more complex. The pattern of transport pathways entering the south end of the Namib Sand Sea, and the sedimentary structures that develop, potentially provide insights which can be applied to consider how the architecture of the system might change in response to marine regression or transgression. Such changes would dramatically alter the boundary conditions under which sand sea development would take place on the south-western continental margin of southern Africa.

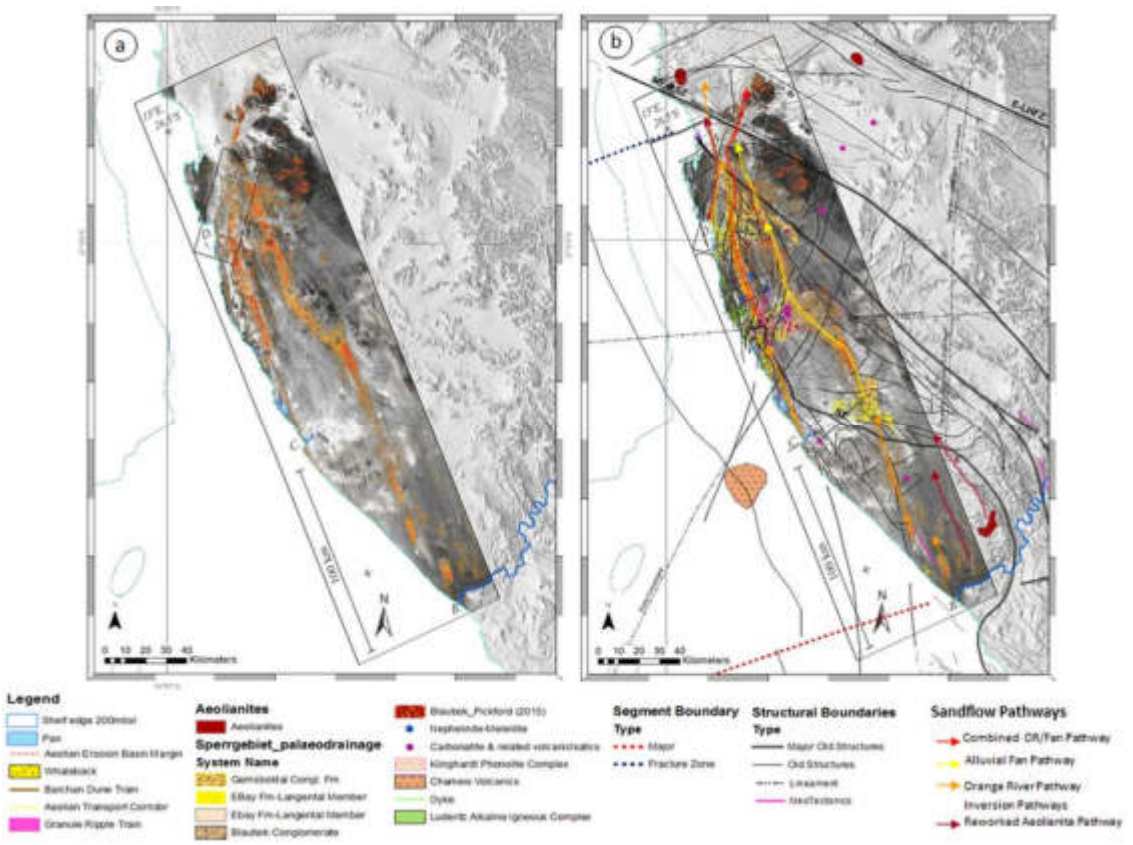

Figure 143. a)Transport pathways mapped by Scheidt (2012) from the analysis of ASTER data; b) The Scheidt pathways integrated with an interpretation of the variation in sand sources for the broader Namib aeolian system showing the sandflow pathways feeding into the present-day Namib Sand Sea based on the GIS dataset compiled for this study together with field-based observations spanning many years of involvement with diamond exploration activities in the Sperrgebiet.

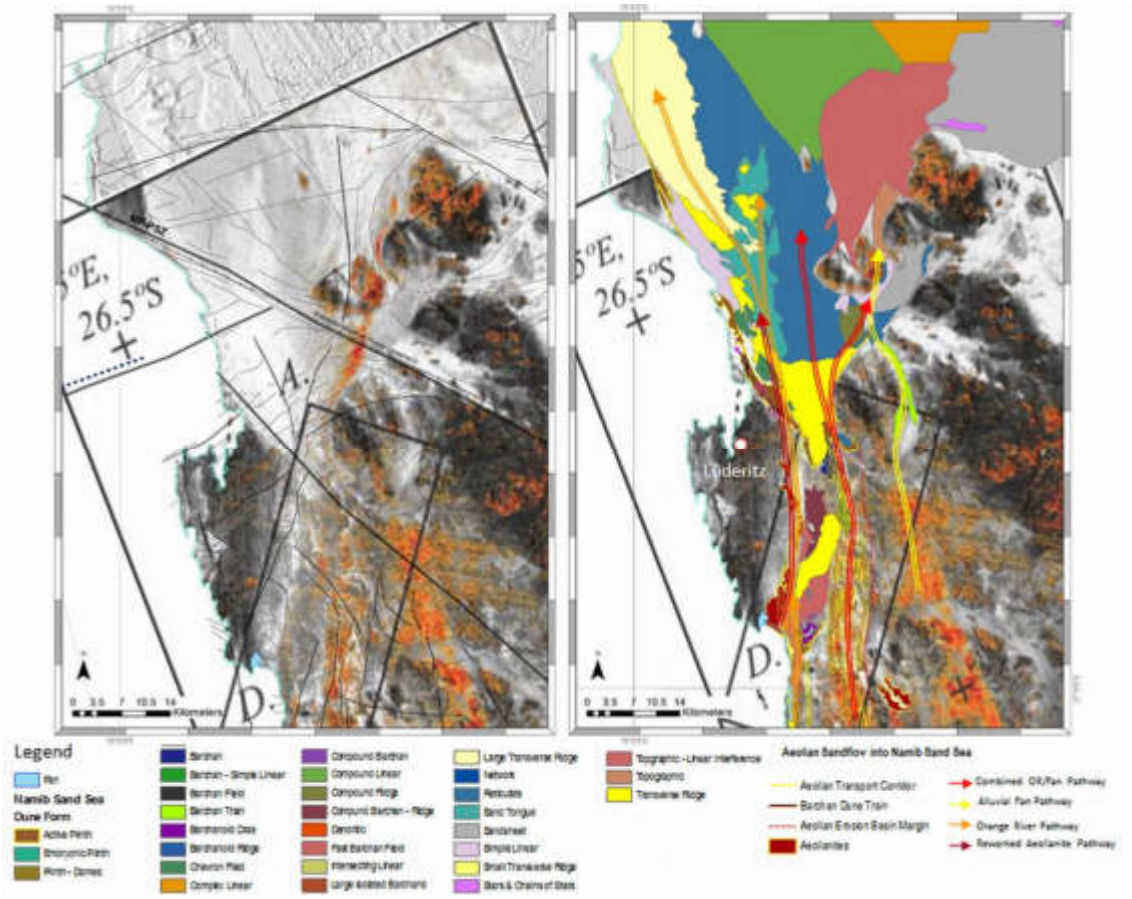

Figure 144. Detailed interpretation of the transport pathways feeding into the modern Namib Sand Sea showing the variability of the sediment sources and the divergence of the NAEB-related Aeolian Transport Corridors in relation to sandflow pathways identified using ASTER data (Scheidt, 2012) in and beyond the NAEB, and COSI-corr analysis (Scheidt & Lancaster, 2013). The spatial distribution of Namib Sand Sea dune forms is modified after the Namib Sand Sea Digital Database of Aeolian Dunes (Livingstone *et al.* 2010).

Aeolian System Response to Changes in Boundary Conditions Driven by Sea-Level Movement

Boundary conditions controlling sand sea development consist of a number of key variables (Ewing & Kocurek 2010) including:-

- Wind regime;
- Sediment supply;
- Source area geometry;
- Areal extent of the existing system;
- Antecedent conditions.

In terms of the wind regime the models of the atmospheric circulation pattern by Parrish & Curtis (1982) indicate that the South Atlantic Anticyclone may have begun to influence the west coast surface-wind pattern during the Cenomanian. The theoretical models suggest that the anticyclonic system would have been more established towards the end of the Cretaceous. Kennett (1982) also considered that the anticyclonic gyre was well established by the Eocene, in reasonable agreement with the model.

Field evidence from the aeolianite sequences preserved in the Sperrgebiet and wider Namib demonstrates that all of the palaeo-aeolian systems were governed by a southerly quadrant wind regime. A similar

conclusion was reached in the Central Namib by Ward (1984, 1987). No evidence for a sustained switch to a dominant northerly quadrant regime, or the breakdown of the zonal atmospheric circulation pattern, has been found in any of the aeolian exposures examined, which means that the wind regime has existed for at least 18 m.y.

Whilst changes in energy might be anticipated through time, it therefore seems reasonable to assume that unimodal windflow conditions would prevail within the coastal tract as it migrates back and forth across the continental shelf and coastal plain. The recognition of palaeo-yardang fields and other features formed by aeolian erosion show that the transport pathways for sandflow have varied through time, and thus are evidence that the boundary conditions within the NAEB have changed through time.

A relationship between surface windflow, sediment flux and dune form was observed by Fryberger & Dean (1979). Applying these findings to dune form and directional variability of wind flow in the context of the Namib system (Lancaster, 2010) it can be predicted that barchan-transverse-crescentic dunes are likely to be characteristic dune forms within the high-energy unimodal tract as it migrates east or west. This pattern can be observed in the present-day architecture of the sand sea (see Fig. 144). Vermeesch *et al.* (2010) have shown that the residence time for the sand in the coastal tract of the Namib Sand Sea is at least 1 m.y. It is possible that the migration of the coastal tract in response to transgression and regression could affect this, where sea-level change has been relatively rapid.

The investigation of diamond placer geometry coupled with the mapping of erosional alluvial terraces along the eastern margin of the NAEB suggest that the influence of the unimodal southerly wind regime may be extending eastwards. This would imply that the areal extent of the NAEB is currently expanding as the process of topographic inversion advances inland along the margin with Kaiser's (1926a) Plain Namib. The present-day architecture may be providing an insight into transport pathways related to transgression. As shown by Lancaster (2010) sharp transitions between aeolian dune types occur within the Namib Sand Sea, indicating that a new generation of dunes is forming under a changed set of boundary conditions – could this be the overprinting produced as sea-level rises?

The Namib Sand Sea Digital Database (Livingstone *et al.* 2010) has been refined for the southernmost area of the sand sea for this research. This is an important transition zone in which major diamond placer formation has occurred (see earlier section). It is also the area that is first influenced by a significant change in sediment supply.

The point of transport pathway divergence at the southern end of the depositional system fundamentally controls the wind regime that transported sediment will be subjected to. The eastern path enters the sand sea in an area in which bimodality and complex surface windflow patterns are characteristic. The western pathway, in contrast, is strongly influenced by the unimodal regime of the coastal tract. Between the two pathways a central zone can be identified in which a sheet-like tongue of sand (Fig. 144) extends deep into the sand sea. It has a feathered northern edge, suggesting it is actively growing in a downwind direction. This may be evidence of an adjustment to the boundary conditions prevailing within this part of the system.

This study has shown that tectonic reactivation has probably played a key role in generating locally derived sediment and the deposition of large alluvial fan systems within the Sperrgebiet. Sediment entrainment from the weathered surfaces of these fans as they undergo topographic inversion undoubtedly contributes to the sediment flux within the Namib aeolian system.

However, wind energy to the east of the NAEB margin declines rapidly. The coastal zone is far more significant as a high-energy pathway (Bluck *et al.* 2007) and adjustments in boundary conditions here are

likely to initiate significant change in the architecture of the depositional basin. Tectonics has also been invoked in this paper to explain the development of the marine sequence preserved in the Buntfeldschuh Escarpment. Extensive micropalaeontological research across the entire continental shelf bordering the NAEB shows that a tectonically-driven regression in the late Eocene saw the shoreline migrate some 45 km west. Consequently a massive area of the continental shelf would have been subaerially exposed. Corbett (1989) predicted that shelf exposure during regression would result in westward displacement of the dynamic coastal belt dominated by the unimodal southerly wind regime.

Under such conditions, instead of localised point sources in widely dispersed bays resulting in a grossly under-saturated wind regime, this would create a 'plane source" (sensu Ewing, 2009). Subaerially exposed shelf sediments would be swept by high-energy unimodal winds as the climatic belt migrated west across it. A massive increase in sediment supply might be expected to result in radical sand sea expansion (Fig. 146a).

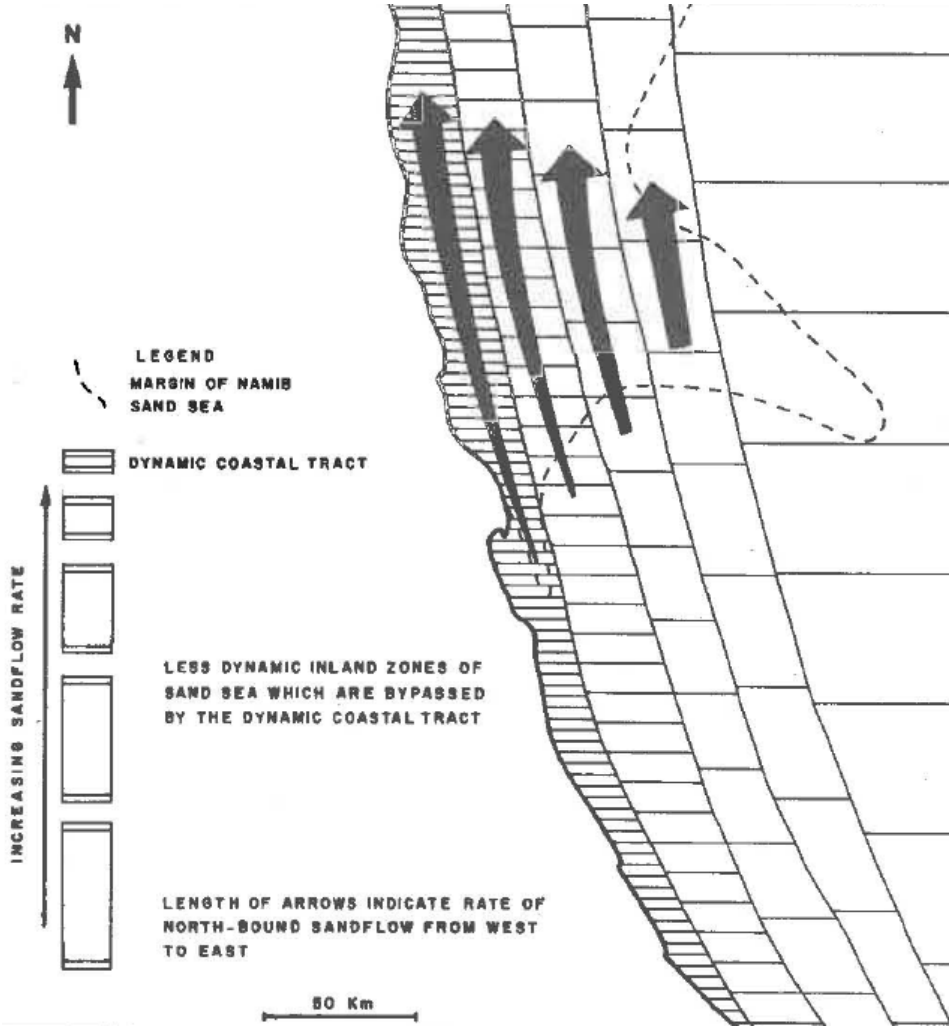

Figure 145. Conceptual division of the aeolian depositional system into a highly dynamic coastal belt influenced by the high-energy unimodal wind regime and a more stable eastern zone which is influenced by a lower-energy bimodal wind regime.

We also know from offshore exploration for, and mining of, diamond placers in deep-water that the Orange River system periodically flushed large volumes of very coarse clastics out onto the subaerially exposed shelf (Murray *et al.* 1970; Corbett, 1996; Jacob *et al.* 1999; Corbett & Burrell, 2001; Bluck *et al.* 2005, 2007). During these episodes large volumes of fine-grained sediment would have been flushed onto the Namibian shelf with the result that sandflow would potentially have increased dramatically due to increased supply further increasing possibilities for transport pathways to sustain sand sea expansion.

The plinth developed in the transition from the NAEB to the depositional basin would act as a barrier to diamond-rich aeolian bedload migrating along the exposed shelf, with the result that aeolian bedload placers could develop over an extensive area. Once transgression ensued an aeolian placer of this type would probably be rapidly eroded by the transgressive front and diamonds would be driven up the shelf. In the process the western margin of the depositional system would be reworked by the marine shoreface and nearshore system. Such a scenario could produce a richly endowed inner shelf with high-grade beach and nearshore diamond placer deposits distributed across it.

During this process the east-west extent of any aeolian sand body would diminish, confined in the east by the Great Escarpment. The coastal high-energy tract would progressively migrate across areas which were formerly influenced by the low- to intermediate-energy wind regime. Linear dune systems developed under the influence of this regime would then be liable to modification by the encroaching higher-energy conditions modifying former linear dunes into a new coastal belt of transverse dunes (Fig. 146b) producing dune transitions similar to those described by Lancaster (2010).

Repeated regression and transgression across the inner shelf and across the western edge of the present-day NAEB would produce complex, embayed coastlines, changing the location and number of point sources for sand to enter the NAEB. As a result transport pathways provided by Aeolian Transport Corridors would shift. Depending upon the number and distribution of suitable log-spiral and south-facing embayments, the degree and point at which the surface-wind becomes sand saturated will probably also change. As studies in the Sahara by Wilson (1972) demonstrated, aeolian depositional systems are sensitive to such changes.

If an aeolian system is saturated, deposition will take place. If the system subsequently becomes under-saturated with respect to sandflow, the sand sea will be eroded and the active plinth defining the south-western margin will progressively migrate northwards.

It is interesting to speculate whether the plinth today is being subjected to erosion or whether it is extending southwards in response to deposition.

There is no doubt that the Elisabeth Bay - Kolmanskop - Charlottental Aeolian Transport Corridor is an example of aeolian diamond placers that formed in response to active aeolian erosion of subaerially exposed shelf placers during regression(s). Diamonds migrated upslope across the exposed shelf as part of the aeolian bedload fraction.

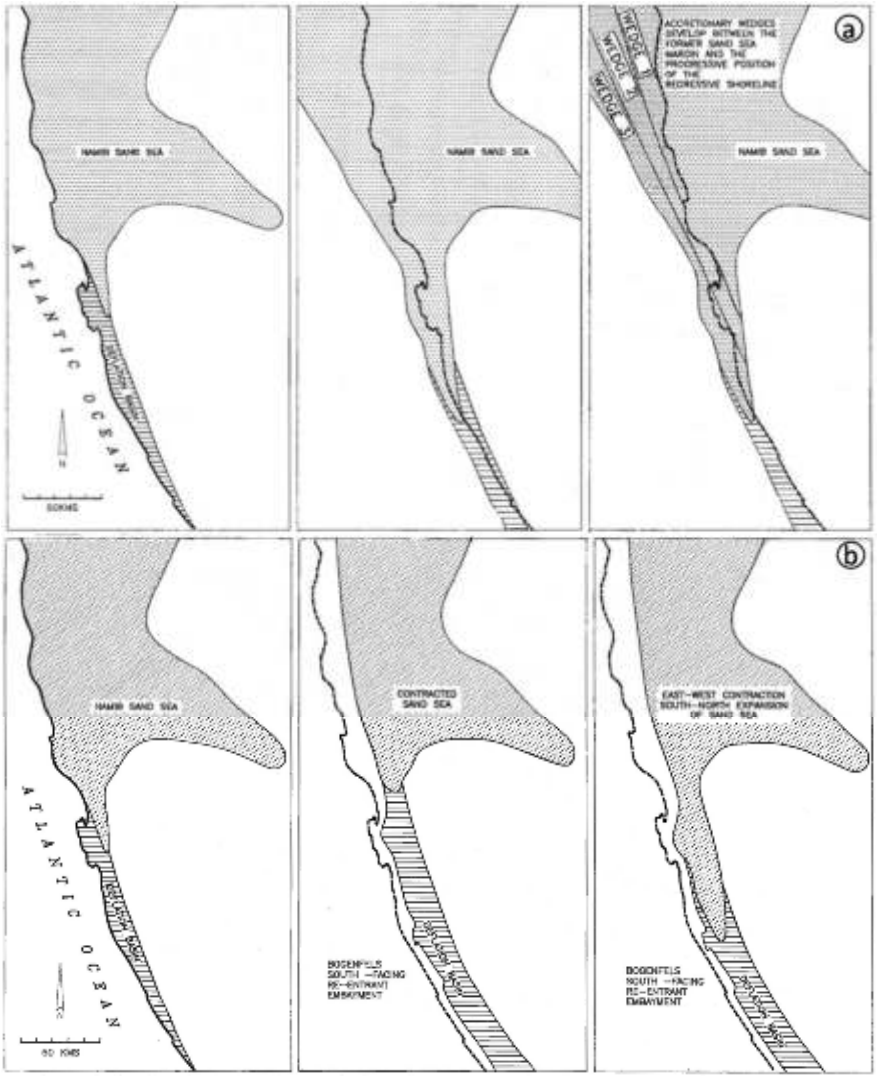

Figure 146. a) Sketch illustrating the addition of accretionary wedges to the western margin of the sand sea during regression. The transition from localised point sources of sediment supply to a plane source would initiate significant changes in boundary conditions – notably availability of sediment to the aeolian system. b) Hypothetical change in boundary conditions leading to sand sea contraction during transgression and the possible configurations that might result in shifts in the location of the active plinth.

Acknowledgements

I would like to thank Dr Jürgen Jacob at Namdeb (Pty) Ltd for providing access to the ALS data, and geophysical and prospecting data that has made this update possible. David Tarboton kindly assisted with TauDEM software and Hartwig Frimmel provided a data set for the Gariep geology.

I benefitted from working with many different people whilst I was with De Beers. I would particularly like to thank Barry Hawthorne for originally enabling me to embark on this research in the early 1980s, and John Ward and Mike de Wit for great discussions in the field over many years.

I would like to thank Martin Pickford for his invaluable input in editing this manuscript. I really enjoyed the opportunity to gain a better understanding of recent developments in solving some of the enigmatic, longstanding challenges presented by the Cenozoic stratigraphy of the Sperrgebiet.

Lastly I would like to thank Gabi Schneider for encouraging me to undertake this project.

References

Allen, J.R.L., 1968. *Current Ripples: Their Relations to Patterns of Water and Sediment Motion*. North Holland Publishing Company, Amsterdam, 433 pp.

Allen, J.R.L., 1982. Sedimentary Structures: Their character and physical basis. *Developments in Sedimentology*, **30** Part A, 535 pp., & Part B, 633 pp. Elsevier, Amsterdam.

Anderson, R.S., 1986. Erosion profiles due to particles entrained by wind. *Geological Society of America Bulletin*, **97**, 1270–1278.

Anderson, R.S., & Haff, P.K., 1988. Simulation of eolian saltation. *Science*, **241**, 820-823.

Apollus, L., 1995. *The Distribution of Diamonds on a Late Cainozoic Gravel Beach, Southwestern Namibia.* Unpublished MSc Thesis, University of Glasgow, 170 pp.

Bagnold, R.A., 1935. The transport of sand by wind. *Geographical Journal*, **85**, 342-369.

Bagnold, R.A., 1941. *The Physics of Blown Sand and Desert Dunes*. Methuen, London, 265 pp.

Bamford, M.K., 2003. *Compilation of Fossil Wood Data from South Africa and Namibia for De Beers 1990-2003*. Internal De Beers Report.

Beetz, W., 1926. Die Tertiarablagerungen der Küstennamib. *In*: Kaiser, E. (Ed.), *Die Diamantenwüste SüdwestAfrikas*, Volume 2, pp. 1-54. Dietrich Reimer (Ernst Vohsen), Berlin.

Best, J.L., & Brayshaw, A.C., 1985. Flow separation - a physical process for the concentration of heavy minerals within alluvial channels. *Journal of the Geological Society of London*, **142**, 747-756.

Blake, W.P., 1904. Origin of pebble-covered plains in desert regions. *Transactions of the American Institute of Mining Engineering*, **34**, 161-162.

Bluck, B.J., Ward, J.D., Cartwright, J., & Swart, R., 2007. The Orange River, southern Africa: an extreme example of a wave-dominated sediment dispersal system in the South Atlantic Ocean. *Journal of the Geological Society of London*, **164**, 341-351.

Bluck, B.J., Ward, J.D., & de Wit, M.C.J., 2005. Diamond mega-placers: southern Africa and the Kaapvaal craton in a global context. *In*: McDonald, I., Boyce, A.J., Butler B.I., Herrington, R.J., & Polya, D.A. (Eds.), *Mineral Deposits and Earth Evolution*. Geological Society of London, pp. 213-245.

Borg, G., Karner, K., Buxton, M., Armstrong, R., & van der Merwe, S.W., 2003. Geology of the Skorpion Supergene Zinc Deposit, Southern Namibia. *Economic Geology*, **98**, 749-771.

Bourke, M.C., Bullard, J.E., & Barnouin-Jha, O.S., 2004. Aeolian sediment transport pathways and aerodynamics at troughs on Mars. *Journal of Geophysical Research, Section E, Planets*, **109**, 1-16.

Bourke, M.C., & Goudie, A.S., 2009. Varieties of barchan form in the Namib Desert and on Mars. *Aeolian Research*, **1**, 45-54.

Brandt, D., Andreoli, M.a.G., & McCarthy, T.S., 2003. Mesozoic fluvial deposits on a rifted continental margin near Vaalputs, Namaqua-land, South Africa. *South African Journal of Geology*, **106**, 11-16.

Brandt, D., Andreoli, M.a.G., & McCarthy, T.S., 2005. The late Mesozoic palaeosoils and Cenozoic fluvial deposits at Vaalputs, Namaqualand, South Africa: possible depositional mechanisms and their bearing on the evolution of the continental margin. *South African Journal of Geology*, **108**, 271-281.

Brayshaw, A.C., Frostick, L.E., & Reid, I.A.N., 1983. The hydrodynamics of particle clusters and sediment entrainment in coarse alluvial channels. *Sedimentology*, **30**, 137-143.

Brüggen, J., 1951. Las Costras de Proteccion en 10 Desiertos. *Revista Universitaria (Chile)*, **36**, 101-104.

Burger, U., 2015. The Geology of the Elizabeth Bay Aeolian Diamond Placer in the Sperrgebiet, Namibia. *In*: *Abstracts of 31st IAS Meeting of Sedimentology. International Association of Sedimentologists, Kraków*, p. 99.

Burke, K., & Gunnell, Y., 2008. The African Erosion Surface: A Continental-Scale Synthesis of Geomorphology, Tectonics, and Environmental Change over the Past 180 Million Years. *Geological Society of America Memoir*, **201**, 1-66.

Butler, R.W.H., & Paton, D.A., 2010. Evaluating lateral compaction in deepwater fold and thrust belts: How much are we missing from 'nature's sandbox'? *GSA Today*, March, 2010, 4-10.

Carrington, A.J., & Kensley, B.F., 1969. Pleistocene molluscs from the Namaqualand coast. *Annals of the South African Museum*, **52**, 189-223.

Chepil, W.S., 1945a. Dynamics of wind erosion: 1. Nature of movement of soil by wind. *Soil Science*, **60**, 305-319.

Chepil, W.S., 1945a. Dynamics of wind erosion: 2. Initiation of soil movement. *Soil Science*, **60**, 397-411.

Clemson, J., Cartwright, J., & Booth, J., 1997. Structural segmentation and the influence of basement structure on the Namibian passive margin. *Journal of the Geological Society of London*, **154**, 477-482.

Clifton, R.E., 1977. Rain Impact Ripples. *Journal of Sedimentary Petrology*, **47**, 678-679.

Cobbold, P.R., Meisling, K.E., & Mount, V.S., 2001. Reactivation of an obliquely rifted margin, Campos and Santos basins, southeastern Brazil. *American Association of Petroleum Geologists Bulletin*, **85**, 1925-1944.

Cogné, N., Gallagher, K., & Cobbold, P.R., 2011. Post-rift reactivation of the onshore margin of southeast Brazil: Evidence from apatite (U-Th)/He and fission-track data. *Earth and Planetary Science Letters*, **309**, 118-130.

Colliston, W.P., Schoch, A.E., & Praekelt, H.E., 2012. Stratigraphy of the Meso-proterozoic Aggeneys Terrane, Western Namaqua Mobile Belt, South Africa. *South African Journal of Geology*, **115**, 449-464.

Cooke, R.U., 1970. Stone pavements in deserts. *Annals of the Association of American Geographers*, **60**, 560-577.

Cooke, R.U., 1981. Salt weathering in deserts. *Proceedings of the Geological Society of London*, **92**, 1-16.

Corbett, I.B., 1989. *The Sedimentology of the Diamondiferous Deflation Deposits within the Sperrgebiet, Namibia*. Unpublished PhD Thesis, University of Cape Town, 430 pp.

Corbett, I.B., 1993. The modern and ancient pattern of sandflow through the southern Namib deflation basin. *In*: Pye, K., & Lancaster, N. (Eds.), *Aeolian Sediments Ancient and Modern*. International Association of Sedimentologists, pp. 45-60.

Corbett, I., & Burrell, B., 2001. The earliest Pleistocene (?) Orange River fan-delta : an example of successful exploration delivery aided by applied Quaternary research in diamond placer sedimentology and palaeontology. *Quaternary International*, **82**, 63-73.

Corner, B., 2008. Crustal Framework of Namibia derived from Integrated Interpretation of Geophysical and Geological Evidence. *In*: Miller, R.M. (Ed.), *The Geology of Namibia*. Geological Survey of Namibia, Windhoek, pp. 2.1-2.19.

Dal Cin, R., 1968. Pebble clusters: their origin and utilisation in the study of palaeocurrents. *Sedimentary Geology*, **2**, 233-241.

Day, R.W., Franzsen, A.J., & Rogers, J., 1992. Coast-parallel palaeochannels off southern Namibia. *Marine Geology*, **105**, 299-304.

de Beer, C.H., 2012. Evidence of Neogene to Quaternary Faulting and Seismogenic Deformation along the Namaqualand Coast, South Africa. *South African Journal of Geology*, **115**, 117-136.

de Vera, J., Granado, P., & McClay, K., 2010. Structural evolution of the Orange Basin gravity-driven system, offshore Namibia. *Marine Petroleum Geology*, **27**, 223-237.

Dewey, J.F., Robb, L., & Schalkwyk, L. Van, 2006. Did Bushmanland extensionally unroof Namaqualand? *Precambrian Research*, **150**, 173-182.

Dong, Z., Wang, H., & Ayrault, M., 2004. Height profile of particle concentration in an aeolian saltating cloud : A wind tunnel investigation by PIV MSD. *Geophysical Research Letters*, **30**, SDE12–1 to SDE12–4.

Dorn, R.I., 2011. Revisiting dirt cracking as a physical weathering process in warm deserts. *Geomorphology*, **135**, 129-142.

Eckardt, F.D., Drake, N., Goudie, A. S., White, K., & Viles, H., 2001. The role of playas in pedogenic gypsum crust formation in the Central Namib Desert: A theoretical model. *Earth Surface Processes and Landforms*, **26**, 1177-1193.

Etheridge, D.W., & Kemp, P.H., 1978. Measurements of turbulent flow down-stream of a rearward-facing step. *Journal of Fluid Mechanics*, **86**, 545-566.

Ewing, R.C., 2009. *Aeolian Dune-Field Boundary Conditions and Dune Interactions Related To Dune-Field Pattern*. Unpublished PhD Thesis, University of Texas (Austin), 117 pp.

Ewing, R.C., & Kocurek, G., 2010. Aeolian dune-field pattern boundary conditions. *Geomorphology*, **114**, 175-187.

Fahnestock, R.K., & Haushild, W.L., 1962. Flume studies of the transport of pebbles and cobbles on a sand bed. *Geological Society of America Bulletin*, **73**, 1431-1436.

Fowler, J.A., 1976. *The Alluvial Geology of the Lower Orange River and Adjacent Coastal Deposits, South West Africa*. Unpublished MPhil Thesis, University of London.

Fowler, J.A., 1982. *Sedimentology and Distribution of Heavy Minerals in the Lower Orange River Valley*. Unpublished PhD Thesis, University of London, 317 pp.

Free, E.E., 1911. Desert pavements and analagous phenomena. *Science*, **33**, 355.

Frimmel, H.E., 2000a. The stratigraphy of the Chameis Sub-terrane in the Gariep Belt in southwestern Namibia. *Communications of the Geological Survey of Namibia*, **12**, 179-186.

Frimmel, H.E., 2000b. The Pan-African Gariep Belt in southwestern Namibia and western South Africa. *Communications of the Geological Survey of Namibia*, **12**, 197-210.

Frimmel, H.E., Basei, M.a.S., Correa, V.X., & Mbangula, N., 2013. A new lithostratigraphic subdivision and geodynamic model for the Pan-African western Saldania Belt, South Africa. *Precambrian Research*, **231**, 218-235.

Fryberger, S.G., Ahlbrandt, T.S., & Andrews, S., 1979. Origin, sedimentary features, and significance of low-angle eolian 'sand sheet' deposits, Great Sand Dunes National Monument and vicinity, Colorado. *Journal of Sedimentary Petrology*, **49**, 733-746.

Fryberger, S.G., & Dean, G., 1979. Dune forms and wind regime. *In*: Mckee, E.D. (Ed.), A Study of Global Sand Seas. *United States Geological Survey Professional Paper*, **1052**, pp. 136-169.

Fryberger, S.G., Hesp, P., & Hastings, K., 1992. Aeolian granule ripple deposits, Namibia. *Sedimentology*, **39**, 319-331.

Garzanti, E., Andò, S., Vezzoli, G., Lustrino, M., Boni, M., & Vermeesch, P., 2012. Petrology of the Namib Sand Sea : Long-distance transport and compositional variability in the wind-displaced Orange Delta. *Earth Science Reviews*, **112**, 173-189.

Garzanti, E., Resentini, A., Andò, S., Vezzoli, G., Pereira, A., & Vermeesch, P., 2015. Physical controls on sand composition and relative durability of detrital minerals during ultra-long distance littoral and aeolian transport (Namibia and southern Angola). *Sedimentology*, **62**, 971-996.

Gerety, K.M., & Slingerland, R., 1983. Nature of the saltating population in wind tunnel experiments with hetergeneous size-density sands. *In*: Brookfield, M.E., & Ahlbrandt, T.S. (Eds.), *Eolian Sediments and Processes*. Elsevier, Amsterdam, pp. 115-132.

Good, M.C., & Joubert, P.N., 1968. The form drag of two-dimensional bluff plates immersed in turbulent boundary layers. *Journal of Fluid Mechanics*, **31**, 547-582.

Goudie, A.S., 2007. Mega-Yardangs : A Global Analysis. *Geography Compass*, **1**, 65-81.

Goudie, A.S., 2008. The History and Nature of Wind Erosion in Deserts. *Annual Review Earth and Planetary Science*, **36**, 97-119.

Goudie, A.S., & Day, M.J., 1980. The disintegration of fan sediments in Death Valley, California, by salt weathering. *Physical Geographer*, **1**, 126-137.

Goudie, A.S., Wright, E., & Viles, H.A., 2002. The roles of salt (sodium nitrate) and fog in weathering: A laboratory simulation of conditions in the northern Atacama Desert, Chile. *Catena*, **48**, 255-266.

Granado, P., de Vera, J., & McClay, K.R., 2009. Tectonostratigraphic evolution of the Orange Basin, SW Africa. *Trabajos de Geologia*, **29**, 321-328.

Greeley, R., Williams, S.H., & Marshall, J.R., 1983. Velocities of wind-blown particles in saltation: preliminary laboratory and field measurements. *In*: Brookfield, M.E., & Ahlbrandt, T.S. (Eds.), *Eolian Sediments and Processes*. Elsevier, Amsterdam, pp. 133-148.

Greenman, L., 1966. *The Geology of Area 2615 C, Lüderitz, South West Africa*. Unpublished MSc Thesis, University of Cape Town, 117 pp.

Groh, C., Rehberg, I., & Kruelle, C.A., 2011. Observation of density segregation inside migrating dunes. *Physics Review, Section E, Statistical Nonlinear Soft Matter Physics*, **84**, 1-4.

Hall, K., 1999. The role of thermal stress fatigue in the breakdown of rock in cold regions. *Geomorphology*, **31**, 47-63.

Hall, K., & André, M.-F., 2001. New insights into rock weathering from high-frequency rock temperature data: an Antarctic study of weathering by thermal stress. *Geomorphology*, **41**, 23-35.

Hallam, C.D., 1964. The Geology of the coastal diamond deposits of southern Africa. *In*: S.H. Haughton (Ed.) The Geology of Some Ore Deposits of Southern Africa. *Geological Society of South Africa*, **2**, 671-728.

Hronsky, J.M. & Groves, D.I., 2008. Science of targeting: definition, strategies, targeting and performance measurement. *Australian Journal of Earth Science*, **55**, 3-12.

Hronsky, J.M., Groves, D.I., Loucks, R.R., & Begg, G.C., 2012. A unified model for gold mineralisation in accretionary orogens and implications for regional-scale exploration targeting methods. *Mineralium Deposita*, **47**, 339-358.

Hunter, R.E., 1977. Terminology of cross-stratified sedimentary layers and climbing ripple structures. *Journal of Sedimentary Petrology*, **47**, 697-706.

Jacob, J., 2001. *Late Proterozoic Bedrock Geology and its Influence on Neogene Littoral Marine Diamondiferous Trapsites, MA1* -

Sperrgebiet, Namibia. Unpublished MPhil Thesis, University of Cape Town.

Jacob, J., 2005. *The Erosional and Cainozoic Depositional History of the Lower Orange River, southwestern Africa*. Volume 1, 167 pp. Unpublished PhD Thesis, University of Glasgow.

Jacob, R., Bluck, B.J., & Ward, J.D., 1999. Tertiary-Age Diamondiferous Fluvial Deposits of the Orange River Valley. *Economic Geology*, **94**, 749-758.

Kaiser, E., 1926a. *Die Diamantenwüste SüdwestAfrikas* Volume I, 321 pp. and Volume II, 535 pp. Dietrich Reimer (Ernst Vohsen), Berlin.

Kaiser, E., 1926b. Die jungen sedimentaren neubildungen om extrem-ariden klima der Namibwüste. *In*: Kaiser, E. (Ed.), *Die Diamantenwüste SüdwestAfrikas* Volume 2. Dietrich Reimer (Ernst Vohsen), Berlin, pp. 317-380.

Kaiser, E., & Beetz, W., 1926. Geological Maps. *In*: Kaiser, E. (Ed.), *Die Diamantenwüste SüdwestAfrikas*, Volume 2. Dietrich Reimer (Ernst Vohsen), Berlin, p. 158.

Kennett, J.P., 1982. *Marine Geology*, New Jersey. Prentice-Hall, 832 pp.

King, L.C., 1951. *South African Scenery*, 2nd Edition. Oliver and Boyd, Edinburgh, 379 pp.

Klinger, H., 1977. Cretaceous deposits near Bogenfels, South West Africa. *Annals of the South African Museum*, **73**, 81-92.

Klinger, H.C., & McMillan, I.K., 2007. Ammonites from offshore deposits near Bogenfels, Namibia. *Palaeontologia africana*, **42**, 25-27.

Koopmann, H., Franke, D., Schreckenberger, B., Schulz, H., Hartwig, A., & Stollhofen, H., 2014. Segmentation and volcano-tectonic characteristics along the SW African continental margin, South Atlantic, as derived from multichannel seismic and potential field data. *Marine and Petroleum Geology*, **50**, 22-39.

Kounov, A., Viola, G., de Wit, M., & Andreoli, M.a.G., 2009. Denudation along the Atlantic passive margin: new insights from apatite fission-track analysis on the western coast of South Africa. *Geological Society of London, Special Publication*, **324**, 287-306.

Krause, C., 1910. Notes on the German South-West African Diamonds. *Transactions of the Geological Society of South Africa*, **13**, 61-64.

Lancaster, N., 1985. Winds and sand movements in the Namib Sand Sea. *Earth Surface Processes and Landforms*, **10**, 607-619.

Lancaster, N., 2010. Global Sand Seas Present Status. *In*: *Global Sand Seas: Past, Present, Future*. The Royal Geographical Society, 39 pp.

Langbein, W.B., & Leopold, L.B., 1968. River Channel Bars and Dunes - Theory of Kinematic Waves. *United States Geological Survey Professional Paper*, **422**, L1-L20.

Laronne, J.B., & Carson, M.A., 1976. Interrelationships between bed morphology and bed-material transport for a small, gravel-bed channel. *Sedimentology*, **23**, 67-85.

Li, Z., & Komar, P.D., 1986. Laboratory measurements of pivoting angles for applications to selective entrainment of gravel in a current. *Sedimentology*, **33**, 413-423.

Lighthill, M. J., & Whitham, G. B. (1955a). On kinematic waves I . Flood movement in long rivers. *Proceedings of the Royal Society A: Mathematical, Physical and Engineering Sciences*, **229** (**1178**), 281-316.

Lighthill, M.J., & Whitham, G.B., 1955b. On Kinematic Waves. II. A Theory of Traffic Flow on Long Crowded Roads. *Proceedings of the Royal Society A Mathematics Physics and Engineering Science*, **229**, 317-345.

Livingstone, I., Bristow, C., Bryant, R.G., Bullard, J., White, K., Wiggs, G.F.S., Baas, A.C.W., Bateman, M.D., & Thomas, D.S.G., 2010. The Namib Sand Sea digital database of aeolian dunes and key forcing variables. *Aeolian Research*, **2**, 93-104.

Lotz, H., 1909. Über die Lüderitzbuchter diamantvorkommen. *Zeitschrift für praktische Geologie*. p. 142.

Lyles, L., Schrandt, R.L., & Schmeidler, N.F., 1974. How Aerodynamic Roughness Elements Control Sand Movement. *Transactions of the American Society of Agricultural Engineers*, **17**, 134-139.

MacDonald, E.H., 1983. Alluvial Mining. *In*: Slingerland, D.G. (Ed.), *Geomorphological Controls on the Distribution of Placer Deposits*. Geological Society of London, pp. 727-737.

Marsh, J.S., 1973. Relationships between transform directions and alkaline igneous rock lineaments in Africa and South America. *Earth and Planetary Science Letters*, **18**, 317-323.

McCuaig, T.C., Beresford, S., & Hronsky, J., 2010. Translating the mineral systems approach into an effective exploration targeting system. *Ore Geology Review*, **38**, 128-138.

McFadden, L.D., Eppes, M.C., Gillespie, A.R., & Hallet, B., 2005. Physical weathering in arid landscapes due to diurnal variation in the

direction of solar heating. *Geological Society of America Bulletin*, **117**, 161.

McFadden, L.D., Wells, S.G., & Jercinovich, M.J., 1987. Influences of eolian and pedogenic processes on the origin and evolution of desert pavements. *Geology*, **15**, 504-508.

McMillan, I.K., & Dale, D.C., 2002. *Progress Report for Micropalaeontology at De Beers Marine*: Unpublished Close-out Report.

McQuivey, R.S., & Keefer, T.N., 1969. The relation of turbulence to deposition of magnetite over ripples. *USGS Professional Paper*, **650D**, 244-247.

Meigs, P., 1966. Geography of coastal deserts. *Arid Zone Research*, **28**, 1-40.

Meisling, K.E., Cobbold, P.R., & Mount, V.S., 2001. Segmentation of an obliquely-rifted margin, Campos and Santos basins, south-eastern Brazil. *American Association of Petroleum Geologists Bulletin*, **85**, 1903-1924.

Merensky, H., 1909. The Diamond Deposits of Luderitzland, German South-West Africa. *Transactions of the Geological Society of South Africa*, **12**, 13-23.

Middleton, G.V, & Southard, J.B., 1984. *Mechanics of Sediment Movement: SEPM Short Course 3*, 2nd Edition. Society of Economic Paleontologists and Mineralogists, Tulsa, Oklahoma, 401 pp.

Miller, J.E., 1983. Basic Concepts of Kinematic-Wave Models, *United States Geological Survey Professional Paper*, **1302**, 36 pp.

Miller, R. McG., 2008. Namib Group. *In*: *The Geology of Namibia, Volume 3, Palaeozoic to Cenozoic*, Chapter 25, pp. 1-66, Ministry of Mines and Energy, Geological Survey, Windhoek, Namibia.

Mosely, M.P., & Schumm, S.A., 1977. Stream Junctions - a probable location for bedrock placers. *Economic Geology*, **72**, 691-697.

Moulden, J.C., 1905. Origin of pebble-covered plains in desert regions. *Transactions of the American Institute of Mining Engineering*, **35**, 963-964.

Murray, L., Joynt, R.H., O'Shea, D.O., Foster, R.W., & Kleinjan, L., 1970. The geological environment of some diamond deposits off the coast of South West Africa. *In*: Delany, F.M. (Ed.), ICSU/SCOR Working Party 31 Symposium: *The Geology of the East Atlantic Continental Margin*. Institute of Geological Sciences Report #70/13, Cambridge, pp. 119-141.

Mvondo, F., Dauteuil, O., & Guillocheau, F., 2011. The Fish River Canyon (Southern Namibia): A record of Cenozoic mantle dynamics? *Comptes Rendus Geoscience*, **343**, 478-485.

Oelofsen, A., 2008. *Late Cenozoic Shallow Marine Diamond Placers off the Northern Sperrgebiet, Namibia*. Unpublished MSc Thesis, University of Cape Town, 193 pp.

Ollier, C.D., 1965. Dirt cracking - a type of insolation weathering. *Australian Journal of Science*, **27**, 236-237.

Parrish, J.T., & Curtis, R.L., 1982. Atmospheric Circulation, Upwelling, and Organic-rich Rocks in the Mesozoic and Cenozoic Eras. *Palaeogeography, Palaeoclimatology, Palaeo-ecology*, **40**, 31-66.

Partridge, T.C., & Maud, R.R., 1987. Geomorphic evolution of southern Africa since the Mesozoic. *South African Journal of Geology*, **90**, 179-208.

Pegler, E.A., 1997. *Final Report on the Geology of the Orange Basin and the History of Diamond Movements*. Cape Town.

Pelletier, J.D., Cline, M., & DeLong, S.B., 2007. High spatial resolution data acquisition for the geosciences: kite aerial photography. *Earth Surface Processes and Landforms*, **32**, 1913-1927.

Pether, J., Roberts, D.L., & Ward, J.D., 2000. Deposits of the West Coast. *In*: Partridge, T.C., & Maud, R.R. (Eds.) *The Cenozoic of Southern Africa*. The Oxford University Press, New York, pp. 33-54.

Pickford, M., 2000. Neogene and Quaternary vertebrate biochronology of the Sperrgebiet and Otavi Mountainland, Namibia. *Communications of the Geological Survey of Namibia*, **12**, 411-419.

Pickford, M., 2015. Cenozoic Geology of the Northern Sperrgebiet, Namibia, accenting the Palaeogene. *Communications of the Geological Survey of Namibia*, **16**, 10-104.

Pickford, M., Sawada, Y., Hyodo, H., & Senut, B., 2013. Radio-isotopic age control for Palaeogene deposits of the Northern Sperrgebiet, Namibia. *Communications of the Geological Survey of Namibia*, **15**, 3-15.

Pickford, M., Sawada, Y., & Senut, B., 2008. Geochronology and palaeontology of the Palaeogene deposits in the Sperrgebiet, Namibia. *In*: *The World at the Time of Messel*. 22nd International Senckenberg Conference, pp. 129-130.

Pickford, M., & Senut, B., 2016. The fossiliferous sands of Hexen Kessel, Sperrgebiet, Namibia. *Memoir of the Geological Survey of Namibia*, **22**, 199-208.

Pickford, M., Senut, B., & Dauphin, Y., 1995. Biostratigraphy of the Tsondab Sandstone

(Namibia) based on gigantic avian eggshells. *Geobios*, **28**, 85-98.

Pickford, M., Senut, B., Mocke, H., Mourer-Chauviré, C., Rage, J.-C., & Mein, P., 2014. Eocene aridity in southwestern Africa: timing of onset and biological consequences. *Transactions of the Royal Society of South Africa*, **69**(**3**), 139-144.

Pietruszka, R.D., & Seely, M.K., 1985. Predictability of two moisture sources in the Namib Desert. *South African Journal of Science*, **81**, 682-685.

Raab, M.J., Brown, R.W., Gallagher, K., Carter, A., & Weber, K., 2002. Late Cretaceous reactivation of major crustal shear zones in northern Namibia: constraints from apatite fission track analysis. *Tectonophysics*, **349**, 75-92.

Raith, J.G., Cornell, D.H., Frimmel, H.E., Beer, C.H. De, The, S., & May, N., 2003. New Insights into the Geology of the Namaqua Tectonic Province, South Africa, from Ion Probe Dating of Detrital and Metamorphic Zircon. *Journal of Geology*, **111**, 347-366.

Range, P., 1909. Die Diamantfelder bei Lüderitzbucht. *Deutsches Kolonialblatt*, **22**, 1039-1048.

Rea, D.K., 1994. The paleoclimatic record provided by eolian deposition in the deep sea: The geologic history of wind. *Reviews of Geophysics*, **32**(**2**), 159-195.

Rogers, J., Pether, J., Molyneux, R., Hill, R.S., Kilham, J.L.C., Cooper, G., & Corbett, I.B., 1990. Cenozoic geology and mineral deposits along the west coast of South Africa and the Sperrgebiet. *In*: Gresse, P.G., Rogers, J., & Minter, W.E.L. (Eds.), *Guidebook Geo-congress '90*. Geological Society of South Africa, pp. 1-111.

Rohrmann, A., Heermance, R., Kapp, P., & Cai, F., 2013. Wind as the primary driver of erosion in the Qaidam Basin, China. *Earth and Planetary Science Letters*, **174**, 1-10.

Scheidt, S.P., 2012. Sand Transport Pathways of Dark Dunes in the Sperrgebiet: Sand Composition and Dune Migration Rates from ASTER data, Abstract #7051. *Third International Planetary Dunes Workshop: Remote Sensing and Image Analysis of Planetary Dunes, June 12-15, 2012*.

Scheidt, S.P., & Lancaster, N., 2013. The application of COSI-Corr to determine dune system dynamics in the southern Namib Desert using ASTER data. *Earth Surface Processes and Landforms*, **38**, 1004-1019.

Schneider, G., 2008. *Treasures of the Diamond Coast: A Century of Diamond Mining in Namibia*. MacMillan, Windhoek, 320 pp.

Scott, M., & Schmaltz, J., 2010. Dust and Hydrogen Sulphide along the Namibian Coast [WWW Document]. *Earth Observatory*. URL http://earthobservatory.nasa.gov/IOTD/view.php?id=44340

Sharp, R.P., 1963. Wind Ripples. *Journal of Geology*, **71**, 617-636.

Siesser, W.G., & Salmon, D., 1979. Eocene marine sediments in the Sperrgebiet, South West Africa. *Annals of the South African Museum*, **79**, 9-34.

South Africa Committee for Stratigraphy (SACS), 1980. Stratigraphy of South Africa. Kent, L.E. (Compilation), Part 1: Litho-stratigraphy of the Republic of South Africa, South West Africa / Namibia and the Republics of Bophuthatswana, Transkei and Venda. *Handbook of the Geological Survey of South Africa*, **8**: 690 pp.

Spaggiari, R.I., 2011. *Sedimentology of Plio-Pleistocene Gravel Barrier Deposits in the Palaeo-Orange River Mouth, Namibia: Depositional History and Diamond Mineral-isation*, Volumes 1 & 2. Unpublished PhD Thesis, Rhodes University, Grahamstown, 389 pp.

Sternberg, H., 1875. Untersuchungen uber langen- und Querprofil geschiebeführende Flusse. *Zeitschrift Fur Bauwessem*, **25**, 483-506.

Sutherland, D.G., 1982. The Transport and Sorting of Diamonds by Fluvial and Marine Processes. *Economic Geology*, **77**, 1613-1620.

Sykes, L.R., 1978. Intraplate seismicity, reactivation of preexisting zones of weakness, alkaline magmatism, and other tectonism postdating continental fragmentation. *Reviews of Geophysics*, **16**, 621.

Tinker, J., de Wit, M., & Brown, R., 2008. Mesozoic exhumation of the southern Cape, South Africa, quantified using apatite fission track thermochronology. *Tectonophysics*, **455**, 77-93.

Tsoar, H., 1983. Wind tunnel modelling of echo and climbing dunes. *In*: Brookfield, M.E., & Ahlbrandt, T.S. (Eds.), *Developments in Sedimentology 38: Eolian Sediments and Processes*. Elsevier, Amsterdam, pp. 247-259.

van Zinderen Bakker, E.M., 1975. The origin and palaeoenvironment of the Namib Desert biome. *Journal of Biogeography*, **2**, 65-73.

Vermeesch, P., Fenton, C.R., Kober, F., Wiggs, G.F.S., Bristow, C.S., & Xu, S., 2010. Sand residence times of one million years in the

Namib Sand Sea from cosmogenic nuclides. *Nature Geoscience Letters*, **3**(**12**), 862-865.

Viola, G., Andreoli, M., Ben-Avraham, Z., Stengel, I., & Reshef, M., 2005. Offshore mud volcanoes and onland faulting in southwestern Africa: neotectonic implications and constraints on the regional stress field. *Earth and Planetary Science Letters*, **231**(**1-2**), 147-160. doi:10.1016/j.epsl.2004. 12.001.

Viola, G., Kounov, A., Andreoli, M.a.G., & Mattila, J., 2012. Brittle tectonic evolution along the western margin of South Africa: More than 500 Myr of continued reactivation. *Tectonophysics*, **514**-**517**, 93-114.

Wagner, P.A., 1910. The diamond fields of southern Africa. *Transactions of the Geological Society of South Africa*, **13**, XLVI-XLVII.

Wagner, P.A., 1914. The diamond fields of southern Africa. *The Transvaal Leader*, Johannesburg, p. 355.

Ward, J.D., 1984. *Aspects of the Cenozoic Geology in the Kuiseb Valley, Central Namib Desert*. Unpublished PhD Thesis, University of Natal, Pietermaritzburg, 310 pp.

Ward, J.D., 1987. The Cenozoic Succession in the Kuiseb Valley, Central Namib Desert. *Geological Survey of Namibia Memoir*, **9**, 124 pp.

Ward, J.D., & Corbett, I.B., 1990. Towards an Age for the Namib. *In*: Seely, M.K. (Ed.), *Namib Ecology*. Transvaal Museum, Pretoria, pp. 17-26.

Wells, S.G., McFadden, L.D., McDonald, E. V, Eppes, M.C., Young, M.H., & Wood, Y.A., 2014. Desert Pavement Process and Form : Modes and Scales of Landscape Stability and Instability in Arid Regions. *Geophysical Research Abstracts*, p. 16.

Wildman, M., 2015. *Reassessing the Structural and Geomorphic Evolution of a 'Classic' Atlantic Type Passive Margin: An Integrated Study of the Namaqualand Sector of the South African Continental Margin*. Unpublished PhD Thesis, University of Glasgow, 374 pp.

Wildman, M., Brown, R., Watkins, R., Carter, A., Gleadow, A., & Summerfield, M., 2015. Post break-up tectonic inversion across the southwestern cape of South Africa: New insights from apatite and zircon fission track thermochronometry. *Tectonophysics*, **654**, 30-55.

Willetts, B., 1983. Transport by wind of granular materials of different grain shapes and densities. *Sedimentology*, **30**, 669-679.

Willetts, B., & Rice, M.A., 1986. Collision in aeolian transport: the saltation/creep link. *In*: Nickling, W.G. (Ed.), Aeolian Geomorphology. *Proceedings of the 17th Annual Binghampton Geomorphology Symposium*. Allen & Unwin, pp. 1-17.

Willetts, B., & Rice, M.A., 1989. Collisions of quartz grains with a sand bed: the influence of incidence angle. *Earth Surface Processes and Landforms*, **14**, 719-730.

Wilson, I., 1972. Aeolian bedforms - their development and origins. *Sedimentology*, **19**, 173-210.

Zalan, P.V., 2005. End members of gravitational fold and thrust belts (GFTBs) in the deep waters of Brazil. *In*: J.H. Shaw, C. Connors, & J. Suppe (Eds.), *An AAPG Seismic Atlas* (AAPG Studies, pp. 147-156). American Association of Petroleum Geologists.

Zhang, D., Yang, X., Rozier, O., & Narteau, C., 2014. Mean sediment residence time in barchan dunes. *Journal of Geophysical Research: Earth Surface*, **119**, 451-463.

Zhang, W., Tan, L., Zhang, G., Qiu, F., & Zhan, H., 2014. Aeolian processes over gravel beds (2) Supplement to : Aeolian processes over gravel beds : Field wind tunnel simulation and its application atop the Mogao Grottoes, China. *Aeolian Research*, **15**, 335-344.

Ferricrete in the Sperrgebiet, Namibia : age, palaeoclimatic and economic implications

Martin Pickford

Sorbonne Universités (CR2P, UMR 7207 du CNRS, Département Histoire de la Terre, Muséum National d'Histoire Naturelle et Université Pierre et Marie Curie) case postale 38, 57 rue Cuvier, 75005 Paris.
(e-mail: <pickford@mnhn.fr>*)*

Abstract: The near-surface ferruginised deposits of the Sperrgebiet, Namibia, have had a chequered history of interpretation with estimates of their formation varying in age from Middle Cretaceous to Pleistocene. Detailed study reveals that there was a single phase of ferruginisation which occurred sometime during the period spanning the Late Oligocene to basal Middle Miocene. Previous reports of ferruginised deposits beneath the Pomona Quartzite (now known as the Kätchen Plateau Formation) are erroneous, all occurrences being banked up against the slopes of the tafelberge and containing reworked blocks of the quartzite within them. At many localities ferruginised deposits line the floors and sides of valleys eroded during the Oligocene, seldom reaching a thickness of more than a metre, but at Buntfeldschuh, the Kakaoberg occurrence is up to 20 metres thick, while the equivalent ferruginised quartz lag at the northern end of the escarpment, previously thought to be of Mid-Cretaceous age, is about 2 metres thick. At Lüderitz Krater ferruginised deposits overlying Kätchen Plateau Quartzite contain agates, and at Langental *Turritella* site they cement agate-bearing fossiliferous marls and limestones. Because the diamond placers of the Sperrgebiet date from at least the Late Eocene (if not considerably earlier) the presence of ferruginised deposits onshore and offshore Namibia is not a reliable criterion for indicating the footwall of the placers. The Sperrgebiet ferricrete field indicates a sub-humid palaeoclimate at the time of its genesis, an inference supported by the local fossil record.

Key Words: Ferricrete, Ferruginised sediment, Oligo-Miocene, Namibia, Diamonds, Palaeoclimate

To cite this paper: Pickford, M., 2016. Ferricrete in the Sperrgebiet, Namibia: age, palaeoclimatic and economic implications. *Memoir of the Geological Survey of Namibia*, **22**, 172-198.

Introduction

Outcrops of ferruginised sediments (ferricrete) occur widely but discontinuously through the Sperrgebiet, Namibia, from Grillental in the North (Liddle, 1971; Pickford, 2015) to Kerbehuk in the South (Haughton, 1932) passing via Pomona (Kaiser & Beetz, 1926) and Buntfeldschuh (Hallam, 1964).

Beetz (1926), Kaiser (1926) and Kaiser & Beetz (1926) mapped ferruginised sediments overlying altered Basement rocks beneath the capping quartzites of the Pomona Tafelberge and deduced that they were the basal portion of the Pomona Schichten of « Prämitteleocän » age (i.e. pre-Priabonian in today's parlance : Pickford, 2015). Beetz (1926) wrote that the encrusted surface of the altered Basement (Verwitterungskruste einer alten Landoberfläche) was probably of Cretaceous age (Wahrscheinlich Kreide). The stratigraphy of the Pomona area was modified by Liddle (1970a, 1970b, 1970c, 1971), Fowler (1970) and Stocken (1978) who subdivided the Pomona Schichten of Kaiser & Beetz (1926) into a lower, unsilicified part which Stocken (1978) called the Pomona Beds and an upper silicified part which he named the Tafelberg Quartzite. An age estimate of Cretaceous became attached to the deposits (Sullivan & Clarke, 1962; Hallam, 1964; Fowler, 1970; Stocken, 1978) an idea that was widely accepted, with the supposed erosion surface beneath the Pomona Beds eventually being correlated to the Middle Cretaceous (i.e. the African Surface of King, 1949) (or in the scheme of Hallam, 1964, the Gondwana Surface), and the Tafelberg Quartzites and related silicified deposits considered to overlie a Late Cretaceous bevel developed atop the Pomona Beds upon which the Tafelberg Quartzite was deposited (Liddle, 1971; Stocken, 1978).

In stark contrast to a Cretaceous age estimate for the Sperrgebiet ferricretes (Sullivan & Clarke, 1962; Barbieri, 1968; Fowler & Liddle, 1970; Fowler, 1970; Stocken, 1978) is the Pleistocene age given to

them by Du Toit (1954, cited in Hallam, 1964) and the Oligo-Miocene correlation published by Pickford (2015).

Re-examination of the succession in the region of the Tafelberge reveals that the Kätchen Plateau Quartzite grades downwards into unsilicified sediment rich in similar quartz pebbles, which itself grades downwards into Bo Alterite beneath, without any obvious « erosion » surface between any of the parts. There is no sign of a ferruginised horizon between the Bo Alterite and the overlying Pomona Schichten or the quartzite. At Tafelberg Nord, the upper part of the Kätchen Plateau Quartzite contains lebenspurren indicating marine reworking of the superficial deposits producing a sand in which organisms contructed vertical burrows. This sandstone and the underlying poorly sorted gravels were subsequently silicified to produce the Kätchen Plateau Quartzite (Pickford, 2015).

At Wanderfeld IV, Cretaceous pebbly limestone lies in and on deeply weathered versions of the same limestone, now represented by variegated marl rich in quartz and quartzite pebbles derived from the Cretaceous limestone. White irregular nodules in the marl represent ghosts of the steinkerns of oysters. From this it is concluded that the marl is a local facies of the Bo Alterite, weathered during the Ypresian (Pickford, 2015), rather than a pre-Cretaceous horizon as interpreted by Klinger (1977).

Since it was (and still is) widely believed that diamonds were transported to the Sperrgebiet during the Eocene (Kaiser & Beetz, 1926) and subsequently (Stocken, 1978) the correlation of the Sperrgebiet ferruginised deposits to the Cretaceous implied that they were formed prior to the arrival of the diamonds and consequently that the presence of ferricrete in a section (both onshore and offshore Namibia) meant that the footwall of the diamondiferous strata has been detected. It turns out that this is false, since the ferricrete in the Sperrgebiet is of Oligo-Miocene age whereas it is generally conceded that diamonds have been in the area from at least the Late Eocene.

Pickford (2015) showed that in the type area of the Sperrgebiet ferruginised sediment, originally diagnosed around Kätchen Plateau and Elfert's Tafelberg, the ferricrete contains reworked blocks of Kätchen Plateau Quartzite (which used to be called the Pomona Quartzite or the Tafelberg Quartzite) and must therefore be considerably younger than the quartzite. The ferruginised deposits drape downslope for about 20 metres, meaning that at least this amount of relief existed adjacent to the tafelberge prior to the phase of ferruginisation. Thus, although the ferruginised deposits are topographically lower than the quartzite, they are stratigraphically considerably younger than it. Evidence for this comes not only from the type area but also from other outcrops as detailed below.

Pickford (2015) adduced evidence for a post-quartzite age for other ferruginous outcrops, including ferruginised sediment containing agates unconformably overlying quartzite at Lüderitz Krater, ferruginised quartz lag at Langer Tafelberg where it contains blocks of Tafelberg Quartzite, at Kakaoberg where it pervasively cemented the Terrestre Sandstone which overlies the deltaic-marine deposits of the Buntfeldschuh Formation of Eocene age, at Wanderfeld IV where reworked Priabonian fossils (shark teeth, bivalves) occur in ferruginised grit and conglomerate, and at Grillental where Early Miocene molluscs have been ferruginised along with clays/silts as well as the overlying coarse grits which yield Early Miocene mammalian fossils. He concluded that the ferruginising processes were active some time between the Late-Oligocene and the Early Miocene (Chattian to Langhian).

During the 2016 field survey in the Sperrgebiet, further observations were made in order to determine firstly, whether there was evidence for more than one episode of ferruginisation and secondly, to estimate more precisely the age of ferruginisation. Many of the reported occurrences of ferricrete in the Sperrgebiet (Kaiser & Beetz, 1926; Barbieri, 1968; Liddle, 1971) were visited. The findings underscore and extend the interpretation published in 2015. The following observations in the Sperrgebiet are treated from north to south.

Definition of ferricrete and its palaeoclimatic significance

Ferricrete is a generic term for iron-rich sedimentary deposits which formed near the land surface, the iron oxide cements being derived from the oxidation of percolating waters containing dissolved iron salts (ferric oxide, being less soluble in water than ferrous oxide and other iron salts, precipitates when the latter salts are oxidised). The term ferricrete is not to be confused with laterite, which is also an iron-rich, near-surface layer, but which is formed by prolonged weathering and associated chemical changes of *in situ* bedrock (Widdowson, 2003). In ferricrete the iron oxides are largely brought into the depositional zone by percolating waters and generally cement near-surface rock layers which differ from the underlying bedrock (sediments, breccias, lags, regs, sands etc.) whereas laterites result from *in situ* physico-chemical changes to the bedrock with little input of iron salts from outside the weathering zone. In the field, ferricretes usually lie with discordance upon the underlying rock layers, as in the Sperrgebiet, where they overlie a variety of bedrock types with sharply discordant contacts, whereas laterite grades progressively downwards from the iron-rich surface crust through zones of heavily weathered bedrock to lightly altered bedrock and then into unaltered bedrock beneath. The latter situation has not been observed in the Sperrgebiet, which means that all of the ferruginised layers in the region are ferricretes.

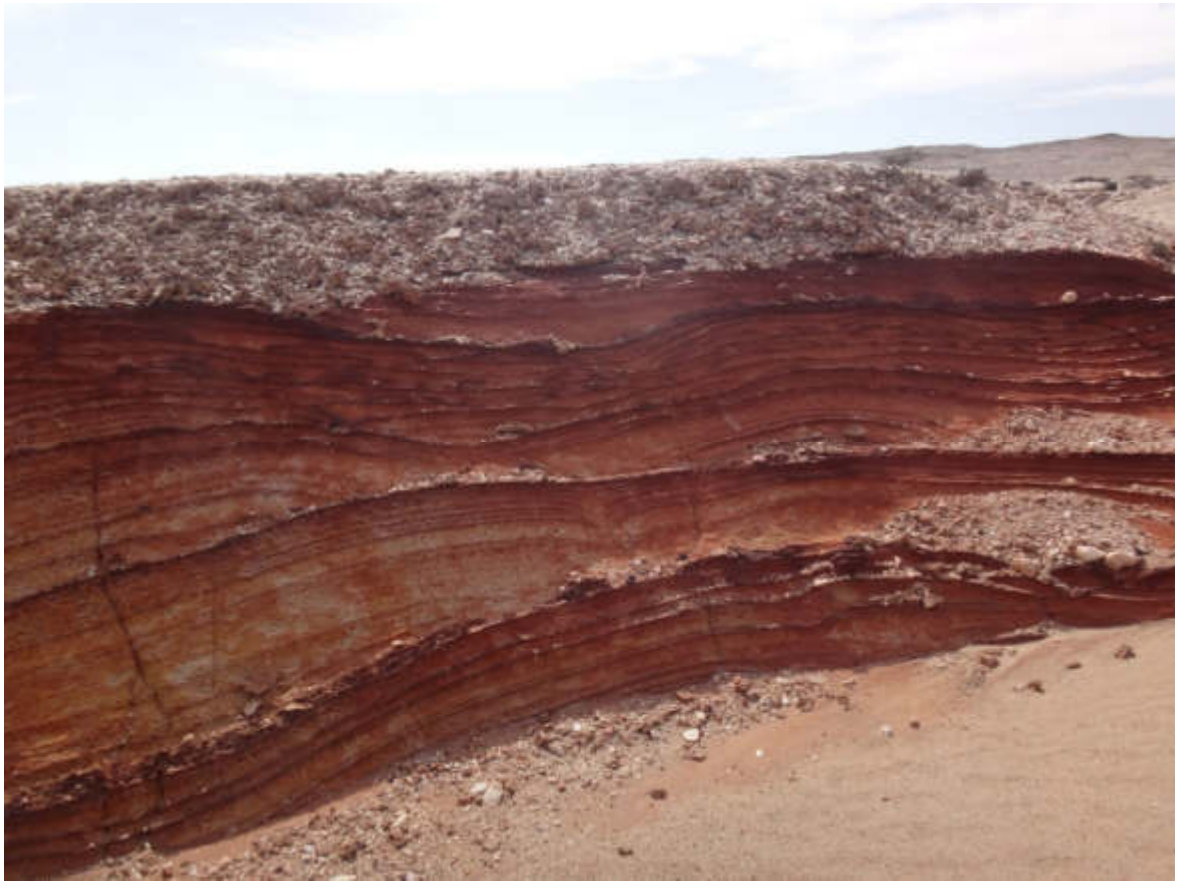

Figure 1. Altered Proterozoic schist (Bo Alterite) in the northern part of Hexen Kessel (27°14'56.3"S : 15°20'32.2"E), overlain by 50 cm of regolith (Desert Waste of Beetz, 1926), showing minor ferruginisation of thin layers within the alterite and at its surface.

There are several categories of ferricrete, including alluvial (cementing conglomerates, for example), colluvial (cementing breccias and regolith for example) and bog ferricrete (with little or no clastic fraction) (Verplanck *et al.* 2007). In addition, there are pisolithic varieties (murram, bohnerz or « bean ore »). The ferricretes of the Sperrgebiet are

predominantly colluvial, but there are examples or bohnerz, of bog-type ferricrete infilling fissures in alterite and of colluvial ferricrete cementing well-rounded clasts of various lithologies. In brief, at the time of oxidation, the iron-rich waters of the Sperrgebiet cemented whatever near-surface sediments and fissures they were percolating through.

According to Verplanck *et al.* (2007) colluvial ferricrete can be defined as « *iron oxyhydroxide cemented, clast supported with angular clasts of limited lithologic variation, poorly to moderately sorted, massive to minor layering subparallel to hillslope* ». In Colorado, colluvial ferricretes occur in steep tributaries, avalanche chutes and hillslopes, whereas bog ferricrete usually occurs in valley floors but also along hillslopes near bedrock contacts and fissures.

The above definitions fit well with the ferricrete observed in the Sperrgebiet, the ferruginised deposits often comprising lag deposits of angular quartz cobbles, poorly sorted with weak bedding disposed in valley floors and draping up the sides of valleys, corresponding to colluvial facies. There are also ferruginised fissure infillings, sometimes with angular clasts, sometimes without, corresponding to bog ferricrete, and there are minor occurrences of alluvial facies with well-rounded clasts of diverse rock types.

It is understood that, for ferricretes to form in the Sperrgebiet, which is currently an extremely arid part of the continent, there must have been an appreciably more humid palaeoclimate at the time that they formed than typifies the area today. Fossilised hives (*Namajenga mwichwa*) of a genus of polycalate termite, probably *Hodotermes*, are preserved in the Early Miocene fluvio-paludal deposits in Grillental, Fiskus, Chameis and elsewhere in the Sperrgebiet. The presence of these hives indicates that the region at the time of their construction lay within or close to a zone with summer rainfall between 250 and 750 mm mean annual rainfall (Pickford, 2008). Such palaeoclimatic conditions would be sufficient for ferricretes to form, given that the other physico-chemical conditions were met.

Note on the Geological Time Scale

As was pointed out by Pickford (2015) the geological time scale has evolved since the pioneer surveys of Kaiser & Beetz (1926) who adopted the common view of the time that the Miocene was preceded by the Eocene which was preceded by the Cretaceous (without the Oligocene and Palaeocene recognised as distinct epochs). In broad terms, what the latter authors called « Mitteleocän » is equivalent to Priabonian (i.e. Late Eocene) in today's terms (Gradstein *et al.* 2004) and what they called Late Eocene would be Oligocene in today's version of the scale. Many of the previous reports on Sperrgebiet geology failed to take this time-scale offset into account.

Location of ferruginised deposits in the Sperrgebiet

Ferruginised rocks occur widely but sporadically in the Sperrgebiet between Grillental in the north and Kerbehuk in the south a distance of 160 km, and from the coast as far inland as the Klinghardt Mountains (30 km) (Pickford, 2015). They are also known to occur offshore Namibia, but the latter deposits are not discussed in this paper, but they do imply that sea-level must have been lower for them to form in areas that are today under the sea. Table 1 lists the main onland outcrops examined during this study, but several of the locations such as Idatal, Hexen Kessel, the valleys north of Lüderitz Krater and the Idatal-Granitberg Road contain important outcrops in addition to the ones listed. Most of the occurrences examined are in the Trough Namib, but there are outcrops in the Plain Namib around Swartkop and near the Klinghardt Mountains (Barbieri, 1968; Fowler, 1970; Pickford, 2015).

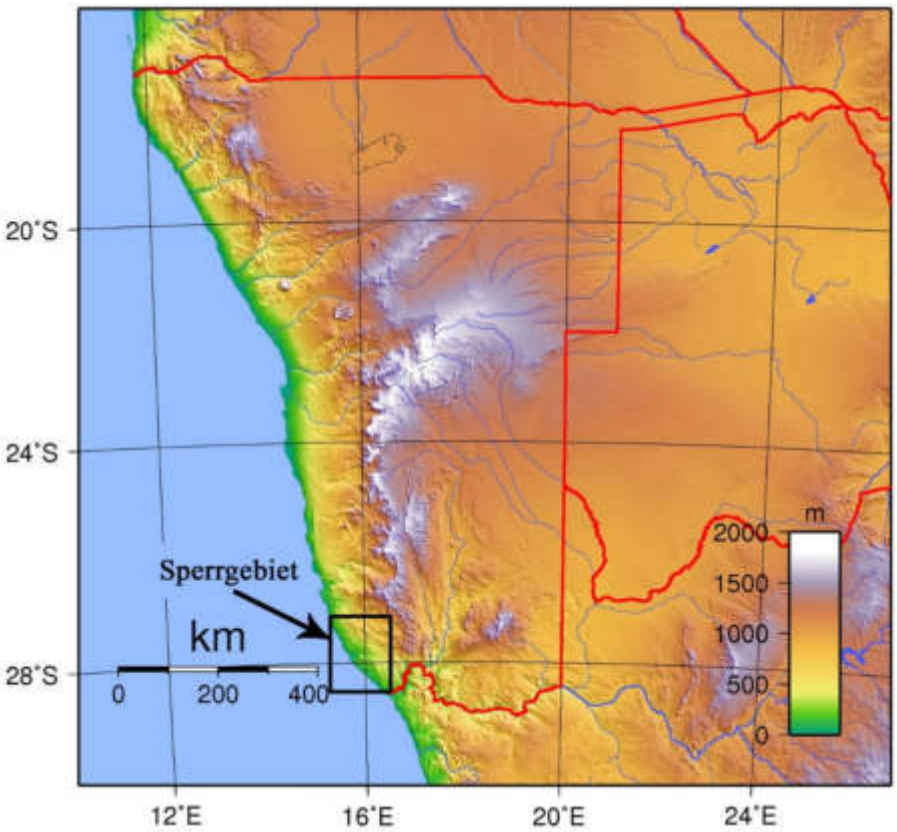

Figure 2. Relief map of Namibia showing the Sperrgebiet in the southwest, where the ferricretes occur.

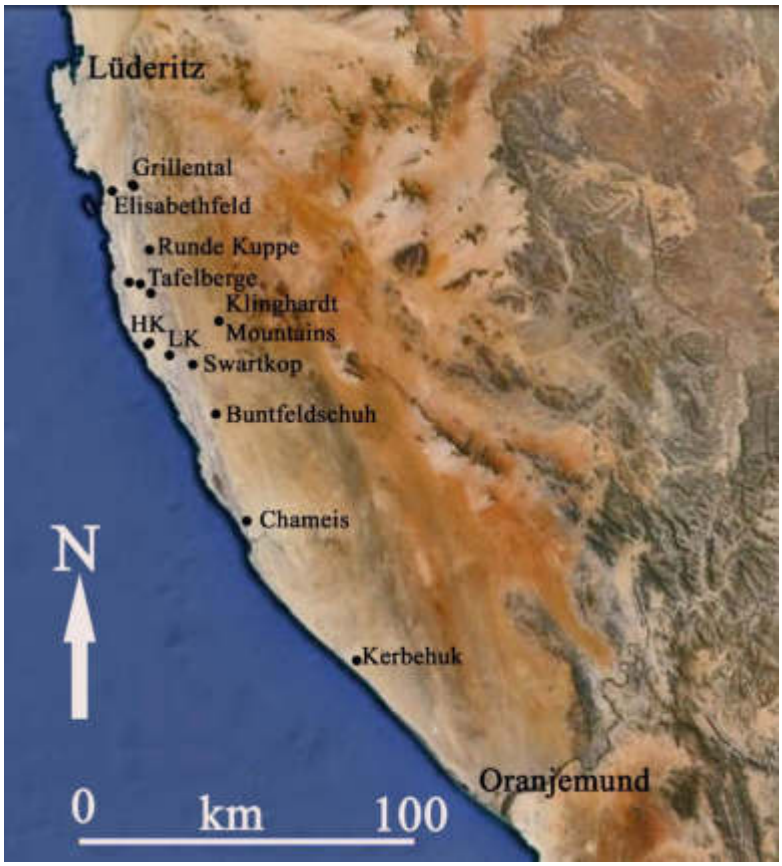

Figure 3. Distribution of ferricrete outcrops in the Sperrgebiet, Namibia (black dots). Map modified from Google Earth (HK - Hexen Kessel, LK - Lüderitz Krater).

Table 1. Ferruginised deposits of the Sperrgebiet studied for this report, arranged from north to south.

Locality	Latitude	Longitude	Altitude	Ferricrete facies
Grillental	26°58'19.7''S	15°19'29.3''E	71 m	Alluvial
Elisabethfeld	26°58'55.3''S	15°15'54.2''E	0 m	Alluvial
Runde Kuppe	27°09'24.3''S	15°20'52.4''E	147 m	Colluvial
Kaukausib Tafelberg	27°12'56.3''S	15°19'03.3''E	131 m	Colluvial
Tafelberg Sud	27°13'02.5''S	15°18'56.6''E	120 m	Colluvial
Katchen Plateau	27°14'03.9''S	15°19'25.6''E	118 m	Colluvial
Elfert's Tafelberg	27°15'00.9''S	15°19'11.1''E	94 m	Colluvial
Between Kätchen Plateau and Elfert's	27°14'34.4''S	15°19'16.0''E	88 m	Bog
East of Elfert's Tafelberg	27°14'43.3''S	15°19'45.1''E	97 m	Bog
North of Lüderitz Krater	27°17'39.9''S	15°21'41.8''E	76 m	Colluvial & Bog
Idatal	27°18'03.0''S	15°20'21.7''E	38 m	Colluvial & Bog
Hexen Kessel ferricrete	27°17'49.7 ''S	15°19'53.3''E	50 m	Bog
Idatal-Granitberg Road	27°22'02.4''S	15°21'58.2''E	38 m	Colluvial & Bog
Lüderitz Krater	27°17'58.8''S	15°21'42.2''E	77 m	Alluvial
Hill west of Blaubok Beacon	27°22'57.2''S	15°25'48.0''E	141 m	Alluvial
Langental *Turritella* Site	27°23'42.7''S	15°24'18.9''E	66 m	Colluvial
Between Wanderfeld IV & Langental Mammal	27°24'04.7''S	15°24'20.8''E	59 m	Bog
Swartkop North area	27°24'55.9''S	15°31'26.1''E	224 m	Colluvial
Swartkop South area	27°25'33.6''S	15°32'26.0''E	193 m	Colluvial
Kakaoberg	27°35'27.8''S	15°34'22.2''E	200 m	Colluvial & Bog
Buntfeldschuh Escarpment 1	27°33'32.6''S	15°34'29.8''E	149 m	Colluvial
Buntfeldschuh Escarpment 2	27°33'39.1''S	15°34'37.3''E	151 m	Colluvial
North of Chalcedon Tafelberg	27°15'51.8''S	15°22'47.9''E	166m	Colluvial & Bohnerz
Klinghardt Ferruginised Conglomerate	27°18'49.4''S	15°36'41.3''E	401 m	Alluvial
Buntfeldschuh upper slopes at north end	27°33'45.4''S	15°34'53.8''E	219 m	Colluvial & Bohnerz
Chameis Road Borrow Pit	27°51'05.0''S	15°40'09.0''E	48 m	Alluvial
Kerbehuk	28°13'43.1''S	15°59'56.4''E	89 m	Alluvial
Kerbehuk Valley	28°12'30.8''S	16°01'52.0''E	117 m	Colluvial & Alluvial

Grillental and Elisabethfeld

Ferruginised sediments occur at Elisabethfeld and Grillental in the Northern Sperrgebiet. At the former site, sand and grit has been ferruginised in patches. Some rhizoliths, gastropods and mammal bones have also been partly ferruginised. At Grillental VI, ferruginisation has affected the basal clays/silts and their contained fossils, producing irregular goethitic nodules, plate-like concretions and goethitic gastropods. The overlying coarse grits are extensively ferruginised in layers and patches. Because both Elisabethfeld and Grillental VI have yielded early Miocene faunal assemblages (Stromer, 1926; Corbett, 1989; Pickford & Senut, 1999) it is inferred that the ferruginising processes were active until this period, and perhaps for some time afterwards.

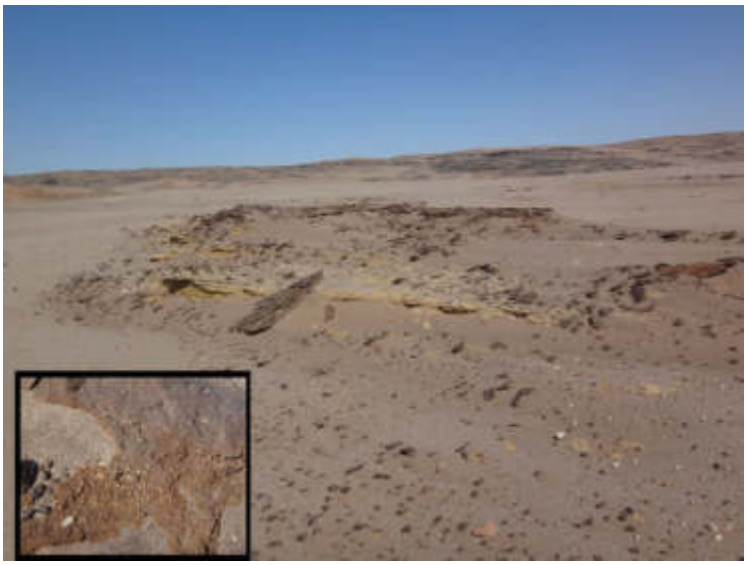

Figure 4. Ferricrete cementing coarse grit at Grillental VI, overlying green-yellow silts rich in the remains of Early Miocene mammals, termite hives and terrestrial gastropods indicative of a sub-humid palaeoclimate (between 250 and 750 mm mean annual rainfall). Inset shows detail of the surface of the outcrop.

Runde Kuppe

Liddle (1971) mentioned « *ferrugination* (sic) *of the Late Cretaceous erosion surface …. short distance to the north and west* (of Runde Kuppe) ». The Runde Kuppe ferruginised quartz lag directly overlies Bo Alterite and has no cover, but its distribution in the floors and up the sides of the valleys in which it occurs indicate that it has a similar geomorphological history to other outcrops further south in the region between Chalcedon Tafelberg and Lüderitz Krater. These outcrops stand proud in the valleys, indicting that three to four metres of downwasting of the surroundings has occurred since their formation.

Kaukausib Tafelberg and Tafelberg Sud

Liddle (1971) reported that « *Ferruginous beds only occur below the Pomona Quartzite on Tafelberg Sud and Kaukausib Tafelberg* » (i.e. Middle Cretaceous in Liddle's 1971 correlation) whilst at the Kätchen Plateau and the north-western corner of Elfert's Tafelberg he reported similar « *ferruginous sands and quartz breccias* » overlying the « *Late Cretaceous Erosion Surface* ». This interpretation implies at least two phases of ferruginisation widely separated in time.

Examination of the occurrences reveals that at Tafelberg Sud, the ferruginised deposits contain derived blocks of Kätchen Plateau Quartzite and that they are not only banked against the hillside but also occur as a thin layer on top of the quartzite at the summit of the hill. Thus ferruginisation occurred long enough after the silicification of the quartzite for it to be eroded into blocks and for at least several metres of relief to be developed around the residual Tafelberg before the ferruginising process started. At the nearby Kaukausib Tafelberg, the same situation occurs, with the ferruginised deposits banked up against the quartzites and the underlying basement rock. The demonstration that the ferruginised deposits at these two hills are younger than the quartzite effectively erodes support for the existence of sub-quartzite ferruginised horizons (i.e. Middle Cretaceous in the correlation scheme of Liddle, 1971, and Stocken, 1978).

Figure 5. Outcrop of ferruginised conglomerate at Tafelberg Sud (red arrows show some of the iron oxide cement) containing derived blocks of Tafelberg Quartzite (yellow arrows). This outcrop was previously mapped as underlying the quartzite (Liddle, 1971).

Figure 6. Kaukausib Tafelberg viewed from Tafelberg Sud. Red arrow shows the outcrop of ferricrete on the top of the Kätchen Plateau Quartzite. The inset shows a close-up view of a veneer of ferricrete cementing sand that accumulated in shallow depressions in the surface of the quartzite. Similar ferricrete is banked up against the cliffs of quartzite.

Kätchen Plateau

Pickford (2015) already illustrated some ferricrete at Kätchen Plateau. Further outcrops amplify the conclusions, including an occurrence on the northern face of the tafelberg where blocks of Kätchen Plateau Quartzite are observed caught up in intensely ferruginised lag overlying alterite with a sharp contact.

Figure 7. Ferricrete outcrop on the northern flank of Kätchen Plateau containing large and small blocks of Katchën Plateau Quartzite and various other rock types, predominantly milky quartz, cemented by ferricrete, unconformably overlying Bo Alterite (contorted, laminated pink and white rock exposed under the ironstone overhang). Above the ferricrete is a gravel lag cemented by the Namib I Calc-crust.

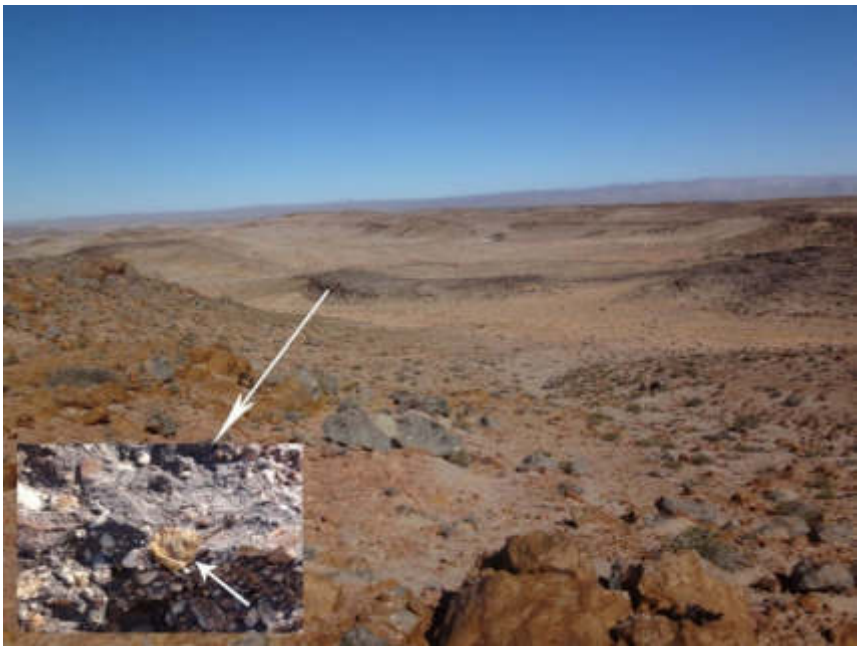

Figure 8. Ferruginised alluvial infilling of a palaeovalley descending ca 20 metres below Kätchen Plateau towards the southeast, now standing 5-10 metres proud of the surrounding countryside. The white arrow in the inset shows a slightly rounded cobble of Kätchen Plateau Quartzite caught up in the ferricrete along with abundant angular milky quartz clasts.

Hexen Kessel and Idatal

At Hexen Kessel and Idatal, there are several impressive outcrops of ferricrete which overlie Bo Alterite, and which are overlain in places by fossiliferous Pliocene onyx and grey sand. This stratigraphic relationship indicates that Du Toit's (1954, cited in Hallam, 1964) estimate of a Pleistocene age for the ferricrete is not tenable, at least for these outcrops.

Figure 9. Two-metre thick bog ferricrete outcrop overlying Bo Alterite at the southern end of Hexen Kessel, not far from Idatal.

The outcrops of ferricrete at Hexen Kessel are up to two metres thick, but they are generally areally too small to figure on the maps by Kaiser & Beetz (1926). The distribution of the ferricrete patches indicates that the deposit possibly covered much of the Idatal – Hexen Kessel depression but that, during the Miocene and Pliocene, erosion removed much of it.

In Hexen Kessel, it can be inferred that the ferricrete is older than the onyx (travertine) and grey indurated sand (« esi » in the map legend of Kaiser & Beetz, 1926). Examination of these outcrops led to the discovery of fossils at two localities, one a mass of tubes attributed to *Phragmites* or a similar plant, in orange sandy marl, the other scattered shells of *Patella* in indurated grey sand.

The supposed *Phragmites* tubes are significant on account of the fact that many of the individuals are *in situ* in their growth positions, but some have broken and lie at various angles. Some tubes penetrate the alterite underlying the sand. The insides of many of the tubes are generally smooth, with no sign of infillings or patterns on the walls but some of them show patterns compatible with the nodes and leaf bases of *Phragmites*. The deposits are probably Pliocene, like similar deposits at Elisabethfeld/Grillental, Gamachab and Klinghartfelder 24, opposite Buntfeldschuh. These deposits top out locally at about 40-50 metres above sea level (estimated from Google Earth imagery).

The presence of shells of *Patella* in the grey sand at Hexen Kessel support the interpretation that these deposits accumulated close to the sea. Such shells are unlikely to have been carried in by ancient humans, or brought in by birds. Small outcrops of indurated grey sand occur sporadically in the floor of the valley west of the onyx ridge downwards to ca 25 masl, indicating that the valley had already been eroded by the Pliocene.

Figure 10. Sandy marl at Hexen Kessel containing abundant *in situ* calcified tubes (probably *Phragmites*). The roots of some of the tubes penetrate the underlying alterite exposed in the undercut (in shadow).

The outcrops indicate that Idatal and environs were inundated by the sea sometime during the Pliocene. It is likely that these deposits accumulated at the same time as the marine terraces at an altitude of ca 50 metres preserved sporadially along the coast north of Lüderitz as far as Meob where the terraces were carved into aeolianite and are covered in vast concentrations of marine shells.

Figure 11. Shells of *Patella* in calcified grey sand intercalated in onyx travertine at Hexen Kessel at an altitude of ca 30 masl. Further north correlative sandstones occur up to 50 metres above sea-level.

North of Chalcedon Tafelberg

Pickford (2015) described some pisolithic iron nodules in an exposure 1 km north of Chalcedon Tafelberg. At the time it was thought that this bohnerz was formed prior to the Sperrgebiet Silicification Event, but it is now considered more likely that this bean ore formed during the same phase of ferricrete genesis as the rest of the ferruginised deposits in the region. The bohnerz at this locality is similar to an occurrence on the upper slopes of the northern end of the Buntfeldschuh Escarpment.

Valleys North of Lüderitz Krater

In the broad north-south valleys between Lüderitz Krater and Scheibergeysir there are several impressive outcrops of ferruginised sands and quartz lags. These deposits mould the ancient profiles of the valleys, being low in the valley floors and draping upwards onto the sides of the valleys above and as such conform to the definition of ferricrete lining hillslopes. The valleys existed more or less in their present form prior to ferruginisation, but have been downwasted by several metres since the ferruginising processes were active.

Figure 12. Outcrops of ferricrete are common in the valleys between Lüderitz Krater and Chalcedon Tafelberg as well as in Idatal, Hexen Kessel and other valleys in the Trough Namib. Many of the outcrops now stand proud of their surroundings due to downwasting of the surrounding rock.

Lüderitz Krater

Lüderitz Krater, despite its name, is not a volcanic structure, but is a saucer-shaped remnant of Kätchen Plateau Quartzite (Pickford, 2015). The infilling of the saucer is comprised of agate-rich beach deposits, some of which have been ferruginised by alluvial ferricrete.

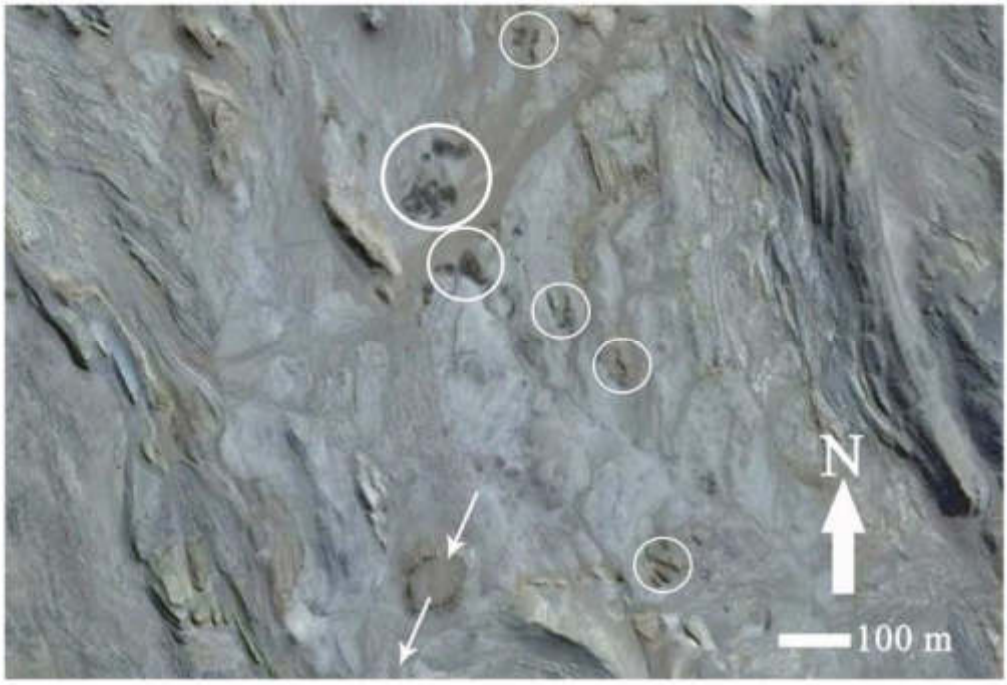

Figure 13. Ferricrete outcrops in the valleys north of Lüderitz Krater (white circles). Lüderitz Krater itself is shown by the white arrows (map modified from Google Earth).

Figure 14. Alluvial ferricrete from Lüderitz Krater containing well-rounded agates and quartz clasts up to 3 cm in diameter. The ferricrete at this locality is younger than the Kätchen Plateau Quartzite which forms the saucer-shaped outcrop at Lüderitz Krater.

Goethite Ring

In the sandy marl derived from altered bedrock (alterite) north of Steffenkop, there is a circular outcrop of intensively ferruginised sand (goethite cement) up to 20 cm thick forming a circle of 30 metres diameter overlying marl and alterite. A few metres to the west of the circle there is a ridge of Blaubok Conglomerate overlying altered basement rock, indicating that at this locality ferruginisation preceded the deposition of the conglomerate.

Figure 15. Circular outcrop of ferricrete cementing sandy marl at Goethite Ring. The diameter of the circle is ca 30 metres. Note the bedrock ridge covered in Blaubok Conglomerate in the background.

Blaubok Area

In the type area of the Blaubok Conglomerate, a layer of intensively ferruginised marl and quartz lag containing large rounded cobbles of Nama Quartzite (Proterozoic) and other rock types typical of the Blaubok Conglomerate overlies altered basement rocks (Stocken, 1978). This outcrop is at the top of the hill 1 km west of the

Blaubok Beacon and it is clear that at this locale, the basal part of the Blaubok Conglomerate is older than the ferruginisation because cobbles of Nama Quartzite are enclosed in gravel-rich goethite. At other localities, however, layers of reworked cobbles of Blaubok clasts repose unconformably on ferruginised layers, and are thus younger than the iron impregnations. It is evident that most of the deposits hitherto included in the Blaubok Conglomerate have been redeposited since their first arrival in the area. This is the case at Langental Mammal site where a channel infilling comprised of typical Blaubok clasts overlies fossiliferous marls of Early Miocene age (Stromer, 1926). The same can be said of the Wanderfeld IV *Turritella* site, where ferruginised fossiliferous limestones of Late Eocene age (Siesser, 1977) are unconformably overlain by Blaubok Conglomerate (Corbett, 1989).

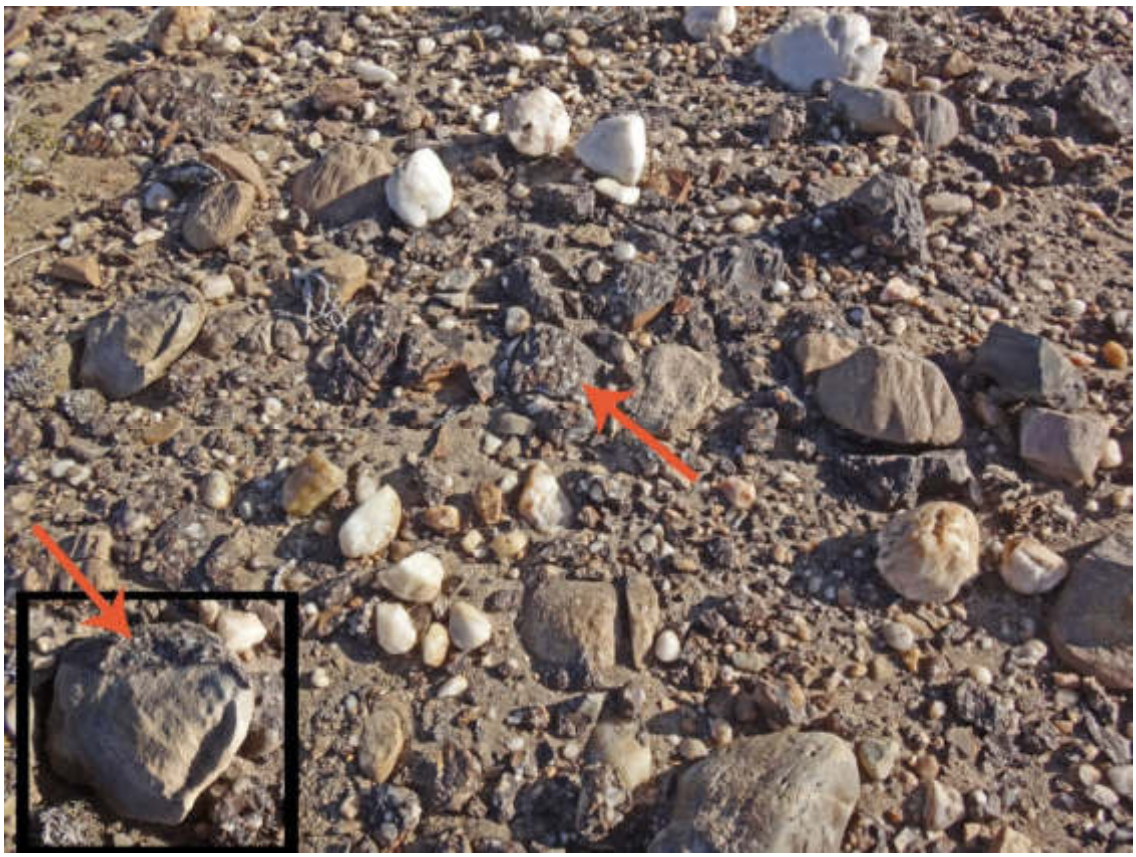

Figure 16. Ferricrete (brown arrows) at the summit of the hill west of Blaubok Beacon, cementing polymict lag deposit and large cobbles of Nama Quartzite (Proterozoic) and typical of the Blaubok Conglomerate. The inset shows a 10 cm cobble of Nama Quartzite coated on one side by ferricrete containing fine gravel lag.

Wanderfeld IV *Turritella* Site and Cretaceous occurrence

On the ridge between the Wanderfeld IV *Turritella* site and the Langental Mammal site, there is an outcrop of ferruginised gravel and marl overlying weathered bedrock (alterite). Although the area has been heavily disturbed by mining, some of the ferruginised deposits are *in situ* and underlie the numerous cobbles attributed by previous authors to the Blaubok Conglomerate (Stocken, 1978) but evidently in its redeposited manifestation. 50 metres south of the Cretaceous occurrence at Wanderfeld IV, there are fissures in alterite (weathered dolomite) infilled with quartz lag which has been intensively ferruginised.

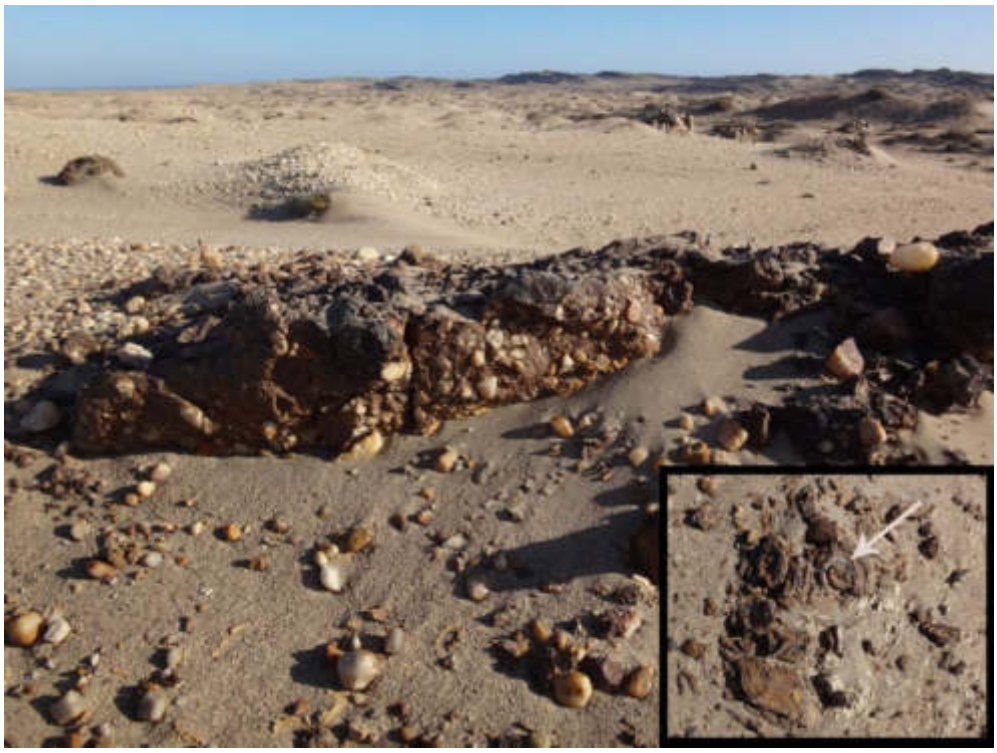

Figure 17. Ferricrete at Wanderfeld IV, near Bogenfels, Namibia, cementing a quartz lag deposit with well-rounded and angular clasts. The main image shows ferricrete containing abundant quartz pebbles overlying marl (alterite) near the Cretaceous occurrence. Note the abundant trommel screen heaps in the upper third of the image, residues of diamond mining activity during the 1919-1920 operations. The inset depicts ferruginised Late Eocene limestone at the Langental *Turritella* site (the white arrow points to a lamellibranch in the ferruginised limestone).

Swartkop

Barbieri (1968) reported that a thin layer of ferricrete was widely distributed « *almost everywhere* » in the surroundings of Swartkop, but occurred as small patches usually overlying marl (i.e. alterite) which forms a « *capping on the End Cretaceous surface, although relatively younger than the silcrete* ». Despite the existence of reasonably clear exposures, none of this ferricrete has been observed to underlie the phonolite lava or tuff at Swartkop : as elsewhere in the Sperrgebiet, it is a superficial manifestation of ferruginised deposits banked up against pre-existing relief. It was evidently emplaced long after the phonolites had been erupted and after the two Swartkop hills had had time to be eroded more or less into their present day appearance. Barbieri's (1968) observation that the ferruginisation occurred later than the silicification is correct.

Northern End of the Buntfeldschuh Escarpment

Kaiser & Beetz (1926) mapped two prominent black hillocks in the northern end of the Buntfeldschuh Escarpment as « Braun-eisenquarzit der Pomonaschichten » (« bqf » at 27°33'32.6''S : 15°34'29.8''E : 149 masl and 27°33'39.1''S : 15°34'37.3''E : 151 masl). Hallam (1964) wrote that the Buntfeldschuh Escarpment « *has a capping of calcrete though this changes to ferricrete at the south end of Kakaoberg* ». In fact the calc-crust that caps the northern parts of the escarpment extends onto the upper surface of Kakaoberg where it occurs as small mesas of Namib 1 Calc-crust containing reworked fragments of ferricrete (Kaiser & Beetz, 1926 ; Corbett, 1989) and it is thus considerably younger than the ferricrete. Liddle (1970b) noted that the two black hillocks at Buntfeldschuh are « *identical in appearance to those found on the Kätchen Plateau in the Pomona Area* ». In agreement

with Corbett (1989), Miller (2008) wrote that « *the lower marine unit rests on an uneven basement and overlies a remnant of the Pomona Beds and their capping of Kätchen Plateau Silcrete Formation at the northern end of the Buntfeldschuh Escarpment* ». There are serious problems with such an interpretation.

Examination of these two hills reveals that they are not silicified but are heavily ferruginised quartz-rich gravel lags (i.e. colluvial ferricrete). Genetically they are the lateral equivalent of the vast ferruginised mass at Kakaoberg three km to the south, the only difference being that, in the north the host-rock comprises quartz-rich gravel lag overlying alterite, while in the south it comprises aeolian sand overlying deltaic-marine deposits.

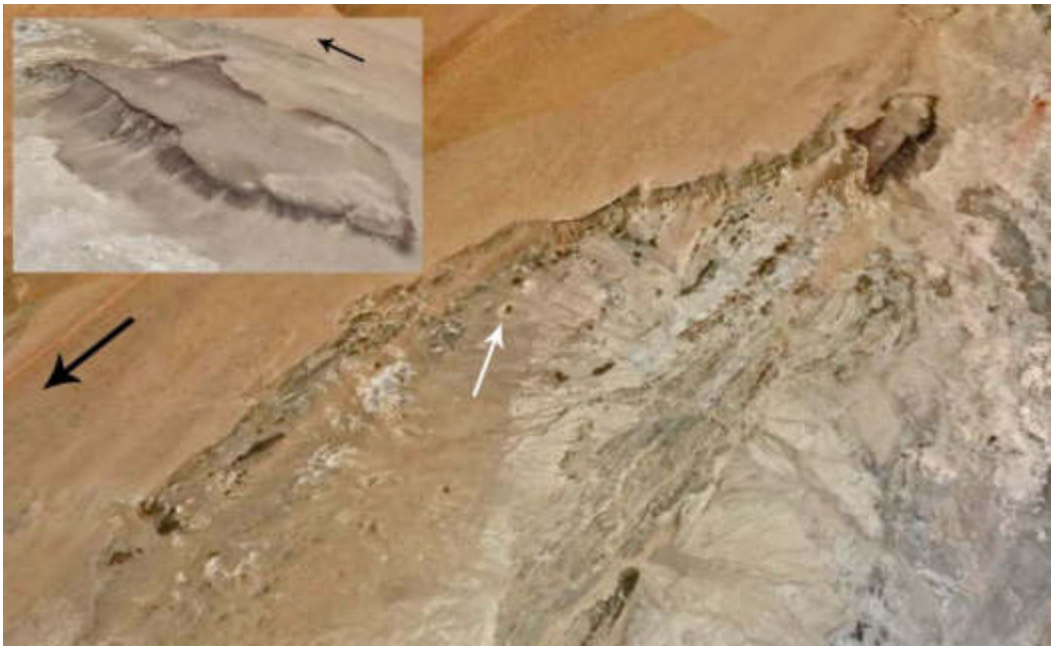

Figure 18. Oblique view from the northwest of Buntfeldschuh and Kakaoberg and (inset) of Kakaoberg from the southwest. Note the Namib I Calc-crust forming the upper rim of the Buntfeldschuh Escarpment and a discontinuous cover on top of the ferricrete at Kakaoberg. Black arrows point approximately North. The dark patches in the north of the Buntfeldschuh Escarpment (opposite the large black arrow) are ferricrete overlying Bo Alterite. The white arrow points to the ferricrete knolls illustrated in Figures 19 and 22. In the south at Kakaoberg the ferricrete overlies deltaic-marine sediments overlying Bo Alterite. The small red patch with a downwind tail at the top right of the image is a borrow pit excavated into Bo Alterite. The Buntfeldschuh Escarpment is ca 5 km long and 120 metres high. Kakaoberg is 1.5 km from north to south (images modified from Google Earth).

Study of the area surrounding the northern ferricrete hillocks in the Buntfeldschuh Escarpment reveals that the ferruginised deposits drape upwards almost to the level of the Namib I Calc-crust which forms the skyline at the top of the Buntfeldschuh Escarpment. At some of the higher outcrops, ferruginisation has reached the stage of producing « murram » nodules (i.e. pisoliths of goethite (bohnerz in German = pisolithic iron ore)). Thus the ferruginised deposits in the northern part of the Buntfeldchuh exposures are younger than the deltaic-marine levels, and not older than them. They underlie the Namib 1 Calc-crust. Since these layers were ferruginised there has been about 10-15 metres of downwasting of the floor of the Buntfeldschuh depression. In this area the situation recalls that in Idatal and several of the other valleys in the region between Chalcedon Tafelberg and Lüderitz Krater, in which the ferruginised layers mould the ancient profiles of the valleys, being low in the floors of the valleys and draping upwards along their sides. These outcrops indicate that the Buntfeldschuh Escarpment was formed at the latest by Late Oligocene times, with about 10-15 metres of downwasting since the formation of the ferricrete.

Figure 19. Quartz-rich ferricrete in the northern end of the Buntfeldschuh Escarpment. The sloping, poorly bedded layers record the original dip, indicating that the sediments accumulated as a veneer of lag deposits sub-parallel to the ancient hillslope prior to being cemented. Note the massif of Kakaoberg in the background, 3 km to the south.

Figure 20. Ferricrete (between the pink arrows) in the northern part of the Buntfeldschuh Escarpment slopes upwards towards the base of the Namib Calc-crust (white arrows) which forms the skyline.

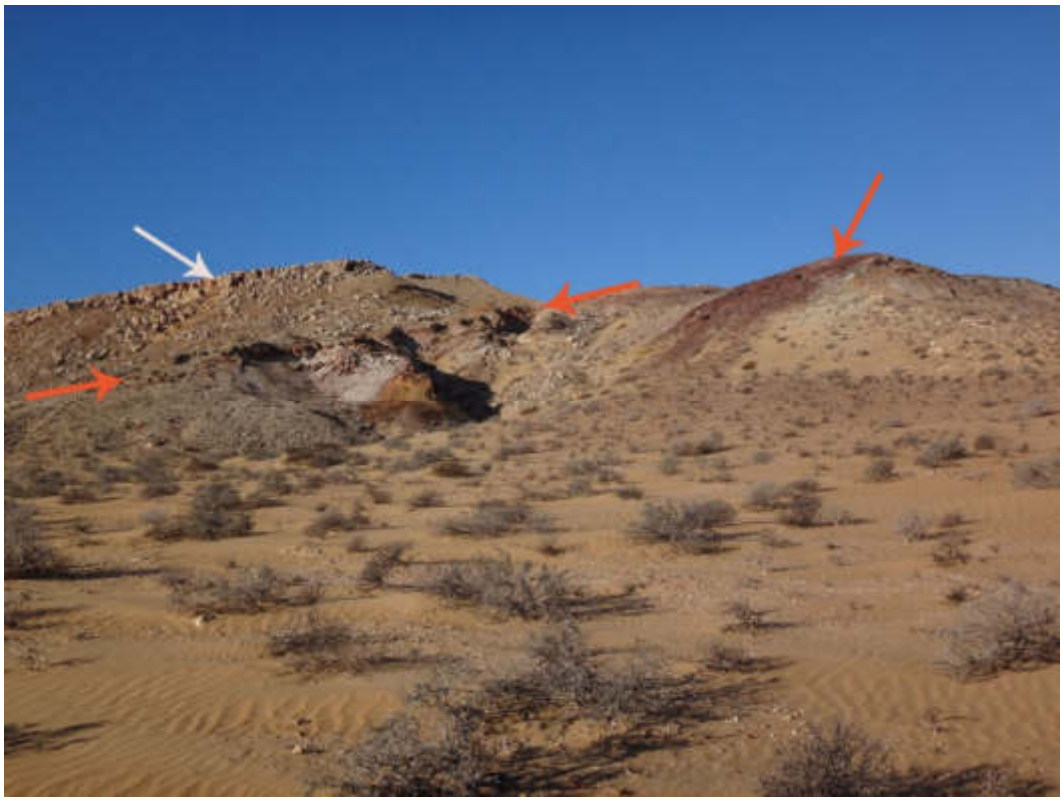

Figure 21. Ferricrete (pink arrows) overlying a sloping surface of weathered bedrock (Bo Alterite on relatively fresh Gariep Dolomite) in the northern end of the Buntfeldschuh Escarpment. The Namib 1 Calc-crust (white arrow) forms the skyline.

Figure 22. Two remnants of ferricrete in the northern part of the Buntfeldschuh Escarpment viewed from the escarpment edge indicate that up to 15 metres of downwasting has occurred since the ferricrete was formed. Vehicle (circled) provides a scale. Atlantic Ocean in the background.

Figure 23. Bohnerz (pisolithic iron ore) and ferruginised aeolian sand occurs on the higher slopes at the northern end of the Buntfeldschuh Escarpment.

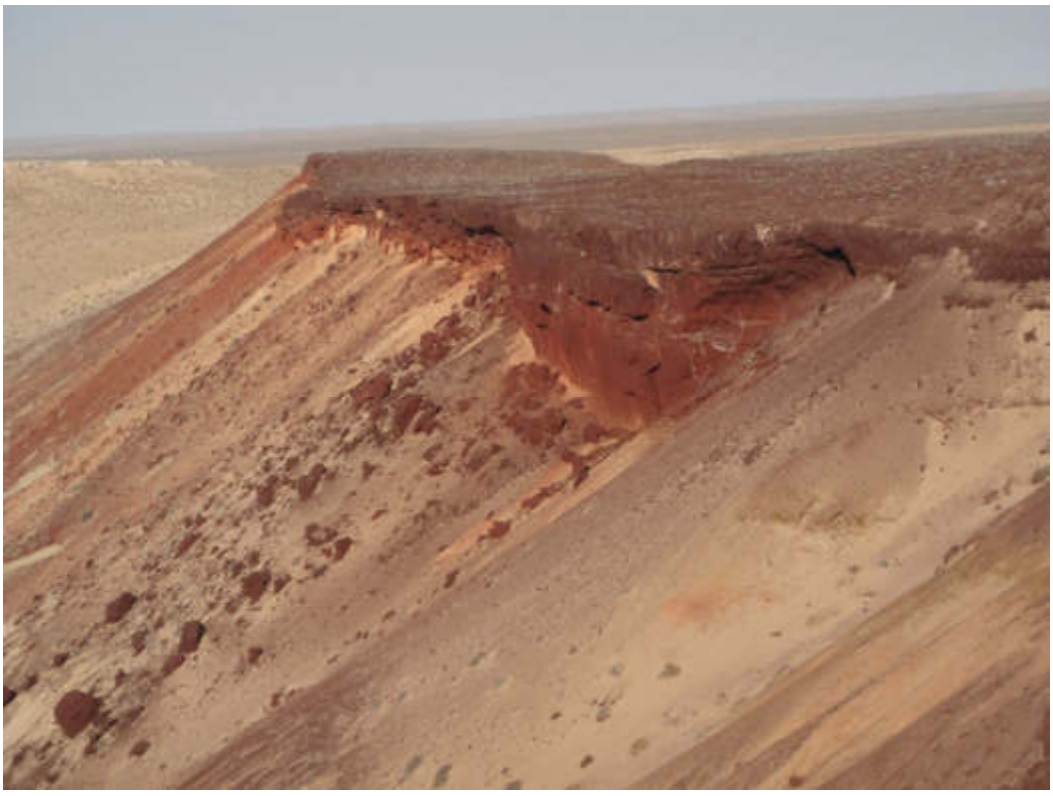

Figure 24. The eastern edge of Kakaoberg looking southwards, exposing the thickest occurrence of ferricrete (up to 20 metres) which has pervasively cemented Terrestre Sandstone overlying deltaic-marine deposits. Note the Namib 1 Calc-crust capping the hill in the left distance.

Figure 25. The ferricrete at Buntfeldschuh is overlain by the Middle Miocene Namib 1 Calc-crust, well exposed at the southern end of Kakaoberg, but also as outliers near its top, as shown in the inset (telegraph pole for scale).

Chameis

A borrow pit northeast of the Chameis-Baker's Bay road (27°51'05''S : 15°40'09''E : 48 masl), shows a thick succession of fluvial and terrestrial gravels and breccias which have been ferruginised, weakly in some patches but intensely in others. The sediments overlie altered basement. This occurrence is deduced to be older than the Namib I Calc-crust which crops out in a large, slightly saucer-shaped plateau to the north-northwest of the quarry at 27°49'08''S : 15°39'44''E : 94 masl).

Kerbehuk

Haughton (1932) described the cover of the basement series at Kerbe Hock (sic) as consisting of «*Pomona Quartzites, which in places are highly ferruginous – formed of two or three prominent bands of quartzite separated by sandy clays. This cover dips at a slight angle seawards*». Stocken (1978) inverted the diagenetic sequence in writing that «*at Kerbehuk a somewhat different exposure in the form of a silicified ferricrete is recognised as belonging to the same formation*», an interpretation accepted by Miller (2008). Stocken (1978) considered that the Kerbehuk deposits accumulated in an ancient pan on the Late Cretaceous land surface. The occurrence of these rocks offshore has been used as an indicator of the presence of the footwall of the Sperrgebiet diamond placers.

Examination of the ferruginous deposits at Kerbehuk reveals that they are not quartzites, but are ferruginised gravel lag and channel fills, often with coarse cross-bedding. In places the ferruginisation is moderate, but at some outcrops it is intensive. The quartz cobbles and pebbles in these deposits are predominantly angular although there are some well-rounded clasts. Far from resembling the «Pomona Quartzites», these deposits recall the ferruginised rubble found north of Chameis, in the north of the Buntfeldschuh Depression and widely over the region north of Bogenfels (i.e. they are colluvial and alluvial ferricretes). We here correlate them to the same ferruginising phase as the ferricretes in the north, and if this is correct, then the Kerbehuk outcrops are likely to be of Late Oligocene to Early Miocene age, and thus to post-date the footwall of the diamond placers.

Figure 26. Ferricrete at Kerbehuk, Namibia (inset shows details of the quartz-rich lag which has been pervasively ferruginised).

Figure 27. Layers and lenses of ferruginised mostly angular gravel with weakly expressed bedding fills ancient channels, now exposed along the southern flanks of the Kerbehuk Valley. These ferricretes overlie alterite with sharp discordance (under the overhang).

The Age of the Sperrgebiet Ferruginised Deposits

A Late Cretaceous label got attached to the ferruginised deposits of the Sperrgebiet on the scantiest of evidence. In the area of Kätchen Plateau and Elfert's Tafelberg such rocks were first described by Kaiser & Beetz (1926) as being below the Pomona Quartzite which they correlated to the Prämitteleocän. However, even though the ferruginised deposits at both these localities are topographically lower than the quartzites, they are not stratigraphically beneath them. Undoubtedly influenced by Merenksy's (1909) (erroneous) claim for the presence of Cretaceous marine fossils in the Northern Sperrgebiet, and Haughton's (1930a, 1930b) descriptions of a Cretaceous ammonite from Wanderfeld IV, Sullivan & Clarke (1962) followed by Hallam (1964) thought that the Pomona Quartzites represent « *residuals of the End-Cretaceous geomorphological surface* ». In the same line of logic, Sullivan & Clarke (1962) and Liddle (1971) correlated the surface beneath the Pomona Quartzite and the ferruginised lag (erroneously) thought to lie beneath the quartzite at Tafelberg Sud to the Middle Cretaceous, and the ferruginised deposits around Kätchen Plateau to the Late Cretaceous, but without providing any substantiating evidence. Kalbskopf (1976) wrote that the « *silicified freshwater limestone* (at Chalcedon Tafelberg) *represents the Late Cretaceous land surface* ». Stocken (1978) modified Liddle's (1971) stratigraphy by insisting on the supposed presence of two erosion surfaces of Cretaceous age, one Middle Cretaceous beneath what he called the Pomona Beds, the other Late Cretaceous truncating the Pomona Beds upon which the Tafelberg Quartzite was supposedly deposited. By these dubious means, with frequent repetition, the ferruginised deposits in the Sperrgebiet became correlated to the Cretaceous.

However, in several places in the Sperrgebiet, ferricrete deposits are underlain and overlain by strata which can be dated on the basis of their fossil content, and these occurrences bracket the ferruginisation phase within confidently constrained geochronological contexts. Near Wanderfeld IV, the Langental *Turritella* site, marls and grits derived from the marls contain redeposited Priabonian marine fossils (gastropods, bivalves, sharks) (Böhm, 1926; Siesser, 1977; Siesser & Salmon, 1979). Some of these redeposited layers have been ferruginised, and are overlain by Blaubok Conglomerate (not underlain by Blaubok Conglomerate as thought by Haughton, 1930a and Kalbskopf, 1976). At Kakaoberg, aeolian sands overlying the Buntfeldschuh Formation (deltaic-marine sediments) containing shark teeth, have been pervasively ferruginised (Hallam, 1964), and are overlain by the Namib I Calc-Crust of Middle Miocene age (Pickford, 2015). At Elisabethfeld and Grillental, sands and grits overlying Early Miocene clays rich in mammalian fossils (Stromer, 1926; Pickford & Senut, 1999) have been ferruginised from which it is deduced that impregnation with iron oxides occurred during the Early Miocene or possibly as recently as the basal Middle Miocene.

From a geomorphological perspective, the determination of the Oligo-Miocene timing of ferruginisation is coherent. In many places in the Northern Sperrgebiet the ferruginised deposits mould the form of the ancient valleys in which they occur but are now generally standing slightly proud of the immediately neighbouring countryside due to subsequent downwasting of the surroundings. These valleys were probably incised during the Oligocene low sea-stand, a long period of incision and erosion (Pickford, 2015). This was the period during which the Pomona Tafelberge were eroded into more or less their present forms, with at least 20 metres of relief between the summits of the tafelberge and the adjacent valley floors, best seen east of Kätchen Plateau. Ferruginisation occurred at the end of this incision phase, possibly when sea-level rose during the Aquitanian-Burdigalian (Late Oligocene-Early Miocene) when the Sperrgebiet enjoyed a more humid climate (250-750 mm mean annual rainfall) than today's, as shown by the presence of fossilised hives of the harvester termite (*Hodotermes*) preserved at Grillental, Fiskus and Chameis. Subsequently, with a drop in sea-level and increased desertification, downwasting continued (driven largely by a combination of bioturbation which brought fine clastic material to the surface and aeolian activity which removed it, a process which is still active in the region), leaving the ferruginised masses « perched » a few metres above their surroundings (Fig. 22).

Figure 28. Aspects of redeposited clasts of Blaubok Conglomerate in its type area. A) Low ridge of conglomerate overlying ferricrete and alterite on the slope leading down towards Neue Anlage, 2-3 metres lower than *in situ* conglomerate (behind the photographer); B-D) insect activity brings fine sediment from the underlying alterite to the surface where it is blown away by the wind (red sediment shadows on the downwind side of the heaps). Such activity repeated many times leads to regional downwasting of the coarse fraction.

It is necessary to stress the fact that there is no evidence for the presence of two or more ferruginising events in the Sperrgebiet. Pickford (2015) mentioned the presence of bohnerz at the Bo Alterite outcrop north of Chalcedon Tafelberg (implying a pre-Eocene age for its formation), but the bohnerz at this locality looks similar to the deposit high on the side of the Buntfeldschuh Escarpment at its northern end, and it is likely to be a manifesation of the same ferruginising event which affected alterite and the overlying lag deposits in many other places in the Sperrgebiet. The only difference is the facies of the end product, ferruginised sands and quartz lags in most places, rarer bohnerz at Bo and Buntfeldschuh.

Palaeoclimatic implications of Sperrgebiet ferricretes

Ferricrete forms where mineral-charged water percolating through pervious rock reaches a zone of oxidation whereupon ferric iron oxide precipitates. The iron salts are generally transported into the zone of precipitation by ground water, and they precipitate preferentially near the land surface where there are relatively high levels of oxygen. The formation of ferricrete thus implies sufficient quantities of water percolating through superficial layers of the earth for the transport of the iron salts in solution. This in its turn implies a humid palaeoclimate. Under the present-day climatic regime of the Sperrgebiet, no ferricrete is being formed.

The fossil record reveals, however, that the Early Miocene palaeoclimate of the Sperrgebiet was more humid than it is today. Hives of the harvester termite are common at Grillental, Fiskus and Chameis (Fig. 29) and they indicate annual rainfall between 250 and 750 mm, and therefore sufficient for the genesis of ferricrete in favourable situations. Other indications of a more humid climate in the Sperrgebiet during the Early Miocene are the common presence of pipid frogs at Langental, Grillental and Elisabethfeld, as well as a rich and diverse mammalian and chelonian fauna which includes freshwater turtles (Pickford & Senut, 1999).

The fact that some of the Early Miocene deposits are ferruginised (Grillental, Elisabethfeld) supports the inference that this was the main period of humid palaeoclimate and of ferricrete genesis, the two phenomena being two sides of the same coin.

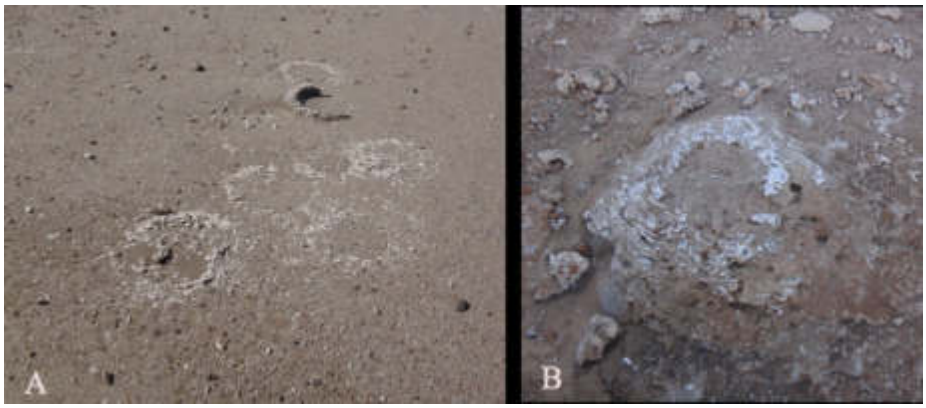

Figure 29. Early Miocene polycalate hives (*Namajenga mwichwa*) of the harvester termite (probably *Hodotermes*) from Grillental (A : a group of 8 hives) and Chameis (B : one of a pair of hives). The hives are 30-40 cm in diameter.

Conclusions

The main conclusion drawn from this study is that the presence of ferricrete or ferruginised sediments is not a reliable indicator of the presence of the footwall of the Sperrgebiet diamondiferous placers. This conclusion applies both to onshore and offshore deposits.

The second conclusion is that there was only a single phase of ferruginisation in the Sperrgebiet, and that it occurred sometime between the end of the Late Oligocene and the beginning of the Middle Miocene. It thus represents a reliable marker horizon applicable widely within the Sperrgebiet.

The ferricrete outcrops of the Sperrgebiet indicate the former presence of a relatively humid palaeoclimate in the region, an inference supported by the occurrence in Early Miocene sediments of fossilised hives of the polycalate termite *Hodotermes*. The present day distribution of this genus of termite suggests that the palaeoclimate would have been either within a summer rainfall zone or close to such a zone, with a mean annual rainfall between 250 and 750 mm (Pickford, 2008).

Acknowledgements

Authorisation to carry out palaeontological research in the country was provided by the National Monuments Council of Namibia (Mr Karipi). Thanks to the Geological Survey of Namibia and the French Embassy in Windhoek. Funding for the survey was provided by Namdeb, the French CNRS and the Muséum National d'Histoire Naturelle de Paris. Support from the Franco-Namibian Cultural Centre (M. Portes) and the Ore Reserves Department of Namdeb (J. Jacob) is greatly appreciated.

References

Barbieri, S., 1968. Sperrgebiet Geological Investigation Report, Swartkopp Mapping Report. *Unpublished Report, The Consolidated Diamond Mines of South West Africa, Ltd*, 6 pp.

Beetz, W., 1926. Die Tertiärablagerungen der Küstennamib. *In*: E. Kaiser (Ed.) *Die Diamantenwüste SüdwestAfrikas*, **2**, 1-54, D. Reimer, Berlin.

Böhm, J., 1926. Über Tertiäre Versteinerungen von den Bogenfelser Diamantefeldern. *In*: E. Kaiser (Ed.) *Die Diamantenwüste SüdwestAfrikas*, **2**, 55-87, D. Reimer, Berlin.

Corbett, I.B., 1989. *The Sedimentology of the Diamond Deflation Deposits within the Sperrgebiet, Namibia*. PhD Thesis, University of Cape Town, 430 pp.

Du Toit, A.L., 1954. *The Geology of South Africa*. (3rd Edition), Oliver & Boyd, London, 611 pp.

Fowler, J.A., 1970. Report on the mapping of the Klinghardt Mountains. *The Consolid-*

ated Diamond Mines of South West Africa, Limited. Sperrgebiet Geological Investigation. Unpublished Report, 24 pp.

Fowler, J.A., & Liddle, R.S., 1970. Sperrgebiet Prospect. Klinghardt Mountains, Unpublished Geological Map, 1 : 36,000. *Consolidated Diamond Mines of South West Africa (Pty) Ltd*.

Gradstein, F., Ogg, J., & Smith, A., (Eds) 2004. *A Geological Time Scale 2004*. New York, Cambridge (UK), Cambridge University Press, 589 pp.

Hallam, C.D., 1964. The Geology of the coastal diamond deposits of southern Africa. *In*: S.H. Haughton (Ed.) The Geology of Some Ore Deposits of Southern Africa. *Geological Society of South Africa*, **2**, 671-728.

Haughton, S.H., 1930a. Note on the occurrence of Upper Cretaceous marine beds in South West Africa. *Transactions of the Geological Society of South Africa*, **33**, 61-63.

Haughton, S.H., 1930b. On the occurrence of Upper Cretaceous marine fossils near Bogenfels, S.W. Africa. *Transactions of the Royal Society of South Africa*, **18**, 361-365.

Haughton, S.H., 1932. The Late Tertiary and Recent Deposits of the West Coast of Africa. *Transactions of the Geological Society of South Africa*, **34**, 19-57.

Kalbskopf, S., 1976. Sperrgebiet Geological Investigation, Progress Report, March, 1976. *Unpublished Report, Consolidated Diamond Mines of South West Africa (Pty) Ltd*. 3 pp.

Kaiser, E., 1926. *Die Diamantenwüste SüdwestAfrikas*. D. Reimer, Berlin, Vol. 2, 535 pp.

Kaiser, E., & Beetz, W. 1926. Geological Maps *In*: E. Kaiser (Ed.) *Die Diamantenwüste SüdwestAfrikas.* Reimer, Berlin, **2**, p. 158.

King, L.C., 1949. On the ages of African land surfaces. *Quarterly Journal of the Geological Society of London*, **104**, 438-459.

Klinger, H., 1977. Cretaceous deposits near Bogenfels, South West Africa. *Annals of the South African Museum*, **73**, 81-92.

Liddle, R.S., 1970a. Sperrgebiet Investigation Report, Progress Report for September, 1970. *Unpublished Report, Consolidated Diamond Mines of South West Africa (Pty) Ltd*. 3 pp.

Liddle, R.S., 1970b. Sperrgebiet Investigation Report, Progress Report for October, 1970. *Unpublished Report, Consolidated Diamond Mines of South West Africa (Pty) Ltd*. 3 pp.

Liddle, R.S., 1970c. Sperrgebiet Investigation Report, Progress Report for November, 1970. *Unpublished Report, Consolidated Diamond Mines of South West Africa (Pty) Ltd*. 2 pp.

Liddle, R.S., 1971. The Cretaceous deposits of the North West Sperrgebiet. Sperrgebiet Geological Investigation, *Unpublished Report, Consolidated Diamond Mines of South West Africa (Pty) Ltd*, (Namdeb archives ref. 78127). 22 pp + 2 annexes of 10 pp.

Merensky, H., 1909. The Diamond deposits of Lüderitzland, German South-West Africa. *Transactions of the Geological Society of South Africa*, **12**, 13-23.

Miller, R. McG., 2008. Namib Group. *In*: *The Geology of Namibia, Volume 3, Palaeozoic to Cenozoic*, Chapter 25, pp. 1-66, Ministry of Mines and Energy, Geological Survey, Windhoek, Namibia.

Pickford, M., 2008. Arthropod bioconstructions from the Miocene of Namibia and their palaeoclimatic implications. *Memoir of the Geological Survey of Namibia*, **20**, 53-64.

Pickford, M., 2015. Cenozoic Geology of the Northern Sperrgebiet, Namibia, accenting the Palaeogene. *Communications of the Geological Survey of Namibia*, **16**, 10-104.

Pickford, M., & Senut, B., 1999. Geology and Palaeobiology of the Namib Desert, Southwestern Africa. *Memoir of the Geological Survey of Namibia*, **18**, 1-155.

Siesser, W.G., 1977. Upper Eocene age of the marine sediments at Bogenfels, South West Africa, based on nannofossils. *In*: Papers on Biostratigraphic Research. *Bulletin of the Geological Survey of South Africa*, **60**, 72-74.

Siesser, W.G., & Salmon, D., 1979. Eocene marine sediments in the Sperrgebiet, South-West Africa. *Annals of the South African Museum*, **79** (**2**), 9-34.

Stocken, C.G., 1978. A Review of the Late Mesozoic and Cenozoic Deposits of the Sperrgebiet, *Unpublished Report, Consolidated Diamond Mines of South West Africa (Pty) Ltd*, 1-33.

Stromer, E., 1926. Reste land- und süsswasserbewohnender Wirbeltiere aus den Diamantfeldern Deutsch-Südwestafrikas. *In*:

E. Kaiser (Ed.) *Die Diamantenwüste SüdwestAfrikas*, **2**, 107-153, D. Reimer, Berlin.

Sullivan, P., & Clarke, N., 1962. Progress Report for December. *The Consolidated Diamond Mines of South West Africa, Limited. Sperrgebiet Geological Investigation*. Unpublished Report.

Verplanck, P.L., Yager, D.B., Church, S.E., & Stanton, M.R., 2007. Ferricrete Classification, Morphology, Distribution, and Carbon-14 Age Constraints. *In*: Environmental Effects of Historic Mining, Animas River Watershed, Colorado. *US Geological Survey Professional Paper,* **1651**, 724-744.

Widdowson, M., 2003. Ferricrete. *In*: A.S. Goudie (Ed.), *Encyclopedia of Geomorphology*, London, Routledge, pp. 365-367.

The fossiliferous sands of Hexen Kessel, Sperrgebiet, Namibia

Martin Pickford and Brigitte Senut

Sorbonne Universités (CR2P, UMR 7207 du CNRS, Département Histoire de la Terre, Muséum National d'Histoire Naturelle et Université Pierre et Marie Curie) case postale 38, 57 rue Cuvier, 75005 Paris.
(e-mail: <pickford@mnhn.fr> : <bsenut@mnhn.fr>)

Abstract : The timing of the geological processes which led to the formation of the diamond placers of the Northern Sperrgebiet (sources, transport pathways, concentration mechanisms) has been a matter of discussion for more than a century, indeed, ever since the first diamonds were found there in 1908. German geologists realised early on that fossils provided crucial information concerning the timing of events, but they found only a handful of localities of Priabonian and Early Miocene age, which nevertheless provided secure chronological anchor points for interpreting the deposits in the Granitberg-Bogenfels sector and the Grillental-Elisabethfeld area. However, there was no time control for the immensely rich diamond placers of the Pomona-Idatal zone, and as a result most scenarios concerning their genesis and enrichment derived their timing from neighbouring areas, notably the succession at Bogenfels. In the end, most hypotheses, starting with the researches of Kaiser (1926) were anchored to a supposed Eocene input of diamonds, followed by the action of aeolian deflation and fluvial reworking.

During the 2015 field survey of the Namibia Palaeontology Expedition, fossils were found at Hexen Kessel, not far from Idatal, in light brown marly sand and grey sand associated with onyx travertine. Marine fossils *in situ* in the grey sand are most likely to be of Pliocene age, correlating to the 50-metre marine package mapped elsewhere along the Atlantic coast, notably in Namaqualand, South Africa. This evidence indicates that the Idatal – Hexen Kessel area was inundated by the sea during the Pliocene, in which case there was likely to have been an input of diamonds into the basin, adding to those that were introduced during the Eocene and possibly at other times. This discovery impacts on hypotheses concerning the timing of, and the processes leading to, the genesis of the diamond placers, not only of the Pomona area, but also of other occurrences dispersed along the Atlantic coastal strip of Namibia and South Africa.

Key Words : Pliocene, Biostratigraphy, *Patella*, 50-metre package, Diamond placers, Sperrgebiet, Namibia.

To cite this paper: Pickford, M., & Senut, B., 2016. The fossiliferous sands of Hexen Kessel, Sperrgebiet, Namibia. *Memoir of the Geological Survey of Namibia*, **22**, 199-208.

Introduction

The endorheic depressions south of Pomona, in the Northern Sperrgebiet, Namibia, were the locale of immensely rich diamond placers (Kaiser, 1926). Various theories about the provenance of the diamonds and of the processes that led to the formation of diamond-rich surface 'lags' were proposed. It has generally been accepted that the diamonds originated from kimberlites in the interior of Southern Africa, were delivered to the Atlantic Ocean via the Orange River, and worked their way northwards along the Atlantic shoreline pushed by the Benguela Current and longshore drift. Fluctuations in sea-level led to the formation of beach placers at various altitudes, some now on land, others now below sea-level (Bluck *et al.* 2005, 2007).

The role of the wind in deflating the diamond-bearing deposits, once they were above sea-level, was early recognised (Kaiser, 1926) as was the role of centrifugal processes due to rainfall which tended to transport diamonds from the margins of depressions towards the sumps of endorheic basins, especially evident at Idatal and Hexen Kessel. The combination of aeolian winnowing, salt breakdown of sediment clasts (Corbett, 1989) and fluvial reworking, followed by further aeolian action, finally produced immensely rich concentrations of diamonds, the bulk of

which were found in the floors of the north-south valleys that extend from Chameis in the south to Lüderitz in the north.

The winnowing action of the wind has been so complete in some of the valleys such as Idatal, Hexen Kessel and Scheibetal, that there remain few signs of the original deposits that accumulated at the time that the diamonds were input to the depressions. This lack has given rise to a certain amount of doubt about the timing of the diamond input, with estimates ranging from Cretaceous (Merensky, 1909; Krause, 1910) to Eocene (Kaiser, 1926). Naturally, estimation of the rates of deflation, downwasting of the floors of the depressions and other geomorphological processes depends to a great extent on the timing of geological events in the region being studied.

During the 2015 field survey of the Namibia Palaeontology Expedition, fossiliferous deposits were encountered in Hexen Kessel, which indicate that this endorheic basin was likely inundated by the sea during the Pliocene, and that during the transgression, diamonds were probably transported into it by the usual processes related to pocket-beach formation and allied deposits (Bluck *et al.* 2005, 2007; Jacob *et al.* 2006). The implications of this discovery are sufficiently interesting for them to warrant publication.

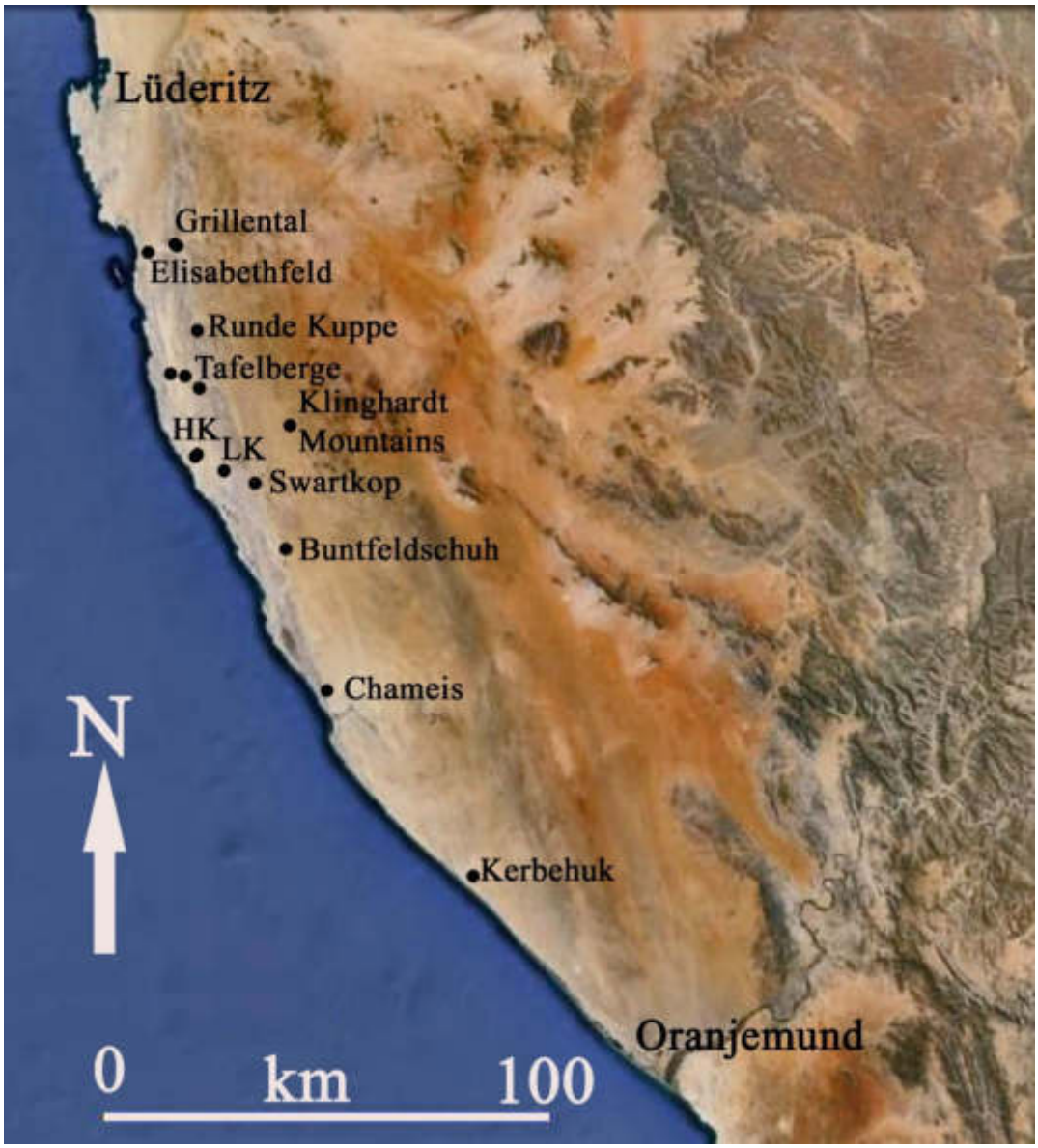

Figure 1. Location of Hexen Kessel (HK) and other localities in the Sperrgebiet, Namibia (LK – Lüderitz Krater).

The fossiliferous sands at Hexen Kessel

Kaiser & Beetz (1926) mapped an occurrence of travertine and sandstone ("esi" in the map legend) in the southern extremity of Hexen Kessel, not far from Idatal. Examination of this outcrop by the authors, led to the discovery of fossils at two localities, one a mass of tubes in pale brown marly sandstone tentatively attributed to *Phragmites* or a similar plant, the other scattered shells of *Patella* in indurated grey sand. The *Phragmites*-like tubes are significant on account of the fact that many of the individuals are *in situ* in their growth positions. Some individuals penetrate into the underlying alterite. These deposits are probably Pliocene. The fossil occurrences at Hexen Kessel are at an altitude of ca 30 masl, but elsewhere in the vicinity correlative deposits top out at about 40-50 metres above sea level. Small outcrops of indurated grey sand occur sporadically in the floor of the valley west of the onyx ridge at altitudes as low as ca 25 masl.

Figure 2. Intercalations of grey sandstone and onyx travertine overlying Bo Alterite at Hexen Kessel. These deposits are at an altitude of ca 30 masl but nearby, correlative deposits top out at ca 40-50 metres above sea level.

Figure 3. Onyx travertine veins deposited in fissures in Bo Alterite (brown outcrop at bottom left) and cementing grey sand at Hexen Kessel, Sperrgebiet, Namibia. This outcrop indicates that the carbonate was deposited as groundwater rose towards the land surface. Even today there is a spring near this outcrop.

Figure 4. Onyx travertine overlying Bo Alterite and intercalated with grey sands at Hexen Kessel, south of Elfert‘s Tafelberg in the background, Sperrgebiet, Namibia.

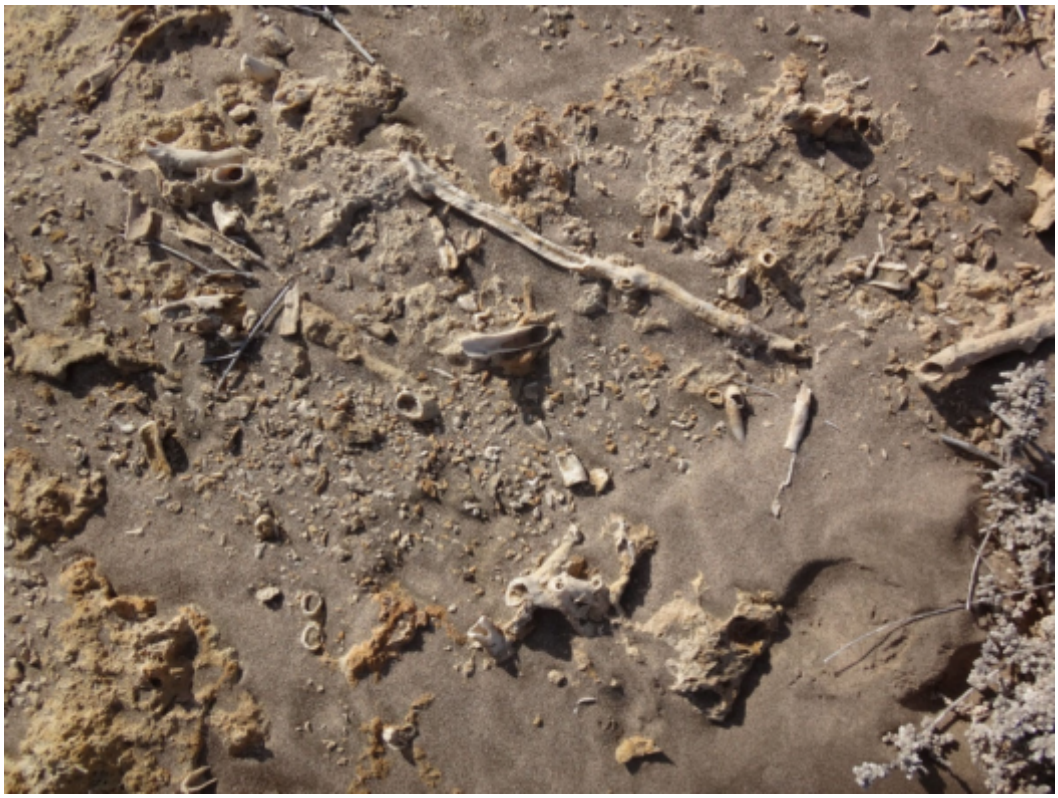

Figure 5. Sandy marl at Hexen Kessel containing abundant calcified tubes attributed to *Phragmites*, an aquaphile plant. The roots of the tubes penetrate the underlying alterite.

Figure 6. Shells of *Patella* in calcified grey sand intercalated in onyx travertine at Hexen Kessel. Nearby, these sandstones occur up to 50 metres above sea level, although at this locality they are at ca 30 masl.

Figure 7. *Patella* in indurated grey sand at Hexen Kessel, Northern Sperrgebiet, Namibia.

It is likely that the Hexen Kessel deposits accumulated at the same time as marine terraces at an altitude of ca 50 metres preserved sporadically along the coast north of Lüderitz as far as Meob. These marine terraces were carved into aeolianite and are covered in vast concentrations of marine shells (principally *Donax*). Further south in Namaqualand, South Africa, deposits at this altitude are richly fossiliferous (Haughton, 1932) and were attributed to the 50-metre marine package by Pether (1986, 1994) for which an age of Pliocene has been estimated (Pether *et al.* 2000). These outcrops indicate that Idatal and environs were likely to have been inundated by the sea sometime during the Pliocene.

Figure 8. Elevated beach terrace at an altitude of 48 masl, in the region south of Meob, Namib Sand Sea, Namibia. The white « clasts » on the beach comprise a vast accumulation of bivalves (dominated by *Donax*) and rarer gastropods and lithic clasts.

Figure 9. View of the 48-metre beach south of Meob, Namibia. Inset shows the concentration of bivalves, predominantly *Donax*, and other clasts that armour the surface.

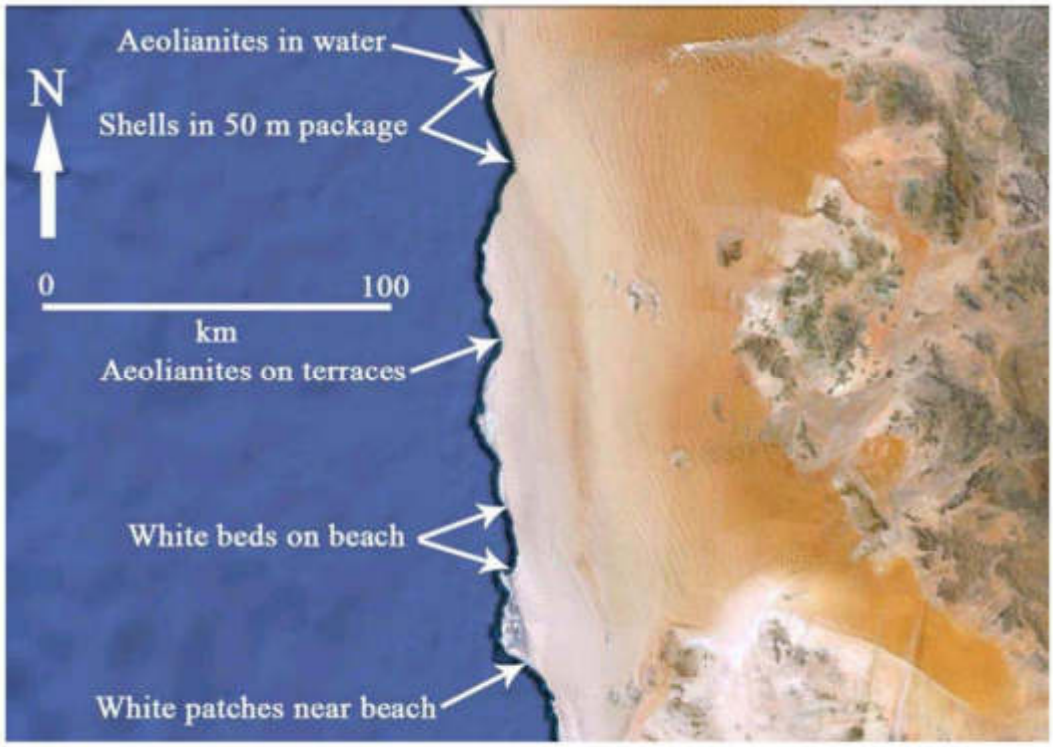

Figure 10. Map showing the southern part of the Namib Sand Sea and the disposition of beaches and some aeolianite deposits along the Atlantic coast between Lüderitz and Meob, Namibia. Figures 8 and 9 were taken at the arrows labelled « 50 m package » (map modified from Google Earth).

Geomorphological implications

Several geomorphological implications flow from the discovery of Pliocene fossils at Hexen Kessel. The first is that rates of aeolian winnowing and regional downwasting of the floors of Idatal and Hexen Kessel could have been considerably more rapid that previously estimated when an Eocene age was assigned to marine deposits endowed with agates, jaspers and diamonds. This is not to imply that there are no Eocene clasts in the region, but the possibility of diamond input during the Pliocene, along with a suite of other clasts can no longer be avoided. What it means is that there were probably several pulses of diamond input into the basins.

The second implication concerns eustacy and tectonics. As currently exposed, the endorheic basins of Hexen Kessel and Idatal would not be flooded were the sea-level to rise to 30 metres above present day levels, but a transgression up to 50 metres would drown the valleys. Thus, with a Pliocene age for the Hexen Kessel fossils, there would be no requirement to invoke vertical land movements to explain their presence in the depressions.

A third implication of this discovery is that extensive areas further south in the vicinity of Bogenfels would have been drowned by a 50-metre transgression of the sea, with a concomitant input of diamonds to the local placers. There is little if any direct evidence of this transgression left in the Bogenfels sector, so complete has been the aeolian winnowing.

North of Lüderitz, the seaward margin of the Namib Sand Sea shows a number of outcrops of fossil-rich beaches at altitudes of 48-50 masl, overlying wave-cut terraces in aeolianite. These beaches probably represent the same eustatic event as that recorded at Hexen Kessel and further south in Namaqualand, called the 50-metre package (Pether, 1986). If this is so, then it speaks for a relatively stable continental margin since the Pliocene. This in turn implies that the Pleistocene beach deposits that are now above or below sea-level (Hallam, 1964; Stocken, 1978; Bluck *et al.* 2005, 2007), were influenced more by eustatic changes in sea-level rather than by uplift or downdrop of the land.

Conclusions

The discovery of fossiliferous marine deposits of Pliocene age at Hexen Kessel, south of Pomona, Sperrgebiet, Namibia, is important for throwing light on aspects of the geomorphological history of the Northern Sperrgebiet. By providing a chronological anchor, it impinges on previous concepts of rates of geomorphological processes such as aeolian deflation, which led to the concentration of diamonds in the placers at Idatal, Hexen Kessel and other endorheic basins and valleys in the region between Chameis and Lüderitz. Rates of deflation could have been appreciably more rapid than estimates made when the marine deposits were considered to be of Eocene age. This is not to imply that there was no diamond input in the Eocene, but that later inputs of sediment and diamonds cannot be excluded. Thus, diamonds probably arrived in the region in several pulses related to eustatic changes in sea-level, those onland owing their origin to sea-levels higher than at present.

Mapping in the Namib Sand Sea reveals the presence of fossiliferous beach terraces at an altitude of 48 masl in the sector south of Meob, which are here correlated to the deposit at Hexen Kessel and strata in Namaqualand, South Africa, referred to as the 50-metre marine package, which is estimated to be Pliocene (Pether *et al.* 2000). The regional extent of the 50-metre package supports an eustatic explanation for its origin rather than uplift of the continental margin since the Pliocene.

Acknowledgements

Authorisation to carry out palaeontological research in Namibia was provided by the National Monuments Council of Namibia (Mr Karipi). Thanks to the Geological Survey of Namibia and the French Embassy in Windhoek. Funding for the survey was provided by Namdeb, the French CNRS and the Muséum National d'Histoire Naturelle de Paris. Support from the Franco-Namibian Cultural Centre (M. Portes) and the Ore Reserves Department of Namdeb (J. Jacob) is greatly appreciated. Thanks to Ian Corbett for comments about the tube-like fossils from Hexen Kessel and to John Pether (via Ian Corbett) for comments about the 50-metre package.

References

Bluck, B.J. Ward, J.D., Cartwright, J., & Swart, R., 2007. The Orange River, southern Africa: an extreme example of a wave-dominated sediment dispersal system in the South Atlantic Ocean. *Journal of the Geological Society*, **164**, 341–351.

Bluck, B.J., Ward, J.D. & de Wit, M.C.J., 2005. Diamond mega-placers: southern Africa and the Kaapvaal Craton in a global context. *In*: McDonald, I., Boyce, A.J., Butler B.I., Herrington, R.J., & Polya, D.A. (Eds). *Mineral Deposits and Earth Evolution*. Geological Society, London, pp. 213–245.

Corbett, I.B., 1989. *The Sedimentology of the Diamond Deflation Deposits within the Sperrgebiet, Namibia*. PhD Thesis, University of Cape Town, 430 pp.

Hallam, C.D., 1964. The Geology of the coastal diamond deposits of southern Africa. *In*: S.H. Haughton (Ed.) The Geology of Some Ore Deposits of Southern Africa. *Geological Society of South Africa*, **2**, 671-728.

Haughton, S.H., 1932. The Late Tertiary and Recent Deposits of the West Coast of Africa. *Transactions of the Geological Society of South Africa*, **34**, 19-57.

Jacob, J., Ward, J.D., Bluck, B.J., Scholz, R.A., & Frimmel, H.E., 2006. Some observations on diamondiferous bedrock gulley trapsites on Late Cainozoic, marine-cut platforms of the Sperrgebiet, Namibia. *Ore Geology Reviews*, **28**, 493-506.

Kaiser, E., 1926. *Die Diamantenwüste Südwest-Afrikas*. D. Reimer, Berlin, Vol. 2, 535 pp.

Kaiser, E., & Beetz, W. 1926. Geological Maps *In*: E. Kaiser (Ed.) *Die Diamanten-wüste SüdwestAfrikas.* Reimer, Berlin, **2**, p. 158.

Krause, G., 1910. Notes on the German South-West African Diamonds. *Transactions of the Geological Society of South Africa*, **13**, 61-64.

Merensky, H., 1909. The Diamond deposits of Lüderitzland, German South-West Africa. *Transactions of the Geological Society of South Africa*, **12**, 13-23.

Pether, J., 1986. Late Tertiary and Early Quaternary marine deposits of the Namaqualand coast, Cape Province: New perspectives. *South African Journal of Science*, **82**, 464-470.

Pether, J., 1994. *The Sedimentology, Palaeontology and Stratigraphy of Coastal-Plain Deposits at Hondeklip Bay, Namaqualand, South Africa*. MSc Thesis, University of Cape Town.

Pether, J., Roberts, D.L. & Ward, J.D., 2000. Deposits of the West Coast. *In*: T.C. Partridge & R.R. Maud (Eds). *The Cenozoic of Southern Africa*. New York, The Oxford University Press, pp. 33–54.

Stocken, C.G., 1978. A Review of the Late Mesozoic and Cenozoic Deposits of the Sperrgebiet, *Unpublished Report, Consolidated Diamond Mines of South West Africa (Pty) Ltd*, 1-33.

MEMOIR OF THE GEOLOGICAL SURVEY OF NAMIBIA

INSTRUCTIONS FOR CONTRIBUTORS

Instructions for contributions to the Memoirs of the Geological Survey of Namibia are the same as those for the Communications, provided below. Contributors are requested to adhere to these requirements.

COMMUNICATIONS OF THE GEOLOGICAL SURVEY OF NAMIBIA

Communications first appeared in 1985 with the aim to disseminate information about research and mapping projects carried out by Geological Survey staff, as well as by visiting scientists, on an annual basis. Although for a number of years this goal has not been met, it is planned with this issue to return to its original objective. If warranted by the number of contributions, bi-annual publication will be considered. Communications is published in digital format and distributed to universities and research institutions worldwide; copies can also be purchased at the Geological Survey's sales office at 1 Aviation Road, Windhoek.

INSTRUCTIONS FOR CONTRIBUTORS

General

1. Manuscripts must be written in English.
2. A short abstract of less than 200 words must accompany research papers and reports.
3. Short geological notes (commonly less than 1000 words) may also be submitted. Notes do not require an abstract.
4. Contributions have to be submitted in digital format. The preferred format for text is Microsoft Word, for figures jpg or tiff.
5. Papers will be reviewed by external and internal referees; reports will be reviewed by internal referees. In addition, manuscripts submitted by students should be critically reviewed by their supervisors before submission. It is the responsibility of the supervisor to ensure that a high standard is maintained.
6. Proof copies will be sent to the corresponding author for final checking before publication and should be returned within two weeks.

Text

1. A recent issue of *Communications* should be consulted for the general style and format to be adopted.
2. The format and sequence of headings are as follows:
   - a. **Bold upper and lower case**
   - b. ***Bold italics upper and lower case***
   - c. *Italics upper and lower case*

   If further subdivision is needed, numerals or letters (lower case) should be used.
3. An alphabetical list of all references must follow the text, with a format as follows:

Gentry, A., 2010. Bovidae, *In*: L. Werdelin & W.J. Sanders (Eds) *Cenozoic Mammals of Africa*. Berkeley, Los Angeles, London, University of California Press, Chapter **38**, 741-796.

Wells, L.H., & Cooke, H.B.S., 1956. Fossil Bovidae from the Limeworks Quarry, Makapansgat, Potgietersrus. *Palaeontologia africana*, **4**, 1-55.

Note that journal titles are not abbreviated

Illustrations

1. Figures and photographs must be of good quality; ensure that lettering is readable after reduction.
2. Figures and tables may be included in the text document to indicate their positioning, but must also be provided separately in one of the above-mentioned formats.
3. Figure captions must be provided as a separate list.
4. Headings of tables and appendices should appear above the table.
5. All illustrations or photographs are termed figures, and are referred to as Fig. or Figs in the text.